Proyecto Puerto Talcahuano

Evaluating Port Expansion

Multi-Disciplinary Research Project
MP251

TU Delft

Proyecto Puerto Talcahuano

Evaluating Port Expansion

An analysis of the Port of Talcahuano and a proposed port expansion design. Report on the proposed scenarios, the multi-criteria Analysis, the detailed design and recommendations to the port.

Sponsor:

Tensar®

Name	**Student number**
Job Bottemanne	4211200
Martijn van Gils	4317696
Roland Martens	4298233
Thomas Taks	4185889
Jelle Teeling	4243099

Project duration: November 19, 2018 – January 18, 2019

Supervisors: Dr. ir. R. Aránguiz, Universidad Católica de la Santísima Concepción
Dr. ir. H. Hendrikse, Delft University of Technology
Ir. A. van der Hout, Delft University of Technology

TU Delft

Preface

This report contains a detailed design for an expansion of the port of Talcahuano. The report serves an advisory role during the orientation phase that the port is currently in. This report is the result of an eight week Multidisciplinary Project conducted by five master students from the Delft University of Technology. The members of the group follow specializations in Hydraulic Engineering and Offshore and Dredging Engineering. Together with bachelor experiences in Civil Engineering, Mechanical Engineering and System Engineering, Policy Analysis and Management, a wide base of knowledge has been applied during this project.

The project is commissioned by the port operator, Puerto de Talcahuano. Together with the port authorities they are responsible for the exploitation of the port of Talcahuano. An expansion of the port is desired in order to grow with the increasing import of goods. The report contains a problem analysis and a solution in the form of a detailed design in which the quay contains two berthing spaces for 180 m vessels. During the project meetings with the port operator, port authority and the project group were organized.

The Universidad Catholica de la Santísima de Concepción has provided the project group with an office and a supervisor, dr. ir. Rafael Aránguiz. From the Delft University of Technology dr. ir. Hayo Hendrikse and ir. Arne van der Hout have supported the project and provided guidance and feedback. We would like to thank dr. ir. Rafeal Aránguiz, dr. ir. Hayo Hendrikse and ir. Arne van der Hout for their support during the project. Thanks to Matías Felipe Gómez Canto for helping us out with Delft3D modelling. Also, we would like to thank Jan de Bont from Royal Haskoning who has given advice about dredging activities. Finally, we would like to thank our sponsor Tensar, in special Leo Kuljanski and Angel Conde who supported us and shared valuable information with us.

Concepcion, January 2019

Abstract

The port authority of the Port of Talcahuano has the desire to expand the port. The goal of the expansion is to increase the berth space and attract more vessels, thus increasing their throughput. This report is an advise to the port authority on the possibilities of expanding. Four preliminary port designs are made with the requirement of the ability to berth two 180 *m* vessels. A Multi-Criteria Analysis has been used to determine the most suitable scenario. The detailed design for this scenario is composed of a quay design, a dredging plan, an earthquake and tsunami impact analysis, market prospect analysis and a financial analysis. A technical design for port expansion, as well as a market strategy has been advised to the port authority.

Executive Summary

After the 2010 earthquake and tsunami a large part of the port of Talcahuano was destroyed. Some parts of the quay have been rebuilt, but their capacity is less than what it was. This is why the port of Talcahuano has the desire to expand their capacity and increase their throughput. Their goal is to obtain a potential design for a port which is able to berth two 180 m vessel at the same time.

Located in the south-west corner of the Concepcion Bay, the port is sheltered from severe wind and waves. The bathymetry requires modification before an extended quay can be used. Based on historical data it follows that the design of the new quay should take earthquake and tsunami impact into account as well.

For the port expansion four preliminary designs have been made. In a Multi-Criteria Analysis (MCA) these scenarios have been evaluated on the following five criteria, namely dredging costs, construction costs, loss of revenue, potential market value and environmental impact. The first scenario is an extension to the north of Sitio 1, the current commercial quay. This scenario has very low costs for dredging and construction activities, but also the potential market value is rather low, causing it to be not the best option. The second scenario in which Sitio 1 is extended in south and north direction has the same strengths and weaknesses, but scores just a little higher. In the third scenario a jetty is constructed north of Sitio 1. It will be directing to the east and will provide the second berth. The construction costs of this jetty are however very high and the potential market value does not make up for this. The third scenario scores the lowest of all four scenarios. The final scenario connects Sitio 1 to the Maria Isabel quay in the south. The result is one long quay extension to the south of Sitio 1. The costs of this long quay are high, but the high potential market value outweigh these costs. Also Sitio 1 can continue its operations during most of the construction and dredging activities. This results in Scenario 4 being the most favourable design for the desired port expansion.

The new quay design "Nieuw Delft" of 240 m consists of the following elements: a sheet pile wall and anchoring, fender piles, mooring bollards, piles and the quay apron. The sheet pile wall and anchoring are designed using the current quay as reference. After determining the dimensions and sheet pile type the design was modelled in PLAXIS 2D, to assess its stability when subjected to different load cases (operational and earthquake) with different groundwater tables. The same is done for the current sheet pile wall, to check if it doesn't fail with the new water depth. The design is a Hat-type sheet pile wall with a total length of 20 m, an embedded depth of 6.5 m and 25 m long anchors every 2.5 m. The fenders and bollards are designed based on the properties of the design vessel, using literature and guidelines. The fenders and bollards are founded on piles. The dimensions of the quay apron are determined by using the same basis of design as used at Sitio 1. The design for the reinforcement in the concrete is determined by using the maximum moment and the maximum shear force as the governing design factors. The length of the quay apron is 240 m, the width of the quay apron is 25 m and the thickness is 1.16 m. The main reinforcement that is needed is 10 bars of 28 mm diameter every 1 m of length. The stirrup reinforcement that is needed is 4 bars of 14 mm diameter every 1 m of width.

For the design of the navigation channel and manoeuvring area, Dutch as well as Chilean guidelines have been used to determine the dimension. The current navigation channel will be expanded until a depth of 10.6 m below MSL, and the berthing pocket will be introduced to allow vessels to berth even if the other berth is already occupied. The berthing pocket will be dredged until a depth of 10.6 m below LAT. In order to reduce the dredging volume, and with that the dredging costs, it is chosen to implement a one-way navigation channel and a tidal window. A total volume of 600.000 m^3 has to be dredged. Also, a maximum angle of the slope of 12.5 degrees along the dredged area is defined to mitigate the need for dredging maintenance.

The risk of a significant earthquake hitting argues that a proper emergency protocol should be in place and has to be trained in all of the ports components. This includes the use of back-up communication devices and power supplies. Also for a tsunami impact measures need to be taken in order to reduces the possible damage and casualties. Reinforced concrete and placement of port equipment and storage can minimize the

number of objects to be picked up and colliding with buildings outside of the port. For the vessels in the port an emergency protocol must make sure they are able to leave the port as quick as possible and sail to a safe location in the bay.

In the market prospect chapter, two future scenarios are explained. The future throughput is determined for a scenario where the port keeps its current market strategy of handling general cargo and bulk, and for a scenario where the port changes the market strategy and choose to handle containers only. For the base case of the general cargo scenario with an occupancy of 35 %, $0.73*10^6$ $tons$ of throughput is expected to be handled. The current available land area is found to be sufficient to handle the maximum throughput of $1.57*10^6$ $tons$. However, it is advised to build transfer sheds secure a smooth cargo transfer. For the base case of the container scenario, $0.22*10^6$ TEU are able to be handled. Re-arranging the port into a container port would mean a big extra investment for the port and the uncertainty of not attracting the container market in the region due to much competition.

In the financial analysis the quay costs, dredging costs and revenue are calculated. The quay costs are calculated by doing a literature study on quays. The dredging operational costs are calculated by using a cost estimation tool. The dredging transportation costs are estimated by using available information from Royal Haskoning and dredging companies that have done activities in the region in the past. The revenue is calculated by doing a future projection for the throughput and by assuming a gross price per tonnage of throughput. An NPV analysis has been carried out for a low, base and high case. The different sensitivities that have been implemented are: dredging costs, total quay wall costs, discount rate, occupancy and gross price. The base case is expected to generate an NPV of 11 million USD after 30 years with a positive NPV after 16 years.

The project planning can be split in four overlapping phases, namely the Front-End Engineering Design (FEED), site preparation, dredging and the quay construction. As the planning changes during the project a provisional schedule is made which is a live document to be updated along the whole project. The total duration of the project is calculated to be 110 weeks.

Contents

List of Figures

List of Tables

[s] r Radius

List of Symbols and Abbreviations

BCR	Benefit Cost Ratio
CBR	California Bearing Ratio
CF	Cash Flow
DCF	Discounted Cash Flow
DWT	Dead Weight Tonnage
EA	Axial Stiffness
EI	Bending Stiffness
FEED	Front End Engineering Design
GWT	Ground Water Table
HAT	Highest Astronomical Tide
IRR	Internal Rate of Return
LAT	Lowest Astronomical Tide
MCA	Multi-Criteria Analysis
MEH	Metros, Eslora, Horas - Usage of a quay defined in Metres * Length * Hours
MSL	Mean Sea Level
NPV	Net Present Value
SF	Safety Factor
SPT	Standard Penetration Test
TEU	Twenty foot Equivalent Unit
UKC	Under Keel Clearance
USCS	Unified Soil Classification System
USD	United States Dollar
W	Section Modulus
WBS	Work Break Down Structure

β	Wedge angle
Δ	Relative buoyant density
γ	Specific or Unit weight
ω	Angular frequency
ø	Diameter

ϕ	Internal friction angle
ψ	External friction angle
ρ	Density
σ	Stress
$\widetilde{F}$	Fetch
B	Breadth
C	Seismic coefficient
c	Wave speed
C_b	Berthing coefficient
D	Depth
d_{50}	Median particle size
D_s	Directionalitiy
f_w	Force due to dynamic water pressure during an earthquake
f_y	Yield strength
G	Shear Modulus
h	Height
H_{m0}	Significant wave height
I	Importance Factor
L	Length
M	Moment
m	Mass
N	Normal force
P	Force fender plate
P	Weight of the active soil wedge
q	Line load
q_0	Horizontal load due to earthquake accelerations
R	Discount rate
S	Shear strength
s_{max}	Maximum sinkage
T_p	Peak period
T_s	Significant wave period
u	Displacement
υ	Poisson's ratio
W	Width

A	Area
B	Stability coefficient
c	Cohesion
E	Young's modulus
e	Void ratio
F	Point load
G	Shear modulus
g	Gravity constant
I	Moment of inertia
k	Wave number
n	Porosity
S	Maximum depth scour hole
v	Velocity
v_0	Velocity at main propeller of jet stream
v_{bmax}	Velocity of jet stream at sea bed
$v_{thruster}$	Velocity at thruster of jet stream

1 Introduction

Puerto Talcahuano is situated in the Bay of Concepcíon, in the Bío Bío Region of Chile. The port in the south west corner of the bay has three berths directed to the east and can be reached via the navigation channel in north east direction. This part of the Chilean coastline is subject to regular earthquakes and consequential tsunamis. In 2010, an earthquake of magnitude 8.8 on the moment magnitude scale struck the area, the epicenter being around 150 km away from the port. This resulted in a tsunami which reached 4 km inland. The port was heavily damaged and had to be rebuild in 2010. The leftovers of the damaged quay wall had to be removed in order to rebuild the port. Currently the port has three operational quay walls of which one is commercial and two are used for fishery. Between the quays the rubble of the original port is still visible.
The port of Talcahuano is a public port and therefore it has to comply with national law N19 542 [23]. This means that the State of Chile is the owner of the land, but the operator is a private company in this case the Talcahuano Terminal Portuario. The public port authority, Puertos de Talcahuano, pays the concession for a maximum length of 30 years after which re-bidding takes place for renewal of the concession. As the concession has been renewed in 2012 the current concession lasts till 2042. The control of the maritime territory and pilotage services are both in hands of the Maritime Authorities (Navy) which are located in the Asmar Port nearby. The taxes equal a 24% corporate tax, a 40% tax on public companies and a tax on land. Furthermore, half of the remaining net port revenues have to be paid to the State of Chile.
Investments in the super-structure of the harbour need to be done by the private terminal operators, but the depreciated value of private investments are reimbursed by the State at the end of the concession. In practice, this law allows the State to retrieve all of the remaining net revenues and even future earnings. As a result public ports depend on the State for required investments. The budget for the port expansion is limited by the viability of the business plan.

Figure 1.1: Satellite image of the Bay of Concepción with the Port of Talcahuano indicated by the pin.[27]

1.1. Problem Description

Even though most of the damage has been repaired the capacity of the current port is significantly less than before the earthquake and tsunami. During the last few years the throughput of the port has increased. Until today the capacity of the port limits further growth. Therefore the port authorities are looking into possibilities to expand. The current layout of the port gives multiple possibilities for expanding the quay wall and the number of berths. Determining the most suitable solution requires information about the costs, the benefits and other effects from the expansion. Currently the port authorities seek assistance to select one or more viable options for evaluation by an engineering company.

1.2. Goal of report

This report is meant to be an exploration of possible expansions. First, the current situation is evaluated and the requirements for a future design are determined. Based on these requirements several new designs are developed and compared. The result of the analysis is one design which is worked out in more detail. This final design must give a clear and complete picture of what the possibilities are for port expansions and plays an advisory role to re-evaluate the future strategy for the port operator.

1.3. Scope

Due to limited time and resources some subjects can not be touched upon in depth. Below is summed up what subjects are included in the scope of the project and in what level of detail.

1.3.1. Technical evaluation

The technical design is split into two parts, namely the dredging activities and the design of the quay wall. The layout of the port can be divided in the navigation channel, manoeuvring area, berths including berth basin and work space and storage depot. Because the on-land logistics are not in the scope of this project the work space and storage depot are not designed. It should also be noted that only for the final scenario a detailed design is made. Even though the final design is a detailed design, due to time and resource limitations some design aspects are not taken into account. For the technical design a combination of Dutch and Chilean design standards is used.

1.3.2. Economical evaluation

For the market analysis the current activities of the port of Talcahuano and nearby ports are reviewed. As it is unknown in which market the highest future potential lays it is assumed that the port of Talcahuano is able to increase its revenue according to its capacity. Also only the commercial site, Sitio 1, is taken into account for the economic analysis. The costs of the port expansion are included in the analysis and these are estimates based on calculations, experience and comparisons with similar projects.

1.3.3. Earthquake and tsunami impact analysis

As the west coast of South America is a seismically active area earthquakes and tsunami are common. These extreme events will be taken into the environmental conditions. During the design phase specific earthquake design guidelines are used and an evacuation plan will be set up for the vessels in the harbour. As designing a structure to resist a tsunami impact is unheard of due to the enormous costs it would bring, it is not considered in this report. Design choices which reduce damage in and around the port are taken into account.

1.4. Approach

The first step to be taken, is to get a clear view on the differences between the current situation and the desired situation of the port. By reviewing the current design of the port, discussing with the port authorities and analyzing the regional market the requirements for the new design are determined. The new port is designed for a future outlook of 30 years. This means the new port design should be able to handle the expected market share for the port of Talcahuano for the upcoming 30 years.
Based on these requirements four scenarios are made. A Multi-Criteria Analysis (MCA) is used to determine the best alternative out of the four scenarios. In the MCA the alternatives are scored on criteria which are decided to be important by the project team as well as the client, the port operator. For the MCA literature, calculations and comparisons with equivalent projects are used to score the alternatives. The most suitable

port design, as determined by the MCA, is then worked out in detail. Here a full quay wall/jetty design is made. The manoeuvring area and navigation channel are designed in detail and the dredging activities are mapped. Finally, a conclusion and recommendations will be provided for the client to help them create their strategy for the port expansion. During the project, knowledge from Delft University of Technology courses is used throughout as well as international standards and guidelines as set by PIANC [53]. Apart from this, experience and expertise was shared by multiple sources such as professors from Delft University of Technology and Universidad Católica de la Santísima Concepción and engineers from commercial companies in the dredging and construction industry. Even though this report contains a detailed design for the new port, more research is needed before all aspects of the design can be made final.

In Figure 1.2, the approach used for the design in this report is shown.

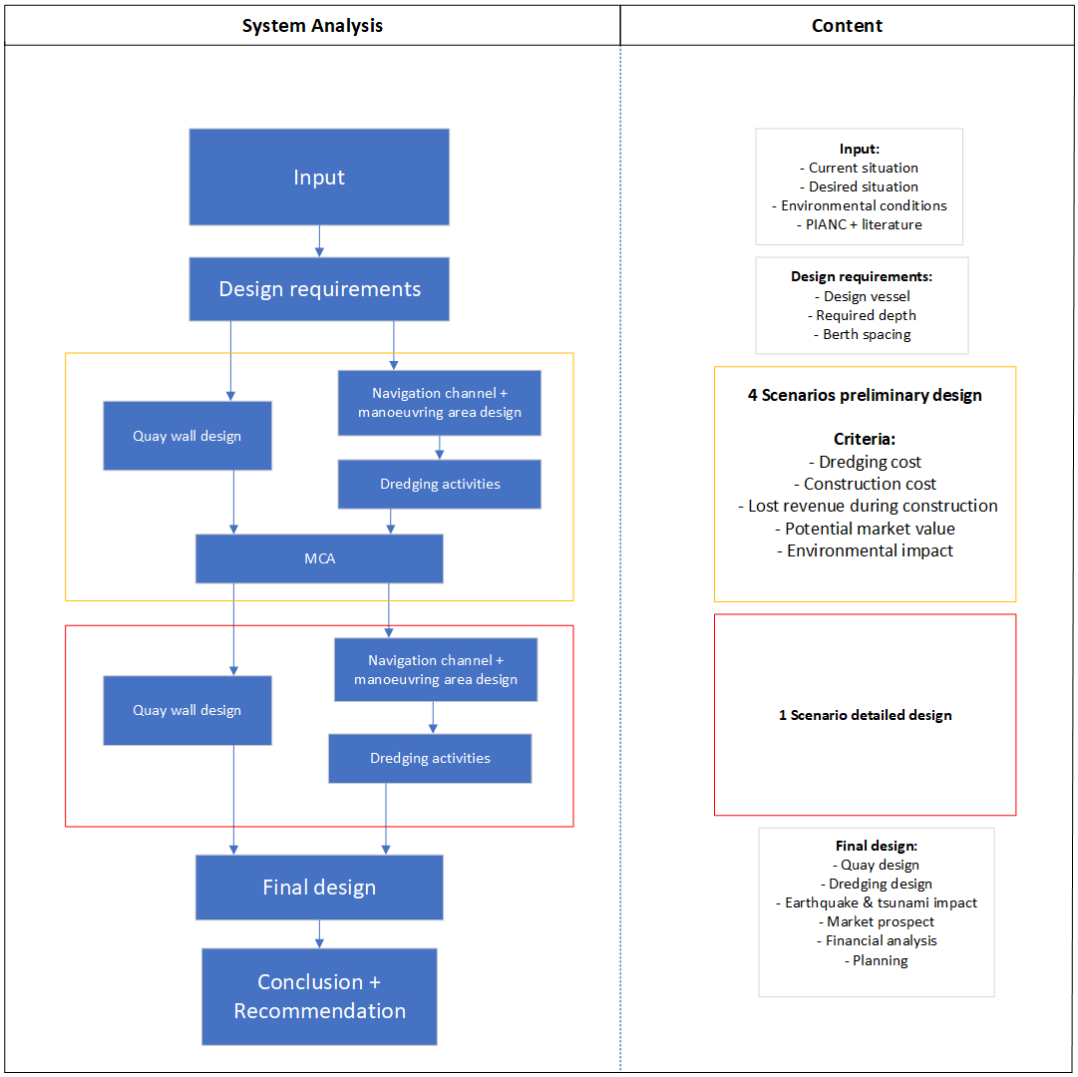

Figure 1.2: Approach for the design

1.5. Report

The report is divided into 5 main subjects: analysis, preliminary design, final design, conclusion and appendices.

In Part I, the current situation of the port is evaluated in order to determine the requirements and limitations for the new design. Chapter 2 describes the port layout, technical design and market of the port and surrounding ports in detail. The environmental conditions include the tidal, wind, wave and soil data and are

elaborated upon in Chapter 3. With all the necessary information available future scenarios can be designed.

Part II describes the preliminary design, which consists of 4 different scenarios. In Chapter 4 these designs are explained, scored and ranked according to an MCA. Finally, for one scenario a detailed design is made on which a recommendation is based for the port operators.

Part III describes the final design. Chapter 5 contains the new lay out of the port. This includes the lay out of the port including the new quay. Chapter 6 includes the design of the new quay wall that is necessary for the extension. The design of the new navigation channel, manoeuvring area and berthing pocket are explained in Chapter 7. Chapter 8 contains the calculation of the dredging volume and a description of a dredging execution plan. An earthquake and tsunami impact analysis is provided in Chapter 9. In Chapter 10, the future projection for the throughput and occupancy are discussed for two different future scenarios. Chapter 11 describes the financial analysis of the project. After that, a planning of the total project is provided in Chapter 12.

Finally, part IV contains the conclusions and the recommendations for the port authorities.

I

Analysis

2

Current Situation

In this chapter the current situation of the port is described. First, the port layout and technical details are discussed in Section 2.1. After that, a market analysis of the different kind of products handled in the port of Talcahuano is discussed in Section 2.2. Finally the stakeholders related to the expansion of the port are described.
The engineering firm which designed the current port have used their own standards, which are based on their experience. Therefore most design criteria are not documented, nor shared for this project.

2.1. Port layout

The port of Talcahuano consists of 3 quays: Sitio 1, Sitio 2 and Maria Isabel. The port also contains a container storage area and offices. The stored containers are used by trucks only as no container vessels berth at the port. Figure 2.1 shows a schematic layout of the port in its current situation. In blue the current sites being used by the port can be seen. The red line in Figure 2.1 shows the navigation channel to the port of Talcahuano. Appendix A shows a more detailed layout of the port including the storage area for containers.

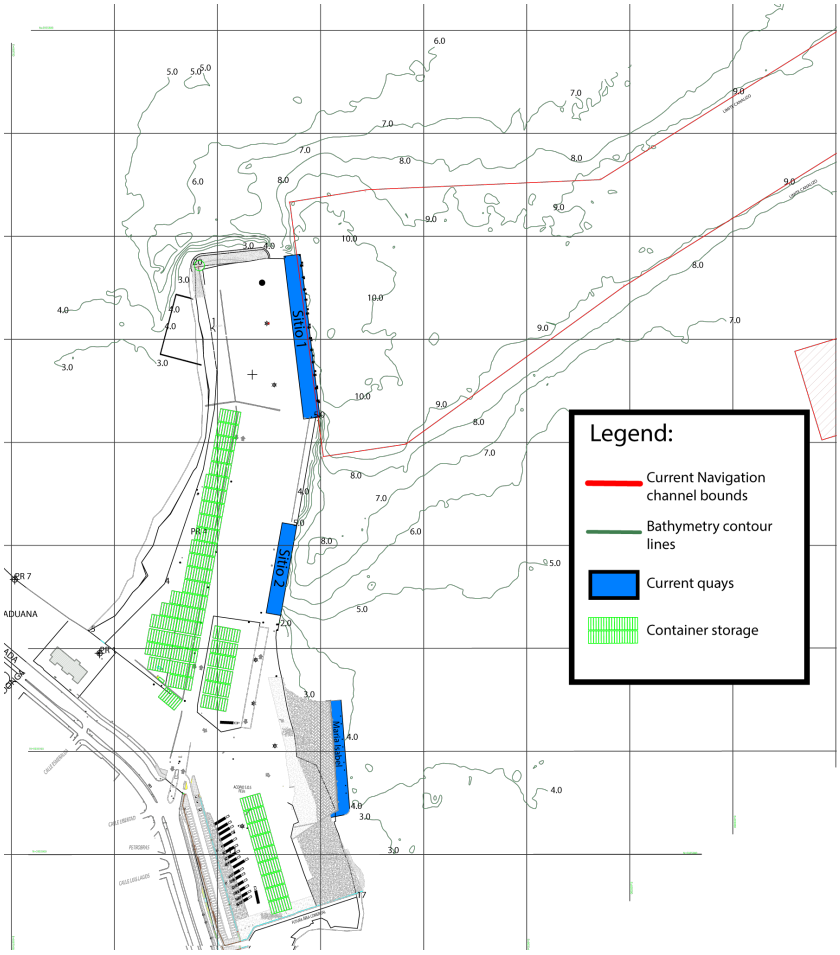

Figure 2.1: Schematic port layout

2.1.1. Sitio 1

Sitio 1 is the commercial berth of the port and is mainly used for transfer of general cargo and break bulk, mainly being metal scrap and salt. Vessels ranging from 140 to 230 meters currently berth here. The total length of the quay is 160 m. A mooring dolphin 30 meters northwest from Sitio 1 is present. This makes it possible for vessels larger that 160 m to berth at Sitio 1. The current depth in front of the quay at Sitio 1 is approximately 9.5 m measured from LAT.

The quay wall at Sitio 1 consists of a concrete structure, concrete piles into the soil, fenders, mooring bollards and a large sheet pile wall. The floor of the quay at Sitio 1 is built on artificially placed soil (composed of medium sand and fine sand) and supported by piles. The quay has a U-profile sheet pile wall supported by anchors which are placed 1.26 m away from each other. The concrete floor continues after the sheet pile wall, creating a cantilever supported by piles. An impression of this construction is given in Figure 2.2. The technical drawing of the current quay wall is shown in Appendix A in Figure A.2. More technical details of the quay are given in Chapter 6.

2.1.2. Sitio 2

Sitio 2 is used for fishery for human consumption. The total length of the quay is 100 meters, constructed after the earthquake in 2010. The depth is approximately 6.5 m LAT. This quay has special equipment on it for unloading, processing and distributing fish onto trucks. Sitio 2 is used all year with its peak period in the months October, November, March, April and May. A simple technical drawing is shown in Figure A.3.

The quay of Sitio 1 used to be connected to Sitio 2. The 2010 earthquake and tsunami destroyed this part of the quay, separating it. The rubble from collapsing is still there, as well as the sheet pile wall.

Figure 2.2: (a) An impression of Sitio 1 and (b) the front of the quay.

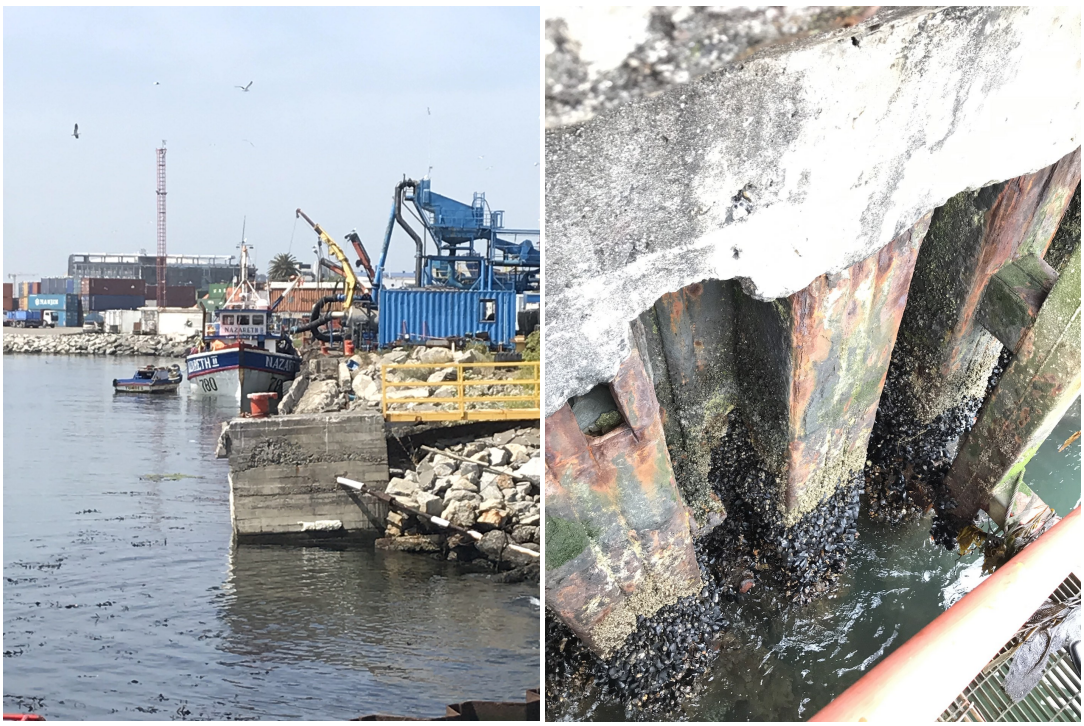

Figure 2.3: (a) An impression of Sitio 2 and (b) the front of the quay showing the sheet pile wall.

2.1.3. Maria Isabel

The site Maria Isabel is currently used for small fishery. The port wants to keep this berth for fishery in the future. The imported fish is used for industrial fish production. The depth around Maria Isabel is approximately 3.5 meters. The total length of the berth is 106 meters. A technical drawing is given in Figure A.4.

2.1.4. Navigation channel and manoeuvring area

The current navigation channel is 1800 m long and 100 m wide. It is designed for a one-way channel. The depth of the seabed level in the navigation channel differs throughout the channel. A drawing of bathymetry of the navigation channel and manoeuvring area is provided in Appendix A, in Figure A.5. In Appendix D a more detailed drawing of the bathymetry can be found. These values are seabed levels with a reference to LAT. The manoeuvring area can be seen in Figure 2.1 as indicated by the red line.
The maximum length of a vessel that is currently accepted has a length of 230 meters and a draught of 8.4 meters. Vessels with a draught of 9.1 meters can still enter the port in a tidal window according to the port authorities. Vessels are guided to the berth with tugboats. The minimum under-keel clearance that is cur-

Figure 2.4: Rubble still present between Sitio 1 and 2 after the collapse of the quay during the 2010 earthquake.

rently implemented in the navigation channel and manoeuvring areas is 0.6 m as determined by the port authorities based on their experience.

2.1.5. Land area

The port owns a land area of 80.000 m^2 in total. A part of this land area is rented out for storing empty containers. These containers are moved around by a reach stacker which is able to stack containers to a maximum height of four containers. Along the quays unloading equipment is present. Near Sitio 1 a mobile crane is present, and near Sitio 2 there is unloading equipment for fishing activities. No transfer sheds are present for the unloading of general cargo. If for instance general cargo is imported, it is either directly loaded onto trucks for transport or the cargo is loaded into empty containers for temporary storage, making transfer sheds unnecessary. This can be seen in the photos presented in Figure 2.5.

Figure 2.5: (a) An impression of storing the containers and (b) the loading of general cargo into empty containers.

In Figure 2.1 container storage areas are shown. In practise, storage of containers does not occur in a fixed location. Containers are stored at the location which is most convenient at that point in time. Since the land area is sufficiently big, a fixed location for container storage is not necessary.

2.2. Port activity and the market

This section shows the current activity of the port and its position within the regional market.

2.2.1. Current activities

The amount of vessel calls for Sitio 1 over the past 5 years is depicted in Table 2.1.

Type	2014	2015	2016	2017	2018
Multipurpose vessels	7	15	18	10	29*
Bulk vessels	2	4	6	9	11*
Container vessels	0	1	0	0	0*
Total vessels	9	20	24	19	40*

Table 2.1: Yearly vessel calls per cargo type. *Year of 2018 without November and December

It can be seen that in 2018 a major growth in vessel calls has taken place. These vessels brought in the amount of tonnage as is depicted in Figure 2.6. It is clear that the total handled cargo in the port of Talcahuano has been increasing over the last few years. In addition, it can also be concluded that the amount of salt handled in the port of Talcahuano is substantial. This figure does not contain information about November and December of 2018. This means the actual tonnage of 2018 will turn out higher.

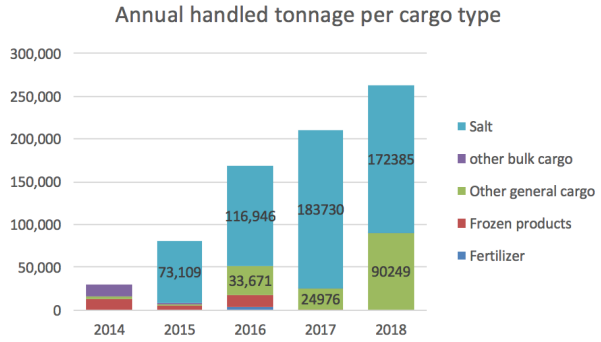

Figure 2.6: Total handled cargo trend-line

As a logical consequence, the increase in handled tonnage also resulted in an increase in occupancy of Sitio 1, as can be seen in Figure 2.7. There is an exception for 2017. In this year the unloading rate was higher than for instance 2016 and 2018 which resulted in short vessel service times and thus reducing the occupancy. The minimum occupancy was 11.43 % in 2014 and the maximum occupancy is achieved in 2018, which is currently 27.45 %. The maximum occupancy in a month reported is 56.32 %.

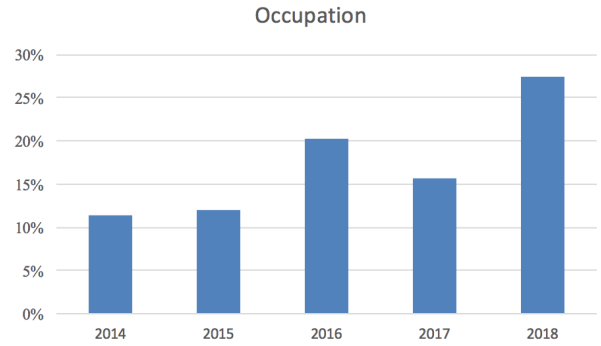

Figure 2.7: Occupation of Sitio 1 of Puerto Talcahuano

From the port statistics found in Appendix B it can be derived that the productivity of Sitio 1 is quite high. A lot of manpower is used at Sitio 1 to obtain an average performance of 153 $tonnes/hour$ in 2017 and 131 $tonnes/hour$ in 2018. Most vessels berthing at Puerto Talcahuano that carry general cargo are equipped with two or more cranes which can also be seen in Figure 2.5. The cranes contribute a lot to the berths performance as the port owns only one mobile crane.

2.2.2. Nearby ports and regional market

The port of Talcahuano is part of the 8th region of Chile, together with the ports of San Vincente, Lirquén, Penco, Coronel and Cabo Froward. In comparison to the other ports, Talcahuano only has a small percentage of the total market value in the 8th region, as can be seen in Figure 2.8. In 2017, Talcahuano had a percentage of 1.36 % of the total market value. The maximum market percentage for the port of Talcahuano is 2.08 %, which was obtained in 2006. The market shares of the players in the 8th region can be seen in Figure 2.9. It is important to note that the percentage for the port of Talcahuano has been growing in the last few years, just like the rest of the market of the 8th region.

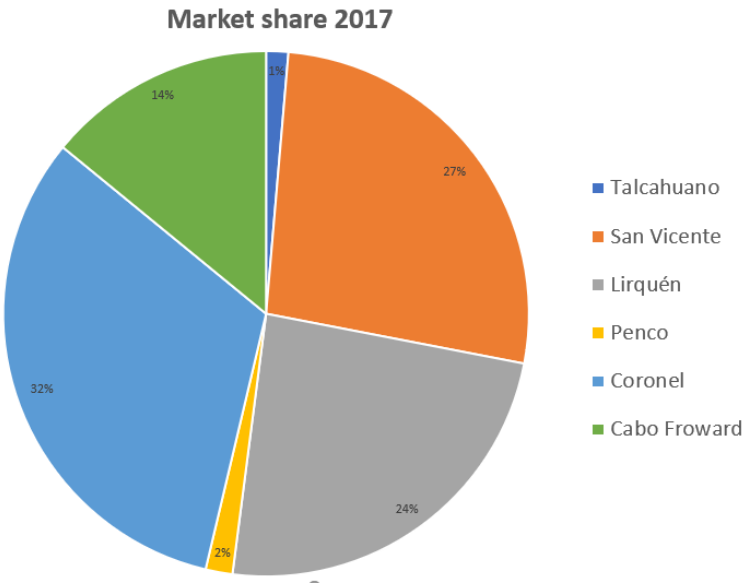

Figure 2.8: Market 8th region

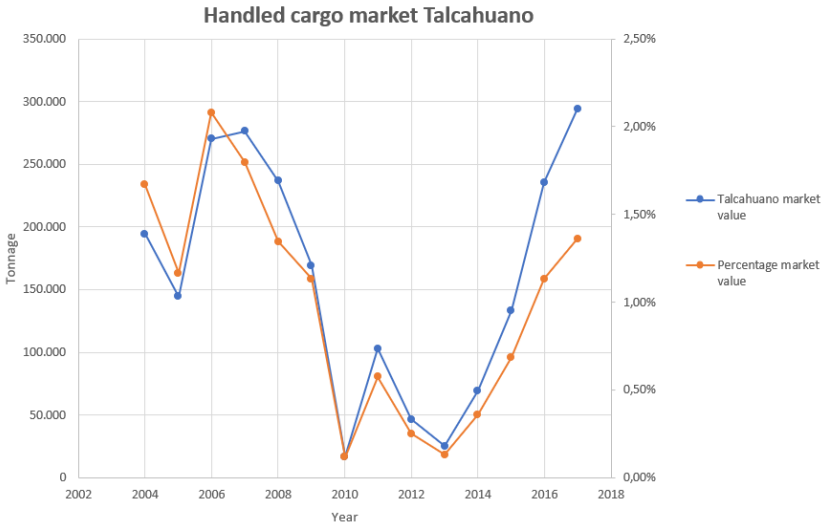

Figure 2.9: Tonnage and percentage total market Talcahuano

2.3. Stakeholder analysis

As briefly described in Chapter 1 the port authorities, who will decide on the port expansion, will need agreements of several other parties. Some parties don´t have an official say in the decision making but are still capable of influencing the decision process. All stakeholders, parties who have in some way an interest in the project, are mentioned in this section. For a better overview of all stakeholders a Power-Interest Diagram is

made. In Figure 2.10 the stakeholders of importance are first displayed. In the diagram they are ranked based on the amount of power they can exert on the decision making and whether this stakeholder has the same or conflicting interests as the problem owner, the port operators.

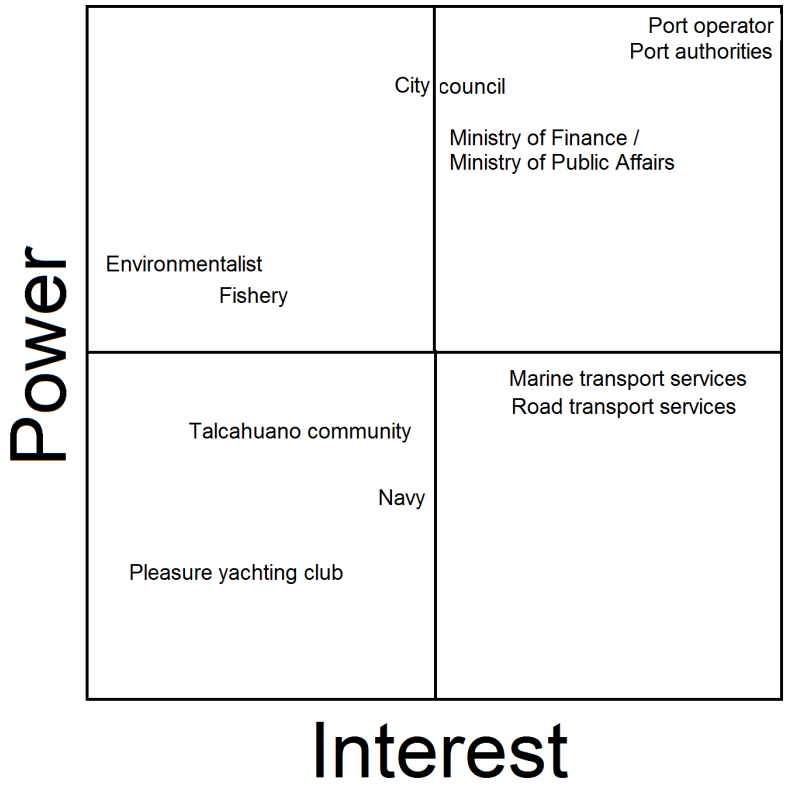

Figure 2.10: Power-Interest Diagram. The bottom of the diagram contains the stakeholders with less power and the stakeholders who can influence the decision the most are on the top half. The stakeholders with opposing interests are on the left and the stakeholders who have the same goals are on the right.

The most important stakeholder is the port operator, Talcahuano Terminal Portuario. This is a private party with financial profits as main goal. They strive towards a large commercial port with profitable activities due to a great throughput. They lease the port area from the port authorities. Even though the port operator is not the owner of the land or the facilities, they do decide about the port expansion and they are the party responsible for the exploitation. The port operator is also responsible for the investment itself. Therefore it is important that the port expansion will provide enough extra revenue to make up for the investment.
The port authorities, Puerto de Talcahuano, is a public party which buys the 30 year concession from the national government. They are responsible for attracting port operators who exploit all berths of the port of Talcahuano, Molo Blanco and Maria Isabel. As a public party they have close relations with the government. Also they are the ones who will need approval from the Ministry of Finance for investments they do. The goal of the port authorities follows from national policy for ports which is to improve the economy in a sustainable way for the environment and surrounding community.
The Ministry of Finance and Ministry of Public Affairs are governmental parties who are responsible for financing and regulating Chile's infrastructure. Not only the marine infrastructure but also the (rail) roads fall under their portfolio. Their goals is to improve the welfare of Chilean people which includes stimulation of the economy by improving the infrastructure. They will have to make a compromise between economic benefits and the well being of the surrounding community.
Apart from the commercial berth there are also berths for fishery. The fishing boats unload their goods after which they go back out to sea for more fish. It is important for them to be able to unload as quick as possible in order to maximize their production. Their berth should be accessible and large enough to provide enough unloading capacity for the whole fleet. When they are unsatisfied with the facilities the port of Talcahuano

offers them they are able to switch to other ports.
The city council serves the interests of many others. Also a lot of parties will try to do their say through the city council. It is assumed one of these parties will be the community which doesn´t want more noise and air pollution. Another one might be a transport company which wants a better infrastructure or the pleasure yacht owners who want to enjoy their recreational vessels. The city council is a powerful stakeholder which can help the port, but also work against them.
Environmentalists will try to prohibit any activities in and around the port which will negatively impact the environment. Because of this, the expansion of the port is something they will oppose. By informing them and minimizing the negative impact their actions can be relieved.
The navy has control of the maritime territory and is responsible for the pilotage services. For them the port expansion creates more work as there will be more vessel to attend. As a stakeholder the navy is expected to have a neutral stance in this project.

From the stakeholder analysis it can be concluded that the most important stakeholders are the port authorities and the ministries of Finance and Public Affairs. They all have economic prosperity and sustainability as high level goals for the Concepcion region and will use the available methods to reach them. The plans of a port expansion don´t necessarily conflict with these goals as long as they take the effects on the surroundings of the port seriously. The port operator should therefore try to mitigate the negative impact on the environment the Talcahuano community by all means reasonable possible.

3

Environmental Conditions

In this chapter, the environmental conditions of the Concepcion bay are described. First, the wind, waves and current in the bay are discussed. After that, the tide, bathymetry and soil properties in the bay of Talcahuano are looked into. Finally the seismic activity of Chile is described and the consequences for the coastal area are explained.

3.1. Wind

For two years, every five minutes, the wind speed and direction have been measured by a meteorological station situated in the port [63].
The dominant wind direction concerning the bay area, is wind coming from the South West direction (36%). Wind coming from the North will occur around 17% of the time, other wind directions will occurs less frequent, as can be seen in Figure 3.1.

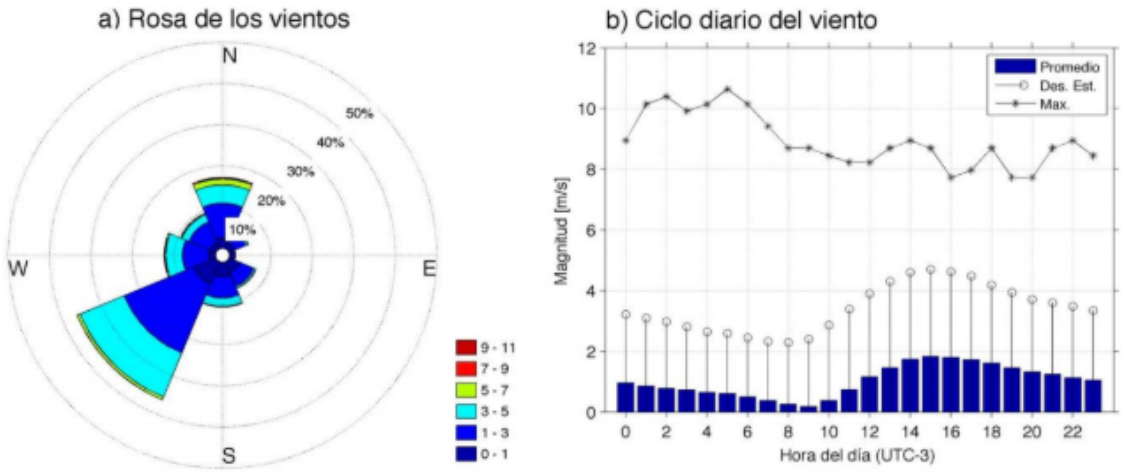

Figure 3.1: Wind Rose and Graph of the yearly distribution

When considering the speeds, the speeds that occur most frequent are between 1 and 4.09 m/s (76%). The higher wind speeds of 7-10.9 m/s will occur only 0.42% of the time. Table 3.1 gives a more detailed look at the wind speeds and their frequency of occurrence.
An extreme event like a cyclone is highly unlikely, due to the location of Talcahuano, being on the south-east side of South America [7].

Magnitude (m/s)	**Occurrence frequency** (%) **of wind directions**								**Total** (%)
	N	NE	E	SE	S	SW	W	NW	
<1.0	2.527	1.636	0.590	2.857	3.517	5.820	1.650	1.610	20.20
1.0 – 2.9	8.449	2.861	0.674	3.672	5.219	18.248	6.346	5.517	50.99
3.0 – 4.9	4.442	0.522	0.140	0.503	2.069	11.607	4.102	1.910	25.29
5.0 – 6.9	1.465	0.100	0.003	0.056	0.147	0.719	0.312	0.292	3.10
7.0 – 8.9	0.328	0.031	0.000	0.002	0.000	0.003	0.003	0.021	0.39
9.0 – 10.9	0.025	0.004	0.000	0.000	0.000	0.000	0.000	0.002	0.03
Percentage	17.236	5.154	1.407	7.090	10.951	36.397	12.413	9.352	100
Maximum	10.6	10.1	5.8	7.0	6.8	7.3	7.7	10.1	10.6
Average	2.7	1.8	1.4	1.5	1.9	2.4	2.6	2.5	1.0

Table 3.1: Wind speed occurrence per wind direction

3.2. Waves

Besides the open water conditions, this section discusses the wave climate in the Bay of Concepción, which is very relevant for the port design. To gain insight in the wave behaviour, a Delft3D model is used. The model definition and validation can be found in Appendix C in Section C.2. In this section only the results and important model inputs are discussed. The analysis of the waves at and around the port is divided in two parts. First, the impact of extreme open water waves is assessed. Then, the impact of wind generated waves is modelled.

3.2.1. Open water waves

Research from the Universidad de Valparaiso done in 2016 provides 35 years of numerically computed wave data at a virtual point, 170 km west of the Concepción bay. Figure 3.2 gives the wave rose for the significant wave height in normal conditions, as well as a rose representing the significant wave height and corresponding period including directionality. Table 3.2 summarizes some relevant parameters.

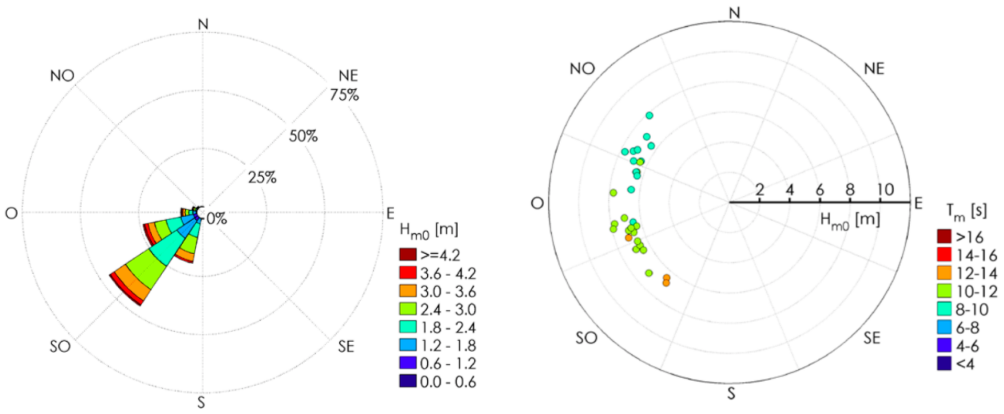

Figure 3.2: (a) The wave rose under averaged conditions and (b) the significant wave height and corresponding period including directionality, both based on numerical modelling at a virtual point 170 kilometers off the coast of Talcahuano. Note: O stands for west in this image. [8]

Parameter	**Value**	**Unit**
H_{m0}	2.42	m
T_s	8.9	s
T_p	13.0	s
D_s	231	$degrees$

Table 3.2: Relevant average wave parameters [8]

3.2.2. The bay

The bay is vulnerable to two environmental situations. The first is an extreme open water wave condition. A Delft3D model shows how these conditions reach the port. Secondly, the bay is vulnerable to wind-generated waves from the North. These situations are modelled in Delft3D to assess their effect at the port.

Extreme open water conditions

Fortunately, it seems that extreme open water waves are mostly coming from a direction between north west and south west, and no extreme events occur from the north. The most critical extreme condition which is likely to occur during the lifetime is chosen to have a significant wave height of 8 m and a period of 9 seconds. This is the extreme event which is coming from the north west as found in Figure 3.2. This situation is simulated in Delft3D to see how it affects the port.

The Delft3D model proves that open water (extreme) wave conditions lead to insignificant wave heights at the port. The model results for the wave heights at the quay and in the channel are given in Table 3.3. A visualisation of the model results can be seen in Figure 3.3, in which the location of the wave height measurements are also marked. For this, it can also be concluded that normal open water wave conditions won't produce high waves in the bay either. Though, different wave lengths and periods have not been modelled. Waves with the same height but a different length and period might enter the bay having more impact at the quay. This is not taken into account in this analysis, although port experience learns that this effects is insignificant.

Location	H_{m0}	
Quay	0.2	m
Channel	0.33	m

Table 3.3: Measured H_{m0} at the quay and the channel for extreme open water wave conditions

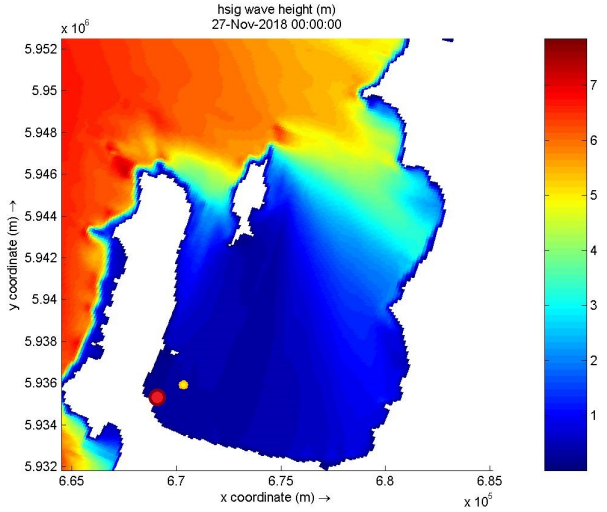

Figure 3.3: Model results for extreme open water conditions. The red dot indicates the location of port and is also the location of measurement for the quay, the yellow dot is the location of measurement for the channel

Wind generated waves from the north

The bay is not shielded when the wind direction is from the North. Waves generated at open sea might enter the bay without losing too much energy. Wind-generated waves in this situation are therefore relevant to investigate. Normal wind conditions are known as described in Section 3.1. From Table 3.1 it can be concluded that the strongest wind from the north observed during the two years of measurements is between 9.0 and 10.9 m/s. A uniform wind speed of 11.0 m/s from the north is simulated in the Delft3D model to investigate how it affects the port. The resulting wave heights at the quay and in the channel are given in Table 3.4, measured at the same location as for the extreme open water conditions. A visualization of the result for the entire bay is given in Figure3.4.

As the available wind data covers only two years it could very well be possible for higher wind speeds to occur over a longer period of time. An arbitrarily chosen wind speed of 15 m/s from the north is also modelled to assess the effect of this condition. The resulting wave heights are given in Table 3.5. Again, a visualization of the model result for the entire bay is given in Figure 3.4.

Location	H_{m0}	
Quay	0.55	m
Channel	0.78	m

Table 3.4: Measured H_{m0} at the quay, mid channel and at the entrance/exit of the channel for wind speeds of 11 m/s from northward direction

Location	H_{m0}	
Quay	0.87	m
Channel	1.16	m

Table 3.5: Measured H_{m0} at the quay, mid channel and at the entrance/exit of the channel for wind speeds of 15 m/s from northward direction

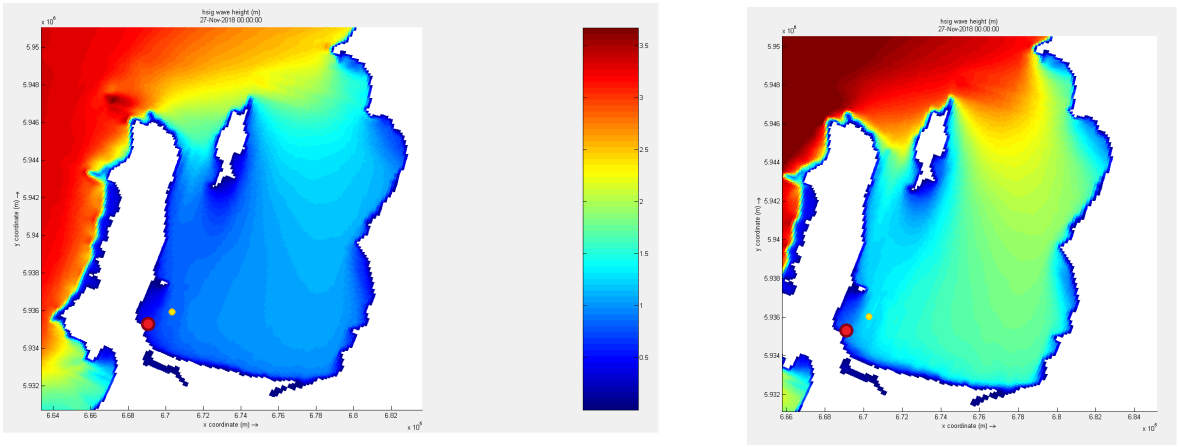

Figure 3.4: Plots for the resulting wave climate for wind speeds of (a) 11 m/s and (b) 15 m/s both from the north. The red dot indicates the location of the port and is also the location of measurement for the quay, the yellow dot is the location of measurement for the channel

3.3. Current

Currents are an important environmental condition to be considered. The current in the bay of Concepcion is analyzed in a report in 2007 ([51]. The maximum tidal current speed measured, according to this report, is 0.43 m/s. For the design, a conservative current speed of 0.5 m/s is used. This value is chosen because for further purposes to analyze the bed slope stability.

3.4. Tide

It is important to calculate the minimum and maximum water level in the bay of Talcahuano in order to be able to make a good design. Measurements of the tide are made at Talcahuano, in the Concepcion Bay. The data concerning these tidal water levels is available on the IOC website [34]. As a reference, the year 2015 is chosen, since there is full wave data available of this year.
Using this data it can be seen that the water level difference during neap tide is approximately 1 m, while the largest difference during spring tide is around 2 m. LAT was found to be -1.04 m in reference to MSL, while the HAT was found to be +1.21 m in reference to MSL. These relevant vertical references are depicted in Figure 3.5.

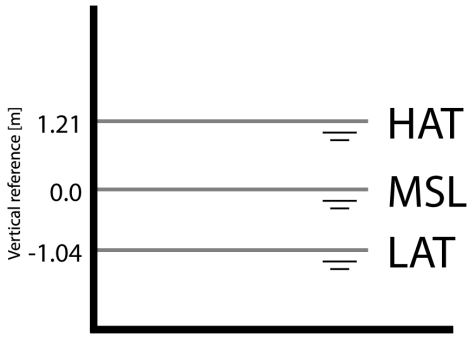

Figure 3.5: Vertical references compared to MSL

3.5. Bathymetry

The bathymetry of the area can be seen in the Figure 3.6, which is acquired by using Global Mapper and bathymetry data.The location of the port is marked by a red frame.

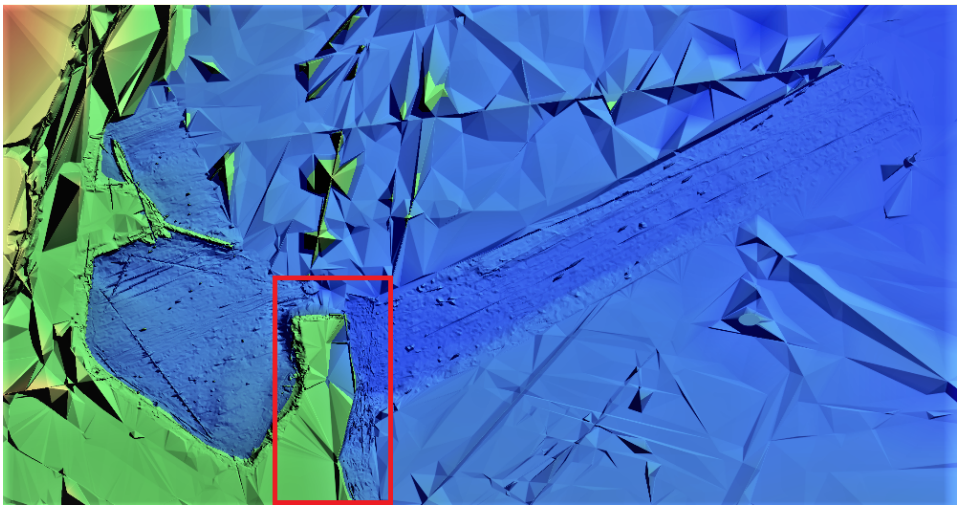

Figure 3.6: The port bathymetry and port location

The location of the navigation channel and the manoeuvring basin can be seen fairly clearly in this figure, indicated by the darker blue color due to the increased depth.
In Appendix B, a technical drawing of the bathymetry including measurements is given, (compared to lowest water level LAT).

According to the port authorities the normal depth of the navigation channel is 8.4 meters measured from MSL, while the average depth in the port is 9.1 meters.

3.6. Soil

3.6.1. Quays

The first layer of soil of the existing quay wall at Sitio 1 consists of artificially placed sand until a depth of 16.6 m. The density of this layer varies over depth and can only be determined by field measurements. As these could not be performed, the soil weight of this layer is assumed the same over depth as defined in Table 3.6. This number is also used for for this layer in the design to rebuild the quay after the 2010 earthquake as performed by the company GEOFUN.
The layer below reaches until -22.6 - just below the bottom of the deepest point of the structure - and its characteristics are based on classification by the of Swiss Road and Engineers and the outcome of a Standard Penetration Test (SPT) (see Figure E.2) performed while building the quay. Terzaghi and Peck defined in 1948 a relationship between the SPT N-value and the relative density. This layer is packed medium-dense. The US

Army Corp of Engineers 1994 related the SPT N-value to a value for the bulk density. Using this relation, the weight of the layer is estimated at 20 kN/m^3. Soil characteristics are summarized in Table 3.6.

Besides the SPT test, also the California Bearing Ratio (CBR) was measured and the soil is classified according to the Unified Soil Classification System (USCS) in the lab, assessing 15 samples taken along Sitio 1. The results are summarized in Table E.1. Though relating CBR test results to the Young's modulus is often not accurate as described by Stevens in 1984, it is possible based on empirical relations. W.D. Powel formulated the Equation 3.1 in 1984, which is used to determine the Young's modulus of the soil at Sitio 1.

$$E_y = 17.6 * CBR^{0.64} \tag{3.1}$$

The exact location of the samples is unknown. The CBR results also have a large standard deviation. For the PLAXIS model used later in this report a single value for the Young's modulus is used, which is the mean value of the CBR results, not taking into account sample number 4 as this result was inacurate due to the presence of solid coal in the soil. The Young's modulus for the natural soil in Sitio 1 is not determined by lab tests and is therefore estimated. This value is assumed to be the same as the Young's modulus for the artificial sand layer, since the densities of these soils are similar.

There is a relation between the Young's modulus and the shear modulus of a soil, as described by Verruijt as Equation 3.2. The shear moduli found are stated in Table 3.7.

$$G = \frac{E}{2(1+\upsilon)} \tag{3.2}$$

All relevant soil characteristics are summarized in Table 3.7. The void and Poisson ratios are not determined by lab tests but are estimated at commonly used values based on experience as described by Verruijt. The cohesion of the considered soils is assumed to be zero as all layers are mainly sand.
Unfortunately there is no soil data available for Sitio 2 and Maria Isabel. In the final design, the same artificial soil will be used for construction which is present in Sitio 1, assuming the same in-situ conditions.
The soil at the bottom of the manoeuvring area and the navigation channel is also of importance, due to the needed dredging. The results of a sieving test with samples taken along the channel are given in Appendix E (the exact locations of these samples are unknown). The results indicate that the soil consists of normal sand, muddy sand (arena fangosa) and fine sand (arena fina).

Depth [m]	**Description**	**Weight** [kN/m^3]
+2.8 until +1.5	Artificial soil, unsaturated	18.64
+1.5 until -16.6	Artificial soil, saturated	20.20
-16.6 until -22.6	Natural soil, medium-dense, saturated	20

Table 3.6: Soil layer definition at Sitio 1

Characteristic	**Natural**	**Artificial**	**Unit**
γ_{dry}	18.5	18.64	kN/m^3
γ_{sat}	20	20.20	kN/m^3
e	0.7	0.5	-
E	229	229	MPa
υ	0.3	0.3	-
G	88	88	MPa
c	0	0	-
ϕ	30	30	deg
ψ	10	10	deg

Table 3.7: Soil particulars at different locations in the port.

3.6.2. Navigation Channel

In the navigation channel, 12 soil samples have been taken at different locations. It is unknown at what exact locations these soil samples have been taken. Sieve tests have been performed in order to be able to

characterize the soil. From these sieve tests, a grain diagram can be computed. In Figure 3.7 below, the results for the most two extreme sieve tests are shown. The summary of all soil sieve tests can also be found in Appendix E.

Figure 3.7: Sieve test results

Sieve Test 1A
The result from sieve test 1A is that the soil is uniformly divided, since the curve is steep [70]. The value of d_{50} is calculated to be 0.23 mm by interpolation, which is classified as a fine sand [69]. Fine sand with a diameter of 0.23 mm has a maximum internal angle of friction of 35 degrees [69].

Sieve Test 3B
The result from sieve test 3B is that the soil contains particles of strongly different grain sizes. This is because the curve of the soil is fairly flat [70], as can be seen in Figure 3.7. The value of d_{50} is calculated to be below 0.063 mm, as can be seen in Figure 3.7 since 52 % of the mass passes the 0.063 mm filter. This is classified as clay or silt [69].

Conclusion soil properties navigation channel
The conclusion of the soil characteristics is that the soil in the navigation channel is classified as fine sand. Based on the average properties mentioned in section 3.6.2 fine sand corresponds best with the test results. This soil is assumed to also be present in the manoeuvring area. The characteristics of the soil used for calculations are summed up in Table 3.8.
It is important to mention that if the actual soil is different at particular spots in the navigation channel, more sediment transport might occur and it might be more difficult to dredge.

Classified soil	d_50 $[mm]$	**Gradation**	ϕ_{max} $[degrees]$
Fine sand	0.23	uniform	35

Table 3.8: Soil properties navigation channel and manoeuvring area

3.7. Seismic activity

Along the coast of Chile and Peru lies a long fault line which is responsible for numerous earthquake in Chile, Argentina and Peru. The Peru-Chile trench is subducted by the South American plate. The trench has a length of 4500 km and reaches depths of up to 8000 m. The pressure build-up pushes the Andes upwards and sudden pressure releases cause a lot of seismic activity in this area. For the design of the port earthquakes and tsunamis are taken into account as environmental conditions.

3.7.1. Earthquakes

Some of the earthquakes that struck Chile are among the greatest ever measured. For this reason it is common practise to use construction codes especially for building in earthquake sensitive areas. Kulikov, Rabinovich and Thomson analyzed historical data and determined the return period for earthquake which caused tsunamis [19]. Table 3.9 shows the magnitude of the earthquakes for certain return periods measured in a period from 1901 to 2003.

Return period [$years$]	2	5	10	20	50	100	200
Magnitude [M]	7.30	7.83	8.10	8.31	8.52	8.64	8.73

Table 3.9: Magnitudes (moment magnitude scale) of tsunamigenic earthquakes per return period [19]

3.7.2. Tsunamis

As the Peru-Chile trench is location under the ocean most of the earthquakes causes tsunamis that have landed on all coastlines along the Pacific Ocean. In Chile especially the 2010 tsunami caused a lot of damage in the Concepcion Bay. Also, before this event many tsunamis have troubled the Chilean coastal region. Lagos has divided all tsunamis from 1562 till 2000 in five magnitudes according the scale of Monge [38], [45]. According to this study the return period of a tsunami of at least magnitude 1 is 9.9 years. A magnitude 1 tsunami will have a wave height of 2-5 m and a maximum inundation or run-up height of 2-3 m. Such a tsunami will cause damage to houses and boats. As the quay height is high enough to not to be topped by a magnitude 0 tsunamis during high tide these have not been taken into this frequency of occurrence. The return period of tsunamis in the Concepcion Bay is obviously longer as not all tsunamis will hit the coast in this bay, but due to a lack of data this value will be used in this report.
The source of tsunamis can be determining for its consequences. Tsunamis coming from great distances can usually be detected a long time before it hits land. This will give people time to evacuate and get to higher ground. Tsunamis which have been generated by an epicenter nearby may cause much more damage as the warning can only be given less than an hour in advance [19]. This results often in more casualties and damage. Also for the port the evacuation time is important to allow its vessels to sail to safety.

II

Preliminary Design

4

Potential Scenarios

In this chapter, different expansion scenarios are defined and assessed. For these four scenarios a preliminary design is made. This provided enough information to determine which scenario will be the most suitable for the port. A Multi-Criteria Analysis (MCA) is performed to evaluate and compare the scenarios. In Part III of this report one of the scenario is worked out in a more detailed design.

4.1. Method

In this chapter, four potential future scenarios for the port of Talcahuano are defined. Both technical aspects and economic aspects are compared for each scenario. The PIANC: Harbour Approach Channels Design Guidelines are used in the preliminary design of the scenarios [53]. However, the port standards regarding Channel Design differ from the PIANC guidelines on a lot of aspects. Compared to the port´s standards the PIANC guidelines can be seen as conservative as the PIANC guidelines prescribe larger safety margins. It is decided to present the scenarios as a midway between the port´s standards and the PIANC guidelines. Based on discussions with the port authorities regarding this subject this design choice is applied consistently to all scenarios.
After the preliminary designs for the scenarios are made a MCA is performed. To determine which scenario is the most suitable for the port of Talcahuano all designs are evaluated on five criteria, namely: dredging costs, construction costs, costs due to loss of revenue during construction, potential market value and environmental impact. For each of the criteria a score is given which is multiplied by a weighing factor. The weighing factors have been determined based on the importance of the criterion and have been discussed with the port operator. More information concerning the criteria and weighing factors is given in Appendix F in Section F.1

4.2. Scenarios

The scenarios are presented in this section, but first general remarks concerning the dimensions, scenario layouts and structure type are given as these apply to all scenarios.

4.2.1. General considerations

The considerations which influenced each scenario equally are discussed in this section. All preliminary designs comply with the boundary conditions specified below.

- The port should be able to process two bulk carriers, with a capacity of 35.000 $tons$ each, simultaneously. The length of such a bulk carrier is 180 m. The chosen design vessel is the SPL Tarapaca. It´s characteristics are summarized in Table 4.1.
- Following the port´s standards, the bow of a moored vessel is allowed to reach further than the quay wall for a maximum of 25% of the vessel length, meaning a minimum of 135 meter quay length is needed for mooring one design vessel.
- The distance between two vessels berthing at the same quay must be at least 25 m. This distance is determined by the port authorities and is based on experience.

- The diameter of the turning basin is two times the vessel's maximum length, 360 m [53]. This turning basin is considered in order to obtain a safe area for the vessels to turn and manoeuvre to the berths.
- In all scenarios the navigation channel, manoeuvring area and quayside are dredged up to 10.6 m below LAT, allowing for a draught of 10 m and an under keel clearance (UKC) of 0.6 m. The latter figure is determined by the port authorities and is based on experience. It allows for the design vessel to enter or exit the port without a tidal window.
- The width of the navigation channel is 100 meters.

Characteristic	Value	Unit
Length	180	m
Width	30	m
Draugth	10	m
Deadweight	34431	$tons$

Table 4.1: Characteristics of the design vessel "SPL Tarapaca".

In each scenario the following assumption is made.

- If one long quay is realized accommodating to two design vessels, this requires a length of 135 + 25 + 180 = 340 m. Hereby it is assumed that only one of these vessels is able to have its bow reaching out for 25%.

Apart from the items just mentioned also some design choices for the scenario layouts and the structure type are made. These will be explained below.

Scenario layouts
The scenarios are depicted in Figures 4.1-4.4. In each figure the current quays are displayed in blue. The red lines represent the current navigation channel and manoeuvring area. The proposed new quay is highlighted in green and the expansion of the navigation channel is highlighted in red. Finally, in gray, a turning basin is indicated. Within this basin the depth is sufficient for the maximum draught of the design vessel. The location of this turning basin is determined in the situation where two vessels are berthed. In the new situation, the manoeuvring area needs to be expanded from the red lines to the area highlighted in red.

Since it is not known which guidelines the port utilizes for dimensioning its manoeuvring area, it is decided to utilize the PIANC guidelines to compare the scenarios and proceed with the MCA.

Structure type
The use of caissons for jetties and quay walls is generally more expensive than open structure types [67]. Furthermore, a production of 3-5 running meters per week is expected when building gravity wall structures such as caissons [67]. When building open-piled quay walls a production of 12 running meters per week can be expected [18]. Thus, the production time of open-structure quay walls is shorter than for caisson-type quay walls. Longer construction time also has a big impact on the economics as there is more loss of revenue during construction due to possible downtime of the existing quays. For these reasons, it is decided that a caisson structure quay wall is not an economically viable option. A pile-supported solution is the most economically advantageous, dispenses underwater work, [preliminary] dredging [of the foundation soil], less equipment and therefore lower costs with mobilization and preparatory work [18]. Also, open-structure quays are already present in the port and also commonly used in similar ports. Open-structure quay walls is the preferred structure type. Since caissons will not be used, the jetty will be founded on piles, which is also common in the region.

4.2.2. Scenario 1: Extension Sitio 1 North

A layout of Scenario 1 can be seen in Figure 4.1. An extension of 180 m to the North for the berthing place is suggested. The planned extension (given by the green rectangle) is a jetty founded on piles, with a width of 40 meters and berthing on one side. The height of the jetty above MSL will be the same as the existing quay wall height at Sitio 1 and is 2.36 m. It is clear to see that a large area of the new manoeuvring are is located on the north side which is less shallow than the south side. Installation can be done by waterborne construction or step by step from land.

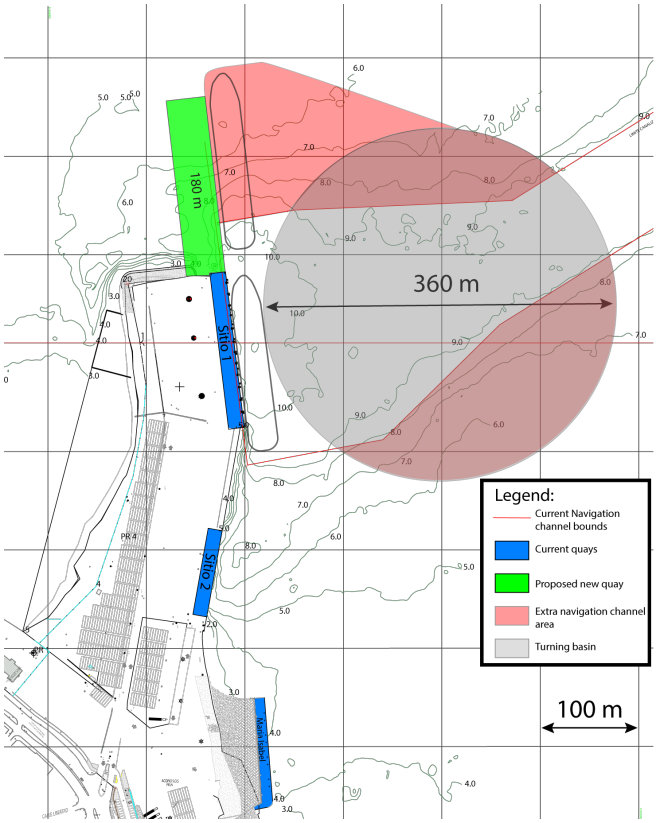

Figure 4.1: Scenario 1

4.2.3. Scenario 2: Extension Sitio 1 North and South

A layout of Scenario 2 can be seen in Figure 4.2. An extension of 90 m (width of 40 m) to the South and 90 m to the north of Sitio 1 is suggested. The extension can either be a closed or open berth structure. Due to lower costs and the shielded location, it is preferred to use an open berth quay. The height of the new quay above MSL will be the same as the existing quay height at Sitio 1 and is 2.36 m. Sitio 1 will have to be closed partly on either side or even closed entirely during construction of this scenario. The south quay wall of the expansion to the south can also function as an expansion of Sitio 2 to be used for fishery. As depicted in the figure, the navigation channel will have to be expanded on both the north and the south side of the current navigation channel.

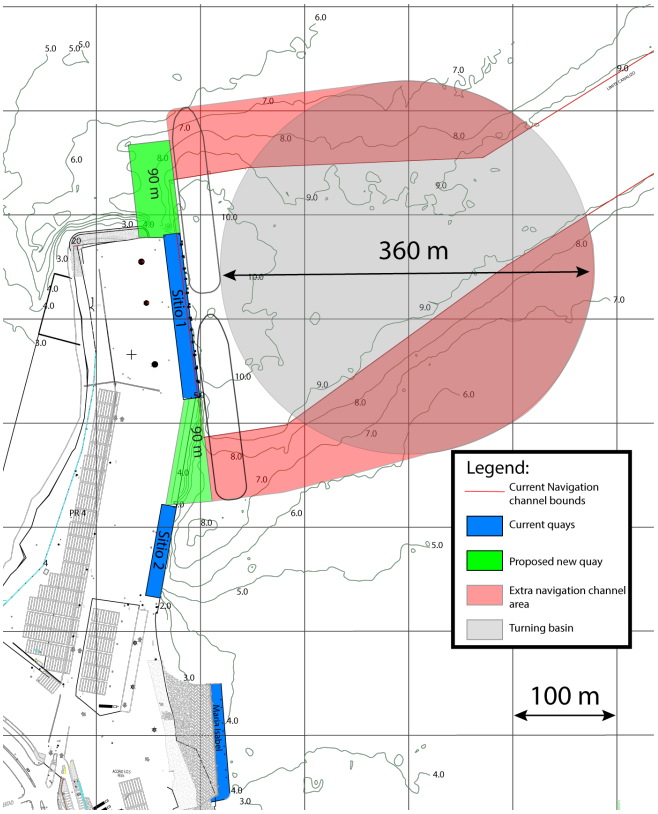

Figure 4.2: Scenario 2

4.2.4. Scenario 3: A Jetty

A layout of Scenario 3 can be seen in Figure 4.3. An extension of 180 m in the direction of the maneuvering area is proposed. The extension (green) is a jetty founded on piles, with a berth on the southern side. To prevent blockage of the navigation channel the jetty is translated 50 meters north. This also allows the original commercial berth to be used. The length of this original berth will become 210 meter. The width is estimated at 40 m. The height of the jetty above MSL will be the same as the existing quay height at Sitio 1 and is 2.36 m. Installation can be done by waterborne construction or step by step from land.

It should be mentioned that the jetty is vulnerable for tsunami impact. If a tsunami occurs it will attack from the north as it has to enter the Concepcion bay there. This will result in maximum hydrodynamic load due to the orientation of the jetty being almost perpendicular to the tsunami direction.

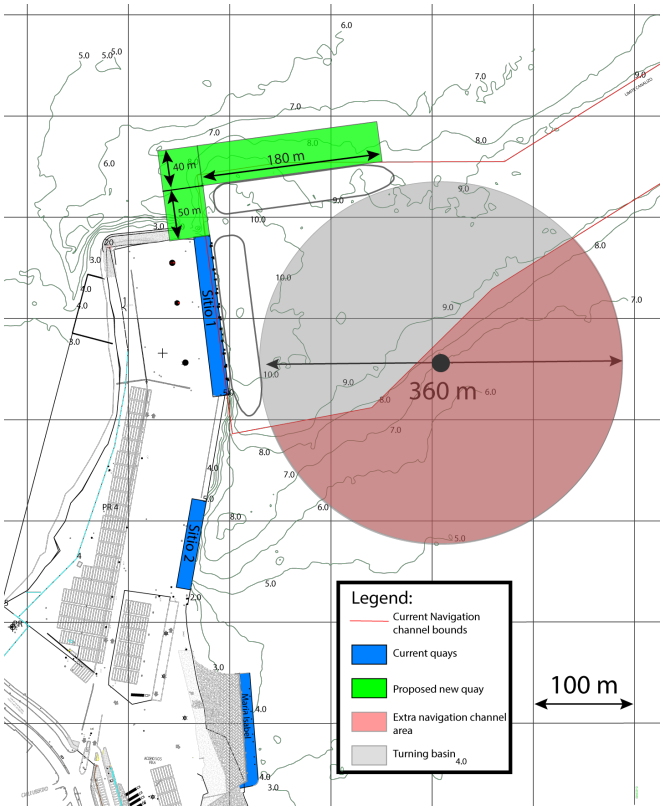

Figure 4.3: Scenario 3

Also, the center of the turning basin as seen in Figure 4.3 must be in a direct line with the middle of the entrance channel, which is not the case in this scenario.
Thus far it is not clear which guidelines exist for the dimensions of the port maneuvering area. However, from the existing maneuvering area it can be derived that from the quay it has a rectangular shape extending from 50 meters north of Sitio 1 to 50 meters south of Sitio 1.

4.2.5. Scenario 4: Connecting Sitio 1 and Maria Isabel

A layout of Scenario 4 can be seen in Figure 4.4. The quay at Sitio 1 will be extended to the south all the way to the most southern existing quay. This extended length is 240 m. The extension can either be a closed or open berth structure. Due to lower costs and the shielded location, it is preferred to use an open berth quay. The height of the new quay above MSL will be the same as the existing quay height at Sitio 1 and is 2.36 m. The length of the total quay becomes 400 m which allows for a lot of flexibility in terms of berthing spaces. There is a lot of dredging to be done as the large part of the dredging area is in the south part.

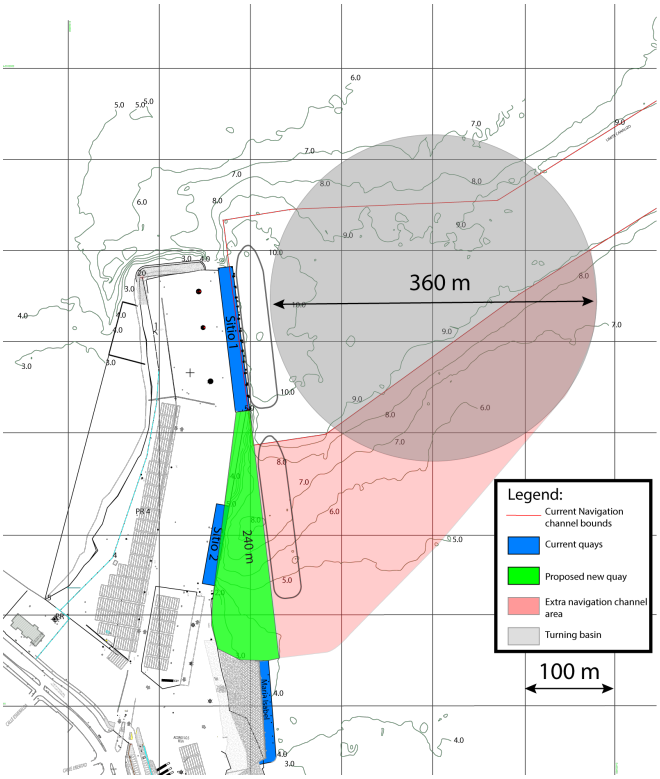

Figure 4.4: Scenario 4

4.3. Multi-Criteria Analysis

In this section the costs will be discussed briefly and the advantages and disadvantages of the scenarios are given. For information about the scores of the scenarios Section F.2 can be consulted. Also the result and conclusion of the MCA is provided here.

The costs of dredging and construction make up most of the budget. As these are investments to be made before any revenue is collected from the expansion each investment is a risk. The total investment should therefore be minimized in order to reduce the costs of capital.

Table 4.3 shows the final result of the MCA. Besides this relative comparison, the estimated costs are given in Table 4.2. For the first three criteria, which are based on costs, 1 weighted point equals approximately 500,000 USD in monetary value. Note that the transportation cost for the dredger are significant but not taken into account in these numbers. The MCA shows that Scenario 4 is most favourable. Though, the results for Scenario 1, 2 and 4 are close. Scenario 4 is particularly favourable thanks to the minimal loss of revenue during construction and the big future market potential with the long new quay wall. The higher investment needed for this scenario (due to the high dredging and high construction costs, see table 4.2), results in this option not being miles ahead of the other three. The pay-off after the initial investment however, is expected to be much larger than of the other options, while also being more future proof, leading it to fit better in the proposed 30 year plan.

Criteria	Scenario 1	Scenario 2	Scenario 3	Scenario 4
Dredging costs	3,900,920	3,795,553	4,025,432	4,305,699
Construction costs	4,153,599	4,224,399	6,230,399	5,711,199
Loss of revenue during construction	877,359	893,306	1,233,093	526,646
Total	8,931,879	8,913,259	11,488,925	10,543,545

Table 4.2: Dredging and construction cost and loss of revenue during construction in *USD*. Note: transportation cost for the dredging vessel are significant and not taken into account in these numbers.

Scenario 1 loses quite some points on because of its lack in potential market value. The quay wall is shorter and the ability to use the extension for a second berth on the other side misses. The same problems are relevant for Scenario 2. The good score of these two scenarios is mostly due to the low dredging costs, due to the relatively great current depth, and the low construction costs because the extension are small.

	Criteria	Weight factors	Scenario 1		Scenario 2		Scenario 3		Scenario 4	
			UW	W	UW	W	UW	W	UW	W
1	Dredging costs	0.10	7.93	0.79	10.0	1.00	5.49	0.55	0.00	0.00
2	Construction costs	0.35	10.0	3.50	9.66	3.38	0.00	0.00	2.50	0.88
3	Loss of revenue	0.15	5.04	0.76	4.81	0.72	0.00	0.00	10.0	1.50
4	Potential market value	0.35	0.00	0.00	0.33	0.11	4.55	1.59	10.0	3.50
5	Environmental impact	0.05	7.00	0.35	10.0	0.50	0.00	0.00	4.00	0.20
	Total	1.00		5.40		5.72		2.14		6.08

Table 4.3: Multi-Criteria Analysis results, both weighted (W) and unweighted (UW).

From Table 4.3 it can be concluded that Scenario 4 is the most suitable design for the port expansion. As discussed with the port operators the fourth scenario fulfills all requirements and provides the largest potential revenue. It is therefore decided to work out Scenario 4 in detail for the final design.

III

Final Design

5

Port layout

In this chapter, the new port lay out is discussed. In the new situation Sitio 2 will no longer exist. Maria Isabel will remain. A new quay of 240 m is chosen as an extension of Sitio 1 to the south. This new quay will be called "Nieuw Delft" for the remainder of this report. The total length of the new quay wall (Sitio 1 and Nieuw Delft) will be 400 m. As a minimum length of 340 m is needed for two design vessels to berth, this quay wall provides sufficient space.

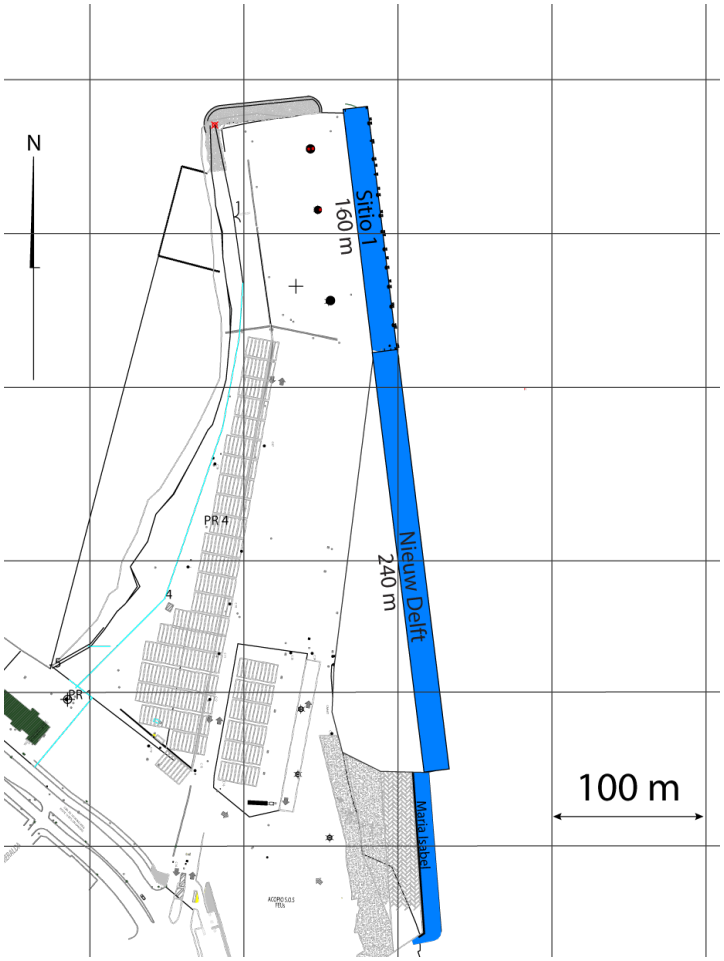

Figure 5.1: Port layout

The fact that one long quay is created also provides other advantages for the port:

- The long quay provides space for a larger amount of smaller vessels.
- The quay can even provide space for a larger vessel than the design vessel given it does not exceed the maximum draught and given the manoeuvring area dimensions are sufficient for this vessel to berth.

Sitio 1 and Maria Isabel are not perfectly aligned and Nieuw Delft is chosen to have the same alignment as Sitio 1. This means the south part of Nieuw Delft will stick out a total of 13.4 m from Maria Isabel. The total amount of land area that is created in the new situation is 12,000 m^2. An area of 25 m wide along Nieuw Delft is appointed as apron area[39]. This means that a total area of $6*10^3 m^2$ of this newly created area can be used for storage and handling of cargo.

The navigation channel will remain in the same position, but the manoeuvring area will be expanded. This will be elaborated on in Chapter 7.
This new port layout allows the port of Talcahuano to increase their throughput and play an important role within the market of the eighth region.

6

Quay Design

240 meters of new quay will be built in the proposed design. The basis of design for the new quay, which is called "Nieuw Delft", is defined in Section 6.1, as well as the design method. Then, the applicability of the main structure types is discussed. To dimension the structure, 2D finite element software PLAXIS is used. After this, it is checked whether the design is safe for several failure modes, which are discussed in Section 6.5. These failure modes are assessed for Nieuw Delft, but also for the existing quay at Sitio 1, as here the water depth will be increased. It is investigated whether this leads to instability of the quay.

6.1. Nieuw Delft: basis of design

The design approach, scope lists of boundary conditions and requirements are formulated for the design of Nieuw Delft.

6.1.1. Design approach and scope

As all environmental conditions are determined in Chapter 3, the design starts with the definition of a list of requirements and boundary conditions the design should comply with. Potential structure types are assessed by literature study. A choice is made on the structure type and the structure is modelled in PLAXIS using 2D finite element theory. The model results give insight in the soil-structure interaction and force distribution. Two load cases are defined to act on the structure. Then, the system is assessed for five main failure mechanisms:

- Sheet pile failure
- Anchor material failure
- Global failure of the entire system
- Failure due to heave and piping
- Failure due to scour

Besides assessment of these mechanisms, the design caps the following:

- Fender and mooring bollard design
- Reinforced concrete floor and qualitative foundation design

The following matters, although relevant, are not taken into account due to the limited project time. Some of these matters are touched upon in Chapter 14 as recommendations.

- Maintenance plan
- Detailed quay equipment such as lighting, drainage and signage
- Safety equipment

- Foundation pile dimensioning and design checks
- Bottom protection design at the quay

Generally, the design is made according to the notes Structures in Hydraulic Engineering by de Gijt, published in 2004. Additional references are consulted along the design procedure which are mentioned when discussed. The calculation procedure is only briefly discussed in this chapter. Additional information is provided in Appendix H. The main findings of the quay design analysis are discussed in this chapter.

6.1.2. Boundary conditions

The boundary conditions are listed here.

- The environmental conditions which the structure has to endure are described in Chapter 3
  - Wave impact plays no significant role in the design.
  - Soil characteristics are stated in Table 3.6
  - Earthquake and tsunami impact should be considered
- Rubble from a quay which collapsed during the 2010 earthquake is an obstacle which needs to be removed before construction

6.1.3. List of requirements

The requirements for the design of Nieuw Delft are as below.

- Dimensional requirements
  - In total a new area of 12,000 m^2 is created in the port by landfill.
  - The newly created surface and the quay height at the waterside levels at 3.94 m above LAT, being the same height as the existing quay at Sitio 1. The exact height of landfill can be calculated using bathymetry data.
  - The new quay to be built is 240 m in length. Together with the existing quay at Sitio 1 this creates a total quay length of 400 m (Maria Isabel excluded).
- Nautical requirements
  - The quay must enable berthing of two design vessels simultaneously. The design vessel particulars are stated in Table 4.1.
  - The two design vessels should be able to stay berthed independent of the tide.
- Bearing requirements
  - The width of the apron area is 25 m following the minimum of the PIANC guidelines.
  - Not taking into account the apron area, the newly created storage area is 6,000 m^2.
  - Mainly bulk will be transferred at the quay.
- Retaining requirements
  - As the required under-keel clearance (UKC) is 0.6 m, the required minimum water depth is 10.6 m based on the design vessel. An additional depth of 0.3 m is dredged extra to make sure the minimum depth is obtained everywhere.
  - As already mentioned, the height of the new quay surface is 3.96 m above LAT.
- Protective requirements
  - For mooring facilities, there are mooring bollards and fenders per 12 m, copying the design of Sitio 1.
  - The port bottom soil is fine sand and at certain points muddy.
  - Harbour bottom protection may be applied at the quay wall depending on the eventual design.
  - No bank is present in front of the quay, so no bank protection is needed.

6.1.4. Structure choice

There are different structures that can be chosen in the design of a quay wall. They can be categorized in the following four groups:

- Gravity type structures
- Piled structures
- Sheet pile bulkheads
- Structures on special foundations

Gravity type structures are fairly expensive. They are mostly used when there are regular extreme conditions (wind, waves, heavy ice), or when pile driving is not an option. In Concepcion Bay the conditions are fairly mild and pile driving has already been used in 2012 to construct the current quay at Sitio 1. Therefore the construction of a gravity type structure is not the best option.
Construction of a structure on special foundations is not necessary due to the favourable soil and environmental conditions. Since construction on special foundations is more expensive, this structure type will not be used for construction.
Therefore a choice is made between a sheet pile bulkhead type and a piled structure type. Both can be a closed or an open berth. The use of an open berth is not preferred due to the port being at risk for tsunamis, which would lead large possible damage with this kind of structure. The sudden increase in water level would lead to large uplift forces, which in turn will also give a large momentum in the attachment point between the open part of the structure and the current existing quay which it will be an extension of. These forces can lead to large failure of the structure, making it entirely unusable after a tsunami. The plan of the port being a 30 year plan, and another large tsunami expected in about 20 years, means making the impact of a tsunami as small as possible, is a large part of the design. Therefore the chosen structure type is a closed quay structure with a sheet pile, comparable with the one that is currently present at Sitio 1. This can either be a structure with a relieving floor and a front sheet pile wall with anchors, or a sheet pile bulkhead with anchors. Ideally, both structure types should be modelled in PLAXIS to find the optimal design and reduce the cost as much as possible. Though, as time is limited, it is chosen to work out only a sheet pile bulkhead with a single anchor, as shown in Figure 6.1. The advantages of a relieving floor structure are touched upon again in Chapter 14.

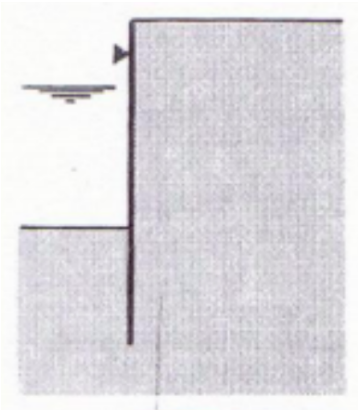

Figure 6.1: A simple drawing of the bulk head with single anchor structure type [12]

6.1.5. Design recommendations based on (tsunami) literature

When designing the structure, the depth of the sheet pile is of importance. The depth will depend either on the needed depth to prevent piping or to prevent failure due to forces/momentum. whichever is dominant.
When piping is dominant, a possible impenetrable bottom protection could help reduce the needed depth. Next to that, the protection would also prevent possible scour, adding to the stability.
When the forces are the dominant factor in determining the depth, the addition of an anchor or a relieving floor to the design would decrease the needed depth. When designing the area for storage etc at the newly added land/above the landfill, it is preferred to use reinforced concrete, considering the impact of the earthquake in 2010 lead to an entire disjointed surface area, which was not usable for vehicles until repaired. Using

reinforcement would greatly decrease the chance of this kind of failure, which would lead to less repair costs and a surface that would still be usable.
Liquefaction induced by earthquakes has shown to have potential devastating influence on seismic performance of anchored quay walls. Therefore, measures to mitigate liquefaction are commonly part of the design of quay walls in seismically active regions. Such mitigation measures are costly. Moreover, these measures are difficult to implement for existing structures in operation [1]. The use of the NCh433 Earthquake Resistant Design of Buildings is consulted for the design of the port expansion in order to resist an earthquake up to certain limits.
An earthquake or tsunami can have devastating impact on the port resulting in high repair cost and loss of revenue due to downtime. Mitigating risks relating this subject should therefore be part of the design. Besides this, a practical evacuation plan can be constructed to minimize the damage and risk to personnel.

6.2. PLAXIS modelling

With the basis of design as discussed above in mind, the design continues with simulating soil-structure interactions in 2D Finite Element software PLAXIS. The model set-up is discussed in Appendix H. Both a single anchor bulkhead structure for Nieuw Delft and the existing quay at Sitio 1 are modelled in PLAXIS. Also, for both quays, two situations with different ground water levels are modelled. Although the soil in the quays is sandy with relatively coarse grains and it can be expected that the water table can follow the tidal movement, there is always an uncertainty on this mechanism. Therefore, the ground water level is modelled at LAT level and at MSL level to assess the effect of additional active pore pressures. The seawater level is assumed at LAT at all times, due to this being the least favorable waterlevel when looking at stability of the structure.

The model has some limitations:

- PLAXIS 2D cannot define two different water levels. Therefore, the variations in ground water levels are defined by setting the dry weight of the soil layer in between the ground water level and the sea water level to the saturated weight. To model the horizontal water pressure, an extra load is added in horizontal direction. This results in slightly conservative results due to an overestimation of the horizontal active forces on the sheet pile in this region.
- Foundation piles for the concrete floor cannot be modelled in PLAXIS 2D. These are therefore left out of the model. Whether or not the concrete is founded on piles doesn't significantly affect the internal forces of the sheet pile wall, as proved in Section H.2.1. Though, loading of these piles does influence the sliding plane [26] and probably also affects the global safety factor (which will be defined later in the report). The global safety factor as reported is therefore only for the situation without piles.

6.3. Load cases

Two load cases are identified which might work on the system, being the operational loading and the earthquake loading. More load cases could be defined, such as impact load of a vessel, though this is not covered in this report.

6.3.1. Operational load case

During normal operations a design vessel is moored at the quay, resulting in fender and mooring bollard forces. These are discussed in Section 6.4.4. Mooring and fender loads are assumed to be transferred to the foundation via the concrete floor to the piles.
The vessel loads its bulk onto trucks on the quay. The weight of these trucks is carried by the concrete floor, which, in its place, transfers the load to the carrying soil directly or via the piles on which the floor is founded. A truck weight of 20 $tons$ is assumed. This can be modelled in PLAXIS by two loads of 10 kN/m, representing the contact point of the truck and the floor in a cross-section if the truck is assumed to have four wheels. These loads work at 5 and 8 meters from the quay waterside. This load might also represent a small temporary crane. How this load case is defined in the model is given in Appendix H.

6.3.2. Earthquake load case

Following the Chilean Standard on Earthquake-Resistant Design of Structures and Facilities (2013), design criteria for earthquakes can be defined. This principle is based on added weight of the active soil wedge due

to earthquake accelerations. A distributed horizontal force representing this added weight can be defined using Equation 6.1, in which C is a seismic coefficient, I is an importance factor, and P is the weight of the active soil wedge.
C depends on multiple factors, like the location of where a structure is built to be built (seismic zone), the kind of structure and the soil type[14]. Based on these factors, the estimated value of our coefficient is taken at 0.23. A more accurate calculation of the seismic coefficient can be done if the natural frequency of the structure is known. Though, this requires a dynamic structural analysis which could not be included in the scope of the project.
The importance factor I is set to 1, based on the structure type and the consequences when failure occurs.
The size of the active soil wedge can be found using the internal friction angle of the soil and the embedded depth. The wedge can be interpreted as a soil body under an angle β, as in Equation 6.2. The wedge can be interpreted as a triangle under an angle β from the toe of the sheet pile, as illustrated in Figure 6.2. From this geometry and the soil properties a weight of the wedge can be calculated and thus the additional horizontal load Q_o can be found. This load is modelled in PLAXIS as a line load, defined per soil layer (due to the variation in weight between the soils).

$$Q_o = CIP \tag{6.1}$$

$$\beta = 45 - 0.5\phi \tag{6.2}$$

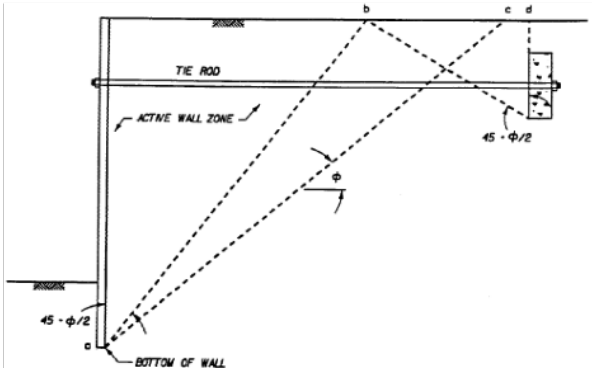

Figure 6.2: The geometry of the active soil wedge used for earthquake load calculation [15].

Besides a force which resulted from accelerations of the soil, also a force is induced by dynamic effects of the sea water. Due to the movement of the structure and the water, suction pressures occur on the sheet pile wall, destabilizing the structure even more. This load F_w can be interpreted by Equation 6.3 [15].

$$F_w = \int_0^H \frac{7}{8} k\gamma_w \sqrt{Hy}\, dy \tag{6.3}$$

in which:

- γ_w = unit weight of water in kN/m^3
- k = seismic coefficient (= C)
- H = height of structure below water surface level in m (in this case the waterdepth)
- y = distance from water surface in downward direction in m

The load is modelled as a point load on the sheet pile wall, working at a distance below the water level of 3/5 times the total water depth. A visualization of both loads is given in Figure 6.3. How these loads are defined in the model is described in Appendix H.

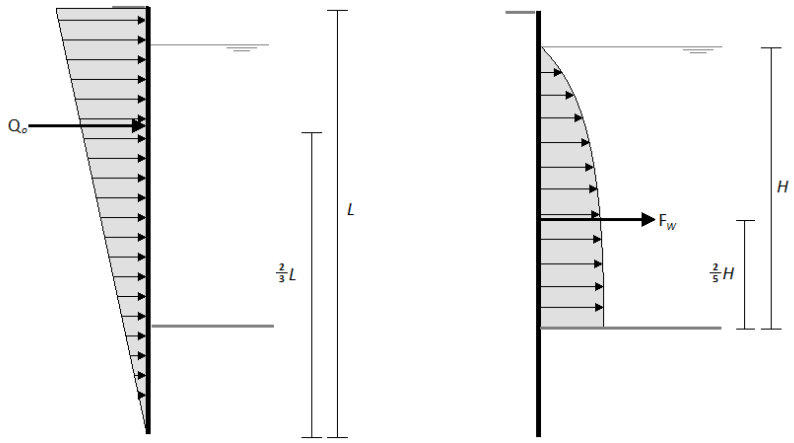

Figure 6.3: The loads on a sheet pile wall due to an earthquake

6.4. Nieuw Delft: dimensioning the structure

There are some important dimensioning decisions to be made for the design of Nieuw Delft. The dimensioning of the structure is based on the operational load case in the most likely situation where the ground water table moves with the tide.

6.4.1. Landfill

Behind the sheet pile wall of the new quay, landfill is needed to level the area. A rough estimation gives that 50.000 m^3 is needed to fill this area with sand. Sand with the characteristics as mentioned in Table 3.7 will be used.

Large earthquakes are likely to cause liquefaction of the soil at the quay, as already mentioned. To reduce excessive pore pressure and the risk of liquefaction, drains are implemented in the soil of the quay.

6.4.2. Sheet pile wall and anchors

For the sheet pile wall to be in equilibrium the embedded depth should be sufficiently large, so that a passive zone of sufficient length can be developed [70]. In case of a very small depth, with a thin passive zone at the toe, the lower end of the wall might be pushed through the soil, with the structure rotating around the anchor point [70]. This failure mechanism is implemented in the PLAXIS software. As will be proven in Section 6.5.4, piping is not a critical factor in determining the embedded depth of the sheet pile. Furthermore, the sheet pile stress capacity is an important criteria for failure. To assess this, a safety factor SF_{SP} is defined as an indicator, its definition is discussed in Section 6.5.1.

The distance of the anchor from the sheet pile wall (the anchor length) should be sufficiently large to enable the necessary passive earth pressure to be developed. In principle, the distance must be so large that the active region of the sheet pile wall and the passive region of the anchor plate do not overlap [70]. This principle is visualised in Figure 6.4. Calculation of this lenght is done in Appendix H.

The design check for the anchors is only based on failure of the anchor rod (deformation of the steel due to excessive tensile stress). An anchor might also fail when the passive soil behind the anchor plate will slide. Although an anchor plate area of 4 m^2 seems sufficient, further assessment of this kind of failure is not performed in this analysis. The definition of the anchor material safety factor SF_{anchor} is given in Section 6.5.2.

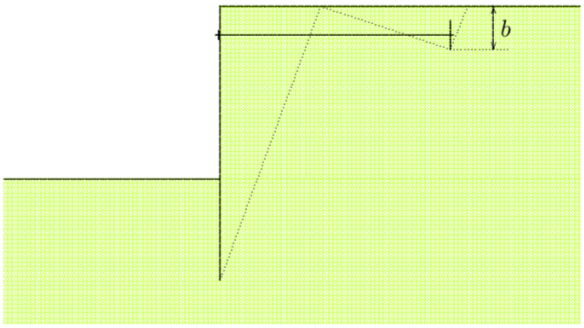

Figure 6.4: The active region of the sheet pile wall and passive region of the anchor must not overlap [70].

The sheet pile wall is chosen to be free in movement at the top. This means the steel is not embedded into the concrete floor. This makes the internal forces in the structure easier to comprehend, but also allows for a displacement of the top which could be significant. The latter is also investigated when determining the anchor depth, as discussed later in this section. The top displacement of the sheet pile wall should not exceed 50 mm under operational loading.
For Nieuw Delft, a hat-type sheet pile wall is chosen as these offer a high bending stiffness, reducing the deformations as much as possible. Each pile of wall has uniform shape and rigidity. Therefore only one type of piling machine is required for installation and the sequential installation in the same direction is possible. This leads to easy installation. Welding can be carried out near the site [46]. The look of the sheet pile wall is shown in Figure 6.5. Initially, a sheet pile is assumed with its particulars as in Table 6.2.

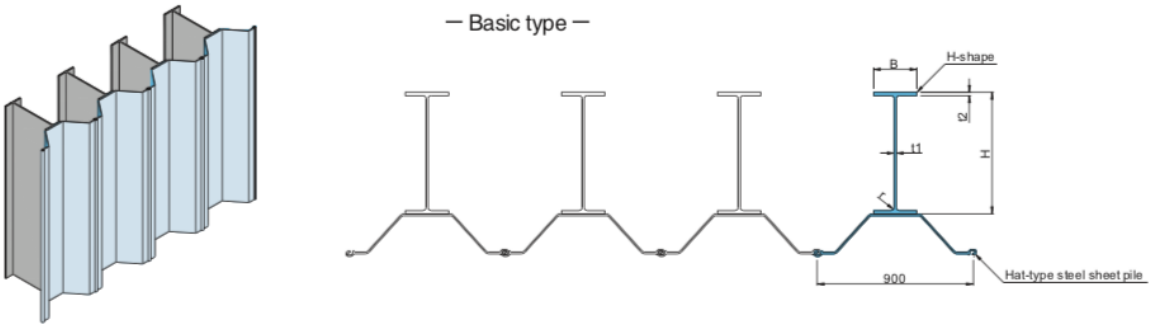

Figure 6.5: The hat-type sheet pile wall [46] chosen for the Nieuw Delft design, its characteristics summarized in Table 6.2

The depth of the anchor below the soil surface should be chosen such that moment is well distributed over the height of the sheet pile. Several runs have been performed with PLAXIS to find the most favourable positioning of the sheet pile and anchors, as well as to define the optimal material properties. This iterative process is visualised in Figure 6.6.

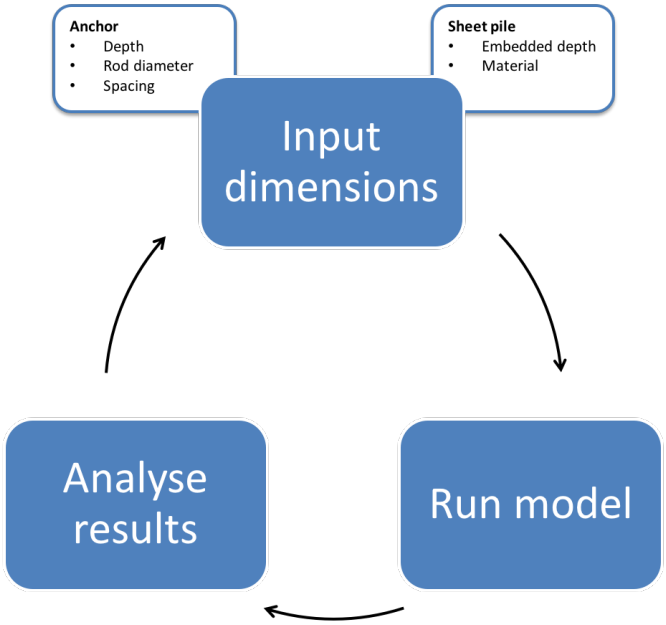

Figure 6.6: Iterative process of finding the optimal dimensions and material properties of the sheet pile and anchors using the PLAXIS 2D models.

The resulting optimal anchor particulars for Sitio 1 and Nieuw Delft are summarized in Table 6.1. An anchor rod diameter of 100 mm is given in this table, which previously was assumed to be 80 mm. The diameter is increased for better performance under earthquake conditions. This is elaborated on in Section 6.5.2.
By further analyzing the results we find that the stress safety factor for the initially assumed sheet pile is rather high. To reduce the amount of steel in the design, and thus the cost, another sheet pile is chosen. The sectional modulus W is reduced by approximately 30% to come to the final sheet pile given in Table 6.2.
Next, in the model, the embedded depth of the sheet pile wall is reduced until failure occurs due to lack of active pressures. An optimal embedded depth of 6.5 m is found, excluding scour. The characteristics of the chosen sheet pile are given in 6.2.
A more elaborate description of this analysis and the route to the conclusions is given in Appendix H.

Parameter	**Sitio 1**	**Nieuw Delft**	**Unit**
Length	36	25	m
Depth	1.2	4.5	m
Anchor plate area	4	4	m^2
Rod diameter	Unknown	100	mm
Spacing	1.26	2.50	m
EA	Unknown	1570	MN
G	200	200	GPa
f_y	Unknown	355	MPa

Table 6.1: Anchor particulars for Sitio 1 and Nieuw Delft

Parameter	Final Nieuw Delft	Unit
Type	Hat-Type NS-SP-10H	-
A	237	cm^2/m
E	200	GPa
I	119100	cm^4/m
W	2970	cm^3/m
f_y	355	MPa
Mass	186	$kg/m/m$
D_{embed}	6.5	m

Table 6.2: The final chosen sheet pile at Nieuw Delft [46].

The new quay features two sheet pile wall corners. In the anchor design, this has to be taken into account. As mentioned before, the anchor length has to be long enough for the passive wedge of the anchor plate and active wedge of the sheet pile not to interfere with one another. However, the anchors themselves should also not interfere with one another. This has to be accounted for in the corners of the structure as well.[22]. This is solved by constructing the corners as visualized in Figure 6.7. Therefore, larger anchor lengths and placement under angles are to be applied in these sections of the structure.

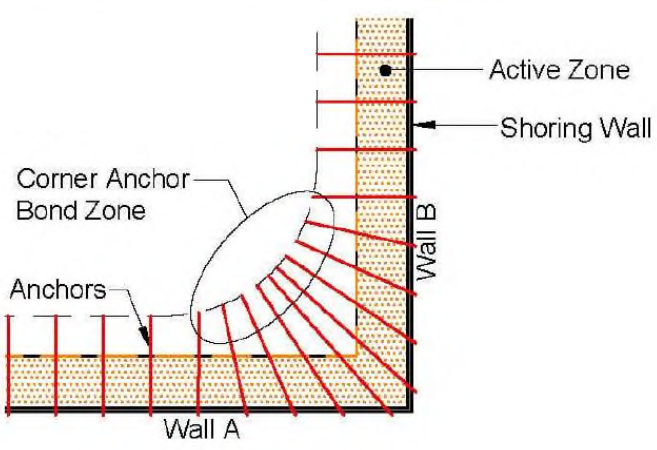

Figure 6.7: Anchor lenghts and placement as implemented in the sheet pile wall corners [22]

6.4.3. Concrete apron floor

Design approach and scope

Next to the fact that a new sheet pile needs to be installed, also a new concrete floor (apron) needs to be constructed and designed. For the apron a reinforced concrete floor will be designed which will be supported by piles. As the new quay is expected to fulfill the same function as Sitio 1, the design of Sitio 1 is used as the basis for the design. The piles are assumed to be 660.4 mm in diameter.

The design scope is to determine the following aspects:

- Dimensions of the reinforced steel bars. A maximum moment and a maximum shear force in the concrete is calculated and used as the governing design factors.

Theory from the books "Toegepaste Mechanica" [31] and "Constructieleer Gewapend Beton" [9] are used as a basis for the design.

Assumptions

The assumptions for the design of the concrete apron floor are as listed below.

- The dimensions of the apron have to fulfill the function of trucks and cranes being able to have enough space. Therefore, the apron of Nieuw Delft will have a length of 240 m and a width of 25 m [39].

- C35/45 type concrete with a thickness of 1160 mm including reinforced concrete will be used. The compression strength is 35 MPa and the tensile strength is 3.21 MPa [21].

- The load case used to assess the strength of the concrete is the operational load case, as used for the sheet pile analysis in section 6.3.

- Concrete with a unit weight of 25 kN/m^3 is used.

Design
In order to be able to determine the dimensions of the concrete floor and the dimensions of the reinforced steel bars, the length between the piles have to be determined. Using the same distances and pile configuration as in Sitio 1, new dimensions for the apron have been determined. This can be seen in Figure 6.8. The highlighted part is used to model a concrete beam in order to be able to determine stresses. The concrete self weight and two points loads from the truck are used in the load case.

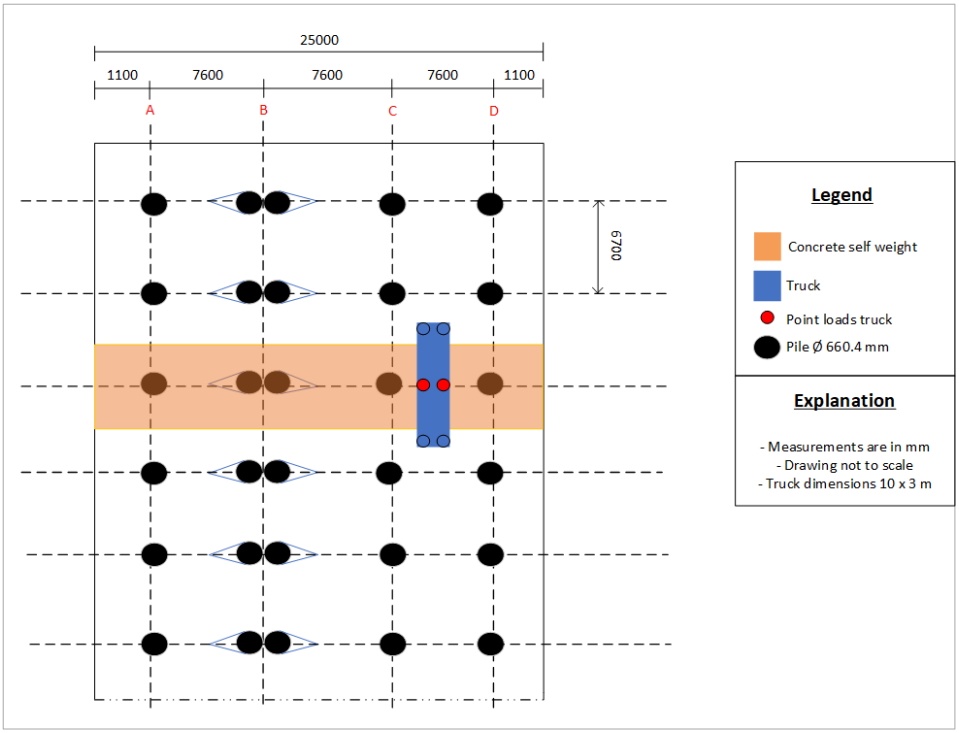

Figure 6.8: Load case description

Loads and model
In this section, the loads in the operational load case are calculated.

- The line load in Figure 6.9 is calculated: q_1 = 25 * 6.7 * 1.16 = 194.3 kN/m

- The point load is calculated: F_1 = 200 / 2 = 100 kN. The truck used for the operational load has a total force of 200 kN.

In order to simplify the situation, the mechanical model seen in Figure 6.9 is used. In this model the apron has been simplified to a beam of concrete with a width of 1.0 m and a height of 1.16 m. Four support points are assumed in the model. The two piles under an angle, which can be seen in Figure 6.8, are assumed to be one support for simplicity.

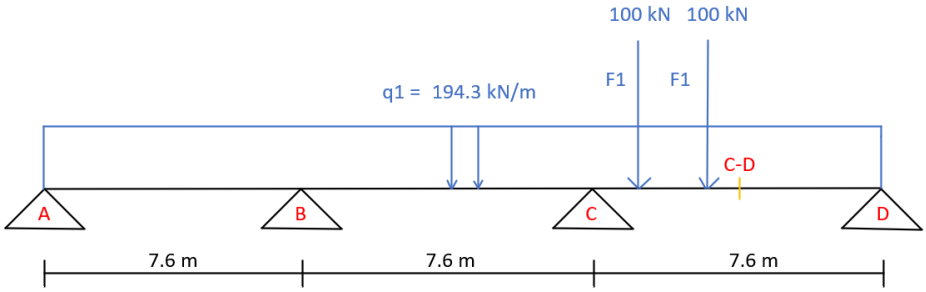

Figure 6.9: Mechanics Model

Next, the maximum moment and maximum shear force in the concrete is calculated.
The maximum moment is calculated to be 1125 kNm and happens at point C-D. The unity check is 0.22 for the concrete section. The maximum shear force is calculated to be 1028 kN and happens on the right side of support C. The moment calculation and shear force calculation is done by hand and can be found in Appendix J.

Reinforcement concrete
Using the maximum moment and the maximum shear force, a concrete design for the apron floor including reinforcement can be made. Main reinforcement is needed for the maximum moment and stirrup reinforcement is needed for the maximum shear force. The design of the concrete apron floor can be seen in Figure 6.10. A full description of the calculation method can be found in Appendix J.

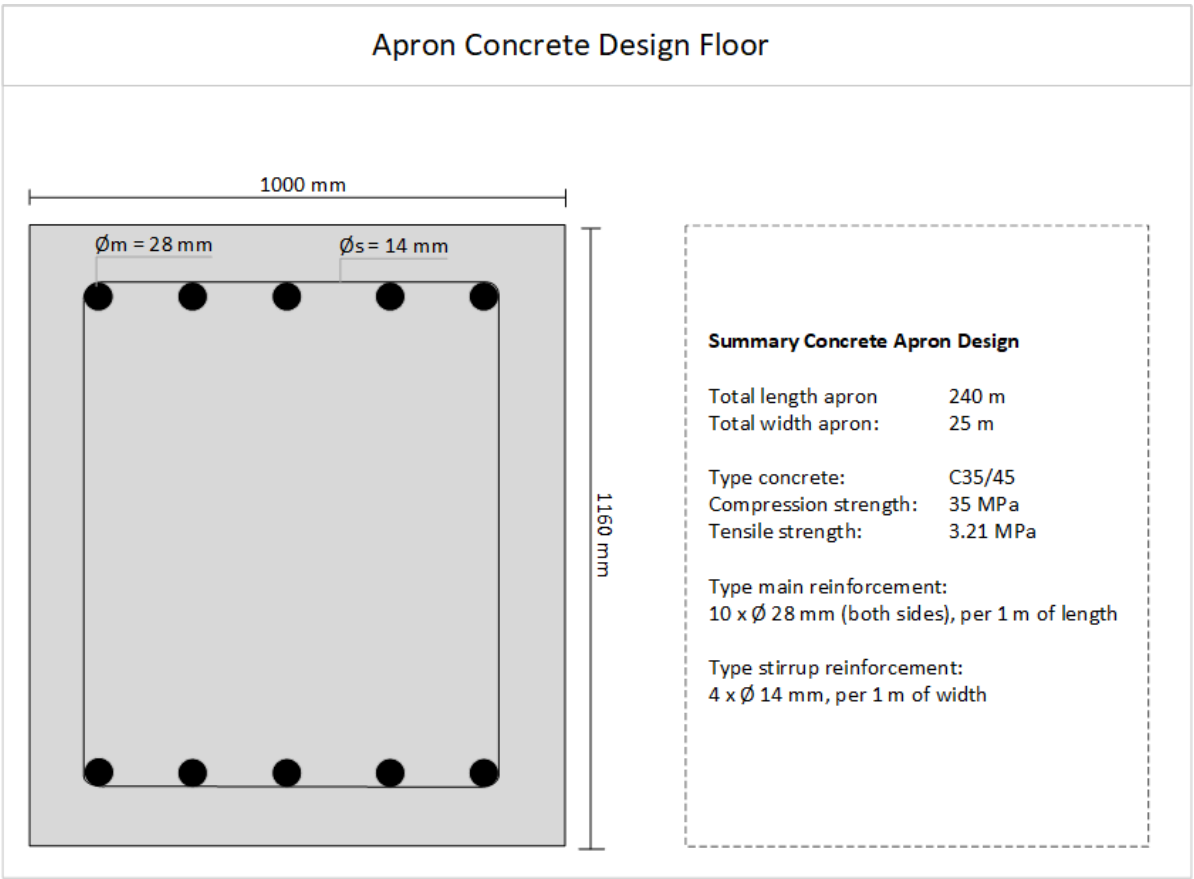

Figure 6.10: Design Concrete Apron Floor

6.4.4. Fenders and mooring bollards

In this section the design of the fenders and mooring bollards is discussed.

Fender Design

For the new quay, fenders have to be installed. These fenders will take up the forces during berthing, so that the berthing of vessels will have no damaging effect on the quay structure. In the design, it is assumed that all the berthing energy is taken up by the fender. This berthing energy is given by [39]:

$$E = \frac{1}{2} * m * v^2 * C_c * C_e * C_m * C_s = \frac{1}{2} * m * v^2 * C_b \tag{6.4}$$

with:

- m = the mass of the vessel [$tons$]
- v = velocity of the vessel [m/s]
- C_b = berthing coefficient (= 0.7)

The mass of the design vessel is 34431 $tons$. The velocity during berthing would at maximum be 0.13 m/s, which would be during difficult conditions in a sheltered area[39]. Using these values, the equation gives a berthing energy of 203.65 kJ = 203.65 kNm.
The fender should be able to absorb this energy entirely, due to it being likely that the vessel will initially only have contact with one fender. Even though this means that the vessel berths with an angle, the contact will be made by the curved part of the hull. It is considered that the fender is compressed parallel [60].

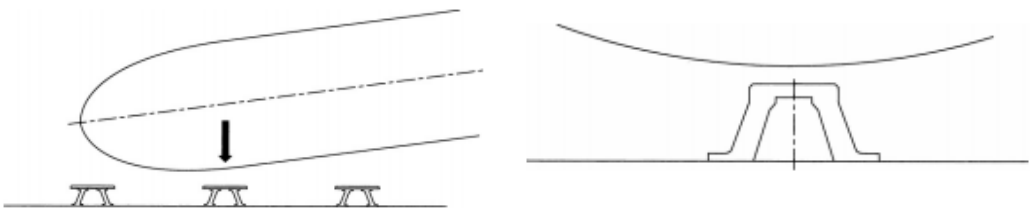

Figure 6.11: (a) A vessel berthing with an angle and (b) a close up at the contact between fender and vessel [60]

The length of the current fenders in Sitio 1 are 900 mm. This means that the ones in the newly designed berth should be equally long, if possible, to eventually create one long quay.
For the new quay, the fenders of Max Groups will be used. Since the kind of fender used in Sitio 1 is a cone fender with a fender plate, it is preferred to also use this kind of fender at the new quay. The cone fender with a length of 900 mm is CO900 (see Figure 6.12a). A fender type with enough absorption is the FO type. With this fender type, the maximum absorb-able energy is 312 kJ [60]. This means that berthing energy for vessels up to 52700 tonnes can be absorbed. The fender type statistics are given in Table 6.3.

Parameter	Value [mm]
H	900
øU	765
øS	585
h	41

Table 6.3: CO900 fender dimensions

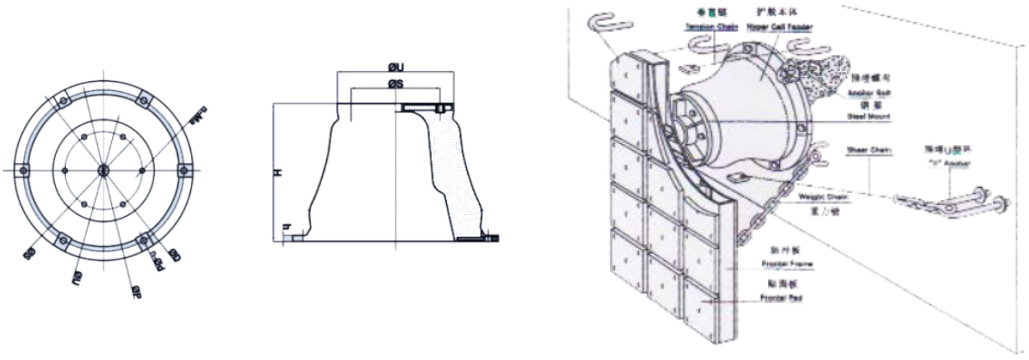

Figure 6.12: (a) The CO900 fender design and (b) the fender and fender plate [29]

This fender has a maximum reaction force of 648 kN [29]. The hull of the vessel should be able to withstand this reaction force. The allowable force on the hull differs per vessel type and size. Since for General Cargo vessels the acceptable pressure on the hull is between 300 and 600 kN/m^2 [30], a value of 300 kN/m^2 is chosen. Although the design vessel is fairly large, it is a conservative choice.

The force of the fender is transferred to the vessel via fender plate (see figure 6.12b). The size of this plate can be determined using the following formula [30]:

$$P = \frac{\sum R}{A_1 * B_1} \leq P_p \tag{6.5}$$

With a value for P_p chosen, the minimal area for the fender plate ($A_1 * B_1$) can be determined. This comes down to 648/300 = 2.16 m^2. The fender plates at Sitio 1 are approximately 2.00 x 1.50 = 3.00 m^2. This means that these plate sizes are still sufficient. Therefore it is chosen to install the same kind of plates at Nieuw Delft, due to it being sufficient and also taking into account aesthetics, making both Sitio 1 and the new quay look like one component.

The distance between the fenders has to be below a certain value to be sufficient for a certain vessel size. The maximum space between the fenders (given as $2l$) can determined by the following equation:

$$2l \leq h\sqrt{\frac{1}{2}B + \frac{L^2}{8B} - h} \tag{6.6}$$

For the design vessel, this maximum distance comes down to 34 m. Currently, the space between fenders is 12 m. Due to smaller vessels needing a smaller distance $2l$, at the Nieuw Delft quay a distance of 12 m will also be implemented, making it possible for the port to still receive their current vessel sizes, also at the new quay.

Mooring Bollard

When moored, the vessel will attach its mooring lines to bollards, to keep the vessel in its place while berthed at the quay. Due to this, mooring forces will be exerted on the bollard via the mooring lines. These forces are determined by currents, waves and wind at the port.

It is of importance that the bollards are strong enough to take the line forces that are exerted on them. Otherwise, the bollard will fail and might damage the quay structure. The EAU guidelines (2004) relate a vessels deadweight to the horizontal component of the mooring line force on the bollard. The DWT of the design vessel is 34431 $tons$, which places it in the category of up to 50000 $tons$ at which the line forces are 800 kN or smaller. This means that the representative line force will be chosen at 700 kN, considering the design vessel is around 15000 $tons$ lighter than 50000 $tons$.

The bollard type used in Sitio 1 is the "Tee Bollard" type. Therefore it is chosen to also use this bollard type on the new quay. Using a Tee type also has the advantage that it can be used for a large range of rope angles. A bollard with the following dimensions should be able to take the line forces[62]:

	A	B	C	C	E	F	G	I	J	K
Size [mm]	70	380	550	640	550	160	250	280	320	230

	L1	L2	L3
Degrees	15	40	N/A

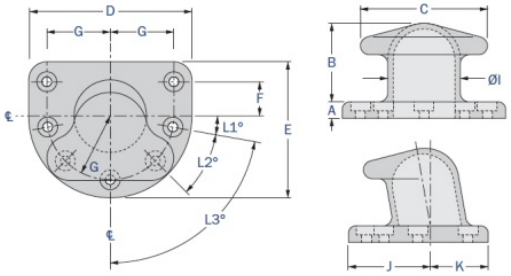

Figure 6.13: Mooring bollard dimensions [62]

As mentioned before, with these kinds of bollards, vessels up to 50000 $tons$ should be able to moor without chance of failure. If the port eventually aspires to receive vessels with a DWT > 50000 $tons$, than these bollards need to be replaced by a stronger type.

Foundation
Since significant forces are working on the mooring bollard (max. 700 kN) and fender (max. 648 kN), and these forces work at the same location, it is common practice to design a separate foundation for these elements. The mooring bollard and fender are connected to a concrete block. The foundation of this block can be designed in multiple ways, being by means of anchoring or piling. The use of anchors is only working properly with the mooring bollard forces, working away from the quay. Though, fender forces are directed towards the quay, and in this direction the anchors don't offer additional capacity. The foundation of the block is therefore chosen to be a concrete pile, its dimensions the same as the other foundation piles for ease of procurement. The piles are situated just behind the sheet pile wall. As the apron floor will also be founded on piles there are no additional mobilisation cost for the equipment, as the driving of these piles can be done simultaneously with the driving of the concrete floor foundation.

6.5. Assessment of failure mechanisms

The five failure mechanisms which are identified are discussed for both Sitio 1 and Nieuw Delft.

6.5.1. Sheet pile failure

A sheet wall is a flexible structure, in which bending moments will be developed by lateral loading, and it should be designed such that it can withstand the largest bending moments [70]. The wall is anchored to obtain more passive soil capacity and to reduce the maximum moment in the sheet pile wall. There are two criteria for stability of the quay wall: equilibrium of moments and horizontal forcing. The checks for stability will be based on the stress that will occur in the sheet pile at the point where the absolute maximum moment occurs. The safety factor is calculated by Equation 6.8. A safety factor of 1 indicates that the yield stress of the steel has been reached. The safety factor should therefore be larger than 1. More detail is given in Appendix H.

$$\sigma(h_{crit}) = \frac{N(h_{crit})}{A} + \frac{M(h_{crit})}{W} \tag{6.7}$$

$$SF_{SP} = \frac{f_y}{\sigma(h_{crit})} \tag{6.8}$$

Sitio 1
The sheet pile stability at Sitio 1 is assessed for the two groundwater level situations, at LAT level and at MSL level. The seawater level is constantly taken as LAT, since this is the most unfavourable water level when looking at the stability of the sheet pile wall. This assessment is described in Appendix H. Its results are given in Table 6.4.

	Operational		**Earthquake**	
	GWT = LAT	GWT = MSL	GWT = LAT	GWT = MSL
M_{min} $[kNm/m]$	384	535	1189	1307
M_{max} $[kNm/m]$	413	617	1705	1992
N_{max} $[kN/m]$	274	310	408	452
N_{crit} $[kN/m]$	169	204	328	372
Q_{min} $[kN/m]$	168	227	453	743
Q_{max} $[kN/m]$	200	275	650	504
u_{max} $[mm]$	35	55	160	192
SF_{SP}	2.60	1.76	0.65	0.56

Table 6.4: Sitio 1 sheet pile assessment, numbers obtained from PLAXIS model.

Nieuw Delft
For Nieuw Delft the same assessment is done as for Sitio 1, with both load cases at both groundwater levels. The seawater level is again taken at LAT level for all cases. The results of both load cases are shown in Table 6.5. The safety factors for the operational loadcase are well above 1. For earthquake loading, the stress in the sheet pile gets close to the yield stress, but still, the safety factors are above 1. Therefore failure will not occur.

	Operational		**Earthquake**	
	GWT = LAT	GWT = MSL	GWT = LAT	GWT = MSL
M_{min} $[kNm/m]$	212	267	733	886
M_{max} $[kNm/m]$	224	310	716	783
N_{max} $[kN/m]$	260	275	286	329
N_{crit} $[kN/m]$	180	198	106	150
Q_{min} $[kN/m]$	127	169	373	475
Q_{max} $[kN/m]$	166	223	483	569
u_{max} $[mm]$	18.0	25.0	69	68
SF_{SP}	4.28	3.15	1.41	1.17

Table 6.5: Nieuw Delft sheet pile assessment, numbers obtained from PLAXIS model.

6.5.2. Anchor failure
The safety factor for the anchor is defined as below, using the material properties of the anchor as in Table 6.1.

$$SF_{anchor} = \frac{f_y * A_{rod}}{F_{anchor}} \tag{6.9}$$

Sitio 1
Anchor forces are obtained from the PLAXIS model for the different situations and load cases and are summarized in Table 6.6. Unfortunately, an anchor failure check cannot be performed due to missing information on the anchor dimensions.

	Operational		**Earthquake**	
	GWT = LAT	GWT = MSL	GWT = LAT	GWT = MSL
F_{anchor} $[kN]$	344	496	1241	1443
SF_{anchor}	-	-	-	-

Table 6.6: Anchor forces for Sitio 1 with $L_{spacing}$ = 1.26 m.

Nieuw Delft
The anchor force which is generated during the earthquake load case is much larger than under the operational load case. To bear this force, it is decided to increase the anchor rod diameter form 80 to 100 mm, resulting in stresses in the rod just below the yield point for earthquake loading. The anchor material properties are summarized in Table 6.1 and the PLAXIS results are given in Table 6.7.

	Operational		**Earthquake**	
	GWT = LAT	GWT = MSL	GWT = LAT	GWT = MSL
F_{anchor} $[kN]$	697	982	2141	2607
SF_{anchor}	4.00	2.84	1.30	1.07

Table 6.7: Anchor forces and safety factors for Nieuw Delft with $L_{spacing}$ = 2.50 m.

6.5.3. Global failure
The above mentioned failure mechanisms focus on a specific part of the structure. Though, it can also be the case that the whole system, being the sheet pile wall, the anchors and the soil body, fails when loading result in an exceedance of the soil shear capacity. This is called global failure. The PLAXIS model is used to assess this failure potential. PLAXIS gives results which are very close to the commonly used Bishop method for assessment of global failure. The difference between the Bishop results and the PLAXIS 2D results equals 0.4% [55]. PLAXIS defines a safety factor based on shear.

$$SF_{GF} = \frac{S_{maximum \quad available}}{S_{needed \quad for \quad equilibrium}} = \frac{c - \sigma_n * tan}{c_r - \sigma_n * tan_r} \tag{6.10}$$

The latter ratio can be found when implementing the Coulomb condition. S represents the shear strength and σ_n a normal stress component. This is the principle on which the PLAXIS global failure assessment algorithm is based. An elaboration of this method can be found in PLAXIS 2D Tutorial Manual 2018.

The safety factor is preferred to be at least 1.5 to have a reliable system. Though, this factor can only be determined for the operational load case. Since an earthquake results in complex dynamic soil conditions and the earthquake is only modelled by adding extra loads on the sheet pile, the model does not give a correct global safety factor.
Besides the safety factor the software gives more. It calculates the total displacement increments and plots those, resulting in Figures 6.14 and 6.15. These figures indicate the sliding plane if global failure occurs. The magnitude of these displacements doesn't say much about the failure mechanism, though from the plots a failure plane can clearly be identified. This is the plane along which the system will fail. Though, as already mentioned, the model does not implement the foundation piles of the concrete. The sliding plane as indicated is only valid for a situation without piles. The anchors plates should be situated outside the sliding zone to optimize the stabilizing effect. The plots of the sliding planes can give an indication whether this criteria is achieved.

Sitio 1
Figure 6.14 and 6.15 give an indication of the failure plane of the system. With an anchor length of 36 meters the plates are well outside the indicated failure zone.

	Operational		**Earthquake**	
	GWT = LAT	GWT = MSL	GWT = LAT	GWT = MSL
SF_{GF}	1.92	1.95	-	-

Table 6.8: Global safety factors for Sitio 1.

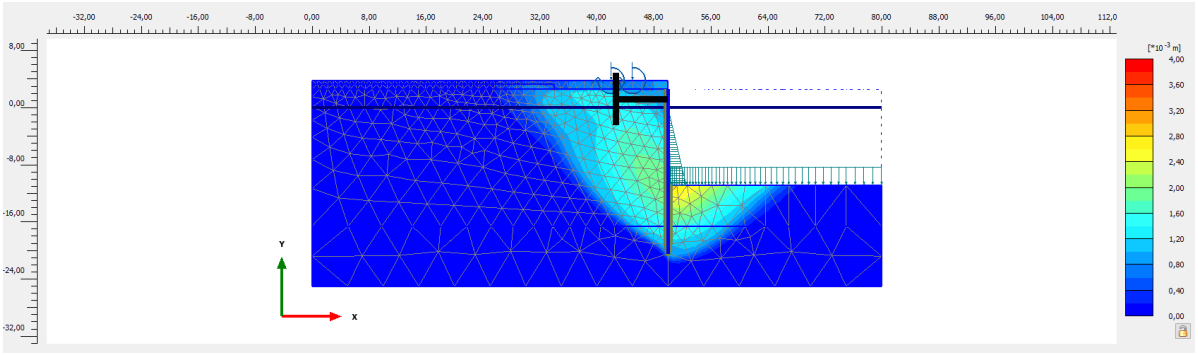

Figure 6.14: An indication of the failure mechanism when GWT = LAT at Sitio 1, indicating the sliding plane, as predicted by PLAXIS, similarly to Bishop's method.

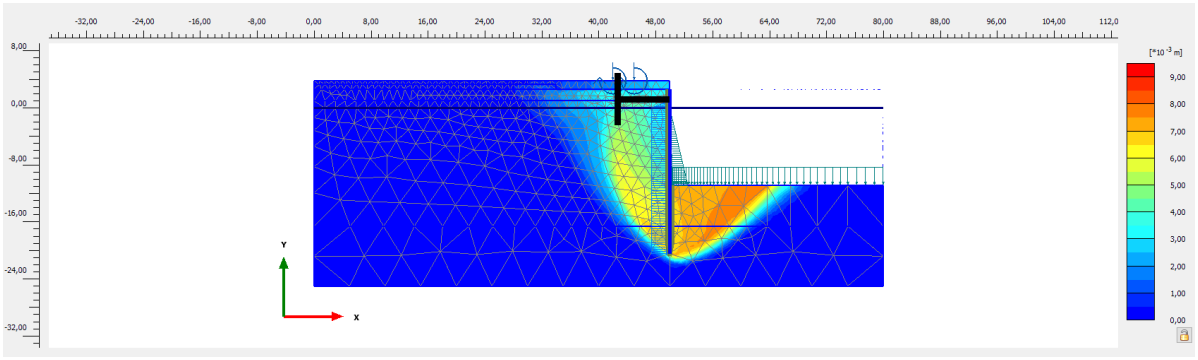

Figure 6.15: An indication of the failure mechanism when GWT=MSL at Sitio 1, indicating the sliding plane, as predicted by PLAXIS, similarly to Bishop's Method.

Nieuw Delft

With an anchor length of 25 m the anchor plates are situated well outside of the indicated sliding plane.

	Operational		**Earthquake**	
	GWT = LAT	GWT = MSL	GWT = LAT	GWT = MSL
SF_{GF}	2.39	3.47	-	-

Table 6.9: Global safety factors for Nieuw Delft.

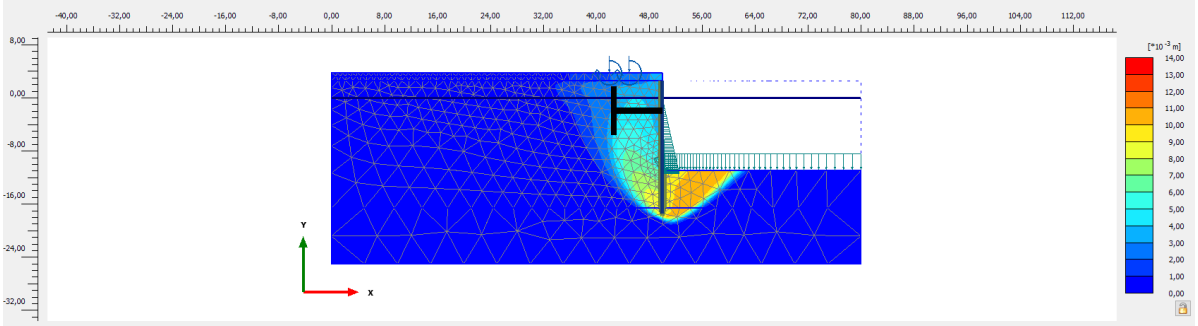

Figure 6.16: An indication of the failure mechanism when GWT = LAT at the new quay "Nieuw Delft", indicating the sliding plane, as predicted by PLAXIS, similarly to Bishop's Method.

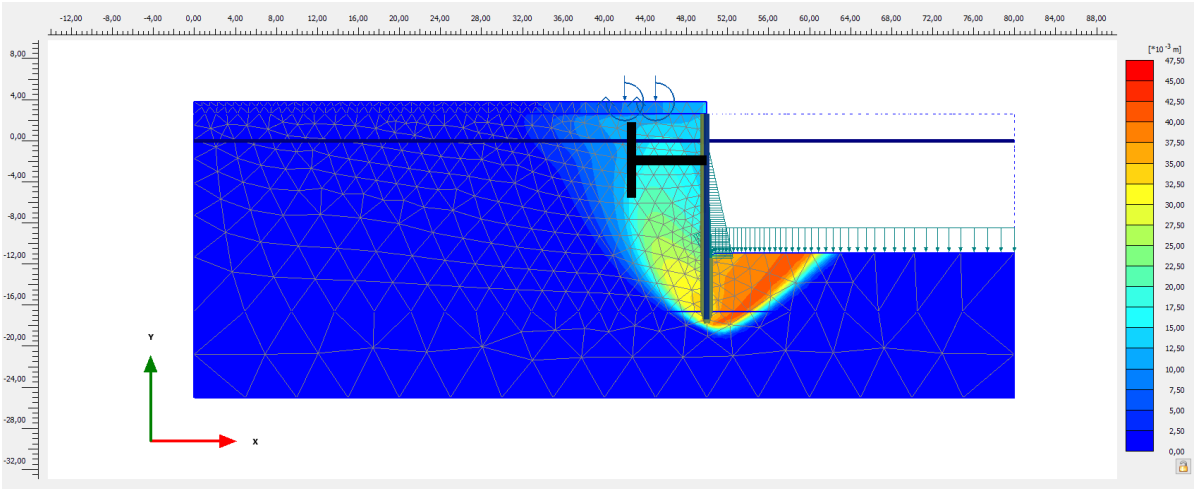

Figure 6.17: An indication of the failure mechanism when GWT=MSL at the new quay "Nieuw Delft", indicating the sliding plane, as predicted by PLAXIS, similarly to Bishop's Method.

6.5.4. Heave and Piping

When analyzing the impact that the new situation has on the current quay wall, the possibility that heave and eventually piping will occur should be assessed. When heave or eventually piping occurs, it can lead to the failure of the structure, which would render part of the quay useless.

Heave occurs when flow force in porous flow is larger than the weight of the grains in the soil, leading to these grains to float and possibly being transported [25]. If heave occurs, or eventually piping, it can greatly influence the bearing capacity of the ground layer on the passive side of the quay wall [12].
Due to the soil being coarse sand, the assumption is made that the groundwater table will move along with the tide. However, in the unlikely event that the groundwater table doesn't change while the seawater level does, the following calculation is made. The difference in GWT and sea level is taken to be the difference between LAT and MSL, which is 1.04 m.

If piping will occur, this can be checked by using the approaches of Bligh and Lane and these are given below [70].

Approach by Bligh:

$$\Delta h \leq \frac{L}{C_B} \tag{6.11}$$

Approach by Lane:

$$\Delta h \leq \frac{\frac{1}{3}L_H + L_V}{C_L} \tag{6.12}$$

The value of $L = L_1 + L_2$. In the Lane formula, the value for L_H will be so small that it will be negligible, due to the construction being a sheet pile wall and $L_v = L$. In the figure below, a visual representation of the parameters are given for a sheet pile wall:

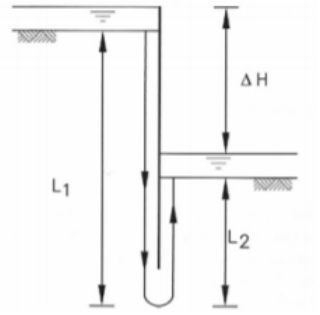

Figure 6.18: Piping parameter definition according to Bligh/Lane

Sitio 1 Piping Check
For the structure at Sitio 1, the computed parameter values are given in Table 6.10. For the soil, a porosity of n = 0.5 is assumed (which is conservative).

$\Delta h[m]$	$L1[m]$	$L2[m]$	L
1.04	20.29	7.85	28.14

Table 6.10: Piping parameter values Sitio 1

The value taken for C_B is 12 (Bligh) and for C_L is 5 (Lane), which are both still chosen conservative considering the soil. When the safety factors (SF) are equal or larger than 1, piping won't occur. Both approaches indicate that piping will not occur, see Table 6.11. Even when implementing a safety factor γ_{piping} of 2 in the Lane formula, the equilibrium criteria is still met.

$\Delta h[m]$	L/C_B	L/C_L	SF_{Bligh}	SF_{Lane}
1.04	2.345	5.628	2.255	5.412

Table 6.11: Values of piping check Sitio 1

So even in the unlikely event that GWT will not be equal to sea level, piping won't occur.

Nieuw Delft Piping Check
When doing the same checks for the Nieuw Delft structure, table 6.12 shows the computed parameter values. For C_L, C_B and n the same values are used as for Sitio 1.

$\Delta h[m]$	$L1[m]$	$L2[m]$	$L[m]$
1.04	18.44	6	24.44

Table 6.12: Piping parameter values Nieuw Delft

Using these parameters it is calculated if the construction meets the Bligh and Lane checks. For both checks, Δh is smaller than L/C, as can be seen in table 6.13. Due to this, the safety factors are again higher than 1. These values implicate that also in the design for Nieuw Delft, piping won't be an issue.

$\Delta h[m]$	L/C_B	L/C_L	SF_{Bligh}	SF_{Lane}
1.04	2.037	4.888	1.959	4.7

Table 6.13: Values of piping check Nieuw Delft

6.5.5. Scour
The increase in vessel sizes can also lead to a difference in the amount of scour at the berth. Since larger vessels often have more power, the jet stream from the bow thrusters or main propellers can also be larger, which could lead to a larger scour hole in front of or close to the quay wall. This of course could influence the stability.

Transverse thruster scour
The tugboats could also produce jet streams that could lead to scour. However, it is very unlikely that they will come close enough to the quay to create large scour holes. Still, to take into account the unlikely event that they will use their thrusters while very close to the quay wall, a scour calculation is still made.
Since the type of tugboat is unknown, the Azistern 3360 is taken as reference vessel. The calculation of the scour depth is described in detail in Appendix K.
The maximum scour that is calculated for this vessel type and the soil properties are given in Section 3.6. The calculated (unlikely) scour depth of 0.5 meters is implemented in the PLAXIS 2D model for Sitio 1 and Nieuw Delft, which is used to assess the sheet pile in Section 6.5.1.

Main propeller scour
The new design vessel (the largest vessel that will berth at the quay) does not have transverse thrusters and will be berthing with the help of tugs, as is procedure with all berthing vessels that arrive at the port. The engine is put in slow ahead mode, leading to the used power of the engine being only a fraction of the full engine power (taken at 5%) of the main vessel. The full engine power is 7900 kW [32]. The calculation of the scour depth is described in detail in Appendix K.

The calculated maximum scour hole depth due to this main propeller is 9.7 m. Even though it is not situated directly against the quay wall, it will be situated close by (around approximately 15 meters, which is half the design vessel width).

Conclusion
The scour depth due to transverse thrusters will not lead to failure of the current structure. However, if the choice is made by the port to attract container vessels as well, the situation could change. Most container vessel do have bow thrusters, which would also lead to larger scour holes at the quay. Therefore it is recommended to install bottom protection if this is considered.
For scour due to the main propeller of the design vessel, the calculated maximum scour depth is much larger. The size and depth of such a hole will negatively influence the stability of the structure. Also, a mound will form due to the scoured soil, which will at certain points decrease the water depth close to the quay. Due to this, a bottom protection has to be installed. This will need to be installed along the bottom of the quay wall. Based on the available information, such as no mentioning of scour holes and no implication of a installed bed protection, an assumption was made about the berthing and unberthing procedure of the vessels. In the initial calculation it was assumed that during the berthing and unberthing of the main vessel, engine power would be shut off, leading only to scour due to the tugboat thrusters. This turned out to be a wrong assumption, as it is common for a vessel to use its engine during unberthing, which will thus lead to scour. Therefore it is recommended to install a bottom protection at the quay. This has been included in the scour calculations, but not in modeling of the design of the sheet pile wall. As the model is still based on the wrong assumption, the model of the sheet pile wall does include the scour of 0.5 m due to the tugboats directly at the quay and does not include bottom protection. Implementation of the bottom protection would take away this scour, leading to more stability concerning the sheet pile wall. Therefore, the new sheet pile design is slightly conservative.

6.6. Conclusions

The results of the design checks on the failure mechanisms for Nieuw Delft and Sitio 1 are summarized in Table 6.15 and 6.14. An impression of the proposed design is given in Figure 6.19. Further visual impressions of the new quay can be found in Appendix I.

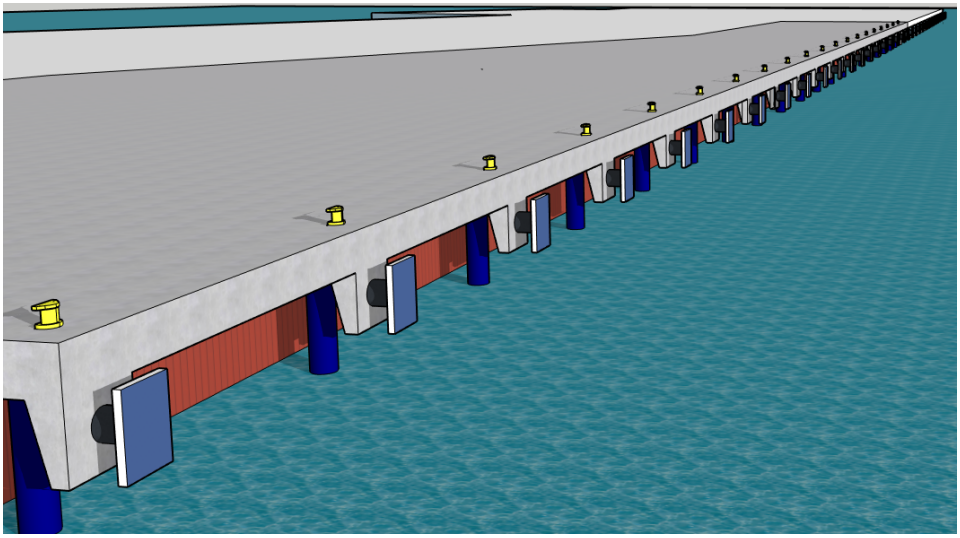

Figure 6.19: Nieuw Delft Quay Structure

The results show that the internal stress in the sheet pile of Sitio 1 under earthquake loading exceeds the yield point, resulting in plastic deformations and a high probability of failure. This is mostly because the yield point of the sheet pile is already low due to the damage of the 2010 earthquake.
Scour due to main propeller flow can be a large problem if no measures are taken. A scour hole of up to 9.7 meters might occur if large vessels visit more frequently. The presence of bottom protection at the quay will prevent this scour from happening.
All other assessed situations pass the design checks.
The bollards and fenders are founded on piles, and designed such that vessels of up to 50,000 *tons* can be moored at the quay.

	Operational		**Earthquake**	
	GWT = LAT	GWT = MSL	GWT = LAT	GWT = MSL
SF_{SP}	2.60	1.76	0.65	0.56
SF_{anchor}	-	-	-	-
SF_{GF}	1.92	1.95	-	-
Scour	Pass[1]	Pass[1]	-	-
Piping	Pass	Pass	-	-

Table 6.14: Results of design checks for Sitio 1.

	Operational		**Earthquake**	
	GWT = LAT	GWT = MSL	GWT = LAT	GWT = MSL
SF_{SP}	4.28	3.15	1.41	1.17
SF_{anchor}	4.00	2.84	1.30	1.07
SF_{GF}	2.39	3.47	-	-
Scour	Pass[1]	Pass[1]	-	-
Piping	Pass	Pass	-	-

Table 6.15: Results of design checks for Nieuw Delft.

[1] Pass if bottom protection is applied at the quay.

Sheet pile wall		
Type	Hat-Type NS-SP-10H	-
E_{Youngs}	200	GPa
I	119100	cm^4/m
W	2970	cm^3/m
f_y	355	MPa
Mass	186	$kg/m/m$
D_{embed}	6.5	m
Anchors		
A_{plate}	4	m^2
r_{rod}	50	mm
f_y	355	N/mm^2
$F_{anchor,max}$	2788	kN
EA	0	kN
G	200	GPa
D_{anchor}	4.5	m
L_{anchor}	25	m
$L_{spacing}$	2.5	m
Fenders		
Type	CO900	
H	900	mm
øU	765	mm
øS	585	mm
h	41	mm
Fender Plate		
Height	2000	mm
Width	1500	mm
Mooring Bollard		
Type	Tee Bollard	-
Bollard capacity	80	$tonnes$
Concrete Apron Floor		
Length	240	m
Width	25	m
Thickness	1.16	m
Type Concrete	C35/45	-
f_c	35	MPa
f_t	3.21	MPa
ø$_{main}$	10 x 28	mm/m length
ø$_{stirrup}$	4 x 14	mm/m width

Table 6.16: Summary of the dimensions and material properties of the sheet pile wall, its anchoring, the fenders, the mooring bollards and the concrete apron floor. Note that the embedded depth is not including scour.

7

Manoeuvring Area and Navigation Channel Design

In this chapter, the manoeuvring area design and navigation channel design are discussed.

7.1. Manoeuvring area

The manoeuvring area dimensions are determined by the turning basin and the berthing area. The berthing area must have a width of 250 m parallel to the quay according to the port standards, which is highlighted in Figure 7.1. This width is in compliance with PIANC, as it states that a manoeuvring area should be $5 * B_v + 100 = 250m$ wide taken perpendicular to the berth, where B_v is the design vessel breadth (30 m). This manoeuvring area allows vessels to manoeuvre around other berthed vessels safely and is taken into account in the detailed design.

In the current situation, the port standards do not prescribe a turning basin within the manoeuvring area. It is also known that in the current situation a vessel of 180 m is able to berth and the port experience confirms that the current manoeuvring area bounds are sufficient for such a vessel. Thus a turning basin, prescribed by PIANC, can be seen as conservative. A midway between the port standards and the PIANC guidelines is implemented. In Figure 7.1 it can be seen that the northern part of the turning basin is cut off to the bounds of the manoeuvring area which currently exists. This is done to reduce the dredging volume but still maintain a sufficiently big area of manoeuvrability for the vessels. In the new situation, the manoeuvring area will be expanded to the gray and red area depicted in Figure 7.1. This new manoeuvring area is of sufficient dimensions for the manoeuvrability of two berthing design vessels in the new situation.

In Section 8.1 the dredging volumes are calculated for different dredging depths. These numbers will determine whether a tidal window will be implemented. Implementing a tidal window will result in a difference in dredging depth between the berthing pocket and the rest of the manoeuvring area including the entrance channel. This requires less dredging of this manoeuvring area and entrance channel, thus saving in dredging costs. A decision on this matter is made in Section 8.1.

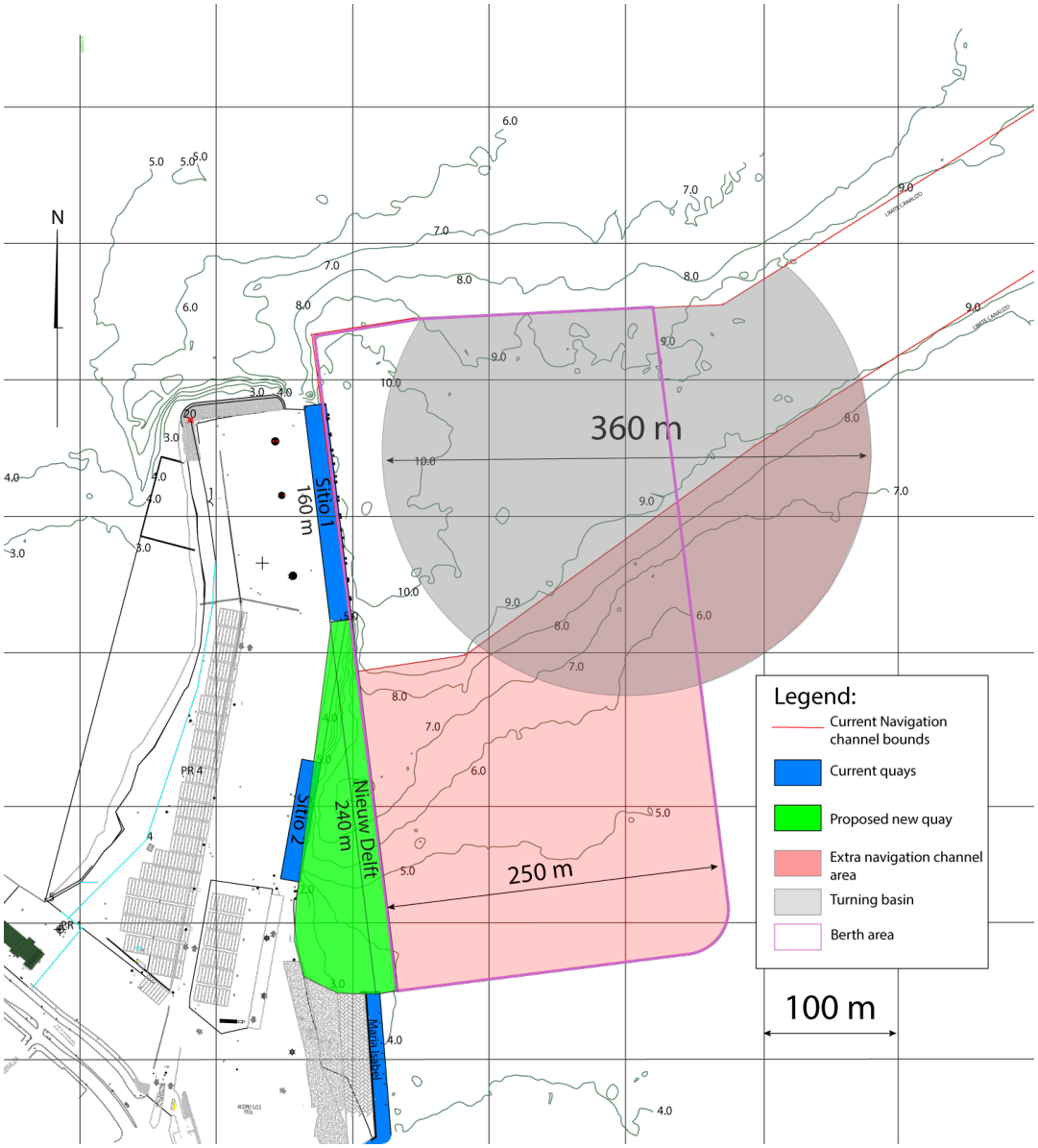

Figure 7.1: Detailed design Scenario 4

7.2. Navigation channel design

In the following section, the new channel design is discussed and worked out in detail.

7.2.1. Basis of design

In order to design the new channel first some important considerations have been made. The channel design is based on the PIANC regulations and on an integrated method for optimal channel design guideline [58].

7.2.2. Boundary conditions

The boundary conditions for the channel design are listed here.

- The environmental conditions considering the navigation channel are described in Chapter 3.
  - Soil characteristics are stated in Table 3.8.
  - A current of 0.5 m/s is considered, as stated in section 3.3.
  - The wind characteristics are stated in Table 3.1.
  - The wave characteristics are described in Chapter 3
  - The navigation channel will be a one way traffic channel

7.2.3. List of requirements

The requirements for the new navigation channel design are listed below.

- The design vessel as stated in Table 4.1 should be able to pass through the navigation channel.

7.2.4. Design scope

The following matters are capped in the design:

- Channel dimensions
- Slope stability in the navigation channel, manoeuvring area and berthing pocket

7.2.5. Width channel

In order to design for the design vessel, the required width of the channel needs to be recalculated. A a sailing vessel makes a sinusoidal track when it is sailing in the navigation channel. This is caused by effects of wind, current, waves and the lack of visibility. Apart from this, certain margins are needed for the width of the channel in order for it to be safe. PIANC describes a method on how to design a channel incorporating all these aspects. The design width for a one way channel is described by equation 7.1.

$$W = W_{BM} + 2 * W_B + \sum W_a \tag{7.1}$$

in which:

- W_{BM} = the basic lane width, being 1.5 * B
- W_B = the bank clearance, being 0.3 * B
- W_a = additional width components

The values for the basic lane width, bank clearance and additional width components are shown in Table 7.1 and are from PIANC.

Width component	Condition	Width [m]
Basic width (W_{BM})	moderate manoeuvrability	1.5* B_s
Bank clearance (W_B)	sloping edge	0.3* B_s
	steep, hard, embankment	0.5* B_s
Additional width (W_a):		
Prevailing cross winds	15-33 kn	0.6* B_s
	33-48 kn	1.1* B_s
Prevailing cross-current	0.2-0.5 kn	0.3* B_s
	0.5-1.5 kn	1.0* B_s
	1.5-2.0 kn	1.6* B_s
Prevailing long current	1.5-3 kn	0.2* B_s
	>3 kn	0.4* B_s
Prevailing wave height	1-3 m	0.5* B_s
	>3 m	1.0* B_s
Aids to navigation	VTS - excellent	0
	good	0.2* B_s
	moderate	0.4* B_s
Seabed characteristics	soft	0.1* B_s
	hard	0.2* B_s
Depth/draught	1.5-1.25	0.1* B_s
	<1.25	0.2* B_s
Separation distance (W_V)	$V = 8-12kn$	1.6* B_s
	$V = 5-8kn$	1.2* B_s

Table 7.1: Width components channel

Basic lane width
The basic lane width is calculated as 1.5 * 30 = 45 m.

Back clearance
The bank clearance is calculated as 0.3 * 30 = 9 m, assuming a sloping edge.

Additional width components
For the new design of the channel, the following additional width components from Table 7.1 are relevant and calculated:

- Prevailing cross winds: The prevailing winds are between 15 and 33 kn, (7.72 m/s and 16.98 m/s), as can be seen in Table 3.1.
- Prevailing cross current: The prevailing cross-current is between 0.2 and 0.5 kn (0.10 m/s and 0.26 m/s).
- Aids to navigation: The aids to navigation is assumed to be good
- Seabed characteristics: The seabed characteristics are soft, since the soil in the navigation channel is mainly fine sand between 0.125 and 0.25 mm, as can be seen in Chapter 3.
- Depth/Draught: The depth (10.6 m) over draught (10 m) ratio is < 1.25.

All additional width components lead to a total of 1.4 * B, leading to an additional width of 42 m.

In conclusion, the total width of the new one way channel is supposed to be 45 + 9 + 42 = 96 m. All width components are summed up in Table 7.2. The current width of the navigation channel is 100 m, meaning the new navigation channel does not need to be any wider. This width accommodates one-way traffic of vessels with a breadth up to 30 m. Also, it accommodates two-way traffic of vessels with a breadth smaller than 13 m, assuming a separation width of 1.2 * B.

Width component	Width	Width (m)
Basic width	1.5*B	45
Bank clearance	0.3*B	9
Prevailing cross wind	0.6*B	18
Prevailing cross current	0.3*B	9
Prevailing long current	0	0
Prevailing wave height	0	0
Aids to navigation	0.2*B	6
Seabed characteristics	0.1*B	3
Depth/draught	0.2*B	6
Seperation distance	0	0
Total width	3.2*B	96

Table 7.2: All width components channel

7.2.6. Soil slope stability under water

In order to guarantee soil stability in the navigation channel and the manoeuvring area, the slope of the sand on the edges of the dredged area is important. As described in Section 3.6.2, the soil is classified as fine sand with a maximum angle of internal friction of 35 degrees. However, the slope under water is less steep than above water [70]. Due to the presence of currents on the bottom and due to the presence of waves, the soil particles can start to move. This phenomena is described by the Shield's criterion.
The morphological process can cause the navigation channel to fill itself with sand and decreases the inclination angle under water after some time [69]. This is elaborated more upon in section 8.2.2.

Soil design slope underneath the water

It is important to determine the soil slopes of the side banks of the channel, manoeuvring area and navigation channel. A design slope angle for the fine sand of 12.5 degrees is chosen (1:4.5). This value is obtained by using Figure 7.2 for a grain diameter d_{50} of 0.23 mm and a current speed of 0.5 m/s, as mentioned in section 7.2.2 . This soil slope is considered to have the lowest possibility of slope failure within one year.

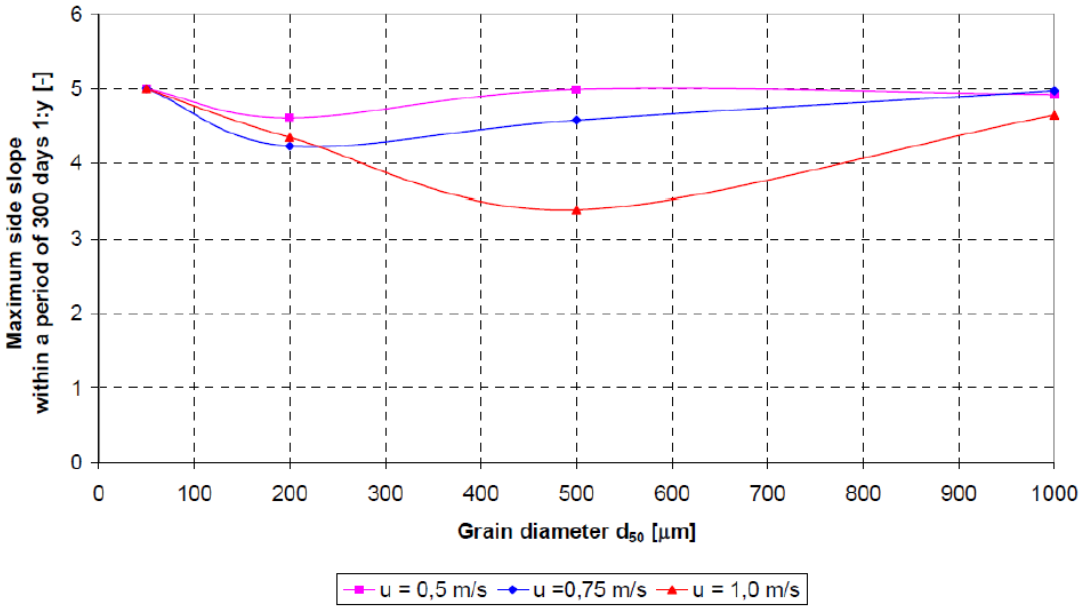

Figure 7.2: Soil slope stability for different current speeds and diameters

In the current navigation channel a maximum slope of 8 degrees is measured by looking at the bathymetry as depicted in Appendix D. This means it makes sense to assume that, due to morphological aspects, the slopes

in the navigation channel and the manoeuvring area will start to decrease over time. This may lead to dredging maintenance in the future. More is elaborated upon this in section 8.2.2

7.2.7. Channel dimensions

A cross section of the design of the navigation channel can be seen in Figure 7.3. For the most shallow situation in the navigation channel this leads to W_{SL} of 12 m and h_t of 2.56 m for a h_{gh} of 10.6 m.

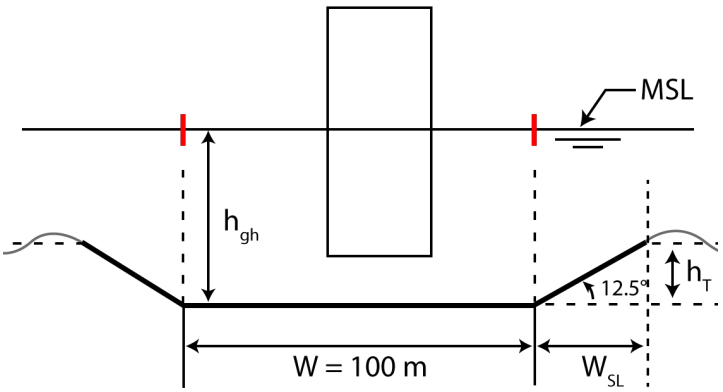

Figure 7.3: Dimensions of the entrance channel from a cross section view

7.2.8. Length Channel

In order to design for a new design vessel, the length of the navigation channel also needs to be re-calculated. Larger vessels require a longer navigation channel for entering the port. The length of the navigation consist of three separate components, namely: the slowing distance (L_1), the tie up distance (L_2) and the stopping distance (L_3). These three distances are calculated according to PIANC.

$$L_{tot} = L_1 + L_2 + L_3 \tag{7.2}$$

$$L_1 = (V_s - 2) * 0.75 * L_s \tag{7.3}$$

$$L_2 = t * 60 * V_{s2} \tag{7.4}$$

$$L_1 = 1.5 * L_s \tag{7.5}$$

For the calculation the following values have been used:

- V_s The entrance speed is assumed to be 2.5 m/s as this is the minimum speed required for control
- L_s The design length is 180 m
- t The tie up time is assumed to be 15 minutes although this is dependent on the experience of the crew and environmental circumstances
- V_{s2} The tie up speed is assumed to be 2 m/s

The total length of the navigation channel according to the PIANC guidelines is calculated to be 2138 m.

The calculated length of the navigation channel is larger than the current length of 1800 m, as stated by the port authorities. The current vessels that enter the navigation channel have a maximum length of 230 m. Since the current channel length is sufficient and does not lead to problems with vessels of a length of 230m, the channel will not have to be enlarged.

This means that the length of 1800 m is used for the new navigation channel design.

7.2.9. Channel depth

The depth of the entrance channel depends on a number of factors: the draught of the design vessel, the squat, the trim, the heel, the vertical response to waves, the tidal difference in water level and channel bottom factors.

The guaranteed depth that is needed can be calculated with equation 7.6 [53].

$$h_{gh} = D + h_t + s_{max} + z + h_{net} \tag{7.6}$$

in which:

- D = draught design vessel (m) = 10 m
- z = Heave motion (m)
- h_{net} = Net underkeel clearance (m)
- h_t = Tidal elevation: -1.04 m (LAT), 0.00 (MSL), +1.21 m (HAT)(see Figure 3.5)
- s_{max} = Maximum sinkage

The values s_{max}, z and h_{net} together form the gross under keel clearance (UKC).
These values can be approximated on basis of experience [39]:

- s_{max} = 0.5 m (general)
- $z = H_s/2$ = 1.16 / 2 = 0.58 m (See Table 3.5
- h_{net} = 0.5 m for a sandy bottom

According to the PIANC, the gross UKC is therefore calculated to be 1.58 m. However, as stated in 4.1 this value is given by the port authorities to be 0.6 m. A value of 0.6 m is used in the design for the navigation channel. It is recommended for the port to re-evaluate the UKC when larger vessels will sail through the navigation channel.

The guaranteed depths h_{gh} can be computed by using an under keel clearance of 0.6 m for the different tidal levels.

- h_{gh} (LAT) = 10 - 1.04 + 0.6 = 9.56 m
- h_{gh} (MSL) = 10 + 0.00 + 0.6 = 10.6 m
- h_{gh} (HAT) = 10 + 1.21 + 0.6 = 11.81 m

All important parameters for the new design of the navigation channel are listed in Table 7.3

Characteristic	**Value**	**Unit**
Width (W)	100	m
Width slope (W_{sl})	12	m
Length (L)	1800	m
Guaranteed depth (measured from MSL) (h_{gh})	10.6	m
Max bed slope at edges	12.5	degrees

Table 7.3: Parameters new navigation channel design

8

Dredging design

In this chapter, the dredging design is discussed. First, the dredging volumes are calculated. After that, the dredging execution plan is discussed, which consists of discussing the dredging challenges and the dredging maintenance.

8.1. Dredging volume

In this section the dredging volume is determined in detail. This is done for two different situations. One situation where a tidal window is implemented and one situation without a tidal window. First the dredging depths are determined. Next, the dredging volume is determined using Global Mapper. The edges of the dredged area will have a slope under a maximum angle, which has to be taken into account when delivering the area. The extra volume to be dredged is determined in order to guarantee this maximum slope. Finally, the total dredging volume is listed and a choice will be made regarding the implementation of a tidal window.

8.1.1. Dredging depths

The dredging volumes will be calculated for two different situations. One where the entire manoeuvring area is dredged to a guaranteed depth of 10.6 m LAT and one where a tidal window is implemented. In case of implementing a tidal window the different guaranteed depths are displayed in Figure 8.1. In this situation, a design vessel is only able to access the entrance channel and manoeuvring area when the tide is equal to or above MSL. The berth area along the quay with a width of 2 times the vessel's breadth will serve as a berthing pocket. This berthing pocket has a guaranteed depth of 10.6 m LAT. The berthing pocket reaches $2 * B_v = 60m$ perpendicular to the quay, as can be seen in Figure 8.3. This is seen as a realistic estimation of the space needed once a vessel is in the berth.

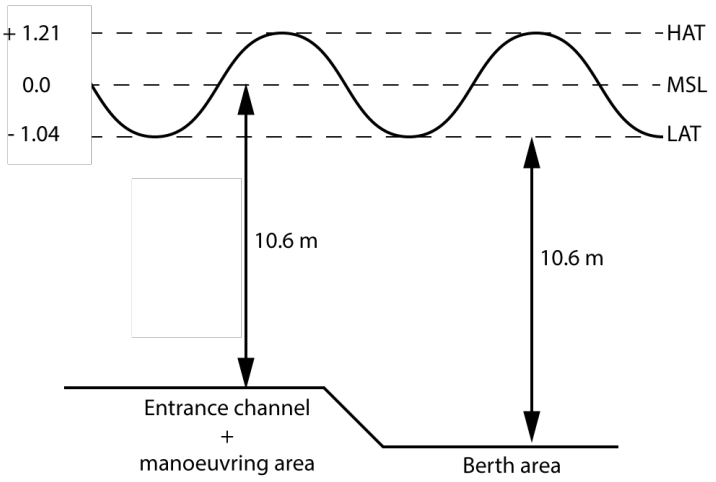

Figure 8.1: Guaranteed depths in the navigation channel, manoeuvring area and berth area using a tidal window

Next, the dredging depth is determined using Figure 8.2. The static draft in ambient water is known, this is 10 m. The net under keel clearance is covered in Section 7.2.9, which is 0.6 m. An overdepth dredging margin of 0.30 m is taken into account [53]. Dredging procedures cannot provide a smoothly excavated surface at an exact defined elevation which is why this margin is taken to guarantee an authorized channel depth.

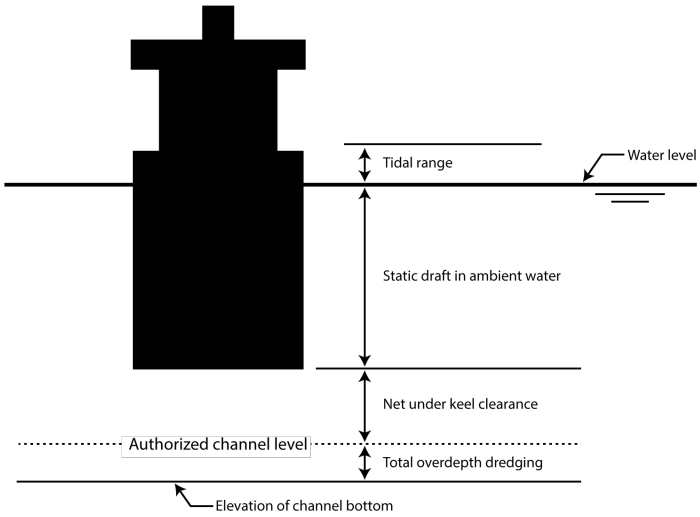

Figure 8.2: Channel depth parameters

From this information it is concluded that the dredging depth in the navigation channel and the manoeuvring area is 11.94 m MSL without using a tidal window. If a tidal window is implemented this depth will decrease to 10.90 m. The dredging depth of the berthing pocket is 11.94 m MSL. These dredging depths are used as input for the dredging volume calculation.

8.1.2. Volumes

The total dredging volume is divided into three different parts, as shown in Figure 8.3.

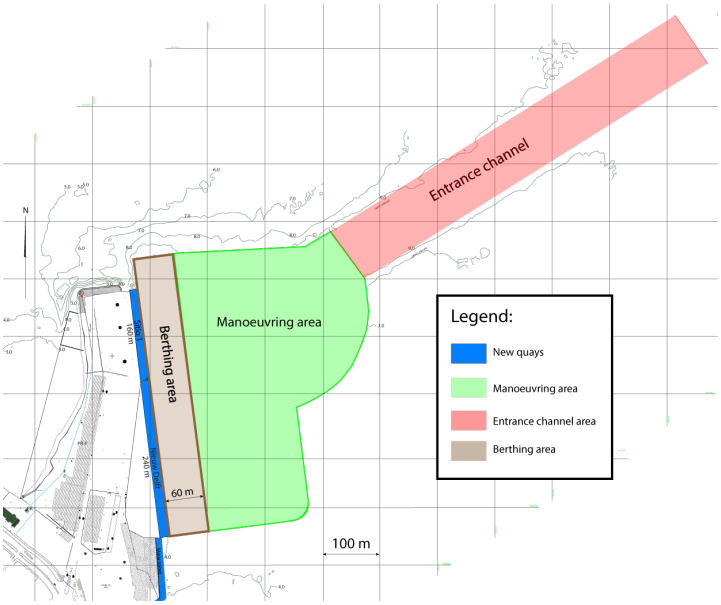

Figure 8.3: Division of dredging parts

The dredging volume is calculated using Global Mapper software. This is a GIS (geographical information system) program in which the bathymetry of the area is imported. Global Mapper provides a function to

calculate the volume of an enclosed area until a prescribed depth. The results of these calculations can be found in Tables 8.1 and 8.2. The inclined area surrounding the navigation channel and manoeuvring area is not taken into account in Global Mapper. This inclined area has a slope of 12.5 $degrees$. In order to guarantee this slope, the volume above this slope needs to be dredged. This volume is determined by doing hand calculations:

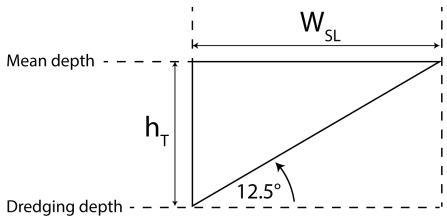

Figure 8.4: Calculation of sloping area volume

- The surrounding area is divided into segments.
- For each segment the depth is plotted over the length of this segment using Global Mapper.
- A mean depth is determined from this plot.
- The difference between the dredging depth and this mean (h_T) is then multiplied with the maximum slope to obtain a width of the sloping area (W_{SL}).
- The surface of the triangle between h_T and W_{SL} is then multiplied by the length of the segment to obtain the volume above the sloping area.
- These steps are repeated for each segment.

The results of these calculations are depicted in Tables 8.1 and 8.2.

Area	**Depth** [m]	**Volume** [$10^3 m^3$]
Manoeuvring area	11.94	533
Entrance channel	11.94	154
Berthing pocket	11.94	111
Surrounding slopes		83
	Total	**881**

Table 8.1: Dredging volumes without tidal window

Area	**Depth** [m]	**Volume** [$10^3 m^3$]
Manoeuvring area	10.90	393
Entrance channel	10.90	49
Berthing pocket	11.94	111
Surrounding slopes		55
	Total	**608**

Table 8.2: Dredging volumes with tidal window

8.1.3. Conclusion tidal window

In conclusion, implementing a tidal window in the port of Talcahuano is recommended, for two reasons:

- As can be seen in Tables 8.1 and 8.2, implementation of a tidal window requires significantly less dredging.
- The current occupancy of the port is significantly low. The maximum occupancy of the port is 27.45 %, as can be seen in Figure 2.6. Logistically, working with a tidal window can cause longer waiting times. In the current situation, a maximum of two bulk vessel berth the port in a month of time. It is assumed that the growth of this occupancy rate is not large enough to pose a risk in the logistical part of utilizing a tidal window.

For the design a tidal window is implemented for vessels to enter the port. A vessel with the maximum allowed draught is only able to manoeuvre to and from the berth during a tide higher than MSL.

8.2. Dredging execution plan

In this section, the dredging method to complete the dredging activities is described. This consists of discussing the challenges encountered when the dredging activities are performed. After that, the expected dredging maintenance for the area is discussed.

8.2.1. Dredging challenges

The dredging execution plan will consist of a hopper dredging vessel completing the dredging activities. The three main dredging activities are:

- Realizing the width of 100 m horizontally on the seabed (see Figure 7.3) in the navigation channel
- Realizing the manoeuvring area and berthing pocket with sufficient depth
- Realizing the side banks with slopes

A hopper dredger usually excavates material in a series of long cuts. Many long cuts are present in the dredging volume area, as can be seen in Figure 8.3. Side bank dredging, including preparing the bed slopes, can be difficult with a hopper dredger because the draghead of the hopper may tend to slide down the bank. A cutterhead or backhoe is more suitable for dredging slopes. Another method to create the sloping edges is to dredge an equivalent box cut at the base of the side slope [65]. A box cut will lead to a natural slope over time. This is only recommended in the navigation channel area, since the steeper slopes in the berthing pocket will more easily lead slope failure. [42].

8.2.2. Dredging maintenance

In this section, it is investigated whether dredging maintenance is needed in the future.

Causes for the movement of sediment

Dredging maintenance is needed when the shape of the seabed changes too much over time, leading to a lower guaranteed depth. Most dredged channels in sand or mud are subjected to deposition and erosion processes of moveable sediments supplied by an upstream river or tidal flow [69].

The main possible causes that lead to the the movement of sediment are:

- Extreme waves
- Currents (perpendicular and parallel)
- Earthquakes
- Main propellers of vessels

These four phenomena have an influence on the shape of the channel. In Figure 8.5, a prediction of the shape of a channel with grain size 200 μm, velocity 0.5 m/s and wave height 1.5 m is shown [69]. It is clear that the slope on the top becomes steeper, whereas the slope near the bottom of the channel becomes smaller. This is a morphological process which happens over time. Once the channel's shape has changed too much it will lead to a decreasing width and depth and dredging maintenance is needed.

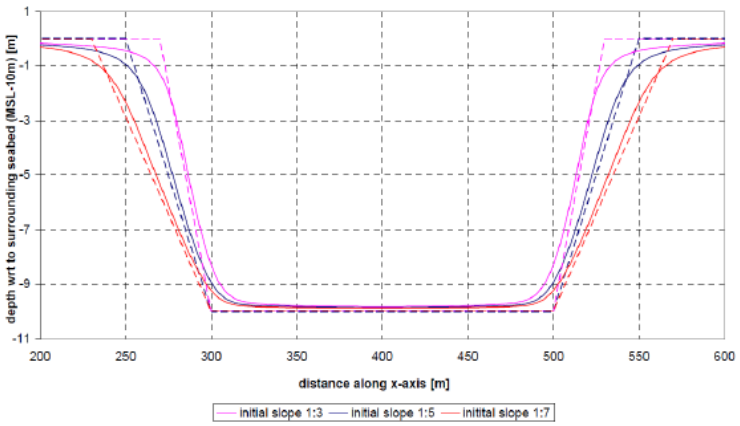

Figure 8.5: Cross section channel over time

Failure mechanisms

The main big failure mechanisms that cause instability for the soil leading to a large irregularities are [69]:

- Liquefaction, possibly caused by an earthquake
- Breaching, possibly caused by extreme waves and currents

- Scour holes, caused by the main propellers of vessels

Liquefaction is a phenomena which can occur, since the Talcahuano bay is regularly exposed to earthquakes. More about this can be read in section 3.7.1. Breaching is a failure mechanism that causes a full sliding mechanism of the complete slope. Breaching is also a phenomena which can occur in the case of extreme met-ocean conditions. Scour holes happen as a consequence of the flow streams created by the main propellers of vessels. Scour holes are most likely to happen since large vessels creating powerful jet streams will enter the port, and the underkeel clearance is relatively small.

Expectations regarding dredging maintenance

The bathymetry of the dredged area will change over time due to the presence of waves, currents, jet streams and possible earthquakes. This means there is a high probability that dredging maintenance is needed. In a study performed by Van Rijn, a bed load transport of 10 $m^3/m/year$ is used to shows that after 10 years there is a significant difference in width and depth in the channel for a grain size diameter of 250 μm. This can be seen in Figure 8.6.

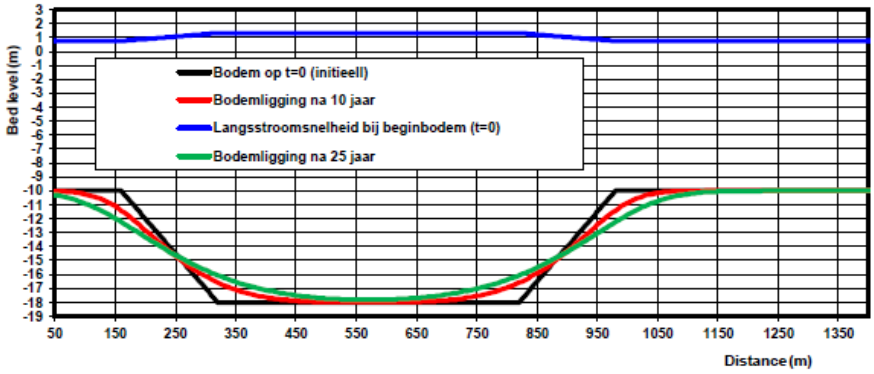

Figure 8.6: Projection cross section channel over 10 and 25 years

In conclusion, dredging maintenance activities can be expected to be necessary after 10 years. In shallow areas the current is generally higher and the seabed is more subjected to turbulence due to waves, meaning erosion and deposition will happen faster. Therefore, extra care should be taken for the south side of the berthing pocket and the manoeuvring area as the surroundings are very shallow. It is advised to closely monitor the bathymetry of this area and perform dredging maintenance activities when needed.

9

Earthquake and Tsunami impact

Apart from the technical amendments due to earthquake and tsunami risk made in Chapter 6 other measures could reduce the impact of an earthquake and tsunami as well. In this chapter first some general consequences and measures are given for earthquake impact. Afterwards the same will be done for a tsunami. The latter will include an evacuation plan based on the 2010 tsunami.

9.1. Earthquake impact

As described in Chapter 3 earthquakes are very common in Chile. Some lessons can be learned from an investigation of the 2010 earthquake that caused a lot of damage in Chile and the Concepcion Bay [66]. By reviewing the impact of this earthquake and tsunami, the damage can be analyzed in order to take measures to prevent equivalent failures. During an earthquake the acceleration of the earth's surface pulls the structures on top with it. When the structure is unable to accelerate with the same speed it will cause failure. Depending on the weakest point failure might occur in the soil, in the structure or at the soil-structure connection. During the 2010 earthquake the maximum Peak Ground Acceleration in Concepcion was measured to be 0.65 g [61]. This acceleration caused soil failure in many places leading to broken cables and pipelines under and above ground. The result is that electricity, water, telephone/internet connections and roads were no longer functional. For the port of Talcahuano it means cranes and lifts might have trouble positioning their loads, or stop working all together if they run on grid power. Computers and servers which are not connected to back-up power, will stop working. For employees evacuation over land can be troublesome as congestion and broken roads block exit routes. Finally foundations and/or structure of the offices can fail causing injuries.

Some problems can be solved by using the Chilean Earthquake Design Standard for the design of the quay as well as the other structures in the port. This has been done in Chapter 6. Other solutions can be found by logical thinking and risk finding. By looking at the failures from the 2010 earthquake solutions for these problems can be found. Some crucial electrical components which are needed for communications and emergency procedures should be provided with backup power instead of only relying on grid power. The same should go for cranes and other equipment related to lifting and/or unberthing operations. As the foundation of the quay might fail it is important that vehicles such as mobile cranes aren't immobilized by derailment for example. Also emergency communications should be available at all times and therefore battery powered receivers and transponders should work on a network separately from the common cellphone network. Finally, it is important that all staff is aware of the emergency procedures for earthquakes as well as tsunamis and are able to act accordingly. This can be achieved by creating emergency protocols, organizing safety training and emergency drills.

9.2. Tsunami impact

Tsunami waves have a great wave length and therefore behave as shallow water waves even in deep oceanic waters. From the source, the Peru-Chile trench, to the Chilean coast the depth decreases from between 8000 and 4000 m to the water surface. For shallow water waves the relation between the wave speed and the depth can be derived from equation 9.1, the dispersion relation [33]. From equation 9.2 follows that the tsunami´s

speed will decrease as it moves to smaller depths. As the speed decrease and the wave energy remains equal the amplitude must increase.

$$\omega^2 = \sqrt{\frac{d}{d}} * tanh(k * d) \tag{9.1}$$

$$c = \sqrt{g * d} \tag{9.2}$$

ω angular frequency $[rad/s]$

g gravity constant $[\ m/s^2]$

d depth $[m]$

k wave number $[rad/m]$

c wave speed $[m/s]$

With this knowledge it is clear to see the water level above MSL, inundation height, will raise the greatest at the coastline. When the tsunami hits the shore the wave will collide and damage whatever is in its way. In the city of Talcahuano a large part of the damage can be contributed to objects from the port that have been picked up by the tsunami. Several containers and small vessels have damaged or destroyed buildings. Figure 9.1 shows the inundation height in the Concepcion Bay. Due to the bathymetry in the bay a lot of the energy is directed to the port of Talcahuano causing large inundation heights. From this it is clear to see that objects in and around the port could have easily be picked up by a 6 m high water column before getting rammed into the buildings inland. In the new port design the layout should be adjusted such that objects like these are stopped or hindered along their path in order to prevent structural damage outside the port.

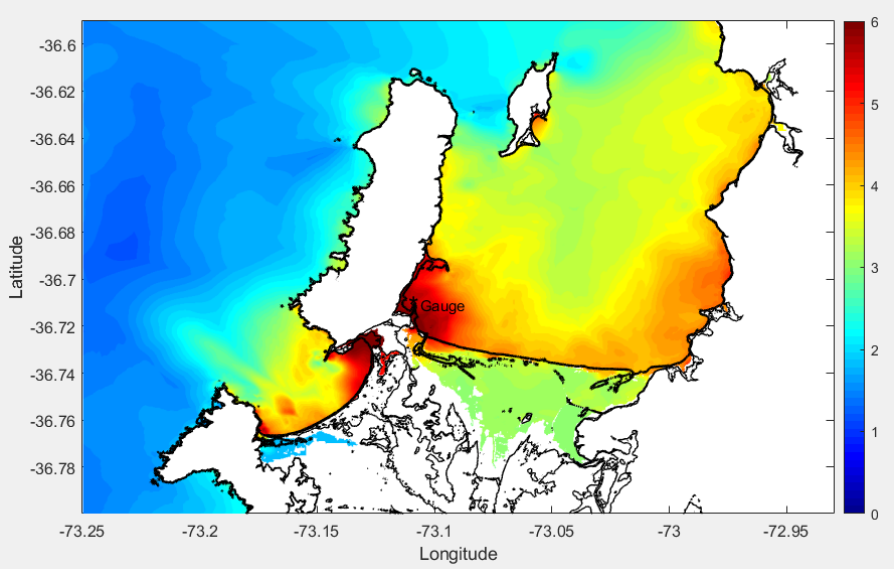

Figure 9.1: Maximum inundation height in meters[3]

9.2.1. Evacuation plan

To prevent damage from vessels colliding with buildings it is currently a standard procedure to send all vessels out of the port in the event of a large earthquake. When the vessels are sufficiently far away from the coastline they will not be pushed on land. This plan poses three challenges. First of all, the vessels need to have enough time to get out of the port far enough to be able to sail over the wave. Secondly, a lot of water is pushed into the port in order the raise the water level which causes high water velocities in counter direction of the vessels evacuation route. Finally, as the tsunami wave has passed, the water level also drops causing vessels to ground if the depth is too small. In order to look into these problems an analysis of the tsunami

impact is done.

Data from the 2010 tsunami is used to create an evacuation plan for the vessel in the port to mitigate damage to the vessel, the port and its surroundings. Apart from the report on the Chile earthquake and tsunami 2010 also a model is used to analyze the tsunami impact [5]. This model is also based on the 2010 earthquake and tsunami. From this model water levels and velocities are taken and displayed in figures below.
Using virtual tide gauges on strategically placed points the arrival time and water levels of the first tsunami wave are plotted against the distance along an evacuation route. Figure 9.2 shows the location of the virtual tide gauges in the Concepcion Bay. The first tide gauges, P01, is located in the port of Talcahuano and all other tide gauges are placed 2 km further out towards the open ocean. As the wave comes from the epicenter in the north, it will hit tide gauge 11 first.

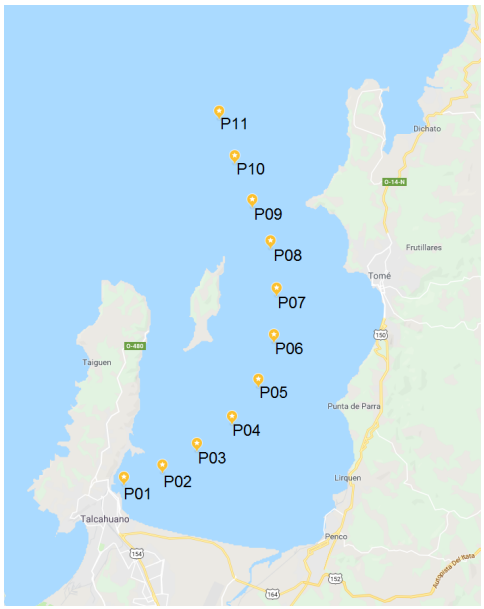

Figure 9.2: Locations of the virtual tide gauges

Figure 9.3 shows the water level and velocities at tide gauge 1, located at the port. The velocity of the water is expressed in a two direction fluid velocity, namely U and V. U is the eastward component and V is the northward component of the fluid velocity. As visible in Figure 9.3 the velocity correlates with the water level. Because the water for the first wave is brought by the tsunami the current is relatively small. When the water from the first wave retreats and the water level lowers the current is directed out of the bay.

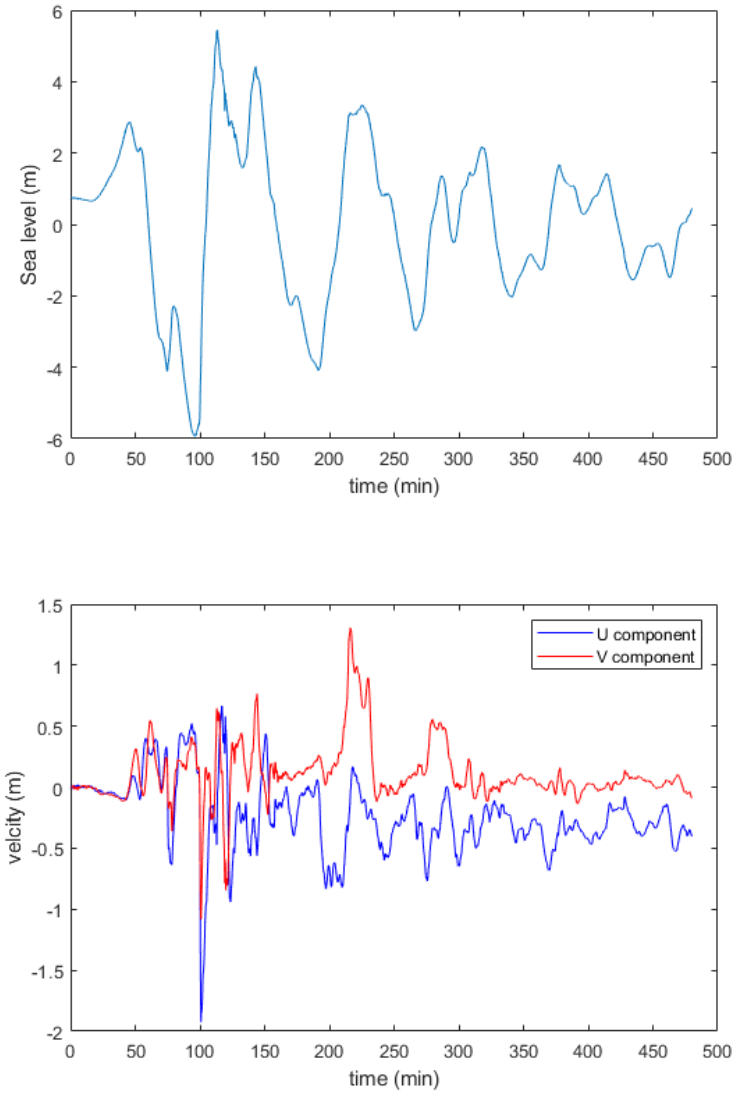

Figure 9.3: The water level and velocities at tide gauge P01

The ETA of the vessel is determined using the unberthing time and the speed of the vessel. The effect of the velocity is not used to check at what location the first peak will hit the vessel because the velocities of the water are insignificant to the vessel speed and the direction of the current and the vessel are equal. Because it is an unplanned emergency unberthing operating lifting operations need to be cut off in a safe manner first, but also some procedures can be skipped. For an exact estimate of an emergency unberthing time a full procedure has to be worked out. It is recommended for the port operations to have such a procedure readily available. For an unplanned emergency unberthing operating 20 minutes are taken as an estimate. For the speed of the vessel after unberthing the average speed of the design vessel is used which equals 6.38 m/s.
The time between the earthquake and the arrival of the first peak of the tsunami wave in the port of Talcahuano takes 45 minutes as displayed in 9.3. In Figure 9.4 the time of arrival of the wave is plotted against the distance from port along the tide gauges. As the distance increases, the location moves towards the north and the travel time for the tsunami decreases. Because the travel time increases along the distance, the vessel and the tsunami will meet. According to this graph they will do so between tide gauge 02 and 03, at approximately 3.5 km from the port.

Looking at the Estimated Time of Arrival of the vessel leaving the port it is clear it will not make it out of the bay. As soon as an earthquake is observed, this will be communicated to the port operators who in turn inform the vessel operators. From that moment on an emergency unberthing procedure must go into action. In this procedure the load on the crane must be secured as soon as possible after which the mooring lines should be released. Due to limited time the vessel is supposed to leave the berth without assistance of tugboats. Following the navigation channel it will reach deeper water in the bay. Here the vessel must turn to face the wave head-on to prevent roll.

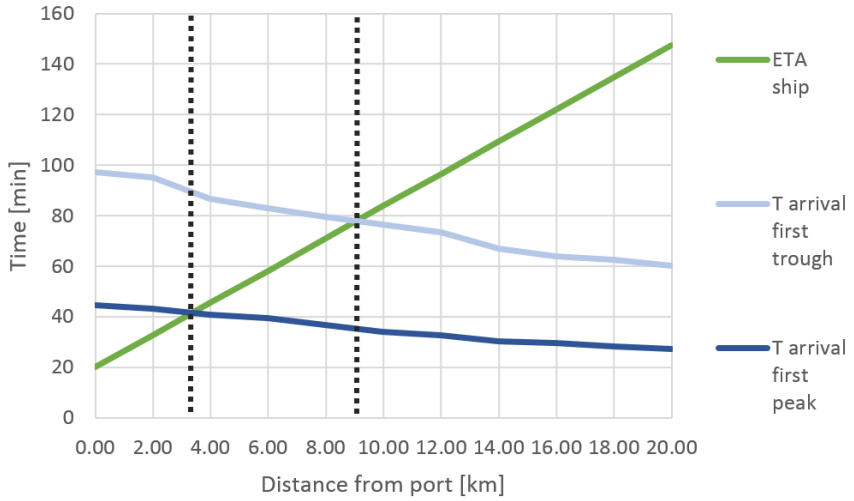

Figure 9.4: The arrival time of the peak and trough of the first tsunami wave[4]

From the water level measured at t=0 minutes, it is clear from Figure 9.3 that it was high tide as the tsunami hit. The worst case scenario for grounding is a tsunami during LAT. The depth taken to determine the minimal distance the vessel needs to clear to prevent grounding, is therefore adjusted to LAT. Figure 9.4 shows that the first wave trough will hit the vessel after approximately 80 minutes. This gives the vessel enough time to sail between tide gauges P05 and P06, at respectively 8 and 10 km. The depth at this point exceeds the draft including Under Keel Clearance.

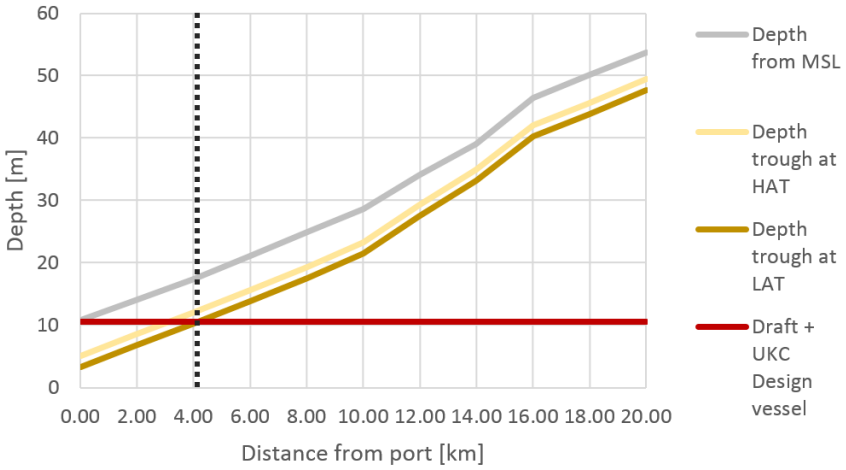

Figure 9.5: The depth during the first trough of the tsunami [4]

Only after the first trough the water velocity turns in counter direction of the vessel. When the vessel is between tide gauges P05 and P06 it is far enough away from shore to be stranded or cause any damage. At this

point the vessel is also safe from rubble being washed out from land. It can therefore be concluded that the design vessel will be able to reach a safe location on the note that the time to unberth takes no longer than 20 minutes. Also the first peak wave of the tsunami is the most critical point and grounding of the vessel is not a threat. It is therefore most important to eliminate all unnecessary steps for the emergency unberthing procedure.

After the first tsunami wave has passed, the vessel should keep continuing towards the end of the bay or another location which has been confirmed to be safe. Depending on the direction of the tsunami some ports will be damaged worse than others. It is therefore important that when the water level has return to normal up-to-date information about the ports in the Concepcion Bay must be used to determine what port is safe to go to.

It should be noted that the 2010 earthquake and tsunami used for this impact analysis is an extreme event not likely to happen in the years to come. The 2010 earthquake which caused the tsunami was very powerful with a magnitude of 8.8 on the moment magnitude scale. From Table 3.9 it is clear that the return period of this earthquake is over 200 years. It is therefore not expected that an earthquake of this magnitude will happen within the 30 year concession of the port operators. Besides this the location of the epicenter was 100 km north of the port of Talcahuano causing a high energy tsunami wave to hit the Concepcion Bay and giving vessels only little time to evacuate. In the Concepcion Bay the energy got even more focused towards the Talcahuano port due to the bathymetry. This can be easily concluded from the inundation height shown in Figure 9.1, which is higher in the Talcahuano port than anywhere else in the bay. To use the 2010 earthquake and tsunami is therefore a worst case scenario for an impact analysis.

The likelihood of the earthquake with the same location from the epicenter is small according to Kulikov, Rabi-novich and Thomson [19]. They claim that energy needs to built up and is released in an earthquake when a threshold level is reached. As the 2010 earthquake released the energy in this seismic region it is more likely that the next big earthquake will happen off the coast of north Chile extending the arrival time of the tsunami wave a lot.
Finally, the breaking of the wave can be looked at in order to estimate the location at which the wave breaks as the vessel can be heavily damaged if it is in that place at that time. However, this location is dependent on the bathymetry, wave height and direction of the wave. As the latter two parameters will vary for every tsunami no reliable conclusion can be given for the safety of the vessel. It is therefore not taken into account in this analysis.

From the earthquake and tsunami impact analysis it can be concluded that the backup power, backup communication systems and emergency protocols should be available and tested throughout the port´s facilities. An evacuation plan for vessels should include an emergency unberthing procedure and has to direct all vessels outside the port towards the entrance of the bay. The emergency unberthing procedure should focus on getting the vessel in the navigation channel within 20 minutes to make sure it has enough time to sail to a safe location before the tsunami wave hits. These recommendations are meant to mitigate risks and reduce the number of casualties and amount of damage to the port and its surroundings.

10

Market Prospect

In this chapter, the market prospect for the future of the port of Talcahuano is discussed. The prospects discussed in this section are matched to the ports aspirations. The port authorities are not only looking into expanding their current activities but are also looking into the possibility of handling containerized cargo. As the port owns a substantial land area and is already making use of a mobile crane, it is worth researching the prospects of expanding the containerized cargo activities. For these reasons, two future scenarios of market prospects are covered in this Chapter. First, the future throughput is determined for a scenario where the port keeps its current market strategy of handling general cargo and bulk. It is also assessed whether changes to the infrastructure or equipment have to be made in order to process this future throughput. Next, a scenario is described where a market strategy change has been made to handling containers only.
These scenarios are assessed for different occupancies of the berths.

10.1. Future throughput

In Chapter 2 it is mentioned what the throughput of the past five years has been. An estimation is made of the future throughput that the port is able to achieve. This estimation is based on the available statistical information provided by the port authorities [64]. The relevant information to calculate a future throughput is depicted in Table 10.1.

The following assumptions have been made in order to obtain a reliable estimate of the future throughput:

- The design vessel has a cargo capacity of 11.540 tonnes [17]. It is assumed that on average the entering vessels carry 75 % of the maximum capacity.
- The r_u is based on the yearly average unloading rates of 2017 (153 $tonnes/hour$) and 2018 (131 $tonnes/hour$) as recorded by the port [64]. A 130 $tonnes/hour$ unloading rate is taken as a base case to compute the port throughput.
- The channel commuting time T_c is based on an entrance velocity of 2 m/s and the mooring and unmooring times are based on averages given in the course book of Ports and Terminals [39].
- Two berths are accommodated by one entrance. Every moment a vessel arrives at or departs from this entrance, this entrance is inaccessible. It is assumed that the moments of arrival or departure of two different vessels do not occur at the same time. This means vessels will not have to wait for another vessel when arriving or leaving the berth. By this assumption, the total throughput for two berths is equal to the sum of two individual berth throughput's.
- The port is not in operation for 15 days per year to account for extreme weather conditions and incidental maintenance. The port is in operation 24 hours per day, which comes down to 8400 operational hours per year

These assumptions have led to the values given in Table 10.1.

Information	Symbol	Value	Unit
Operational hours	n_{hy}	8400	$hours/year$
Average call size	C	8655	$tonnes$
Unloading rate	r_u	130	$tonnes/hour$
Mooring time	T_m	60	$minutes$
Unmooring time	T_{um}	45	$minutes$
Channel commuting time	T_c	30	$minutes$
Unloading time	T_{ul}	66.5	hours

Table 10.1: Port logistical information

The unloading time T_{ul} can then be determined from C and r_u. As in this port only import takes place, the service time T_S consists only of unloading. This is calculated by the following equation:

$$T_S = T_m + T_{ul} + T_{um} + 2 * T_c \tag{10.1}$$

T_S is calculated to be 69 $hours$. The amount of operational hours divided by this T_S gives the total number of calls n_c. Multiplying this n_c with the average call size C gives the throughput for one berth c_b. The total amount of throughput c_{total} is then derived for a situation with two berths using the following equation.

$$c_{total} = n_b * c_b = n_b * \left(\frac{n_{hy}}{T_s} * C * occupancy \right) \tag{10.2}$$

Where n_b represents the number of berths. The throughput for three different occupancy values is depicted in Table 10.2.

Case	Occupancy	c_b [$10^6 tonnes$]	c_{total} [$10^6 tonnes$]
Low	0.15	0.16	0.32
Base	0.35	0.37	0.73
High	0.75	0.79	1.57

Table 10.2: Capacity results

The throughput is calculated for three different cases, as depicted in Table 10.2. Each case represents a different expected occupancy. The occupancy in the base case is assumed to be 35%. From 2014 to 2018 the occupancy in the port has risen from 11.43% to 27.45%, as is explained in Chapter 2. Achieving an occupancy of 35% is considered to be a realistic future outlook considering the steady growth in the last 4 years. An occupancy of 15% is considered to be the lower case, meaning the port is not able to adapt to the new situation in a good way. An occupancy of 75% is considered to be the higher case. 75% occupancy is taken for the high case as it is considered the highest possible occupancy before long waiting times for vessels will arise. These three different cases are also used in Chapter 11 for the financial analysis.

The current maximum throughput of the port is $0.27 * 10^6 tonnes$. The base case of the future throughput represents an estimated throughput of $0.73 * 10^6 tonnes$ which is a growth of 270% compared to the current maximum throughput. The high case is considered as an absolute ceiling of port throughput.

10.2. Waiting times

Looking at the logistical data in Appendix B it can be seen that currently there are no vessel waiting times recorded. As there is no data available on the inter-arrival time of vessels and there seems to be no clear pattern of vessel arrivals, it is hard to make an estimation of the waiting times for the future. To be able to make an estimation it is assumed that significant waiting times are starting to occur if the port's berth occupancy is nearing 45%. This assumption is based on the fact that there have been reported months with a high occupancy of 56% and 46% which crank up the average yearly occupancy. These busy months are expected to become even busier if the average occupancy is to grow, which eventually will cause waiting times to be inevitable.

Now, an estimation is made when the port will reach this 45% occupancy. By taking the average vessel call size of 2018 ($6.58 * 10^3 tonnes$)B and an unloading rate ($130\ tonnes/hour$) an average service time for 2018 is calculated, which is 53.4 $hours$. Then, by using Equation 10.2, a throughput is determined for the situation with an occupancy of 45%. This throughput equals $0.47 * 10^6 tonnes$. If the current growth in throughput of the port, an average $45 * 10^3 tonnes$ per year, is extrapolated, it is expected that the port will reach this occupancy around the year 2023. This means that, in four years, the port will come to a point where it is less attractive for vessels to berth at the port due to higher waiting times. This is why in the next four years, changes will have to be made in order to secure the throughput growth of the port.

10.3. Unloading capacity

In this section it is analyzed whether changes have to be made to the land area or infrastructure in order to maintain a sufficient unloading capacity.

First the amount of available space is assessed. An indication of the available space is given in Figure 10.1. The apron area width, as mentioned in Chapter 6, is 25 m and the area perpendicular to Maria Isabel is considered unusable for storage and handling of commercial cargo. An estimation leaves the two areas enclosed by the red lines in Figure 10.1 consisting of a total of 60.000 m^2 which can be used for handling and storage of cargo. This area excludes offices, a car park and a truck park which remain at their current location.

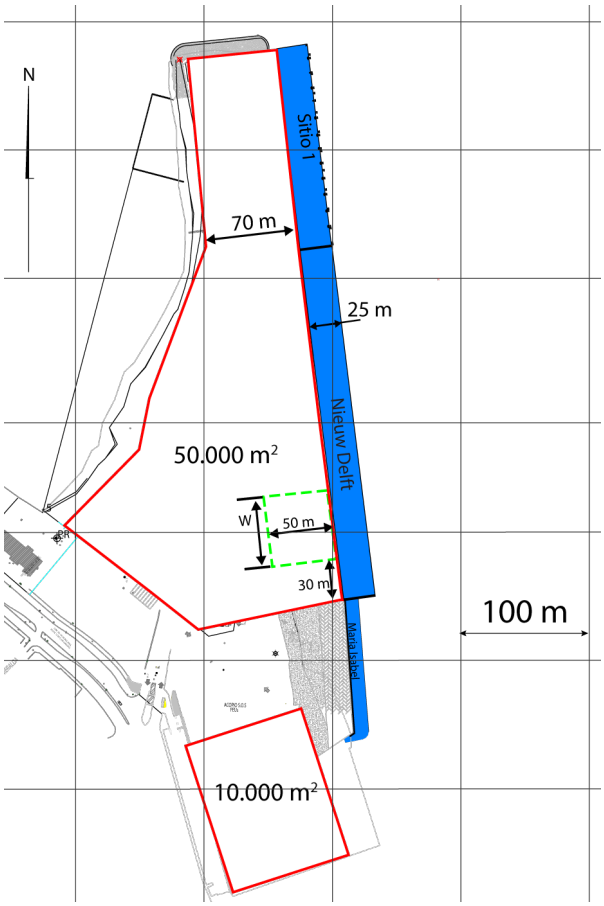

Figure 10.1: Port area layout

In the current situation, when cargo is loaded off the vessel, the port does not make use of transit sheds. The cargo is either directly transported to the client or it is temporarily stored in containers. The unloading capacity is in balance with the rate at which cargo can be removed or delivered. In the new situation with two berths, where the total unloading rate is higher, it is likely that the unloading capacity will exceed the rate at which cargo can be removed or delivered. Normally, ports make use of open storage or transit sheds to account for cargo transfer. In this case a transit shed can be built as salt will need to be sheltered from the rain.

Now it is calculated what size of transit shed is needed in order to secure a smooth cargo transfer. This is done for different outcomes of occupancy. The following equation was used:

$$A_{ts} = \frac{t_d * f_{area} * f_{bulk} * c_{total}}{m_c * h_s * C * 365} \text{[39]} \tag{10.3}$$

Of which:

- c_{salt} = The total throughput of salt. Currently the throughput of salt is 63% of the total throughput. This percentage is also used in this calculation. The total throughput is found in Table 10.2.
- t_d = Average dwell time of cargo, estimated at 5 days.
- f_{area} = The ratio gross over net surface accounting for traffic lanes for forklift trucks in the shed. A common value of 1.50 is assumed [39].
- f_{bulk} = Bulking factor due to stripping and separately stacking. A common value of 1.20 is assumed [39].
- m_c = Average rate of occupancy of the transit shed. This usually lies between 0.65 and 0.75 [39]. 0.70 is chosen for this calculation.
- C = Average relative cargo density as stowed in the vessel, chosen to be 0.6 t/m^3[39].
- h_s = An average stacking height is chosen to be 4 m. Transfer sheds in neighboring ports, for instance the port of Lirquén [28], have a similar stacking height.

The above calculation resulted in the transit shed areas given in Table 10.3.

Case	**Occupancy**	c_{salt} [$10^6 tonnes$]	A_{ts} [ha]	W [m]
Low	0.15	0.20	0.29	59
Base	0.35	0.46	0.68	136
High	0.75	0.99	1.45	291

Table 10.3: General cargo transit shed area

A layout suggestion for the location and size of such transit sheds is highlighted in Figure 10.1 by the green dotted line. The transit shed is placed close to the quay at the edge of the apron area. The transit shed is 50 m in length and has a width of W as indicated in the figure. For each occupancy, the value of W is also indicated in Table 10.3. This means for an occupancy of 0.35, and thus $W = 136m$, the transit shed has a dimension of 50 x 136. In the case of an occupancy of 0.75 and thus $W = 291m$, the transit shed becomes too wide which is why it is divided into two transit sheds that are separated by a traffic lane of 30 m in order to maintain manoeuvrability through the port.

It is thus advised to look into the possibilities of changing the cargo handling method to making use of transfer sheds. It can also be seen that the current amount of available land area is sufficient to accommodate a transfer shed when the port decides to place such infrastructure. Even for the optimistic case with a high occupancy the land area is sufficient.

10.4. Container port scenario

In this section it is assessed what the potential of the future throughput is if a market strategy change is made. Currently the port is active in handling bulk cargo, general cargo and fisheries. The excess storage area is used for empty container storage.

Thus it is researched what a market strategy change to a port which is fully devoted to handling containerized cargo can bring. In this changed strategy the entire area owned by the port will be transformed into a container terminal and all land area is utilized for storage and handling. An estimation of the maximum amount of yearly TEUs is made in the new situation with two berths. This estimation is made using calculations from the Ports and Terminals book [39].

The following assumptions were made in order to determine a future throughput:

- 8400 operational hours per year.
- Unloading rate of 20 moves per hour on average. This is based on one mobile crane per berth. The port owns a Gottwald HMK 300 crane. This crane is similar to a crane from a reference project[28],

which has an average productivity of 20 $moves/hour$. This productivity accounts for "unproductive" intervals such as for crane re-positioning, lost time between shifts and repairs to the cranes.
- A TEU-factor f_T of 1.5 which represents a ratio of 50:50 between 40 foot containers and 20 foot containers.
- The average call size is based on the selection of a new design vessel which is a container vessel with dimensions comparable to the general cargo design vessel. The AS Fiorella is chosen. This vessel has a capacity of 1284 TEU. It is again assumed that, on average, the entering vessels are carrying 75% of its maximum capacity.

This lead to the following results for the throughput estimation, depicted in Table 10.4.

Information	**Symbol**	**Value**	**Unit**
Operational hours	h_{oy}	8400	$hours$
Average transhipment rate	r_{tr}	20	$moves/hour$
TEU-factor	f_T	1.5	
Average call size	S_c	963	TEU
Service time	T_s	35	$hours$
Number of calls per year	n_{yc}	241	$calls$

Table 10.4: Container port logistical information

Case	**Occupancy**	c_{total} [$10^6 TEU$]
Low	0.15	0.07
Base	0.35	0.22
High	0.75	0.48

Table 10.5: Container throughput results

The base case of the estimated throughput of containers is $0.22*10^6 TEU$. The amount of container movements in 2017 of nearby ports such as San Vicente ($0.51*10^6 TEU$), Coronel ($0.43*10^6 TEU$) and Lirquen ($0.31*10^6 TEU$) [43] are all higher than this potential throughput. These ports are also able to attend larger vessels with a larger maximum draught (ranging between 12.4 m and 15.4 m) than Puerto Talcahuano (even when the draught is increased as indicated in this design ($10.0m$). The possibilities to achieve the base case estimated throughput are there, but the port is limited in the size of vessels it is able to attend compared to the surrounding container ports.

10.5. Prospects

Given the current growth of the port, it is only a matter of time before the port logistics become harder to manage and waiting times will start to occur. It is estimated that around the year 2023 waiting times will start to occur. Therefore it is advised to take measures to expand the port.

When implementing this design, it is considered realistic that the port will reach an occupancy of 35%. This will lead to a throughput of $0.73*10^6 tonnes$ under similar working conditions than the port is practising at this time. In order to process this growing throughput it is advised to investigate the possibilities to smoothen the cargo transfer process. A solution to this problem is building like a transit shed to provide secure temporary storage and a smooth cargo transfer. It is showed that the amount of available land area for such infrastructure is sufficient.

Lastly, a scenario of handling containerized cargo is investigated. The port is able to generate a throughput of $0.22*10^6 TEU$ in this scenario. A big investment will have to be made in order to step into this market. This investment contains cranes, cargo transfer equipment and land preparation for storage and transfer areas. Also, it must be noted that surrounding ports activite in containerized cargo are able to attend larger vessels, even if the new design is implemented. This can make it hard to squeeze into this market.

11

Financial analysis

In this chapter, a financial analysis for the final design is discussed. First, the costs of the final design are discussed. These costs can be sub-divided into the quay costs and the dredging costs. After that, the revenue for the future of the port is estimated by doing a future projection for the amount of tonnage processed in the port for the next 30 years. Finally, an NPV analysis is performed over 30 years.

11.1. Quay costs

The costs for the quay wall add up to 5.7 million USD, as elaborated upon in Section F.1 of the Appendix F. Since limited time is available in the project, this number is used for further analysis.

11.2. Dredging costs

In the preliminary phase the total dredging costs were estimated based on a price per cubic metre averaged, given by past performance of used dredgers. In the detailed design it is decided to separate the operational costs from the transportation costs. To give insight in what kind dredger is advised, one dredger with a large capacity and one dredger with a small capacity are chosen to be evaluated. The Yaquina Hopper Dredger is chosen as the low capacity dredger. The HAM 309 Trailing Suction Hopper Dredger (TSHD) is chosen as the high capacity dredger. Finally, the influence of sharing the transportation cost with other ports is investigated.

11.2.1. Operational costs

The operational costs of two different dredgers are estimated. To calculate the operational costs of a dredger, a rough cost price calculation tool is used which can be found in Appendix O. This tool provides a standard method to estimate the operational costs using the input from Table 11.1.

Input	Yaquina	HAM 309	Unit
Length	59	112	m
Vessel lightweight	1686	3980	ton
Dredge pump power	565.2	2080	kW
Jet pump power	0	1080	kW
Free sailing power	1700	5294	kW
Velocity (empty)	12.5	14.4	$knts$
Velocity (loaded)	12	14.2	$knts$
Loading time	13	19	min
Unloading time	10	15	min
Manoeuvring time	5	20	min
Capacity	798	4600	m^3

Table 11.1: Input for cost calculation tool for the Yaquina [48] and the HAM 309 [50]

The loading time, unloading time and manoeuvring times are found by estimates made in a dredging course [44]. As suggested by the author of the calculation tool, Prof.dr.ir. C. van Rhee, the following assumptions

were also made with regard to the cost price calculations:

- A dredging vessel can be assumed to be in operation for 145 hours per week.
- To be able to compute a sailing time, a distance of 20 km between loading and dumping is assumed.
- To account for office employees, project management, execution employees and administration, €50,000 per week is assumed for the Yaquina and €80,000 per week is assumed for the HAM 309.

The equations and formulas used in this tool will not be discussed but a general approach of how this tool computes the weekly costs is given below:

1. *Depreciation and interest.* The value of the vessel is determined using the input in Table 11.1. The vessel value as calculated in this tool is depicted in Table 11.2. Please note that this vessel value is merely used to make estimates of the weekly costs. A prescribed formula is used to compute the weekly depreciation and interest from this vessel value.
2. *Maintenance and repairs.* The maintenance and repairs costs are derived from the value of the vessel and the weekly service hours.
3. *Insurance.* An estimation of the insurance is given as 0.03% of the vessel value.
4. *Crew.* The weekly crew costs is related to the length of the dredging vessel. These costs can directly be derived from the calculations tool.
5. *Fuel and lubricants.* Fuel and lubricants costs are estimated by a given consumption of 0.19 $L/(hour * kW)$. Multiplying this consumption with the vessel propulsion power, weekly service hours and fuel price (338 USD/mt [10]) gives the total fuel costs. Lubricants are taken to be 10% of the fuel costs.
6. *Wear and tear.* A fixed amount of 0.30 per m^3 of dredged material is taken for the wear and tear costs.
7. *Margin and profit.* The approach from 1-6 merely gives the cost price. To account for a margin and profit for the contractor, 20 % of the total weekly cost price is added.

Above mentioned calculations resulted in the weekly costs depicted in Table 11.2.

Costs	**Yaquina**	**HAM 309**	**Unit**
Vessel value	18	36	$*10^6$€
Depreciation and interest	45	92	$*10^3$€/$week$
Maintenance and repair	56	77	$*10^3$€/$week$
Insurance	5	11	$*10^3$€/$week$
Crew	21	53	$*10^3$€/$week$
Gas and lubricants	14	43	$*10^3$€/$week$
Wear and tear	13	69	$*10^3$€/$week$
Margin and profit	30	69	$*10^3$€/$week$
Project management	50	80	$*10^3$€/$week$
Total operational costs	**208**	**493**	$*10^3$ €/$week$

Table 11.2: Weekly costs breakdown

It must be noted that the prices in Table 11.2 are depicted in Euro's. A conversion to Dollars of 1.20 is used, which is conservative compared to the 2018 average [41]. Next, the weekly dredged volume for each dredging vessel is computed. This is done by determining the time of one loading and dumping cycle including sailing time. The number of times this cycle fits in the weekly service hours is then multiplied by its capacity to obtain the weekly dredged volume. This weekly volume determines the total dredging time needed for this project. With this information the total operational costs can be determined. The results of these calculations are depicted below in Table 11.3.

Results	**Yaquina**	**HAM 309**	**Unit**
Cycle time	134	145	min
Weekly dredged volume	52	277	$*10^3 m^3/week$
Production time	12.9	2.4	$weeks$
Weekly costs	208	493	$*10^3 USD/week$
Total operational costs	**3,202,645**	**1,297,864**	USD

Table 11.3: Calculation tool results

11.2.2. Transportation costs

The transportation costs of the dredging vessel sailing to the desired location is of great importance, since this cost can vary very much. The cost of getting a vessel to the desired location mainly depend on market conditions of the dredging vessel used. For instance, if a dredger is available which is near to the port of Talcahuano, the transportation cost is lower. Since the transportation costs are the main cost, it is investigated what the influence of sharing the cost with other ports is, up to a maximum of 4 ports.

For the Yaquina Hopper Dredger, a transportation cost of 3,500,0000 USD is assumed, as stated by Jan de Bont from Royal Haskoning [16]. This cost includes mobilization and demobilization of the hopper dredger to the desired location in Chile. This is the transportation cost of the Yaquina Hopper Dredger from the USA to Chile.

For the HAM 309 Trailing Suction Hopper Dredger, a transportation cost of 10,000,000 USD is assumed, as stated by Rafael Aranguiz [6]. This is the transportation cost of the HAM 309 Trailing Suction Hopper Dredger for sailing from the Netherlands to Chile. This estimate is based on the knowledge of the previous dredging activities performed in the area.

11.2.3. Total costs dredging

The total costs of the dredging activities consist of the operational costs and the transportation costs.
The total costs for 4 different cost options are presented in Tables 11.4 and 11.5. Cost option 1 (C1) means that the port of Talcahauno is the only party participating in the transportation costs, whereas Cost option 4 (C4) means that the port of Talcahuano is sharing the transportation costs with four parties in total. The total dredging results including these sensitivities can be seen in Figure 11.1.

Costs (Million USD)	**C1**	**C2**	**C3**	**C4**
Operational Costs	1.30	1.30	1.30	1.30
Transportation Costs	10.00	5.00	3.33	2.50
Total Costs	**11.30**	**6.30**	**4.63**	**3.80**

Table 11.4: Total dredging costs HAM 309

Costs (Million USD)	**C1**	**C2**	**C3**	**C4**
Operational Costs	3.20	3.20	3.20	3.20
Transportation Costs	3.50	1.75	1.17	0.88
Total Costs	**6.70**	**4.95**	**4.37**	**4.08**

Table 11.5: Total dredging costs Yaquina

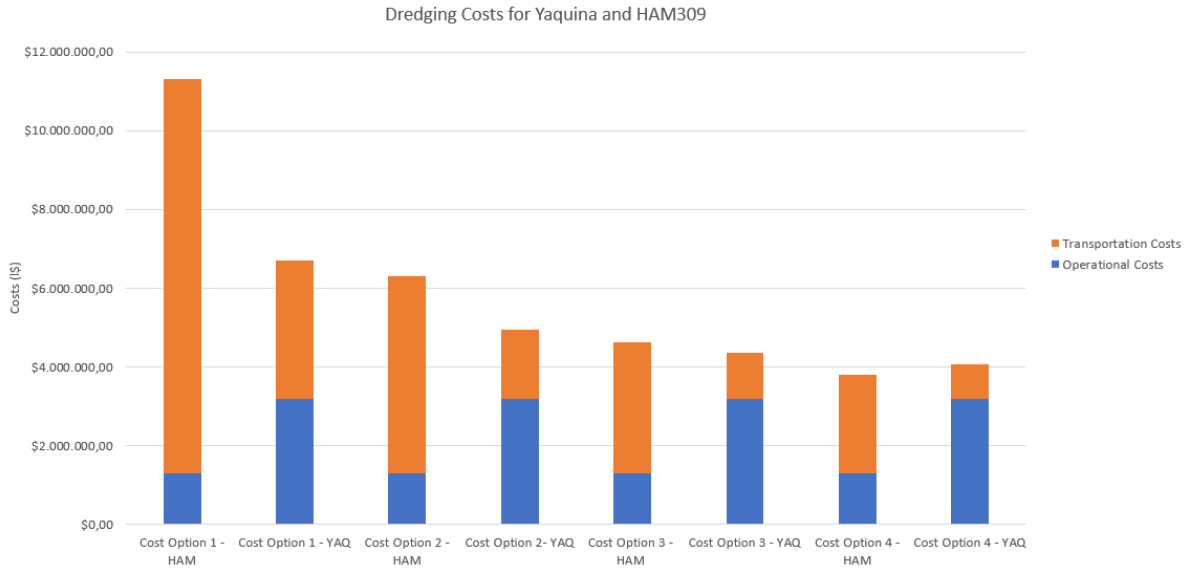

Figure 11.1: Total dredging costs including sensitivities

11.2.4. Validation and conclusion of dredging costs

Regarding the total dredging cost analysis, there are some uncertainties that should be addressed.
First of all, the transportation costs depend on market conditions of dredging vessels, as well as the possibility of collaborating with other ports. Both variables are difficult to project, which is why it is a big uncertainty. Secondly, the loading and unloading times of the dredging vessels are based on estimates which are uncertain. Lastly, the overflow losses in a hopper dredger have not been included. This means the actual hopper capacity is lower than calculated, meaning the numbers are slightly more optimistic.

In conclusion, the HAM 309 has lower operational costs compared to the Yaquina Hopper dredger (see Figure 11.3). This can be explained by the fact that the HAM309 has a higher capacity, meaning the dredging activities will be completed faster. However, the transportation costs of the HAM 309 are substantially higher than the Yaquina Hopper dredger. In general, the recommendation is to use the HAM 309 Hopper dredger and to share the transportation costs with neighbouring ports. The dredging activities are completed faster with the HAM 309, meaning less hinder is caused for Sitio 1. This means less money is lost during dredging. In addition, it is assumable that the HAM 309 from VanOord will complete a better job, VanOord having many years of experience in the dredging branche.

11.3. Revenue

The revenue of the port is dependent on the expected throughput and unit prices in the port of Talcahauano.

The port's revenue consists of the following parts:

- MEH: meter of berth space used per hour for Sitio 1 and 2
- Sale of the processed commercial bulk cargo
- Sale of processed fishery

In general, the revenue can be expressed by equation 11.1.

$$Revenue = P * Q \tag{11.1}$$

in which:

- P is the gross price in $USD/tons$
- Q is the throughput in $tons$

The throughput for all 3 sensitivities can be found in Table 11.7. The average unit price per tonnage is difficult to determine since the average unit price per tonnage depends on:

- The total metres of berthing space used
- The exact throughputs and separate unit prices of fishery and commercial vessels

In order to simplify this, an analysis on the total unit price including the two factors above has been performed. The year 2017 has been used as a reference year. The year 2017 is chosen because 78.44 % revenue is generated by the commercial berth, which is also an assumable assumption for the future since fishery is considered to be less important. The essential numbers of the year 2017 are summed up in Table 11.6 . More details about the financial parameters can be found in Appendix N.

A gross price per tonnage of 7.05 $USD/tons$ is used. Compared to the other years this is found to be an average value. In order to be able to do a sensitivity analysis a sensitivity of -30% and +30% is used for the cases. This leads to a gross price of 4.94 $USD/tons$ for the lower case and a gross price of 9.17 $USD/tons$ for the higher case.

Year 2017	**Value**	**Unit price** [$USD/tons$ **or** USD/MEH]	**Revenue** [USD]
Tonnage Commercial Berth	209,472	5	1,047,360.00
Tonnage Fishery	84,739	1.8	152,530.20
MEH Commercial - S1	193,260	3	579,780.00
MEH Fishery - S2	180,801	1.63	294,705.63
Total tonnage	294,211	-	2,074,375.83
Percentage commercial	78.44%		
Gross price/tonnage	7.05 USD		

Table 11.6: Statistics of the year 2017 for the port of Talcahuano

11.3.1. Future projection

In this section, the future projection for the revenue of 3 different occupancies is discussed.

Assumptions future revenue

The assumptions regarding the future market are listed below:

- The first 3 years are used to build the new construction. 25 % of the commercial revenue is generated during these first 3 years. The year 2017 is used as a reference year for this. This period is called the construction period.

- Starting from year 4 until year 30, a linear growth until the new tonnage production platform as mentioned in Table 11.7 is assumed. This period is called the growth period.

The future projection of the revenue is based on 3 possible occupancies, leading to different maximum values of processed tonnage. The throughput values are shown in in Table 11.7.

Occupancy [%]	c_b [$tons$]	c_{total} [$tons$]
0.15	157,303	314,605
0.35	367,039	734,078
0.75	786,513	1,573,025

Table 11.7: Capacity results for NPV

By combining the assumptions listed above, the occupancies and the gross price per tonnage, revenue projections for the future can be made. The results can be seen in Figure 11.2.

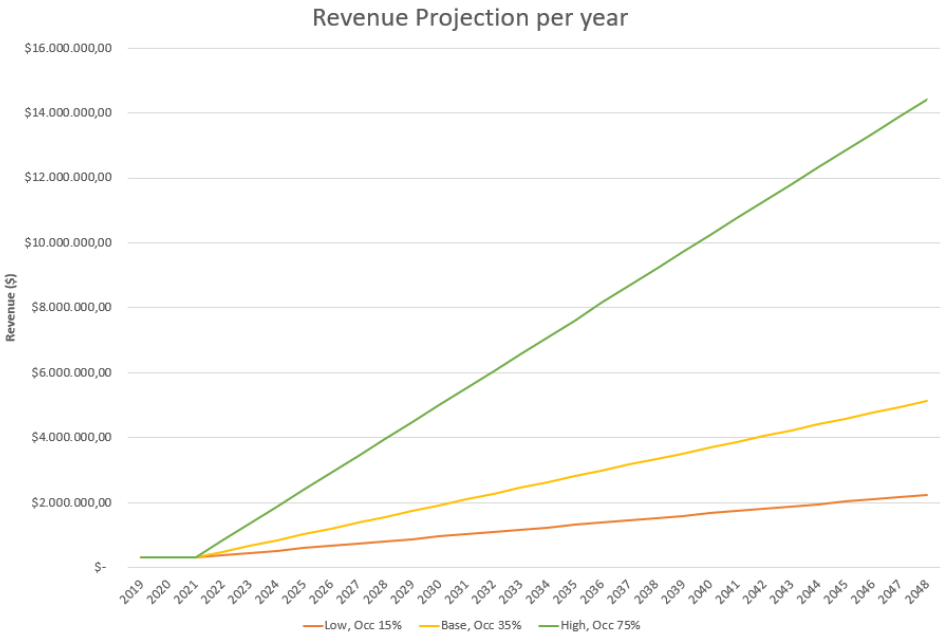

Figure 11.2: Revenue projection per year for different occupancies and different gross prices

11.4. NPV

In the following section, a Net Present Value analysis is carried out. The principle of an NPV is to analyze discounted future cash flows. In general, a PV (present value) is calculated by equation 11.2[2].

$$PV = \frac{CF_t}{(1+R)^t} \tag{11.2}$$

in which:

- PV is the present value
- CF_t is the cash flow generated at year t
- R is the discount factor
- t is the number of the year

By using equation 11.2, the projected future cash flows from the costs and revenue can be combined to make an NPV model.

With equation 11.3 the NPV is calculated [2]. C_0 is the initial cash flow in year 0.

$$NPV = C_0 + \sum_{t=1}^{T} \frac{CF_t}{(1+R)^t} \tag{11.3}$$

11.4.1. Assumptions NPV

In order to be able to do an NPV analysis, first some assumptions must be stated:

- Costs include dredging costs, quay wall costs and operational expenditure.
- Operational expenditure is assumed to be 10 % of the revenue generated in that particular year. This is a simplified way to estimate operational expenditure which is not entirely correct. However, considering the goal of this project this is supposed to be satisfactory. The operational expenditure includes personnel costs.
- Dredging costs and quay wall costs are paid in the first 3 years (capital expenditure).

- Costs exclude tax, permit costs and FEED costs.

- Revenue includes fishery, the commercial vessels and the MEH for Sitio 1 and Sitio 2.

11.4.2. Sensitivities

In Table 11.8, the sensitivities and parameters for the low, base and high case are presented. In the section below, the choice for the sensitivities for dredging costs, discount rate and occupancy are discussed. For the quay wall costs and the gross price a sensitivity of -30 % and +30 % is used.

The dredging costs used are based on using the HAM309 Trailing Suction Hopper Dredger. In all three cases the boundary condition is that the port shares the cost of transportation at least with one other party, since it does not make sense to assume the port will pay for the transportation costs of the dredging vessel if it is the only party participating. The low case means the port of Talcahuano shares the transportation costs with one other party. The base case means the port of Talcahauno shares the transportation costs with two other parties. The high case means the port of Talcahuano shares the transportation cost with three other parties. The values for these dredging costs are taken from Table 11.4 and 11.5.

The discount rate in the base case is assumed to be 7 %. Concerning port investment projects, this discount rate is considered to be acceptable for the base case [68].

The occupancy in the base case is assumed to be 35 %. Achieving an occupancy of 35 % is considered to be a realistic future outlook considering the steady growth in the last 4 years.

Category	Parameter	Sensitivity range	Low	Base	High	Unit
Costs	Dredging costs	-65%,+80%	6,300,000	4,630,000	3,800,000	USD
	Total quay wall costs	-30%,+30%	7,410,000	5,700,000	3,990,000	USD
	Discount rate	-40%,+40%	10	7	5	%
Revenue	Occupancy	-128%,+114%	0.15	0.35	0.75	%
	Gross price	-30%,+30%	4.94	7.05	9.17	$USD/tons$

Table 11.8: Sensitivities for the low, base and high case

11.4.3. Description low, base and high case

In this section, an explanation for the low, base and high case is provided.

In the low case in the sensitivity analysis the least favorable values are assumed. This means the costs and the discount rate are as high as possible, whereas the occupancy and the gross price are as low as possible. In the base case in the sensitivity analysis all most probable values for the parameters are assumed. In the high case in the sensitivity analysis the most favorable values are used. This means the costs and discount rate are as low as possible, whereas the occupancy and the gross price are as high possible.

11.4.4. Results

In this section, the financial results for the three different cases are discussed. The financial results are summed up in Table 11.9. The definitions of the terms shown are listed below:

- BCR: Benefit Cost Ratio, this ratio is calculated by dividing the total discounted revenue of the project by the total discounted costs. If this ratio is above 1, the project will deliver a positive NPV [36].

- IRR: Internal Rate of Return, this is the discount rate that makes the NPV value equal to zero [37].

From the results in Table 11.9, it is clear to see that the base case and the high case are expected to be a good investment. In Figure 11.3, the NPV projection over the years is shown for 30 years. For the base case, it takes 16 years before the NPV becomes positive. Regarding the high case, it takes 8 years before the NPV becomes positive.

	NPV @ 2049 [USD]	**BCR**	**IRR [%]**	**NPV = 0 [years]**
Low	- 5,321,065	0.60	0.00	0
Base	11,003,854	1.92	13.30	16
High	66,520,041	5.25	27.19	8

Table 11.9: Financial results per case

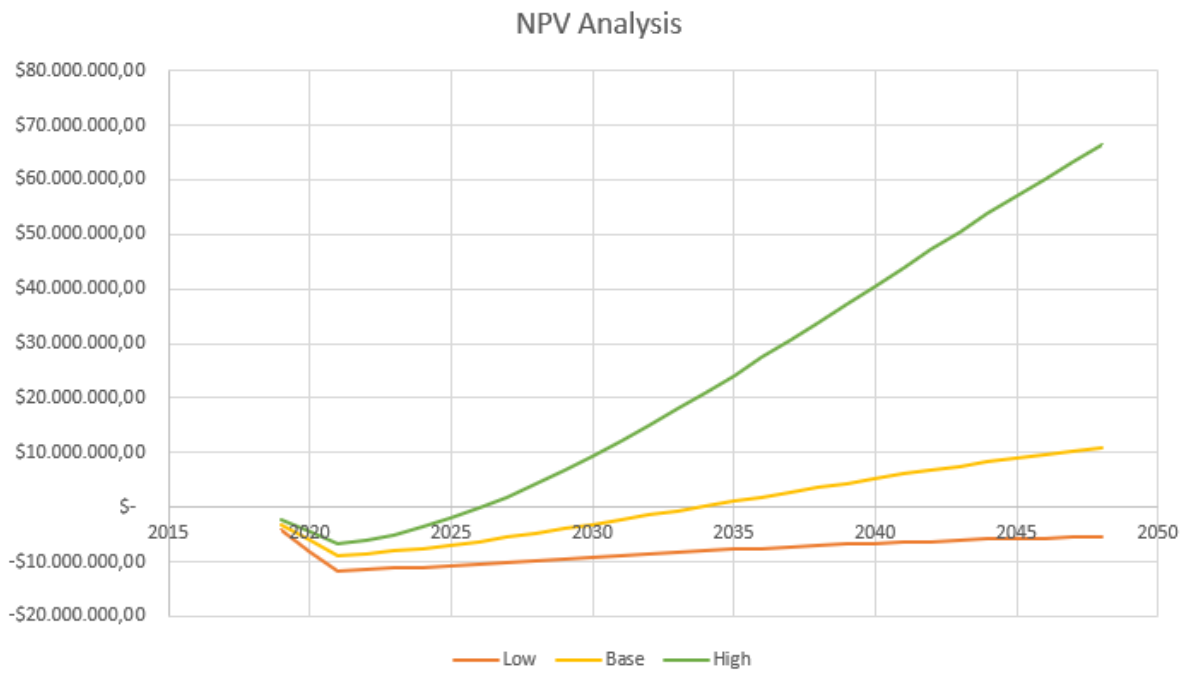

Figure 11.3: NPV Analysis

11.4.5. Recommendations financials

In order for the port project to be profitable, the port of Talcahuano should aim for the following:

- The dredging costs should not exceed 4,630,000 USD.
- The quay wall costs should not exceed 5,700,000 USD.
- The occupancy should reach a minimum value of 35 % by 2049.
- The sale prices of general cargo, bulk and fishery should have a minimum value of the prices used in the reference year 2017. More about this can be read in Appendix N.

12

Planning

This chapter will consist of the work breakdown structure and the the schedule for the project. In these two diagrams the project will be divided into multiple individual components.

12.1. Work breakdown structure

The project is split up in Front-End Engineering Design (FEED), Site Preparation, Dredging and Quay Construction. Each of these categories consist of a number of small components which can be seen as separate tasks with their own starting time and duration.

- The project FEED consist of the preliminary design, detailed design, acquisition and acquisition of the permits. During this stage all of the work is being done in offices and the daily port operation won´t be affected. This phase will take time from the board as meetings and presentations are needed to remain focused on the right design criteria and keep progress going.
- The site preparation contains all activities that need to be finished before construction can start. The activities are divided in the removal of obstacles in order to start the construction of the sheet pile wall and the landfill which is needed for the topside construction. Sitio 2 and the rubble from the earthquake need to be removed before the construction of the new quay can start.
- Before dredging can start a soil analysis is to be performed and the dredging vessel needs to be brought to the Concepcion Bay. Especially the mobilization of the dredging vessel is very important. It has to be planned far ahead and the dredging can not start without it.
- The quay construction is split up in pile driving, sheet wall driving, topside installation and equipment installation. Within these categories there are several sub-activities such as the installation of the fenders, bollards, reinforced concrete floor and so on. In the final work schedule these can be added, but as these depend on the final design they are not specified in this work break down structure yet.

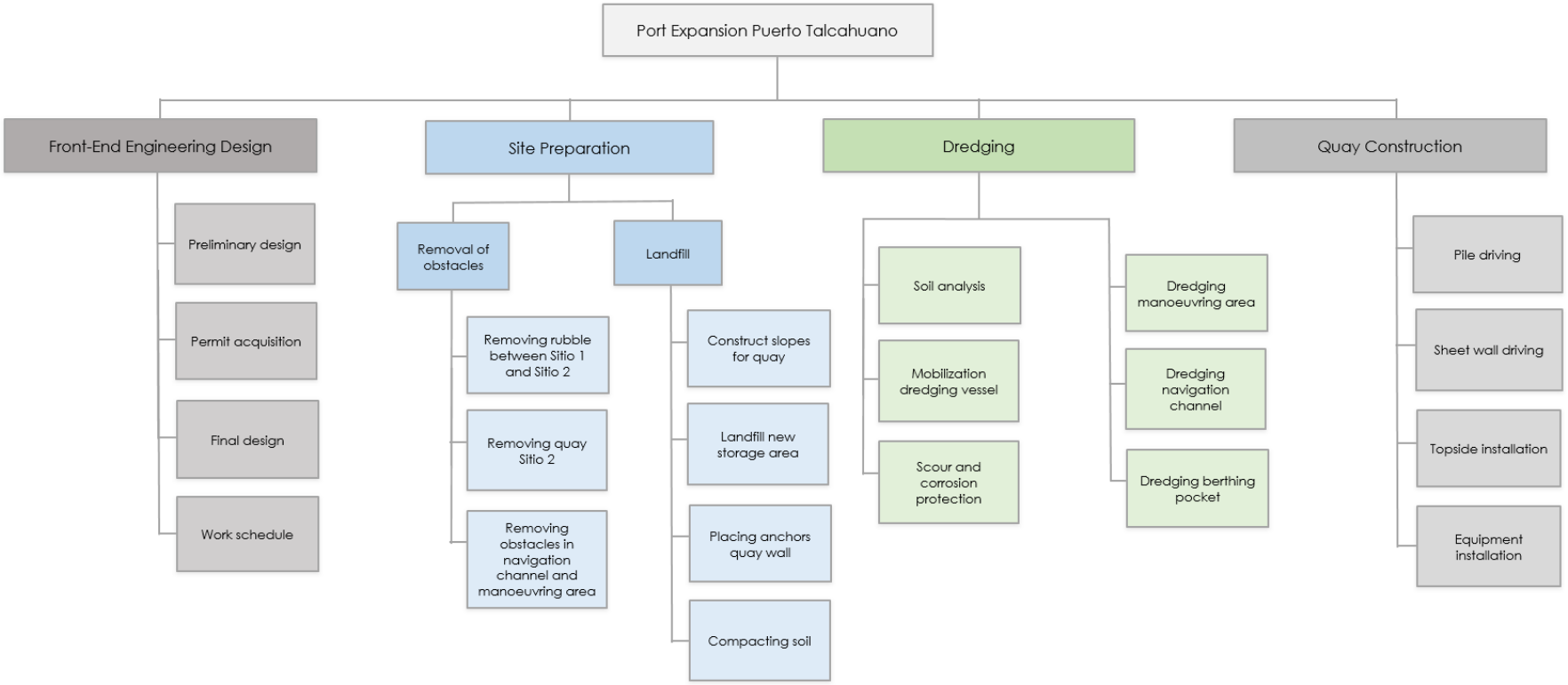

Figure 12.1: Work Breakdown Structure

12.2. Schedule

The work break down structure is used to construct a schedule for the project. In the schedule it should be noted that certain activities can start only when others have finished. Below the most important gate activities are named.

- For the FEED phase of the project it is important to start obtaining the permit as soon as possible, already during the preliminary design phase. If problems for certain permits arise the detailed design can still be adjusted to be in accordance with the permits.
- The work schedule is a live document which will be adjusted and complemented during the project. Also delays and unforeseen obstacles may cause changes.
- The soil analysis for the dredging activities can begin early as no specialized equipment needs to be imported. Obtaining this information early in the progress will help the dredging company plan their dredging strategy and construct an advice for the landfill.
- Even though the final design for the sheet pile wall can be delivered earlier, the fabrication of the components forces the start of construction to hold until the final design is completed.
- The landfill can not start before the sheet pile wall is finished as this structure needs to hold the material in place.
- Also for dredging the berthing pocket it is required that the sheet pile wall is finished. Because the dredging vessel is available for only a limited time, all of the dredging activities are planned around this point.
- During the dredging activities Sitio 1 is likely to have some hinder due to the dredging vessel being in the way of vessels. As the vessels are planning their arrival and departure it should be looked into to plan these action while the dredging vessel is outside the port area to dump its dredged material. While dredging the berthing pocket it is not possible to have a vessel berthed at the quay. Thus especially for this area the the planning should be adjusted such that no vessel is coming until this area is finished.
- The installation of the topside has to wait until the landfill is completed and the material is compacted.
- Finally a clean up and start up is added to the project. During the last two weeks of the project the construction site is cleaned up and all equipment is tested.

From the schedule in Figure 12.2 it is clear that the project will take 110 weeks. The key gates activities are the dredging activities. As advised in Chapter 11 other ports might use the dredging vessel before or afterwards. Therefore the start of the dredging activities may be something the port of Talcahuano is not able to decide for itself. It is therefore important to finish the design of the dredging plan as soon as possible. Also finishing the sheet pile wall allows for the landfill and dredging of the berthing pocket to start. In combination with the just mentioned restrictions of the dredging vessel, the sheet pile wall is also an important gate activity. The mobilization of the dredging vessel and the finishing of the sheet pile wall are therefore marked in red in the schedule. In the current schedule no float is added. In order to reduce the consequence of delays float can be built in before the key gate activities.

It should be noted that the schedule as shown in Figure 12.2 the main focus is on finding the key gate activities and not necessarily the exact length. The total duration of the project depends on many variables such the as bureaucratic system for the permit and the availability of the dredging vessel.

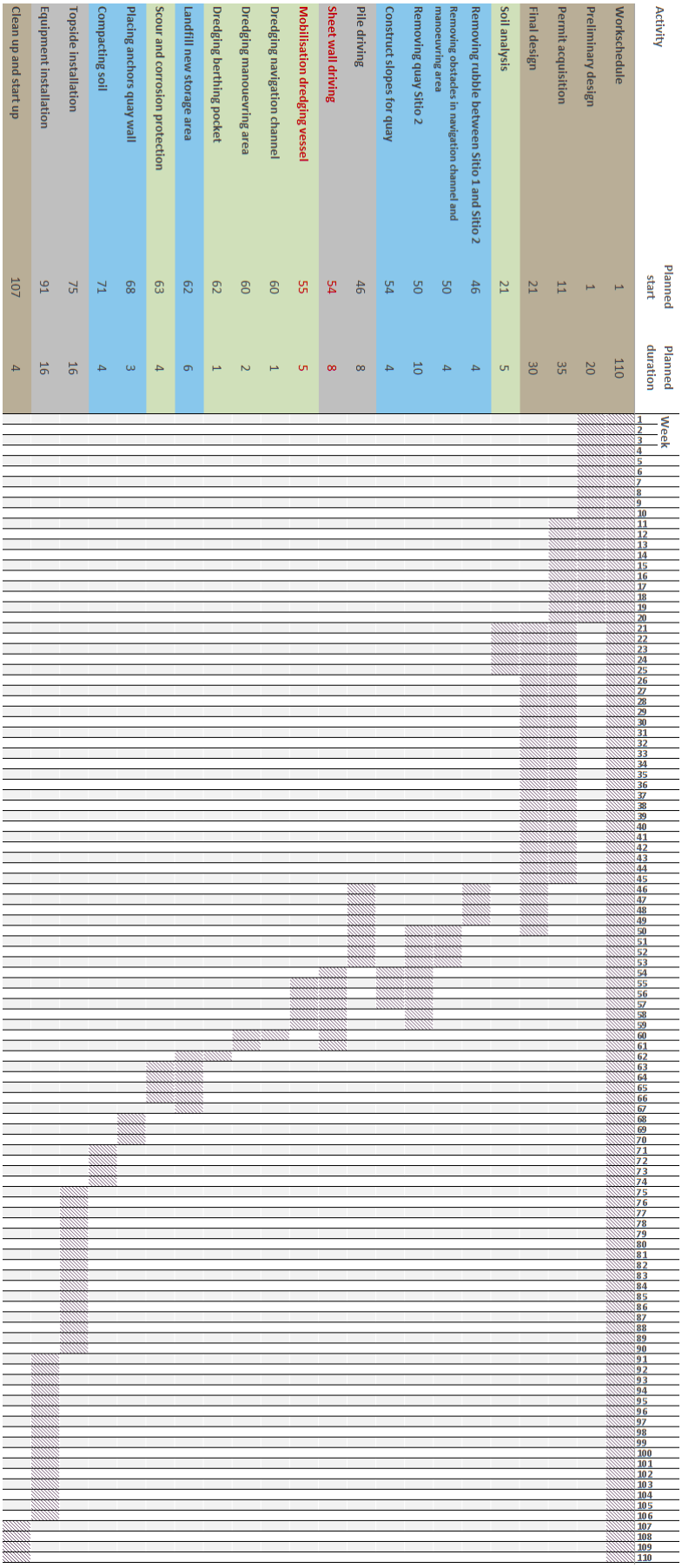

Figure 12.2: Work schedule

IV

Conclusion

13

Conclusions

The operators of the Port of Talcahuano are interested in expanding the port to allow for future growth and a possible new market entrance. The earthquake and tsunami of 2010 has destroyed the port which was only partially rebuilt afterwards. This results in a lower capacity than before the earthquake. After obtaining a new 30 year concession for the port, an expansion is desired in order to re-establish the port´s market share.

As the import of goods in Chile is increasing the market is becoming larger. In order to benefit from the increase in potential throughput, the capacity of the port needs to be increased. The main berth, Sitio 1, is a commercial berth and together with two fishery berths, namely, Sitio 2 and Maria Isabel, and the storage of containers it creates revenue for the port. Because the commercial berth contributes the biggest share of the revenue, it is the most important. In order to create the new berth, which allows two 180 m vessels, one fishery berth may be cut off. The Port of Talcahuano is a public port, but the port operator is a private company. Therefore the city council and ministries of Finance and Public Affairs need to agree on new plans and investments.

The port of Talcahuano is located in the Concepcion Bay which shelters it from harsh conditions outside the bay. The wind and wave climates play only a minor role and also the current is small. The tide is an issue as the depth of the area surrounding the port is relatively small. The difference between high tide and low tide is about 2 m. Together with the bathymetry this is therefore a critical design input for the technical design. Also the occurrence of earthquakes and tsunamis is important to take into account when designing the new port. The seismic activity of the region can cause massive damage to the port as demonstrated in 2010.

Four preliminary designs have been made for the new port. They are designed to provide space for two berths of 180 m long which can both handle a design vessel, the SPL Tarapaca. These designs, referred to as scenarios, consist of a quay design, manoeuvring area and navigation channel design and rough estimates for the costs and potential revenue. Scenario 1, 2 and 4 are an expansion of the current Sitio 1 berth in respectively north, north and south and south direction. Scenario 3 consist of the current Sitio 1 with a jetty towards the east.

The four scenarios have been evaluated by means of a Multi-Criteria Analysis. In the MCA the scenarios scored on the following five criteria: dredging costs, construction costs, loss of revenue during construction, potential market value and environmental impact. Scenario 4, a southward expansion till Maria Isabel, has the highest overall score. This is mainly because the construction can be done without hindering normal operations. Apart from the low losses during construction the potential market value is high.

The most suitable scenario, Scenario 4, is worked out into detail for the final design. The final design consist of the technical design of the old and new quay, a design for the manoeuvring area and navigation channel, a plan for the dredging activities, an earthquake and tsunami impact analysis, a market prospect analysis and a financial analysis.

The dimensions and material properties of the sheet pile (Table 6.2) and anchors (Table 6.1) of the new quay

are found using PLAXIS 2D modelling. An embedded depth of 6.5 m is found for the sheet pile wall, but propeller scour can reduce this depth to 6 m. Based on the fenders of Sitio 1 and the design vessel, the required dimensions of the fenders have been determined. The kind of fender has been chosen from existing fender types. In the current port environment, it can absorb berthing energy for general cargo vessels up to 52700 tonnes. The dimensions are summarized in Table 6.3. Also, the mooring bollard type and dimensions have been determined based on the vessels DWT and the vessel type. Vessels up to 50000 tonnes should be able to moor without failure. The dimensions and type are given in Figure 6.13. The dimensions and material properties of the concrete floor design can be found in Figure 6.10 and Table 6.16. It is found that both main reinforcement and stirrup reinforcement are needed. Per 1 metre length of concrete, 10 main reinforcement bars with a diameter of 28 mm are needed. Per 1 metre width of concrete, 4 stirrup reinforcement bars with a diameter of 14 mm are needed. Several design checks are performed which were all passed for Nieuw Delft. The sheet pile wall at Sitio 1 fails under earthquake loading. The results of all design checks for the two quays are summarized in Tables 6.14 and 6.15.

The manoeuvring area is 250 m wide and runs the full length of the quay as well as an area north of the quay to allow for vessels to extend to the north. On the east side it is extended for accommodate a turning basin with a diameter of 360 m. Along the quay a berthing pocket with a depth of 10.6 m to LAT is designed. The rest of the manoeuvring area is design to a depth of 10.6 m to MSL. This design choice initiates a tidal window on port entrance and exit, but reduces the dredging costs. The navigation channel, designed as a one-way channel, also has a depth of 10.6 m to MSL. It´s length is 1800 m and it´s width is 100 m to which 12 m of slope width is added on both sides to ensure a stable slope and minimal maintenance.

Following from Chapter 8 the dredging design has been determined. In order to save both time and money a tidal window is implemented for the manoeuvring are and navigation channel. This design choice reduces the dredging volume from 881,000 to 607,000 m^3. The berthing pocket is designed to be 10.6 m deep taken from LAT and the rest of the areas will be dredged until 10.6 m below MSL. A sloping angle of 12.5 $degrees$ is used between the dredged area and its surroundings to prevent slope failure. This also reduces the needs for maintenance.

By analyzing the 2010 earthquake and tsunami, lessons can be learned concerning damage prevention. The loss of power and telecommunication can be solved by using backup power and alternatives transponders and receivers for emergencies. Also an emergency protocol should be in place and trained for all staff. An evacuation plan for the vessels in to port must consist of a emergency unberthing procedure and a route for vessel for follow in the case a tsunami is coming towards the port. By analyzing the water level and velocities, a vessel should have enough time to evacuate the port and sail to a safe location within the bay.

The future throughput is estimated to be 0.73 $*10^6 tonnes$ in the base case which is a growth of 270% compared to the current maximum throughput. This future throughput is able to rise even higher until $1.57*10^6 tonnes$ if the port manages to attract business and keep its occupancy higher than 0.35. This high throughput is considered an absolute maximum throughput. To secure a smooth cargo transfer with this growing throughput, infrastructure such as transit sheds can be built. It has showed that the amount of available land area is sufficient to accommodate such infrastructure.

If a market strategy change is made into handling containerized cargo, a throughput of 0.22 $*10^6 TEU$ can be expected. The port is able to make such a change but it is limited in the size of vessels it is able to attend compared to the surrounding container ports.

Regarding the financial analysis of the project, the port expansion project is expected to generate a positive NPV of 11 million USD after 30 years in the base case. The NPV becomes positive after 16 years. A benefit-cost ratio (BCR) of 1.92 is achieved and an IRR of 13.3 %. Therefore, the port expansion project is expected to be profitable.

For the planning of the project it is important to start early with the acquisition of the permits and the planning for the dredging activities. Because a collaboration with other ports is advised for the dredging activities, the planning for the dredging vessel will depend on the other ports as well. Being a gate activity, it is important to plan around the dredging activities. Also float must be built into the schedule to provide room for

changes in the schedule and delays. Following the current planning of the project, from start to completion, should take 110 weeks.

14

Recommendations

During eight weeks of research a lot of analysis have been made in order to develop a design for a port expansion. In this chapter recommendation based on key findings and identified knowledge gaps for the final design are given. The port is advised to pay extra attention to these notes before making further advances on the port development.

14.1. Quay

- Several techniques are available for reducing active horizontal soil pressures on the sheet pile wall of the quay. Such reduction allows for the sheet pile wall to be less rigid, saving material and thus money. One of these techniques is reinforcing the soil. Layers of horizontal grids can be placed in the soil, transforming the active horizontal soil pressure into tensile forces in the grids. A soil column reinforced with such grids can be stable on its own. The sheet pile wall will not be in contact with the soil, and only functions to protect the soil from washing away by the water movement, or as protection for vessel impact. Since the active soil pressure is completely eliminated, a significant saving in material and cost can be realized. Applying such grids with the presence of piles in the ground is still feasible.
  Reinforced soil performs well under earthquake conditions. As the grids absorb a large part of the pressures in the soil, it limits the risk of liquefaction and reduction of the bearing capacity of the soil. For these reasons, this technique might be interesting to implement in the design of the quay. More information and a preliminary design calculation is provided in Appendix L.

- At the quay, the mooring forces and fenders loads result in large shear stress in the foundation pile below. A stress capacity check should be performed to improve the dimensioning of this pile.

- The earthquake analysis of the sheet pile wall is done using design codes and conservative values. For a more thorough and exact analysis of the effect an earthquake will have on the stability of the structure, the following is recommended.

  - A global failure check of the entire structure during earthquake loading should be done. This failure is dependent on the weight of the soil, the shear stress that can be delivered by the soil type and the forces due to the earthquake. For the current stability check, the forces on the sheet pile wall have been modelled to check its stability. However, the structure as a whole, including the anchors, should also be looked at.
  - The free vibration modes of the structure should be determined. This can be done by a modal analysis of the structure. Based on this, the modes of free vibration can be found and the equations from the design code can be used more exact. Next to that, it will be possible to do a spectral analysis.
  - A method that is used often to a more detailed analysis of the effects of earthquakes on a structure is a spectral analysis. It is therefore recommended to do this type of research to further investigate the influence of earthquakes on the structure.

  - Next to these above mentioned analyses, it is also possible to model earthquakes in PLAXIS 2D, using a fitting time series to reenact an earthquake. When a correct time series of a representative earthquake is available, together with the Rayleigh damping coefficients of the structure, it is possible to do a analysis of the influence of an earthquake on the structure. When this information is available, using the model to analyze the influence of earthquakes could also give some useful information.

- For the sheet pile wall in Sitio 1, the earthquake load leads to the internal stress in the sheet pile exceeding the yield point. Due to this, there is plastic deformation and a high probability of failure. Therefore it is recommended to install a new sheet pile wall at this quay.

- As mentioned in Section 6.5.5, due to the strong possibility of large scour holes developing at and near the quay, a bottom protection needs to be installed. This can be done in a few ways, like a block mattress or loose rocks, which can in turn be placed on different filters, like geotextile or a granular filter [25]. Due to there being various possibilities, it is of importance that further research is done to find the best alternative for this particular situatio, from both a financial and a design point of view.

14.2. Dredging and Navigation Channel

- For the dredging activities a vessel is required. Due to the lack of dredging vessels in the west coast of South America it will need to be transported from a different region in the world which is a costly affair. It is therefore recommended to include other nearby ports in this project to share the costs of transportation. Depending on the dredging volumes of the other projects a dredging vessel should be determined. Considering the port of Talcahuano a vessel with the capacity of the Van Oord HAM309 is preferred as the duration of the dredging activities influences not only the costs of the rent of the vessel, but also the hinder caused to the port´s daily business.

- Dredging maintenance activities can be expected to be necessary after 10 years. In shallow areas the current are generally higher and the seabed is more subjected to turbulence due to waves, meaning erosion and deposition will happen faster. Therefore, extra care should be taken for the south side of the berthing pocket and the manoeuvring area as the surroundings are very shallow. It is advised to closely monitor the bathymetry of this area and perform dredging maintenance activities when needed.

- Depending on the quality of the dredged material, it may be used for the landfill of the new area created. In the final design a volume of approximately 50,000 m^3 needs to be filled with sand for to level the quay area. The dredged volume more than covers the landfill volume. The most ideal situation for the planning and logistics would be to fill the extension of the quay with the sand dredged in the extended manoeuvring area. The price and logistics of gaining this amount of sand can be reduced if the dredging vessel is able to pump the dredged material through a pipeline to shore.More about this can be read in Appendix M.

- Implementing a tidal window saves approximately a quarter of the dredging volume. It is up to the port to decide if it can be managed to let the high draught vessels enter or leave the berth only during a tide above MSL.

- The currently used UKC of 0.6 m is concluded to be on the low side compared to the PIANC regulations. When larger vessels enter the navigation channel the UKC will most likely become larger because the squat will become larger. It is therefore recommended to use a larger UKC in the future for the port.

14.3. Earthquake impact

- From the earthquake and tsunami impact analysis it can be concluded that the backup power, backup communication systems and emergency protocols should be available and tested throughout the port´s facilities. An evacuation plan for vessel should include an emergency unberthing procedure and has to direct all vessel outside the port towards the entrance of the bay.

14.4. Market prospect

- Given the current throughput growth, it is estimated that waiting times will start to occur around the year 2023. It is thus advised to execute an expansion plan before the end of 2023.
- It is important to maintain a stable unloading rate with the expected higher throughput. It is expected that the current unloading method of direct transport or temporary container storage will not be able to cope with the growing unloading rate. For this reason it is advised to investigate possibilities of building a transfer shed to secure temporary storage and a smooth cargo transfer.

14.5. Financials

- In order for the port project to be profitable and have a minimum NPV of 11 million USD, the port should aim for a minimum occupancy of 35 % in 2049. Also, the port should aim for the dredging costs not to exceed 4,630,000 USD, and for the quay wall costs not to exceed 5,700,000 USD.

14.6. Planning

- For the schedule of the project it is useful to build in some float before and after the key activities, namely mobilization of the dredging vessel and driving of the sheet wall. This will reduce the consequences of delays significantly.

Bibliography

[1] W A van Elzacker, Floris Besseling, Arny Lengkeek, J.G. de Gijt, S.N. Jonkman, and R.J.Brinkgreve . Evaluation of performance of analytical and numerical methods to account for liquefaction effects on the seismic response of anchored quay walls. PD eartquake journal, 09 2017.

[2] Brealey Myers Allen. *Principles of Corporate Finance*. Mc Graw-Hill/Irwin, 2011.

[3] Dr.ir. R. Aranguiz. maxinundation.m, 2012.

[4] Dr.ir. R. Aranguiz. tidegauges.m, 2012.

[5] Dr.ir. R. Aranguiz. animate$_b$.m,2012.

[6] Dr.ir. R. Aranguiz, 2018.

[7] Jonathan Belles, 2018. URL `https://weather.com/storms/hurricane/news/2018-05-08-subtropical-cyclone-chile`.

[8] J. Beya. Escuela de Ingenieria Civil Oceanica - Universidad de Valparaiso.

[9] C.R. Braam. *Constructieleer gewapend beton*. Aeneas Media, 2000.

[10] Ship bunker. Yearly average fuel price ifo380, 2018. URL `https://shipandbunker.com/prices/am`.

[11] Tensar International BV. Tensar software output for proyecto puerto talcahuano, 2018.

[12] J.G. de Gijt. *Structures in hydraulic engineering - Port Infrastructure*. Delft University of Technology, 2004.

[13] J.G. de Gijt. Cost of quay walls. page 7, 2011.

[14] Instituto Nacional de Normalizacion. Nch 2369: Diseño sísmico de estructuras e instalaciones industriales, 2013.

[15] Universidad Catolica de Santisima Concepcion. Diseño de obras portuarias, 2018.

[16] J. De Bont Port Engineer Royal Haskoning DHV.

[17] Maritime Directory. Spl tarapaca vessel specifications, 2018. URL `https://directory.marinelink.com/ships/ship/spl-tarapaca-9077`.

[18] J.P.L. dos Santos. Construction with prefabricated caissons vs. open-piled quay wall in marine works. page 12, 2011.

[19] R.E. Thomson E.A. Kulikov, A.B. Rabinovich. Estimation of tsunami risk for the coasts of peru and northern chile. pages 185–209, 2005.

[20] EAU. *Recommendations of the Committee for Waterfront Structures Harbours and Waterways*. 2004.

[21] Eurocode.

[22] S. Fagg. Anchored shoring systems with external corners, 2016. URL `http://shirley.net.au/news/anchored-shoring-systems-external-corners`.

[23] International Transport Forum. Ports policy review of chile. page 103, 2016.

[24] GEOFUN. 5.5 informe de mecánica de suelos en sitio 1, 2012.

[25] Henk Jan Verhagen Gerrit J. Schiereck. *Introduction to Bed, bank and shore protection*. Delft Academic Press, 2016.

[26] J. G. de Gijt and M. L. Broeken. *Quay walls*. CRC Press/Balkema, an imprint of the Taylor Francis Group, an informa business, 2014.

[27] Google. Google maps, n.d. URL https://www.google.nl/maps/place/Empresa+Portuaria+Talcahuano+San+Vicente/@-36.6724394,-73.1080877,17909m/data=!3m1!1e3!4m5!3m4!1s0x9668359f6e9f925d:0x7be930d3760860f0!8m2!3d-36.7145733!4d-73.1103706.

[28] Project group CF52. Port expansion lirquen, 2005.

[29] Max Groups. High performance cone fender, 2019. URL https://max-groups.com/products/solid-marine-rubber-fender/cone-fender/.

[30] Max Groups. Choose a suitable marine fender design system, 2019. URL https://max-groups.com/rubber-fender-design-selection/.

[31] Coenraad Hartsuijker. *Toegepaste Mechanica: Spanningen, vervormingen, verplaatsingen*. Academic Service, 2001.

[32] Histarmar. Spl tarapaca, 2011. URL http://www.histarmar.com.ar/MarinaMercanteExtr/MarinaMercanteChile/0Mercantes-S-Z-/SPLTarapaca.htm.

[33] Leo H. Holthuijsen. *Waves in oceanic and coastal waters*. Cambridge University Press, 2015.

[34] IOC, 2015. URL http://www.ioc-sealevelmonitoring.org/index.php.

[35] Kimmo K. Kahma and Charles J. Calkoen. Reconciling discrepancies in the observed growth of wind-generated waves. *Journal of Physical Oceanography*, 22(12):1389–1405, 1992. doi: 10.1175/1520-0485(1992)022<1389:rditog>2.0.co;2.

[36] Will Kenton. Benefit cost ratio - bcr, 2018. URL https://www.investopedia.com/terms/b/bcr.asp.

[37] Will Kenton. Internal rate of return - irr, 2018. URL https://www.investopedia.com/terms/i/irr.asp.

[38] M. Lagos. Tsunamis de origen cercano a las costas de chile, re-vista de geografía norte grande. page 93–102, 2000.

[39] H. Ligteringen. *Ports and Terminals*. Delft Academy Press, 2017.

[40] Calbuco Ingenieros Ltda. Informe tecnico n°594-it-02 rehabilitacion sitio n° 1, 2012.

[41] MacroTrends. Euro-dollar exchange rate - historical chart, 2018. URL https://www.macrotrends.net/2548/euro-dollar-exchange-rate-historical-chart.

[42] Jan Maertens. Stability of underwater slopes realized by means of a suction dredger, 2017.

[43] Mundo Marítimo. Información marítima de latinoamérica, 2018. URL https://www.mundomaritimo.cl/noticias/puertos-chilenos-movilizaron-un-54-mas-de-teus-en-2017-respecto-del-ano-anterior.

[44] Dr.ir. Sape A. Miedema. Oe4607 dredging calculations excel file, 2018.

[45] J. Monge. Estudios de riesgo de tsunami en costas chilenas. jornadas chilenas de sismología en ingeniería antisísmica. page 3–22, 1993.

[46] NipponSteel Nippon Steel Sumitomo Metal Corporation. Steel sheet piles, 2018.

[47] US Army Corp of Engineers. *Engineering Manual EM 1110-2-2504*. US Army, 1994.

[48] US Army Corps of Engineers. Us army corps of engineers website. yaquina dredge brochure, 1981. URL https://www.nwp.usace.army.mil/Portals/24/docs/navigation/vessels/Dredge_Yaquina_brochure.pdf.

[49] Association of Swiss Road and Traffic Engineers.

[50] Van Oord. Van oord - ham 309, 2010. URL http://www.dredgepoint.org/dredging-database/sites/default/files/attachment-equipment/ham_309.pdf.

[51] C.P. TALCAHUANO ORDINARIO. Habilita la operaciÓn del sitio n° 2, de talcahuano terminal portuario s.a. 2017.

[52] OSD-IMT. Osd-imt azistern 3360. Brochure, 2010. URL https://www.osd-imt.com/-/media/damen/osd/portfolio/09_tug_harbour-tugs/azistern-3360/factsheet_azistern_3360.pdf?la=en.

[53] PIANC. *Harbour Approach Channels Design Guidelines*. PIANC, 2014.

[54] PIANC. *Guidelines for protecting berthing structures from scour caused by ships*. PIANC, 2015.

[55] PLAXIS. Phi-c reduction and comparison with bishop's method, 2016.

[56] PLAXIS. *PLAXIS 2D Tutorial Manual 2018*. 2018.

[57] K. Terzaghi R.B. Peck. *Soil Mechanics in Engineering Practice*. Wiley - Interscience, 1948.

[58] Lucas Silveira. Integrated method for optimal channel design. 03 2017.

[59] D.W. Hight M.G.H. Stevens. An analysis of the california bearing ratio test in saturated clays. 1984.

[60] LTD Sumitomo Rubber Industries. New selection of fender, 2018.

[61] USGS (United States Geological Survey. Magnitude 8.8 - offshore maule, chile, 2010. URL http://www.http://earthquake.usgs.gov/earthquakes/recenteqsww/Quakes/us2010tfan.php.

[62] Trelleborg Marine Systems. The bollard guide, 2019.

[63] Terminal Portuario Talcahuano. Estudio de maniobrabilidad sitio 1, 2014.

[64] Terminal Portuario Talcahuano. Estadistica octubre 2018 - statistical information of puerto talcahuano containing throughput data, waiting times, occupation and calls/month infromation, 2018.

[65] John. F. Tavolaro. Overdepth dredging and characterization depth reommenations, 2007.

[66] COPRI Chile Earthquake Investigation Team. *Chile Earthquake and Tsunami of 2010, Performance of Coastal Infrastructure*. 2013.

[67] C.A. Thoresen. *Port Designer's Handbook: recommendations and guidelines*. Thomas Telford Publishing, 2003.

[68] Dr. Cornelis van Dorsser. Economics of port masterplanning, 2018.

[69] Leo. C. van Rijn. Channel slopes of mud, silt and sand. 2018.

[70] A. Verruijt. *Soil Mechanics*. Delft University of Technology, 2012.

[71] J.C. Wasserman. Journal of environmental management. page 8, 2013.

[72] J.F. Potter W.D. Powel. The structural design of bitumenous roads. 1984.

[73] K. Wong. Cost elements to be considered in the design of marine infrastructures – jetties and dredging. page 16, 2016.

V

Appendices

A

Port lay-out

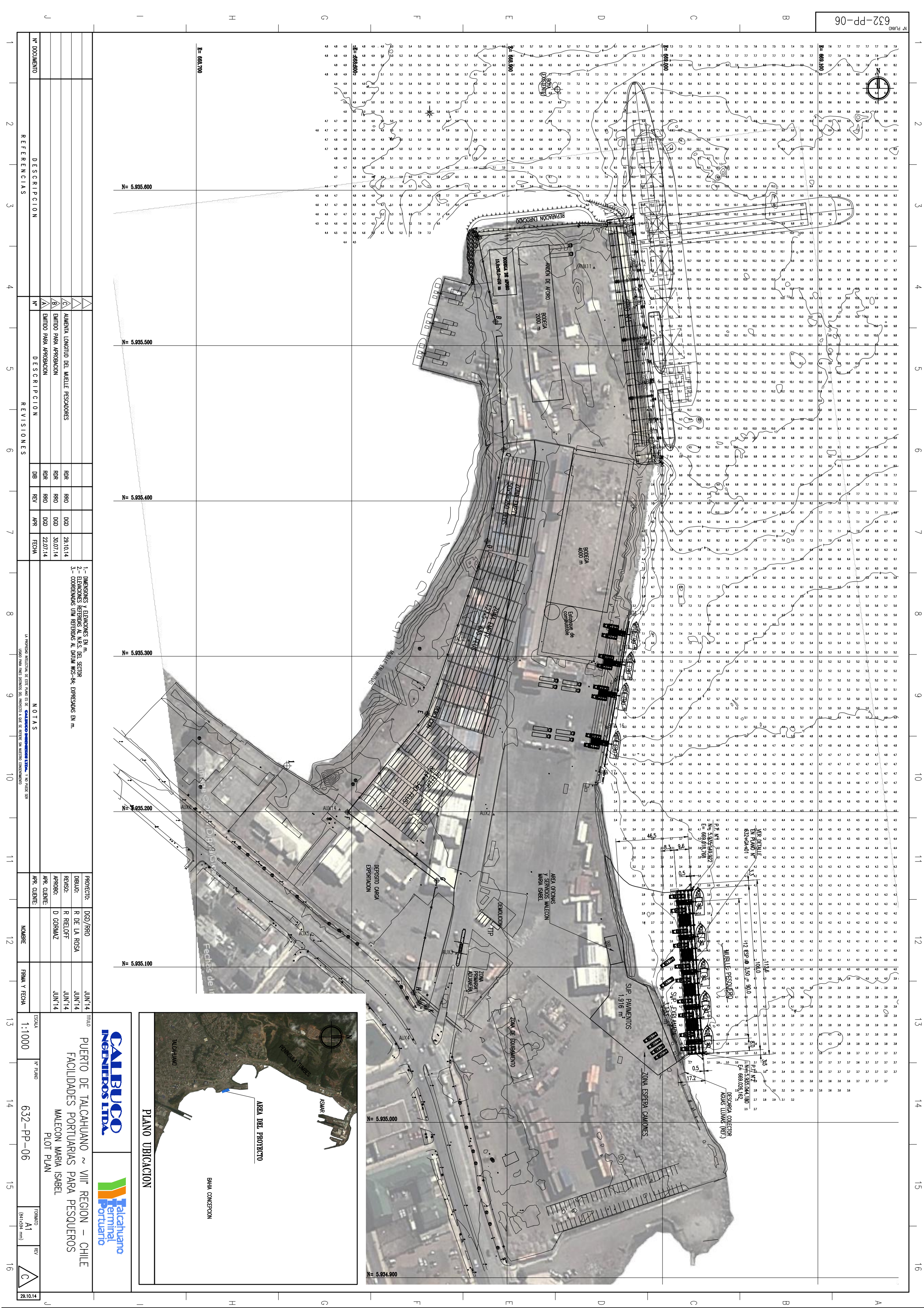

Figure A.1: Port lay-out

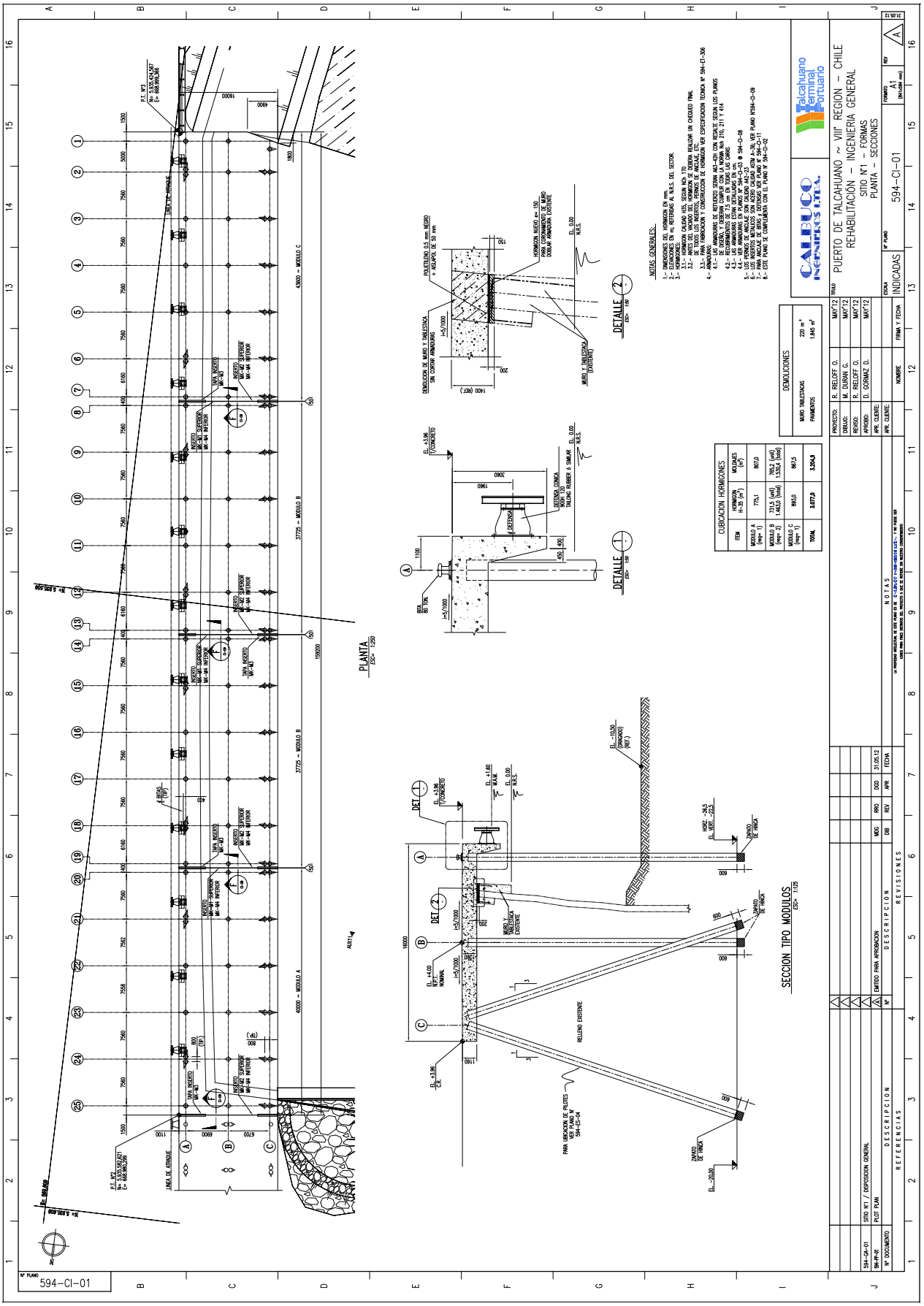

Figure A.2: Technical drawing of the quay wall at Sitio 1.

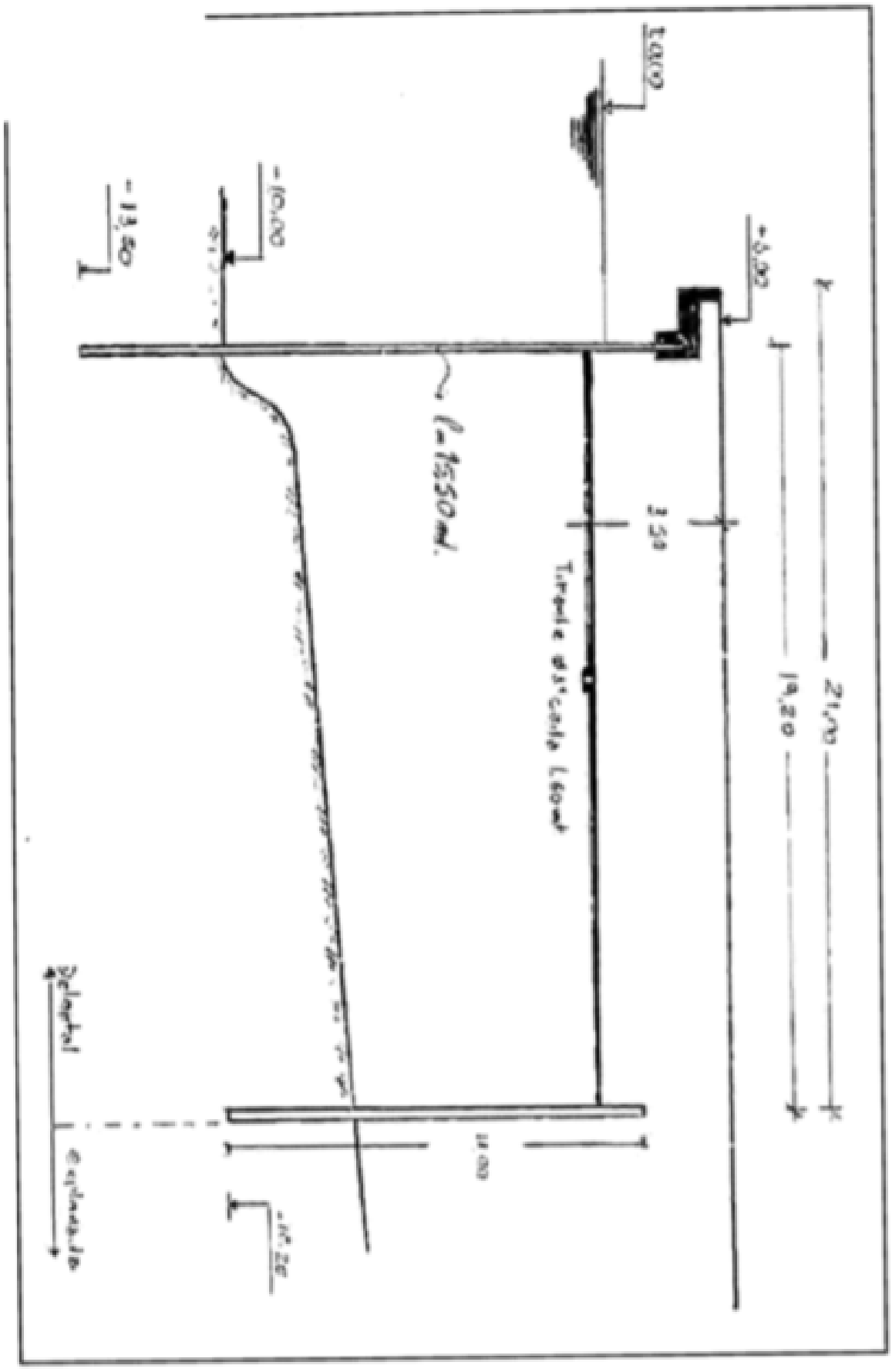

Figure A.3: Technical drawing of the quay wall at Sitio 1.

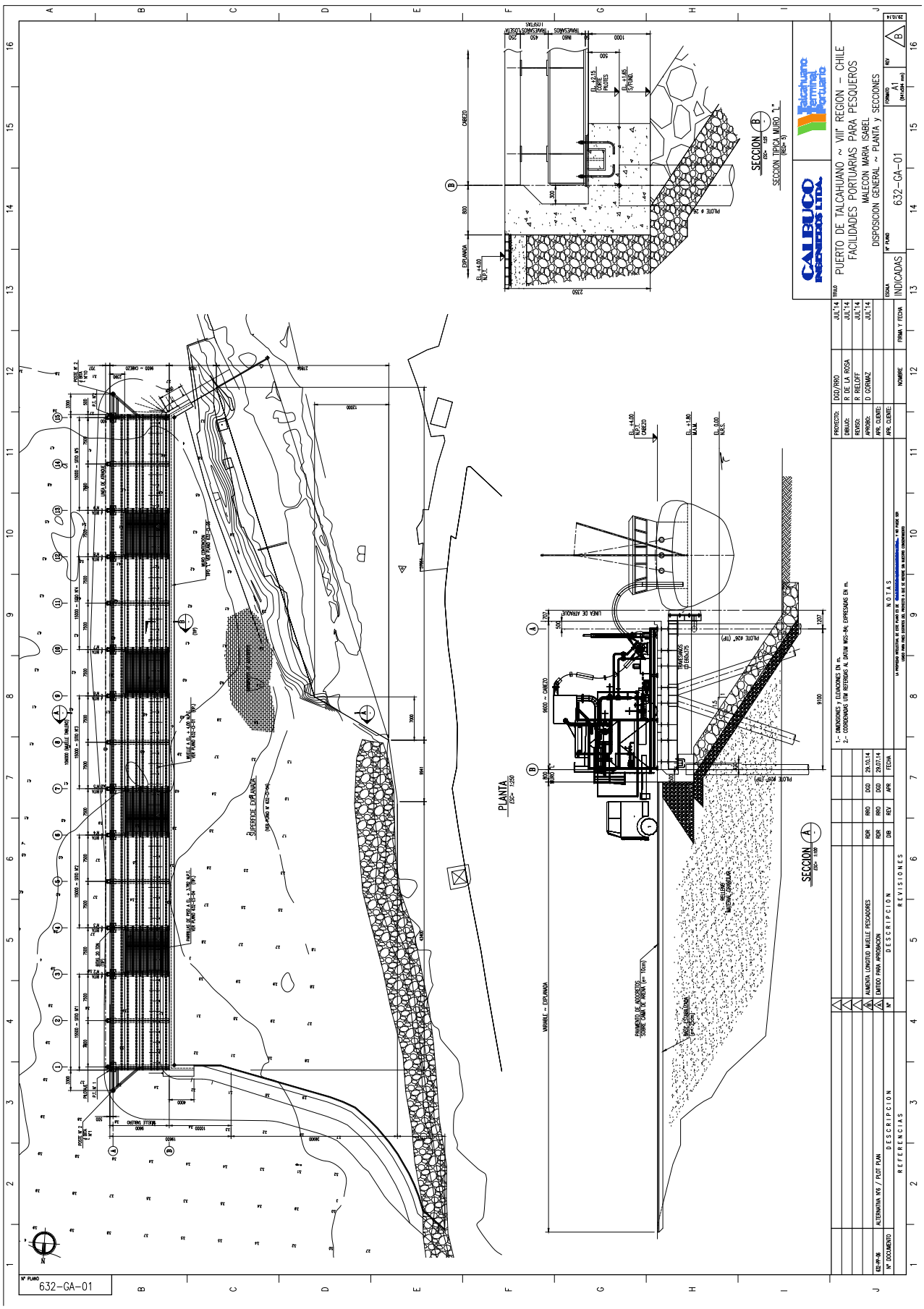

Figure A.4: Technical drawing of the quay wall at Sitio 1.

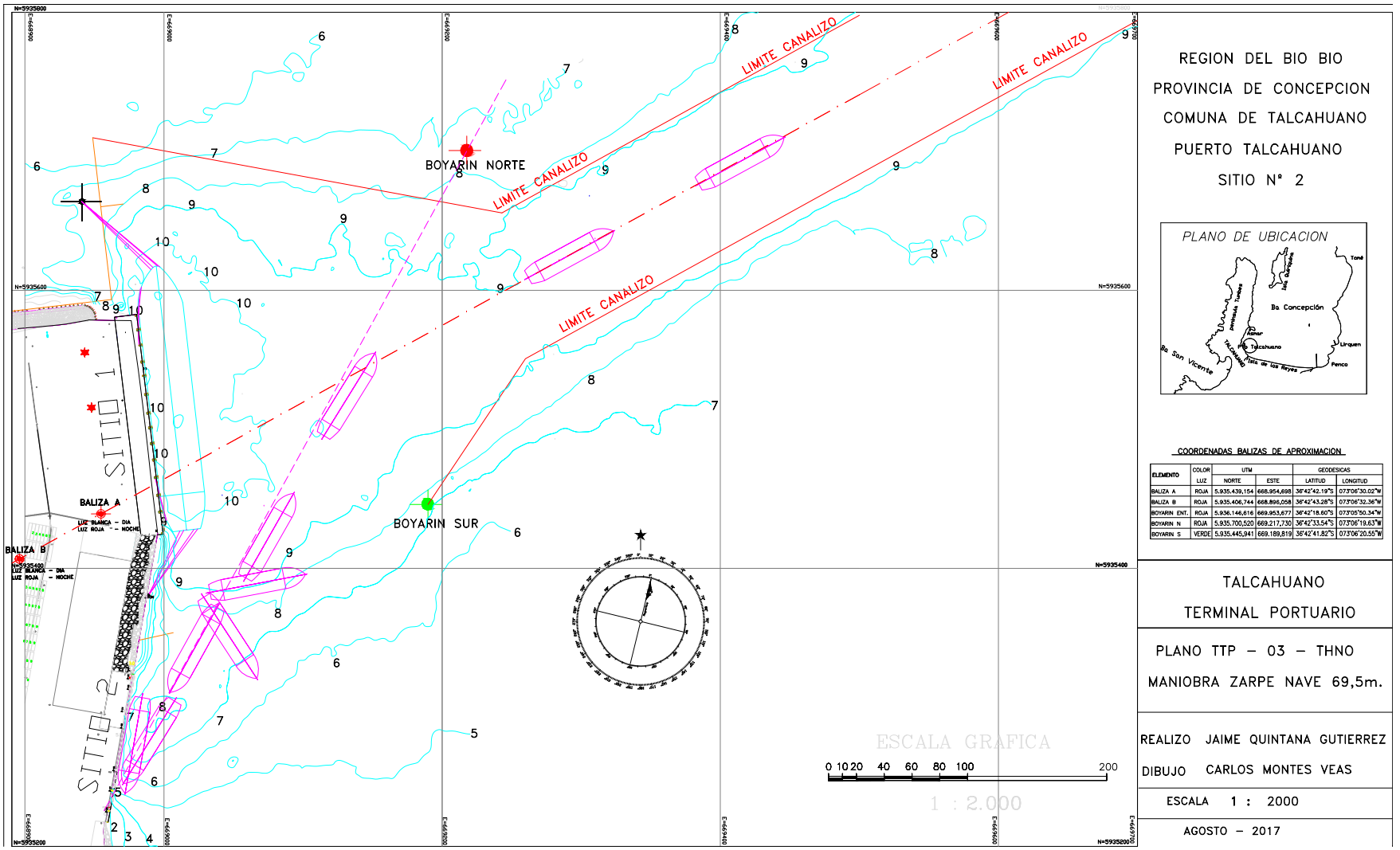

Figure A.5: Bathymetry and Navigation Channel Port of Talcahuano 2017.

B

Statistical information Puerto Talcahuano

INFORMACION ESTADISTICA ADICIONAL MENSUAL - PUERTO DE TALCAHUANO

OCTUBRE 2018

Multipurpose ships

MES	2014	2015	2016	2017	2018
Ene	0	1	0	3	8
Feb	0	0	2	0	1
Mar	0	0	5	3	5
Abr	1	0	1	1	1
May	0	3	9	1	5
Jun	1	1	5	1	2
Jul	0	0	3	3	2
Ago	2	2	3	3	2
Sep	1	1	1	2	2
Oct	1	0	5	2	1
Nov	0	4	7	1	
Dic	1	3	3	1	

Accumulative

2014	2015	2016	2017	2018
0	1	0	3	8
0	1	2	3	9
0	1	7	6	14
1	1	8	7	15
1	4	17	8	20
2	5	22	9	22
2	5	25	12	24
4	7	28	15	26
5	8	8	8	28
6	8	8	8	29
6	12	15	9	29
7	15	18	10	29

Total tonnage

2014	2015	2016	2017	2018
0	900	0	30.952	32.102
0	11.792	18	0	22.759
0	0	23.658	17.714	38.175
5397	0	13.299	11.860	23.629
0	210	12.170	1	23.681
11031	2.400	15.888	0	17.750
0	0	4.830	46.302	53.359
5431	18.859	44.838	11.880	77
5930	177	232	28.751	51.063
902	11.390	31.804	23.424	263
0	11.777	12.071	11.542	
1502	23.543	9.610	27.046	

ACUMULADO

2014	2015	2016	2017	2018
0	900	0	30.952	32.102
0	12.692	18	30.952	54.861
0	12.692	23.676	48.666	93.036
5.397	12.692	36.975	60.526	116.665
5.397	12.902	49.145	60.527	140.346
16.428	15.302	65.033	60.527	158.096
16.428	15.302	69.863	106.829	211.455
21.859	34.161	114.701	118.709	211.532
27.789	34.338	114.933	147.460	262.595
28.691	45.728	146.737	170.884	262.858
28.691	57.505	158.808	182.426	262.858
30.193	81.048	168.418	209.472	262.858

ESPERA ARRIBO-ATRAQUE

2014	2015	2016	2017	2018
0	0	0	0	0
0	0	0	0	0
0	0	0	0	0
0	0	0	0	0
0	0	0	0	0
0	0	0	0	0
0	0	0	0	0
0	0	0	0	0
0	0	0	0	0
0	0	0	0	
0	0	0	0	
0	0	0	0	

ACUMULADO

2014	2015	2016	2017	2018
0	0	0	0	0
0	0	0	0	0
0	0	0	0	0
0	0	0	0	0
0	0	0	0	0
0	0	0	0	0
0	0	0	0	0
0	0	0	0	0
0	0	0	0	0
0	0	0	0	
0	0	0	0	
0	0	0	0	

Container ships

MES	2014	2015	2016	2017	2018
Ene	0	0	0	0	0
Feb	0	0	0	0	0
Mar	0	0	0	0	0
Abr	0	0	0	0	0
May	0	0	0	0	0
Jun	0	0	0	0	0
Jul	0	0	0	0	0
Ago	0	1	0	0	0
Sep	0	0	0	0	0
Oct	0	0	0	0	0
Nov	0	0	0	0	
Dic	0	0	0	0	

ACUMULADO

2014	2015	2016	2017	2018
0	0	0	0	0
0	0	0	0	0
0	0	0	0	0
0	0	0	0	0
0	0	0	0	0
0	0	0	0	0
0	0	0	0	0
0	1	0	0	0
0	0	0	0	0
0	0	0	0	0
0	0	0	0	0
0	0	0	0	0

OCUPACIÓN

2014	2015	2016	2017	2018
0,00	5,51	0	22,04	36,02
0,00	21,43	0,57	0,00	29,91
0,00	0,00	30,65	13,98	38,98
33,19	0,00	14,31	8,89	17,36
0,00	15,59	44,35	3,49	25,13
16,25	17,92	24,17	0,69	19,58
0,00	0,00	12,63	32,66	56,32
42,74	33,06	44,49	14,92	3,90
15,69	0,69	0,56	30,28	45,69
5,38	11,69	41,80	26,48	1,88
0,00	13,89	16,53	11,94	
23,39	24,19	10,22	20,03	

ACUMULADO

2014	2015	2016	2017	2018
0,00	5,51	0,00	22,04	36,02
0,00	13,06	0,28	11,58	33,12
0,00	8,56	10,62	12,41	35,14
8,30	6,42	11,54	11,53	30,69
6,59	8,31	18,23	9,88	29,55
8,20	9,90	19,21	8,36	27,90
7,00	8,45	18,25	11,91	32,06
11,56	11,59	21,58	12,29	28,46
12,01	10,39	19,28	14,27	30,36
11,33	10,53	21,57	15,52	27,45
10,32	10,83	21,12	15,19	
11,43	11,96	20,20	15,61	

M-E-H

2014	2015	2016	2017	2018
0	2.624	0	24.406	36.531
0	11.917	96	0	27.339
0	0	35.861	13.946	43.091
31548	0	27.721	8.896	22.000
0	5.484	36.404	1.144	23.028
17310	18.705	23.580	445	19.206
0	0	12.176	42.336	61.822
42223	33.573	51.156	12.154	1.236
15707	695	320	32.527	45.515
2560	12.093	39.076	25.515	2.002
0	12.074	13.827	11.604	
21054	27605	10.219	20.287	

ACUMULADO

2014	2015	2016	2017	2018
0	2.624	0	24.406	36.531
0	14.541	96	24.406	63.870
0	14.541	35.957	38.352	106.961
31.548	14.541	63.678	47.248	128.961
31.548	20.025	100.082	48.392	151.989
48.858	38.730	123.662	48.837	171.195
48.858	38.730	135.838	91.173	233.017
91.081	72.303	186.994	103.327	234.253
106.788	72.998	187.314	135.854	279.768
109.348	85.091	226.390	161.369	281.770
109.348	97.165	240.217	172.973	281.770
130.402	124.770	250.436	193.260	281.770

Bulk ships

MES	2014	2015	2016	2017	2018
Ene	0	0	0	0	1
Feb	0	3	0	0	2
Mar	0	0	1	0	2
Abr	0	0	1	0	1
May	0	0	0	0	0
Jun	1	0	0	0	1
Jul	0	0	0	2	2
Ago	1	0	2	1	0
Sep	0	0	0	2	2
Oct	0	1	2	1	0
Nov	0	0	0	1	
Dic	0	0	0	2	

ACUMULADO

2014	2015	2016	2017	2018
0	0	0	0	1
0	3	0	0	3
0	3	1	0	5
0	3	2	0	6
0	3	2	0	6
1	3	2	0	7
1	3	2	2	9
2	3	4	3	9
2	3	4	5	11
2	4	6	6	11
2	4	6	7	11
2	4	6	9	11

Rendement Tonnage verwerkt per uur

2014	2015	2016	2017	2018
0,00	21,95	0,00	188,73	119,78
0,00	81,89	4,50	0,00	113,23
0,00	0,00	103,76	170,33	131,64
22,58	0,00	129,12	185,31	189,03
0,00	1,81	36,88	0,04	126,64
94,28	18,60	91,31	0,00	125,89
0,00	0,00	51,38	190,54	127,35
17,08	76,66	135,46	107,03	2,66
52,48	35,40	58,00	131,89	155,21
22,55	130,92	102,26	118,90	18,79
0,00	117,77	101,44	134,21	
8,63	130,79	126,45	181,52	

Accumulatief rendement tonnage verwerk

2014	2015	2016	2017	2018
0	21,95	0	188,73	119,78
0	68,61	4,50	188,73	116,97
0	68,61	102,05	181,59	122,58
23	68,61	110,37	182,31	131,97
23	42,86	73,90	169,07	131,04
117	35,59	77,51	166,74	130,44
117	35,59	74,88	176,29	129,65
134	50,53	90,74	165,56	127,43
186	50,42	90,64	157,71	132,02
209	59,54	92,93	150,96	131,23
209	66,25	93,53	149,78	
218	77,34	94,94	153,23	

PARTICIPACIÓN MERCADO

2014	2015	2016	2017	2018
0	0	0	0	0
0	0	0	0	0
0	0	0	0	0
0	0	0	0	0
0	0	0	0	0
0	0	0	0	0
0	0	0	0	0
0	0	0	0	0
0	0	0	0	0
0	0	0	0	0
0	0	0	0	
0	0	0	0	

ACUMULADO

2014	2015	2016	2017	2018
0	0	0	0	0
0	0	0	0	0
0	0	0	0	0
0	0	0	0	0
0	0	0	0	0
0	0	0	0	0
0	0	0	0	0
0	0	0	0	0
0	0	0	0	0
0	0	0	0	0
0	0	0	0	
0	0	0	0	

HORAS DISPONIBLES

	MES	2014	2015	2016	2017	2018
1	Ene	0	744	744	744	744
2	Feb	0	672	696	672	672
3	Mar	0	744	744	744	744
4	Abr	720	720	720	720	720
5	May	744	744	744	744	744
6	Jun	720	720	720	720	720
7	Jul	744	744	744	744	744
8	Ago	744	744	744	744	744
9	Sep	720	720	720	720	720
10	Oct	744	744	744	744	744
11	Nov	720	720	720	720	
12	Dic	744	744	744	744	

ACUMULADO

2014	2015	2016	2017	2018
0	744	744	744	744
0	1.416	1.440	1.416	1.416
0	2.160	2.184	2.160	2.160
720	2.880	2.904	2.880	2.880
1.464	3.624	3.648	3.624	3.624
2.184	4.344	4.368	4.344	4.344
2.928	5.088	5.112	5.088	5.088
3.672	5.832	5.856	5.832	5.832
4.392	6.552	6.576	6.552	6.552
5.136	7.296	7.320	7.296	7.296
5.856	8.016	8.040	8.016	7.296
6.600	8.760	8.784	8.760	7.296

STAY (hours)

2014	2015	2016	2017	2018
0	41	0	164	268
0	144	4	0	201
0	0	228	104	290
239	0	103	64	125
0	116	330	26	187
117	129	174	5	141
0	0	94	243	419
318	246	331	111	29
113	5	4	218	329
40	87	311	197	14
0	100	119	86	
174	180	76	149	

Accumulative

2014	2015	2016	2017	2018
0	41	0	164	268
0	185	4	164	469
0	185	232	268	759
239	185	335	332	884
239	301	665	358	1.071
356	430	839	363	1.212
356	430	933	606	1.631
674	676	1.264	717	1.660
787	681	1.268	935	1.989
827	768	1.579	1.132	2.003
827	868	1.698	1.218	2.003
1.001	1.048	1.774	1.367	2.003

TIEMPOS DE INACTIVIDAD (TNT)

2014	2015	2016	2017	2018
0	24,52	0	0	0
0	54,47	0	0	0
0	0	45,55	0	0
104,08	0	56,74	0	0
0	0	145,79	0	0
17,58	27,85	75,7	0	0
0	0	0	0	0
228,07	97,96	0	0	0
0	0,00	0	0	0
17,33	23,44	0	0	0
0	46,48	0	0	
23,8	75,81	0	0	

ACUMULADO

2014	2015	2016	2017	2018
0	24,52	0	0	0
0	78,99	0	0	0
0	78,99	45,55	0	0
104	78,99	102,29	0	0
104	78,99	248,08	0	0
122	106,84	323,78	0	0
122	106,84	323,78	0	0
350	204,80	323,78	0	0
350	204,80	323,78	0	0
367	228,24	323,78	0	0
367	274,72	323,78	0	
391	350,53	0	0	

FERTILIZANTES

	MES	2014	2015	2016	2017	2018
1	Ene	0	0	0	0	0
2	Feb	0	0	0	0	0
3	Mar	0	0	0	0	0
4	Abr	0	0	0	0	0
5	May	0	0	0	0	0
6	Jun	0	0	0	0	0
7	Jul	0	0	0	0	0
8	Ago	0	0	3.382	0	0
9	Sep	0	0	0	0	0
10	Oct	0	0	0	0	0
11	Nov	0	0	0	0	
12	Dic	0	0	0	0	

ACUMULADO

2014	2015	2016	2017	2018
0	0	0	0	0
0	0	0	0	0
0	0	0	0	0
0	0	0	0	0
0	0	0	0	0
0	0	0	0	0
0	0	0	0	0
0	0	3.382	0	0
0	0	3.382	0	0
0	0	3.382	0	0
0	0	3.382	0	
0	0	3.382	0	

SAL

2014	2015	2016	2017	2018
0	0	0	20.931	20.361
0	11.271	0	0	11.507
0	0	20.123	17.373	27.822
0	0	12.799	11.808	23.626
0	0	0	0	11.566
0	0	11.695	0	6.449
0	0	0	46.268	30.178
0	15.621	29.355	11.797	0
0	0	0	25.400	40.876
0	11.390	31.555	11.609	0
0	11.604	11.419	11.534	
0	23.223	0	27.010	

ACUMULADO

2014	2015	2016	2017	2018
0	0	0	20.931	20.361
0	11.271	0	20.931	31.868
0	11.271	20.123	38.304	59.690
0	11.271	32.922	50.112	83.316
0	11.271	32.922	50.112	94.882
0	11.271	44.617	50.112	101.331
0	11.271	44.617	96.380	131.509
0	26.892	73.972	108.177	131.509
0	26.892	73.972	133.577	172.385
0	38.282	105.527	145.186	172.385
0	49.886	116.946	156.720	172.385
0	73.109	116.946	183.730	172.385

OTRAS CARGAS A GRANEL

2014	2015	2016	2017	2018
0	0	0	0	224
0	521	0	0	0
0	0	0	336	0
0	0	0	0	0
0	0	0	0	0
7500	0	0	0	0
0	0	0	0	0
178	0	0	0	0
5930	0	0	256	0
0	0	0	32	0
0	173	0	128	
0	320	0	0	

ACUMULADO

2014	2015	2016	2017	2018
0	0	0	0	224
0	521	0	0	224
0	521	0	336	224
0	521	0	336	224
0	521	0	336	224
7.500	521	0	336	224
7.500	521	0	336	224
7.678	521	0	336	224
13.608	521	0	592	224
13.608	521	0	624	224
13.608	694	0	752	224
13.608	1.014	0	752	224

PRODUCTOS CONGELADOS

	MES	2014	2015	2016	2017	2018
1	Ene	0	0	0	0	0
2	Feb	0	0	0	0	0
3	Mar	0	0	0	0	0
4	Abr	5.397	0	0	0	0
5	May	0	0	9.296	0	0
6	Jun	0	2.400	0	0	0
7	Jul	0	0	3.755	0	0
8	Ago	5.253	2.632	1.368	0	0
9	Sep	0	0	0	0	0
10	Oct	0	0	0	142	0
11	Nov	0	0	0	0	
12	Dic	1.502	0	0	0	

ACUMULADO

2014	2015	2016	2017	2018
0	0	0	0	0
0	0	0	0	0
0	0	0	0	0
5.397	0	0	0	0
5.397	0	9.296	0	0
5.397	2.400	9.296	0	0
5.397	2.400	13.051	0	0
10.650	5.032	14.419	0	0
10.650	5.032	14.419	0	0
10.650	5.032	14.419	142	0
10.650	5.032	14.419	142	
12.152	5.032	14.419	142	

OTRAS CARGAS GENERALES

2014	2015	2016	2017	2018
0	900	0	10.021	11.517
0	0	18	0	11.252
0	0	3.535	5	10.353
0	0	500	52	3
0	210	2.874	1	12.115
3531	0	4.193	0	11.301
0	0	1.075	34	23.181
0	606	10.733	83	77
0	177	232	3.095	10187
902	0	249	11.641	263
0	0	652	8	
0	0	9.610	36	

ACUMULADO

2014	2015	2016	2017	2018
0	900	0	10.021	11.517
0	900	18	10.021	22.769
0	900	3.553	10.026	33.122
0	900	4.053	10.078	33.125
0	1.110	6.927	10.079	45.240
3.531	1.110	11.120	10.079	56.541
3.531	1.110	12.195	10.113	79.722
3.531	1.716	22.928	10.196	79.799
3.531	1.893	23.160	13.291	89.986
4.433	1.893	23.409	24.932	90.249
4.433	1.893	24.061	24.940	90.249
4.433	1.893	33.671	24.976	90.249

C

Waves

C.1. Extreme Value Analysis

An extreme value analysis is performed using Gumbell extrapolation to find the 5, 50 and 100 year significant wave heights. Multiplying with 1.67 gives a proper estimation of the maximum wave height and the results are given in Table C.1. A graph visualizing the extrapolation is given in Figure C.1.

Return period	Maximum wave height [m]
5 year	9.85
50 year	14.78
100 year	15.70

Table C.1: Extreme maximum wave heights in open water outside the bay of Concepción.

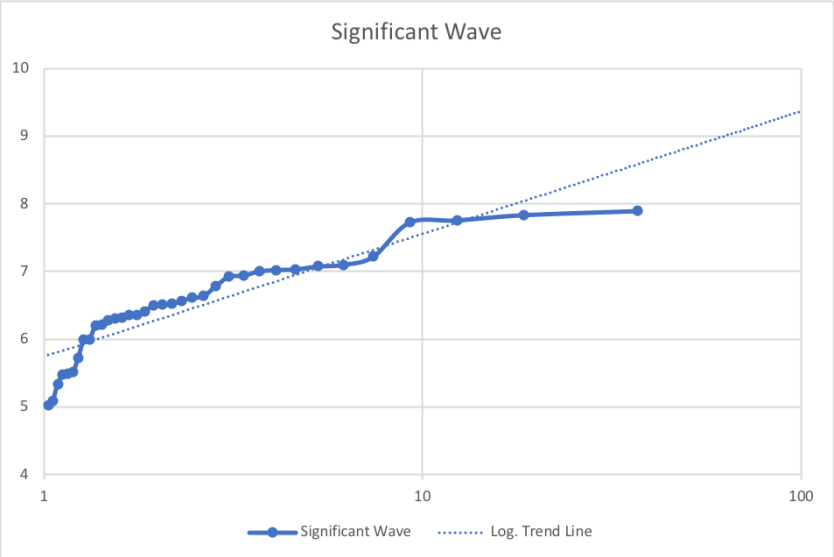

Figure C.1: Visualization of the extreme value analysis using Gumbell extrapolation.

C.2. Delft3D

C.2.1. General model definition

Delft3D requires to define a grid of the bay, as well as boundary conditions and hydraulic and numerical parameters. Fortunately, several grids for the Bay of Concepcion were already available. The grid with the smallest mesh size of 100 m is used for the model and shown in Figure C.2. The boundary conditions de-

scribe the open water conditions at the boundaries of the grid. The boundary conditions and parameters are described further defined in below paragraphs.

Some parameters used in all simulations are defined in Table C.2. In all simulations convention is set to nautical, forces by radiation stress, and wave set-up is activated. Furthermore, wind growth, quadruplets and white-capping is activated, as well as refraction and frequency shift. The geographical space is set to first order (SWAN 40.01) / second order (SWAN 40.11). Concerning spectral space, CDD and CSS are both set to 0.5 determining the nautical scheme.

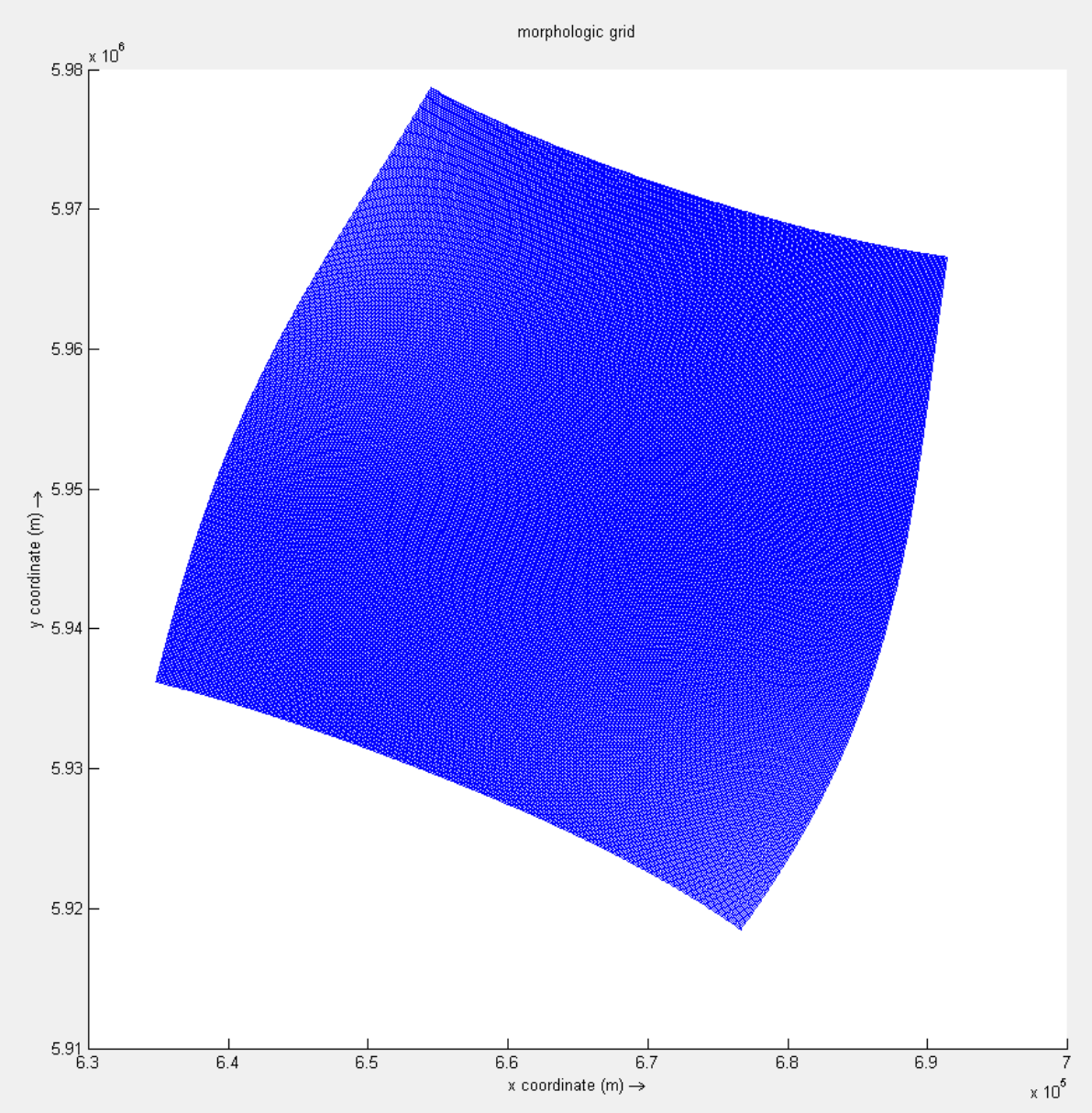

Figure C.2: An impression of the morphological grid used for simulating the wave climate in the bay.

Parameter	Value	Unit
Gravity	9.81	m/s^2
Water density	1025	kg/m^3
North w.r.t. x-axis	90	deg
Minimum depth	0.05	m
Rel. change Hs-Tm01	0.02	-
Wet grid points	98	%
Rel. change w.r.t. mean value Hs	0.02	-
Rel. change w.r.t. mean value Tm01	0.02	-
Max. number of iterations	15	-

Table C.2: General parameters for Delft3D model

Parameter	Value	Unit
H_{sig}	3	m
T_p	12	s
Direction	250	deg
Directional spreading	4	-

Table C.3: Boundary condition definition to simulate normal open water conditions.

C.2.2. Model validation

To do a brief validation of the model, a fetch-limited wind-generated wave calculation is done by hand. The book Waves in Oceanic and Coastal Waters by Holthuijsen[33] is used as a guideline for this calculation.
A maximum fetch of 17.5 km over the bay is taken as shown in Figure C.3. Next, to eliminate the the time element it is assumed that the wave generation is fetch-limited. This allows to define an dimensionless fetch, as in Equation C.1. Assuming deep water and a short fetch, a dimensionless wave height can be calculated by a simple power law as in Equation C.2. Kahma and Calkoen (1992) did an elaborate number study and found values for a_1 and b_1, being 2.88 x 10^{-3} and 0.45 respectively. The obtained dimensionless wave height can be transformed to the actual significant wave height by using Equation C.3. A value for U_{10} of 11 m/s is taken for the hand calculation.
This hand calculation is then compared to the significant wave height which the model computes at the port. For the model simulation the wind speed is set to be the same, at a direction of 35 °following the fetch as in Figure C.3. The outcome H_{sig} of the hand calculation is 0.93 m while the model produces 0.82. The model result has an offset of 12 from the hand calculation. A plot is shown in C.4. As the bay is no perfect smooth fetch, this calculation is not very accurate. Though, it learns that the model output and hand calculation are in the same range.

$$\widetilde{F} = \frac{g * F}{U_{10}^2} \tag{C.1}$$

$$\widetilde{H} = a_1 * \widetilde{F}^{b_1} \tag{C.2}$$

$$H_{sig} = \frac{\widetilde{H} * U_{10}^2}{g} \tag{C.3}$$

C.2.3. Extreme open water conditions

This simulation is based on extreme open water conditions with a significant wave height of 8 m coming from the north-east (315 °). This condition can be modeled by defining boundary conditions at open water with these conditions. Three boundary conditions are defined, orienting south-west, west and north-west. The conditions along these boundaries are defined uniform. Delft3D input for these conditions requires the peak period, so the Relation C.4 is used to find a value of 12.0 seconds, being within the range. The directional spreading parameter is set to the default value of 4.

$$11.1 * \sqrt{H_{sig}/g} \leq T \leq 14.3 * \sqrt{H_{sig}/g} \tag{C.4}$$

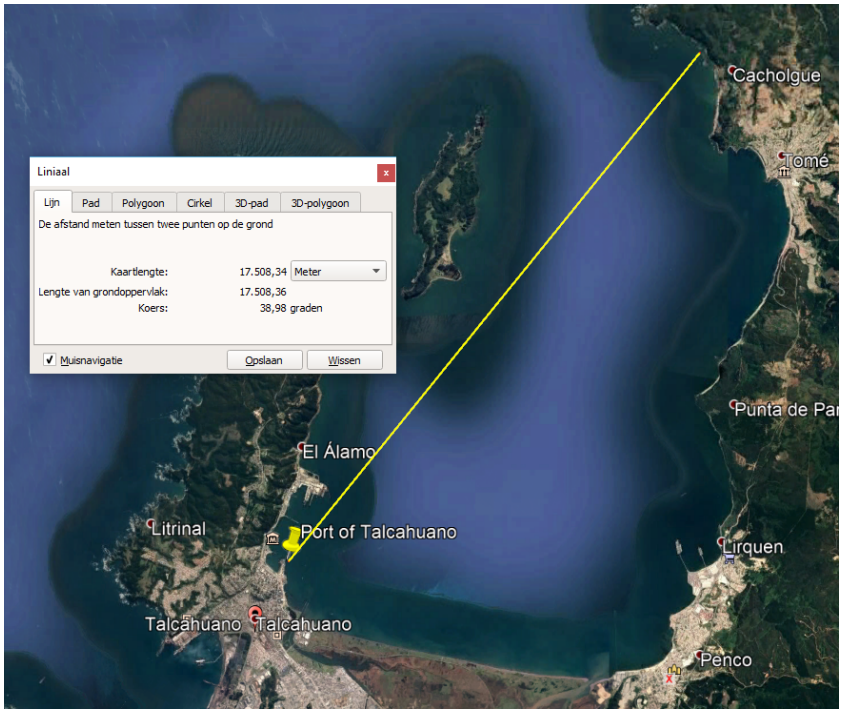

Figure C.3: The fetch used for hand calculation of wind-generated waves (source: Google Earth)

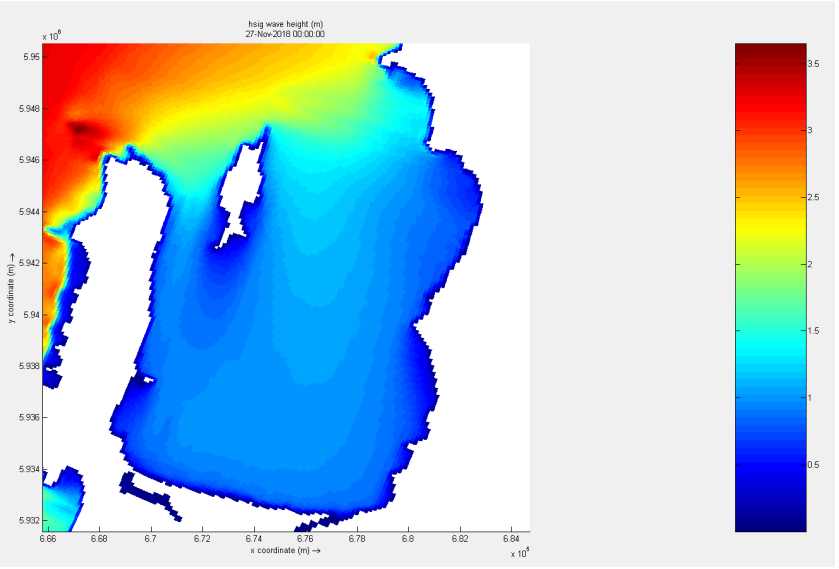

Figure C.4: Model results of wind speed of 11 m/s winds along the fetch as in Figure C.3.

C.2.4. Wind-generated waves from the north

The physical parameter for wind speed an direction are set to 11 m/s and 0 degrees to do the first simulation. The second simulation has a wind speed of 15 m/s and the same direction. The open water waves are defined in the three boundary conditions simulating normal conditions, summarized in Table C.3. The conditions along the boundaries are uniform. All other model settings are unchanged.

D

Bathymetry

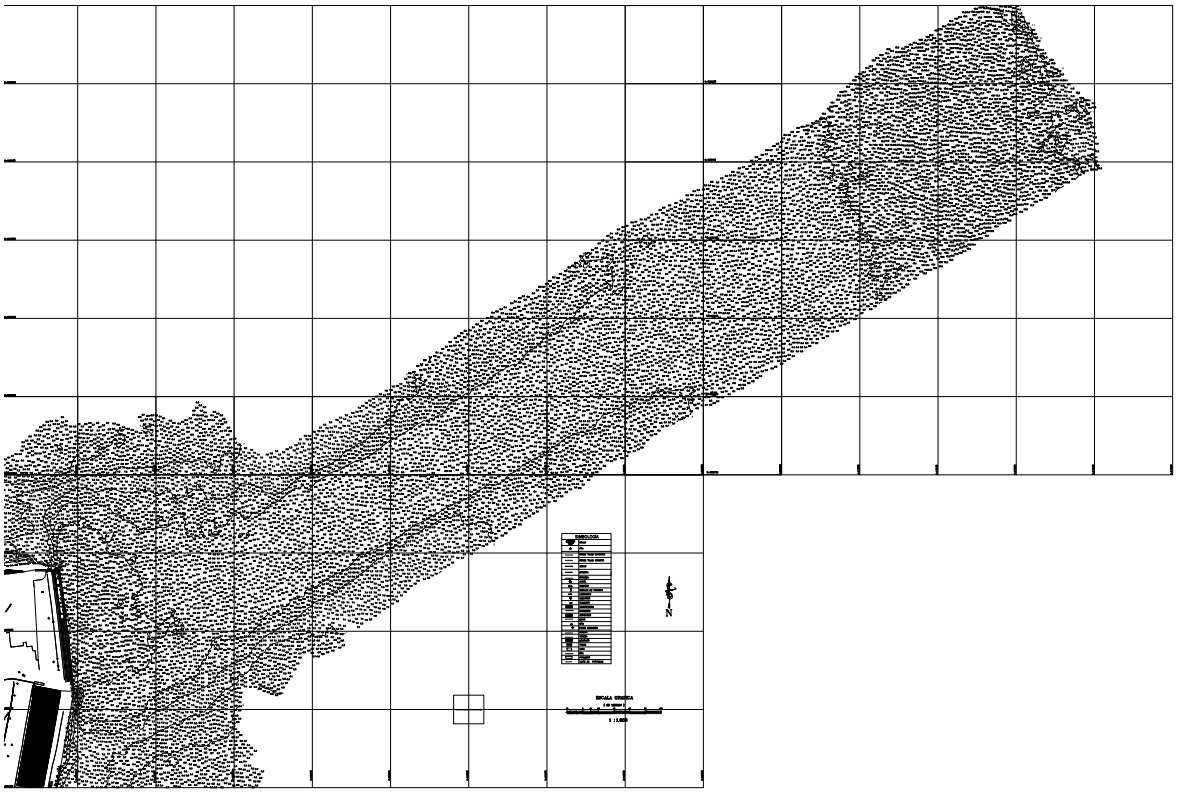

Figure D.1: Bathymetry full navigation channel

E

Soil

E.1. Sieve test

SEASON
Laboratorio de Análisis Medio Ambientales

Resultados ensayos			1A	1B	2A	2B	3A	3B	4A	4B	5A	5B	6A	6B
Fracción sedimentaria (%)	Φ	mm	%	%	%	%	%	%	%	%	%	%	%	%
Grava muy gruesa	-3	8-16												
Grava gruesa	-2	4-8												
Grava muy fina	-1	4-2												
Arena muy gruesa	0	2-1												
Arena gruesa	1	1-0,5												
Arena mediana	2	0,5-0,25	57.66	26.56	30.76	14.91	16.22	2.26	10.37	7.17	5.55	14.63	17.42	10.311
Arena fina	3	0,25-0,125	39.73	30.60	28.70	19.58	20.37	3.39	29.86	24.80	36.05	19.16	21.65	22.047
Arena muy fina	4	0,125-0,062	26.25	43.95	29.25	34.07	19.14	10.58	35.13	48.48	40.66	25.67	24.98	21.772
Fango	5	<0,062	7.61	15.51	17.72	8.93	17.93	17.59	14.28	22.86	10.48	8.39	12.46	15.56
		Media	2.350	2.882	2.827	2.948	3.367	4.612	3.083	3.626	3.085	2.880	2.908	3.425
		Selección	1.049	1.353	1.500	1.272	1.810	1.848	1.268	1.495	1.071	1.318	1.430	1.645
			Pobremente seleccionado	Pobremente seleccionado	Pobremente seleccionado	Pobremente seleccionado	Pobremente seleccionado	Pobremente seleccionado	Pobremente seleccionado	Pobremente seleccionado	Pobremente seleccionado	Pobremente seleccionado	Pobremente seleccionado	Pobremente seleccionado
		Asimetría	0.288	0.060	0.240	-0.001	0.346	0.275	0.143	0.311	0.180	0.068	0.151	0.344
			Asimetrico con exceso de particulas finas	Simetrico	Asimetrico con exceso de particulas finas	Simetrico	Asimetrico con exceso de particulas muy finas	Asimetrico con exceso de particulas finas	Asimetrico con exceso de particulas finas	Asimetrico con exceso de particulas muy finas	Asimetrico con exceso de particulas finas	Simetrico	Asimetrico con exceso de particulas finas	Asimetrico con exceso de particulas muy finas
		Curtósis	0.955	1.353	1.264	1.406	1.314	0.856	1.604	1.873	1.511	1.373	1.382	1.494
			Mesocurtico	Leptocurtico	Leptocurtico	Leptocurtico	Leptocurtico	Platicurtico	Muy leptocurtico	Muy leptocurtico	Muy leptocurtico	Leptocurtico	Leptocurtico	Leptocurtico
		Clasificación textural según Wentworth, 1922	Arena fina	Arena fina	Arena fina	Arena fina	Arena muy fina	Limo muy grueso	Arena muy fina	Arena muy fina	Arena muy fina	Arena Fina	Arena Fina	Arena muy fina
		Clasificación textural según Folk 1954	Arena	Arena fangosa	Arena fangosa	Arena fangosa	Arena fangosa	Arena fangosa	Arena fangosa	Arena fangosa	Arena fangosa	Arena fangosa	Arena fangosa	Arena fangosa

LABORATORIO DE MEDICIONES AMBIENTALES SEASON LTDA

Figure E.1: sieve test results

E.2. USCS, densities and CBR test results

Sample no.	**Clasificacion USCS**		**D.M.C.S. (ton/m3)**	**CBR* %**	**Density In situ (ton/m3)**
Depth of sample	0.9 (m)	1.5 (m)	0.9 (m)	0.9 (m)	1.50 (m)
N°1	SM	SM	1.960	21	1.64
N°2	GP-GM	SC	2.180	71	1.28
N°3	SM	SC	1.890	15	1.31
N°4	GW	SM	2.200	96	0.78**
N°5	GP-GM	GW	2.250	79	1.82
N°6	GP-GM	SP-SM	2.210	75	2.17
N°7	GC	GC	2.230	61	1.87
N°8	GC	SP-SM	2.270	65	1.54
N°9	GM	GM	2.250	74	1.80
N°10	SP-SM	SP-SM	1.990	31	1.39
N°11	GP-GC	SM	2.220	85	1.41
N°12	SM	SM	1.930	23	1.35
N°13	SP-SM	SM	2.020	28	1.11
N°14	SP	SP	1.920	21	1.38
N°15	GC	GM	2.260	83	1.39

Table E.1: Laboratory test results of 15 samples taken along Sitio 1 [24]

* CBR samples are recompacted to 95% D.M.C.S. and the height of the sample is 5.08 cm.
** The soil sample contained solid coal resulting in high a CBR test result and low in situ density. This sample can be considered unreliable.

E.3. Standard Penetration Test

A standard penetration test (SPT) is performed before construction of the quay at Sitio 1.

profile.pdf profile.pdf

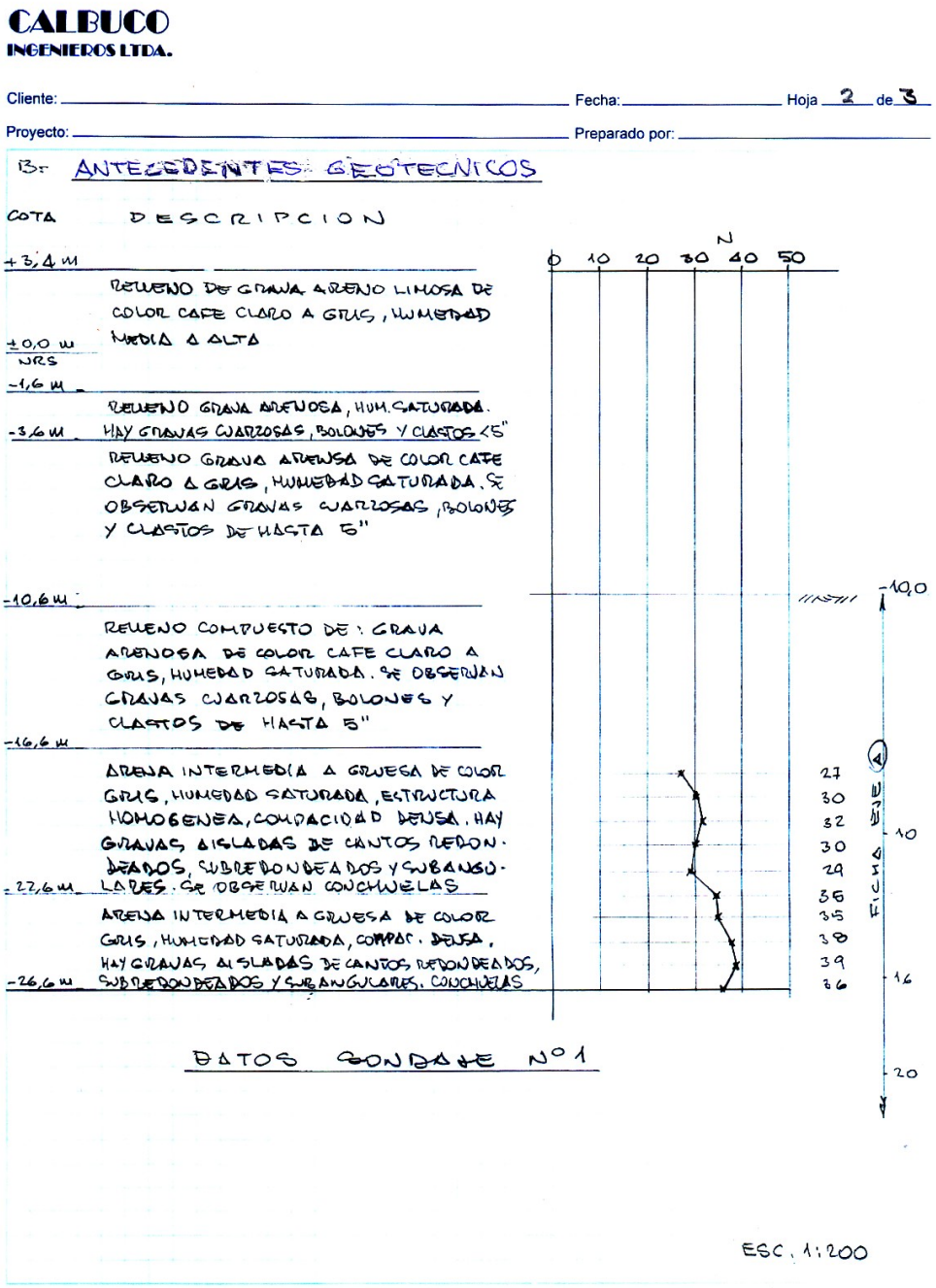

Figure E.2: Soil profile based on Standard Penetration Test

F

Multi-Criteria Analysis

In order to evaluate the most suitable scenario Multi-Criteria Analysis (MCA) is performed on the four scenarios. The MCA scores the scenarios on five criteria which are defined such that they express all important characteristics of the scenarios. The scores are then weighted and summed per scenario to give the final score. The weight of the criteria is determined based on the cost equivalent where possible. By this means the monetary value of all scores is equalized and compared. Below the five criteria and their weights are explained after which the scores per scenario are given. In the Chapter 4 the table with the result of the MCA is presented and the scenario which will be worked out in more detail is elaborated on.

F.1. Criteria definition

In the MCA the scenarios are judged on the criteria as defined in this section. Each criteria has its own weight as defined in Table F.1. The choice for the weights is motivated under each criteria description in this section. The considerations made when determining the criteria were the following.

- The costs of maintenance is not a major aspect concerning in the selection of the structural type of quay walls [13]. Moreover, since wave impact is insignificant as proven in Section 3.2, less maintenance is needed. Maintenance cost are therefore not taken into account in the MCA.

- The total costs are divided into three parts to give insight in how much each category contributes. It is divided into: dredging costs, construction costs and loss of revenue due to construction.

The scores for the criteria are determined for every scenario separately and will be explained in Sections F.2.1 to F.2.4. It should be noted that for all criteria the highest score is the most preferable value. Therefore the lowest costs have the highest score and so does the highest potential market value. The worst scenario is given an unweighted score of 0 and the most favourable scenario for a certain criteria scores a 10 out of 10. All scenarios with values in between the best and worst scenarios are given scores accordingly. The scores for every criteria are then weighed. The sum of the weighing factors for the three criteria concerning costs is 0.6. The costs require an investment to be done beforehand which leads to risk. This means the costs are more important than the revenue. Between the three costs criteria the weighing factor is distributed based on the cost interval between the highest scoring and lowest scoring criteria. By comparing the cost interval, the value of a weighted point in the MCA has an equal value expressed in USD for every cost criteria. The monetary equivalent of one weight point for the costs criteria of a scenario is 500,000 USD. The sum of all weighing factors is 1 and thus the perfect score comes down to 10 points. Per scenario all five unweighted and weighted scores are given and explained.

Criteria	Weight
Dredging cost	0.10
Construction cost	0.35
Lost revenue during construction	0.15
Potential market value	0.35
Environmental impact	0.05

Table F.1: Weights of each criteria of the Multi-Criteria Analysis.

The weights of the criteria as stated in Table F.1 have been discussed with the port operators and are in accordance with their desires.

Dredging costs
The dredging costs consist of two parts which are the transport costs of the vessel for it to come to the Concepcion bay and the operational costs which are proportional to the dredging volume and the distance to the site where the dredged material can be dumped. The costs for transport is equal for all scenarios and also the distance to the dumping site. Therefore, the transportation costs are not taken into account into the MCA. However, it must be noted that this transportation costs can become very high and sharing the costs of transportation might be shared by other ports who also need dredging. The volume to be dredged is the main cause for difference. Because in these preliminary designs it is unclear whether the dredged material is re-used as landfill in the design it is assumed that no material is re-used for landfill during the dredging calculations. For all scenarios the navigation channel and manoeuvring area need to be dredged. Therefore this is calculated and determined for all scenarios equally. As specified in the current situation the dimensions of the navigation channel are 1800 m, 100 m and 8.4 m (though the depth differs throughout the channel) for respectively the length, width and depth. For the estimation of the volume that needs to be dredged for the new scenarios it is assumed that only the depth is increased. The depth is a given number by the port authorities and the channel design will be evaluated in detail in Part III of the report.

Based on the bathymetry that has been provided by the port a manual integration over the area has been used to estimate the dredged volume for each scenario. First the area that needs to be dredged is marked and then this area is divided in smaller blocks of which the average depth is determined. The increase in depth is multiplied by the area and summed with the volumes all other areas. The dredging volume required for the navigation channel for a depth of 10.6 m with the dimension taken equal to the current situation is approximately 198,000 m^3. The additional volume that is specific to the scenario will be calculated later in this chapter.

After the dredging volume is determined this is used to give an estimate of the total dredging costs. The total dredging costs are difficult to estimate since these costs depend on many different parameters. These parameters include:

- Depreciation and interest of the vessel
- Maintenance and repair of the vessel
- Insurance of the vessel
- Crew working on board of the vessel
- Fuel and lubricants used by the vessel
- Wear and tear of the pipelines

However, in order to evaluate the dredging costs for every scenario, the market cost per cubic meter for a hopper dredger is estimated. The hopper dredger is assumed the most suitable for the port of Talcahuano, since the dredged soil is used for landfill. According to the US Army Corps of Engineers, dredging costs vary from 2.99 to 37.02 USD/m^3 This depends on the dredged volume, the used technology (hopper or not-hopper), and whether it is a new work or maintenance work. [71]. In Figure F.1, the estimated cost equation for the Yaquina Trailing Suction Hopper Dredger is shown. It is assumed that the equation is quadratic and this is

therefore a conservative assumption. Using the data from the US Army of Engineers, an estimation has been made for the dredging costs based on the cubic metres of dredged volume per scenario. The used data set contains total costs for dredging projects. It is assumed that all of the above mentioned costs are incorporated in this data set from the US Army of Engineers. The total costs of transportation of the dredging vessel to the location is equal for all the scenarios and therefore not taken into account. However, it must be noted that this dredging cost can become very high.

It is chosen to use the Yaquina Hopper Dredger as the design dredger. This decision is based on the fact that the Yaquina Hopper Dredger is used for "smaller reference projects" in the US and it is based on the fact that it is a relatively cheap hopper dredger. The calculated capacity of the Yaquina Dredger is 678 $m^3/hour$.

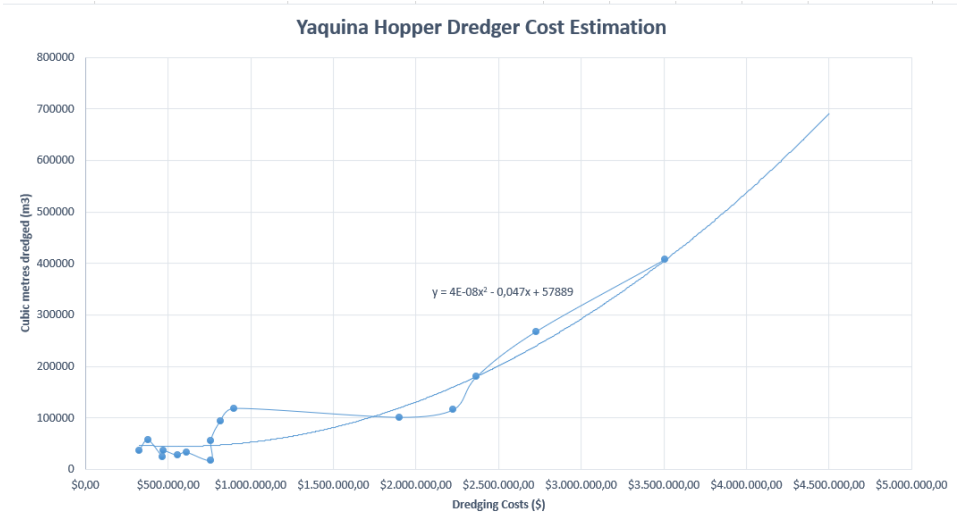

Figure F.1: Yaquina dredger costs per cubic metre of dredged material.

Dredging vessels are generally unavailable in Chile. This makes a competitive market impossible and thus it causes higher prices than usually expected. The dredging costs are therefore uncertain and should be taken within a margin of +30% and -15% [16]. For the MCA this applies for all scenario´s and therefore this uncertainty does not influence the outcome.
By applying the method based on interval difference as described above the rounded weighing factor the criteria of dredging costs is 0.10. This weighing factor is low because the difference between the highest and lowest scoring scenarios is small. The monetary value that can be saved by choosing the best scenario instead of the worst is only little.

Construction costs
These costs refer to the material and installation cost of quay walls or jetties. de Gijt extensively investigated the cost of sheet pile quay walls in 2011 and came up with the relation as shown in Figure F.2. The cost indication of quay walls for the MCA is based on this relation. He also concluded that the costs of quay walls vary within a band width of approximately +/- 25 %, irrespective of the soil conditions, tidal ranges and types of structures.

The cost of a quay wall is similar to the cost of a jetty per running meter for a cost estimate, as concluded by Wong in 2016. The relation in Figure F.2 is therefore also used as a cost estimation for jetties.
The equation used to calculate the approximate cost (given in the graph) is as follows:

$$Costperm' = 627.05 * x^{1.2878} \tag{F.1}$$

in which x is the retaining height of the quay wall/structure. As mentioned before, this can also be used for jetties.
The difference between the most costly scenario and the lowest scenario is large and thus a lot of money can be saved by choosing the cheapest scenario. This results in a high weighing factor: 0.35.

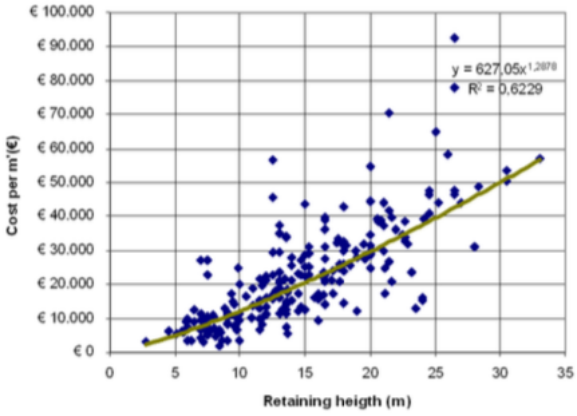

Figure F.2: Quay wall cost per running meter versus the retaining height [13].

Loss of revenue during construction

The current quays may be partially or entirely out of order during construction of a port expansion. If a quay is partially unavailable, larger vessels are unable to berth and the amount of smaller vessels berthing the quay may be less. This may result in a loss of revenue during construction. For each scenario it differs which of the current quays will need to be closed down during construction, partially or entirely. To assess this criterion, the expected operation of the port during construction of each scenario is evaluated. The method for assessment of each scenario is as listed below. An elaboration of these calculations is given in Appendix G.

1. Estimate the construction time
2. Determine whether the existing quays need to be shut down
3. Assign loss factors for the part of throughput lost during construction
4. Calculate the lost revenue based on port tariffs, throughput data, construction time and loss factors

A number of assumptions had to be made to complete the assessment in limited time. These are listed below.

- All main activities are sequential and not parallel, thus the total downtime is a sum of total downtime due to dredging and construction. This is done to gain conservative estimations of the downtime.
- Sitio 2 is not limited by manoeuvring area dredging.
- All fishery is at Sitio 2 and Maria Isabel, the rest at Sitio 1.
- The size of the vessels entering the port is not taken into account in the loss factors. Thus, it could be that if the quay is half closed that the majority of the vessels normally berthing cannot berth anymore.
- No significant landfill is needed in Scenario 1 and 3. Though, significant landfill is needed in Scenario 2 and 4. The volumes are determined at 10,000 and 50,000 m^3 respectively, based on rough calculations.
- Only the prices per ton of handled cargo and the prices per meter/length/hour of the quays are used in estimating the total revenue. Other income from services like tugboat rental/usage, usage of storage space or crane usage are not taken into account.
- The throughput numbers used in the calculations are found by linearly extrapolating the available data of years 2014 - 2017 to the year 2020.
- Maria Isabel is not taken into account as no throughput data was available.
- The construction speeds regarding quay and jetty construction, 10 and 8 running meters per week respectively, are assumed just below the construction speeds as stated by dos Santos in 2011 to get a conservative estimation.

- The dredging speed, 77122 $m^3/week$, is deduced from a project of similar volume, performed by an American Trailing Suction Hopper Dredger called Yaquina and includes relevant cycle time elements. The vessel operates 16.25 hours per day, 7 days per week, which was also the case in the reference project.

- Revenues are calculated based on throughput unit prices per category using current tariffs. Thus, dynamic economic effects such as inflation are not taken into account in this assessment.

The potential loss is not very large compared to the other costs, and also the difference between the best and worst scenario is small. The rounded weighing factor is therefore 0.15.

Potential market value
In order for the port expansion to be future proof, it is important to evaluate the potential market value as a criteria. The indicators used to asses the potential market value are meters berthing space, extra storage area and the possibility to have an extra berth. The indicator berthing space is considered to be the most important indicator and the possibility to have an extra berth is considered to be the least important.

Firstly, the indicator meters berthing space is discussed. Meters berthing space is an important indicator because more berthing space means larger vessels can be handled in the port, creating more revenue for the port. The meters berthing space gained for every scenario are calculated by adding the created extra berthing space to the current berthing space. The berthing space for each of the scenarios is equal to the total quay length created. The operational availability of the port is also implicitly included in this criteria. It is unknown to estimate the occupation of the port in the future. However, it can be concluded that more berthing space means there is a higher probability of the port being occupied more, leading to a higher operational availability. In conclusion, the indicator meters berthing space is given a weight of 50 % within the criteria potential market value since it is the most important indicator.

Secondly, the indicator extra storage area is discussed. Extra storage area means more goods are able to be processed in the future, leading to a higher revenue for the port. The extra storage area gained for every scenario is calculated by estimating the extra land gained in m^2 excluding the quay wall itself. In conclusion, the indicator extra storage area is given a weight of 30 % within the criteria potential market value.

Thirdly, the indicator possibility to have an extra berth is discussed. This indicator describes whether the new quay wall created has the possibility to facilitate an extra berth in the future. This is an indicator which implies whether the port is future proof if they want to expand even further. Since this indicator is the most uncertain a weight factor of 20 % within the criteria potential market value is assigned to this indicator.In conclusion, this indicator is given a weight of 20 % within the criteria potential market value.

The total division of weight percentages of the three indicators used in potential market value are summed up in Table F.2 below.

Indicator	**Weight factor**
Meters berthing space	0.50
Extra storage area	0.30
Possibility to have a extra berth	0.20

Table F.2: Weighing factors of indicators in potential market value

Because potential market value is the only criteria that displays the revenue of the port it is important and thus it has a high weighing factor. This results in a total weighing factor 0.35 for the criteria potential market value.

Environmental impact
The environmental impact of the port expansion is important to review as the dredging activities and construction and operation of a large port can have a negative impact on the air pollution, noise, water quality, ecosystem and overall quality of life in the surrounding area. It is therefore important that already during the

design phase actions need to be taken in order to mitigate the impact. Some scenarios provide more possibilities to avoid CO2-emission, transport of materials or water pollution than other. Actions that should be taken in all scenarios will be named in Chapter 14 and only the scenario dependent action are mentioned for the MCA. An estimation of the effect of the actions taken will form the base for the score. Particularly this criteria receives very subjective scores as the reduced impact is difficult or impossible to monetize. As it also can´t always be expressed in CO2-equivalent emission the scores are open for discussion and the weight is low. Environmental impact does not have a high priority for the port authorities, but it is required to consider actions to mitigate negative impact in order to keep on good terms with the city council and the community of Talcahuano. It is determined that the environmental impact has a minimal influence on the choice process and thus it has a weighing factor of only 0.05.

F.2. Scores

The four scenarios are now assessed for each criteria.

F.2.1. Scenario 1: Extension Sitio 1 North

Dredging cost

In the first scenario the expansion in northern direction means that a lot dredging needs to be done in shallow waters in front of the new quay wall. As the vessel is allowed to extend beyond the end of the quay wall the dredging area also extends beyond the quay wall. Especially in the most Northern part of this area the depth is very small. The total dredging volume is estimated to be 483,000m^3. The costs come down to 3,900,920 USD, as calculated by using Figure F.1 and solving for the dredging volume. The unweighted score is 7.93.

Construction cost

In this scenario, a jetty of 180 m is constructed. Using the equation of de Gijt, this leads to a estimated construction cost of 4,153,600 USD. Other than the jetty, no other construction (like landfill) is needed. The costs as calculated above are the lowest of all scenarios and thus the score is 10 out of 10.

Lost revenue during construction

At Sitio 1 the upper half is closed during the jetty construction. 50% of the total throughput can still be processed. Sitio 1 fully closed during manoeuvring area dredging. Sitio 2 and Maria Isabel are fully operational during construction and dredging. The total lost revenue during construction comes down to 877,359 USD which gives it a score of 5.04.

Potential Market Value

For Scenario 1, a quay with a total length of 340 meter is facilitated. However, no extra storage area is created since the jetty is fully used for other activities. In the future, there is a possibility of facilitating an extra berth with length of 180 m. However, this is not considered to be likely since the extra dredging area including extended manoeuvring area is large and is located in shallow water. This results in a score of 0.00.

Environmental impact

The dredging volume in the first scenario is relatively small and therefore the CO^2-emission should therefore be less than for Scenario 3 and 4. As there is no possibility to use the dredged material for landfill all of the material must be dumped out at sea where it can disrupt the local ecosystem. The transport will also emit CO^2 emission and is also taken into account here. Overall for the dredging activities Scenario 1 scores a positive (compared to the other scenarios). The jetty that will be build will require a lot of steel and concrete which will both cause a lot of emissions during production and transport. The materials are heavy and aren't produced locally. Also some of the construction needs to be done vessel on the water. This is more polluting than construction from land. These are negative aspects of this scenario. Because the jetty is a north wise extension of the quay wall it might be needed to relocate the entrance path for Molo Blanco. Another negative point is that gradient on the seabed along the northern edge of the manoeuvring area is very steep. Morphological change might cause a lot of maintenance and thus dredging. In total this scenario has a less negative impact on the environmental and this result in an unweighted score of 7 out of 10.

F.2.2. Scenario 2: Extension Sitio 1 North and South

Dredging cost

In the second scenario the manoeuvring area needs to be extended a bit in northern and southern direction. In this places the depth is relatively great keeping the dredging volume small. This makes the total dredging volume come done to 456,000 m^3. The costs come down to 3,795,553 USD, as calculated by using Figure F.1 and solving for the dredging volume. There are the lowest dredging costs so the score is 10 out of 10.

Construction costs

This scenario features the construction of a quay (90 m) in southward direction and a jetty (90 m) in northward direction, the same as in Scenario 1. The estimated costs are calculated in the same manner, leading to the same result as in Scenario 1 which is 4,153,600 USD.

When this scenario is constructed, the rubble that is currently present just under Sitio 1 has to be removed before construction can occur. This will add to the cost. The estimated cost is 50,000 USD , considering costs like crew costs, needed equipment etc. Next to that, a landfill will be needed, an estimated 10,000 m^3.

The landfill will be done using dredged soil. An estimate for this is taken to be 23,600 USD, due to the placement of the pipeline for the discharge of sediment and other attached cost for executing the landfill (crew costs, assisting equipment, etc.). The dredger will only have to navigate to the pipeline, discharge its load, and sail back to its next dredging site. Since discharge will at the longest take as long as the suction, along with the small part relative to the total dredged soil needed for the landfill, the influence on the total dredging time will be minimal.

If the dredged soil is not used, the landfill soil (assumed to be sand, priced at approximately 49.56 USD per m^3) has to be bought. This leads to a estimated increase of 495,600 USD. Therefore it is chosen to re-use dredged soil.

These factors lead a total estimated construction cost of 4,224,399 USD. This gives a score of 9.66.

Lost revenue during construction

Sitio 1 is completely down during jetty and quay construction and manoeuvring area dredging. Sitio 2 is slightly limited during quay construction: 80% of throughput can still be processed. Maria Isabel is fully operational during all activities. The total lost revenue during construction comes down to 893,307 USD which leads to a score of 4.81.

Potential market value

For Scenario 2, a quay with a total length of only 340 meter is facilitated. In addition, an extra storage area of 1250 m^2 is created. In the future, there is a possibility of facilitating an extra berth with length of 90 m. However, this is not considered to be likely since the extra dredging area including extended manoeuvring area is large and is located in shallow water. This results in a score of 0.33.

Environmental impact

Because in the second scenario only small extensions in the shallow areas are created is the dredging volume the smallest. Also is it possible to use some of the dredged material as landfill for the southern quay expansion. This is a big positive aspect. Because of this also the amount of other material such as steel and concrete are reduced. This again helps this scenario to minimize the negative impact on the environment. Finally the possibility to construct part of the expansion from land makes this the best scenario and thus scoring a 10 out of 10.

F.2.3. Scenario 3: A Jetty

Dredging cost

The third scenario requires the current manoeuvring area to be moved to the south. Apart from the navigation channel and the manoeuvring area there is no additional dredging needed. The total volume including the navigation channel is 517,000 m^3. Only when in the future the northern side of the jetty might be transformed into a berth a second manoeuvring area and a divergence of the navigation channel need to be added. These adjustments will cause a large increase in dredging volume, but are not considered in this preliminary design. The costs come down to 4,025,432 USD, as calculated by using Figure F.1 and solving for the dredging volume. These costs are average compared to the other scenarios and this is reflected in the score of 5.49.

Construction costs
The jetty in Scenario 2 can be seen as a 90 m jetty connected to a 180 m jetty. The equation of de Gijt for quay walls and jetties gives a estimated construction cost of 6,230,400 USD, making this by far the most expensive scenario. The score for this criteria is 0 because it is the most expensive option.

Lost revenue during construction
At Sitio 1 the upper half is closed during jetty construction. 50% of the throughput can still be processed.Though, Sitio 1 is fully closed during manoeuvring area dredging. Sitio 2 and Maria Isabel are fully operational during jetty construction and dredging. The total lost revenue during construction comes down to 1,233,093 USD. Also for this criteria this scenario score lowest resulting in another 0 out of 10.

Potential market value
For Scenario 3, a quay with a total length of 390 meter is facilitated. However, 25 meters are subtracted from this length because of the 90 degree angle of the quay wall. This gives a quay length of 365 meters. No extra storage area is created since the jetty area is used for facilitating other activities. In the future, there is a possibility of facilitating an extra berth with length of 220 meters. This is considered to be more likely since the berthing area is easily accessible and it is in rather deep water. This result in a score of 4.55.

Environmental impact
The dredging volume of the third scenario is larger than of the first two scenarios but definitely not as large as Scenario 4. This scenario doesn't have the possibility to use dredged material however and thus these dredging activities have a relatively large negative impact on the environment. The long jetty in relatively deep water requires large amounts of steel that needs to be transported to the port and installed from water which will generate lots of emissions. Finally the orientation of the jetty, perpendicular to the current, might be a reason for scour and/or morphological changes along the jetty. The unweighted score of the third scenario is 0 out of 10 because compared to the other scenarios it has the greatest negative impact on the environment.

F.2.4. Scenario 4: Connecting Sitio 1 and Maria Isabel

Dredging cost
For the final scenario the quay wall is extended a lot in southward direction which puts it in smaller water depth. The berth basin however is only dredged till the Maria Isabel site. The commercial berth is thus 400 meter. Especially the southern part is shallow and needs a lot of dredging which makes the total dredging volume 597,000 m^3. The costs come down to 4,305,699 USD, as calculated by using Figure F.1 and solving for the dredging volume. As this is the largest dredging volume and thus the highest dredging costs this scenario scores a 0 out of 10.

Construction costs
In Scenario 4, the quay is extended southward, connecting to the Maria Isabel quay. This extension is 240 meters, which leads to an estimated 5,534,200 USD in construction costs. However, just as in Scenario 2, the rubble that is currently present has to be removed before construction will begin, adding to the cost.
Next to that, a lot of landfill (50,000 m^3) is needed. This can possibly be done using the dredged soil, however, it will still add to the costs. The estimated cost is 59,000 USD.
The landfill will be done using dredged soil. An estimate for this is taken to be 118,000 USD, due to the placement of the pipeline for the discharge of sediment and other attached cost of executing the landfill. The dredger will only have to navigate to the pipeline, discharge its load, and sail back to its next dredging site. Since discharge will at the longest take as long as the suction, along with the fairly small part relative to the total dredged soil needed for the landfill, the influence on the total dredging time is still considered to be minimal.
If the dredged soil is not used, the landfill soil has to be bought (price taken to be 49.56 USD/m^3), leading to a estimated increase of 2,466,200 USD. Therefore it is chosen to use dredged soil.
These factors lead a total estimated construction cost of 5,711,199 USD. The corresponding score is 2.5.

Lost revenue during construction
Sitio 1 is slightly limited during quay construction and landfill: 80% of throughput can still be processed. Sitio 1 is fully closed during manoeuvring area dredging. Sitio 2 is fully closed during construction. Maria Isabel

slightly limited during quay construction and landfill: 80% of throughput can still be processed. The total lost revenue during construction comes down to 526,646 USD. These losses are the lowest compared to the other scenarios and therefore the score is 10 out of 10.

Potential market value
For Scenario 4, a quay with a total length of 400 meter is facilitated. In addition, an extra storage area of 5830 m^2 is created. In the future, there is no possibility of facilitating an extra berth without intensive construction. This scenario scores 10 out of 10.

Environmental impact
By extending the quay wall from the current Sitio 1 to Maria Isabel a large land area is created. This requires a lot of material for land fill which can be taken from the dredging material. Re-using dredged material is better than dumping it out at sea, but the large dredging volume makes the dredging activities very polluting all together. The construction can be done from land for the biggest part as the quay wall doesn´t protrude into the bay. Also the fact that less steel is required for the construction of the new quay wall is positive. Finally the steep depth gradient along the southern edge of the manoeuvring area means a lot of sediment transport takes place here and maintenance has to be done more frequently. The total score of the forth scenario is 4 out of 10, mainly because the amount of dredging in the south area is very large.

G

Loss of Revenue during quay construction

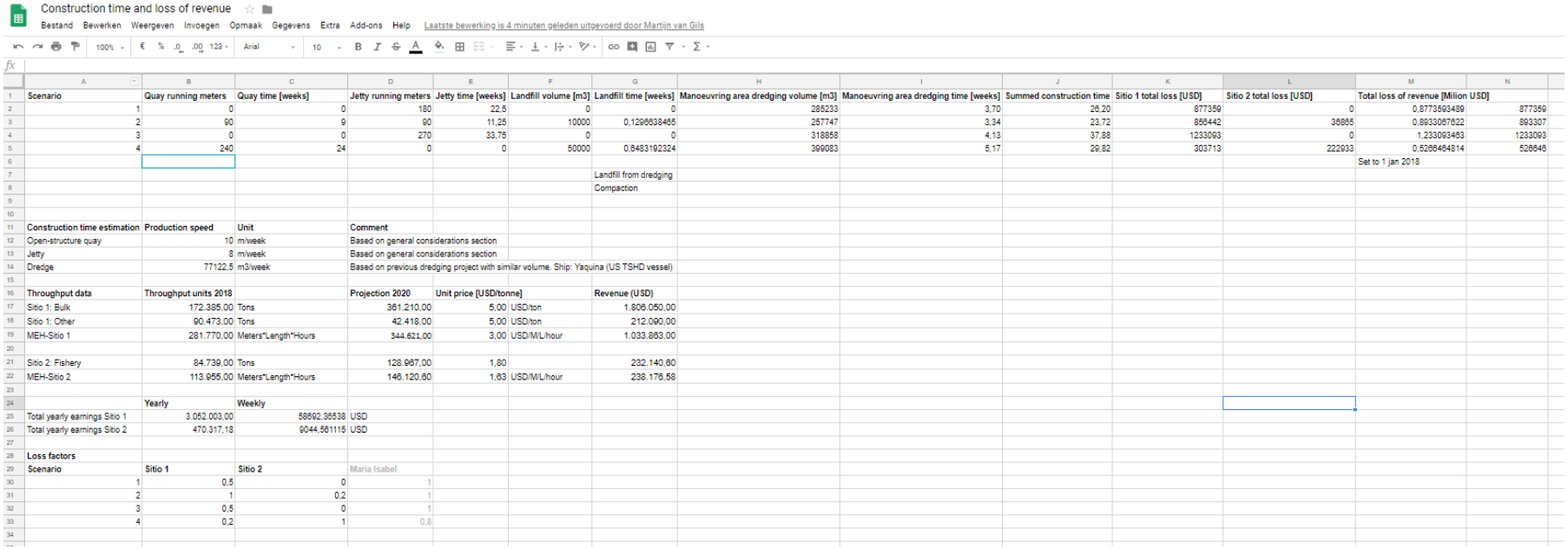

Construction time and loss of revenue

Bestand Bewerken Weergeven Invoegen Opmaak Gegevens Extra Add-ons Help Laatste bewerking is 4 minuten geleden uitgevoerd door Martijn van Gils

Scenario	Quay running meters	Quay time [weeks]	Jetty running meters	Jetty time [weeks]	Landfill volume [m3]	Landfill time [weeks]	Manoeuvring area dredging volume [m3]	Manoeuvring area dredging time [weeks]	Summed construction time	Sitio 1 total loss [USD]	Sitio 2 total loss [USD]	Total loss of revenue [Milion USD]	
1	0	0	180	22,5	0	0	285233	3,70	26,20	877359	0	0,8773593489	877359
2	90	9	90	11,25	10000	0,1296638465	257747	3,34	23,72	856442	36865	0,8933067622	893307
3	0	0	270	33,75	0	0	318858	4,13	37,88	1233093	0	1,233093463	1233093
4	240	24	0	0	50000	0,6483192324	399083	5,17	29,82	303713	222933	0,5266464814	526646
												Set to 1 jan 2018	
						Landfill from dredging							
						Compaction							

Construction time estimation	Production speed	Unit	Comment
Open-structure quay	10	m/week	Based on general considerations section
Jetty	8	m/week	Based on general considerations section
Dredge	77122,5	m3/week	Based on previous dredging project with similar volume. Ship: Yaquina (US TSHD vessel)

Throughput data	Throughput units 2018		Projection 2020	Unit price [USD/tonne]		Revenue (USD)
Sitio 1: Bulk	172.385,00	Tons	361.210,00	5,00	USD/ton	1.806.050,00
Sitio 1: Other	90.473,00	Tons	42.418,00	5,00	USD/ton	212.090,00
MEH-Sitio 1	281.770,00	Meters*Length*Hours	344.621,00	3,00	USD/M/L/hour	1.033.863,00
Sitio 2: Fishery	84.739,00	Tons	128.957,00	1,80		232.140,60
MEH-Sitio 2	113.955,00	Meters*Length*Hours	146.120,60	1,63	USD/M/L/hour	238.176,58

	Yearly	Weekly	
Total yearly earnings Sitio 1	3.052.003,00	58692,36538	USD
Total yearly earnings Sitio 2	470.317,18	9044,561115	USD

Loss factors			
Scenario	Sitio 1	Sitio 2	Maria Isabel
1	0,5	0	1
2	1	0,2	1
3	0,5	0	1
4	0,2	1	0,8

Figure G.1: Total loss of revenue during construction quay

H

PLAXIS Sheet Pile Analysis and Design

This appendix contains the model of Sitio 1 with the new water depth, the design and model of Nieuw Delft, the stability checks for both quays and the quay apron design. For the analysis of the quay wall structure, PLAXIS 2D is used. PLAXIS 2D is finite element modelling software, that can be used to assess the stability, forces, pressures, stresses and deformations, of both the soil and the structures. Thanks to this, it is possible to quickly asses a design, and to explore multiple options.
In the model, first, soil layer properties are defined, just as the structure properties and the water level. Then dimensions of the layers and the structures are defined, to eventually create a model that well represents the design.
After defining the dimensions and the properties, building phases are defined, ending with the final structure. The deformation, forces and bending moments in the structure are given and are also visually displayed. The same goes for the soil deformation, the pressures, stresses and so on.
PLAXIS 2D is used to asses the stability of both the current sheet pile wall at Sitio 1 with the new water depth, as well as for the stability of the newly designed sheet pile wall at Nieuw Delft.

H.1. Sitio 1

Due to the planned increase of the water depth at Sitio 1, the stability of the sheet pile wall is also influenced. Therefore it is re-assessed.
The only data given about the anchor rod is the height above LAT at which it is attached to the sheet pile (1.2 m) and the anchor rods are 1.26 m apart from each other [**?**]. Therefore, some assumptions are made for the dimensions and properties of the anchor:

- For the cross-sectional area, a diameter of 80 mm is chosen as this dimension is unknown
- Using technical drawings, a length of 36 m from the sheet pile wall to the anchor is estimated.
- It is assumed that the anchor is made of steel with a Young Modulus of 200 GPa

Using the above mentioned input, together with the soil properties mentioned in Table 3.7, the following model basis is established:

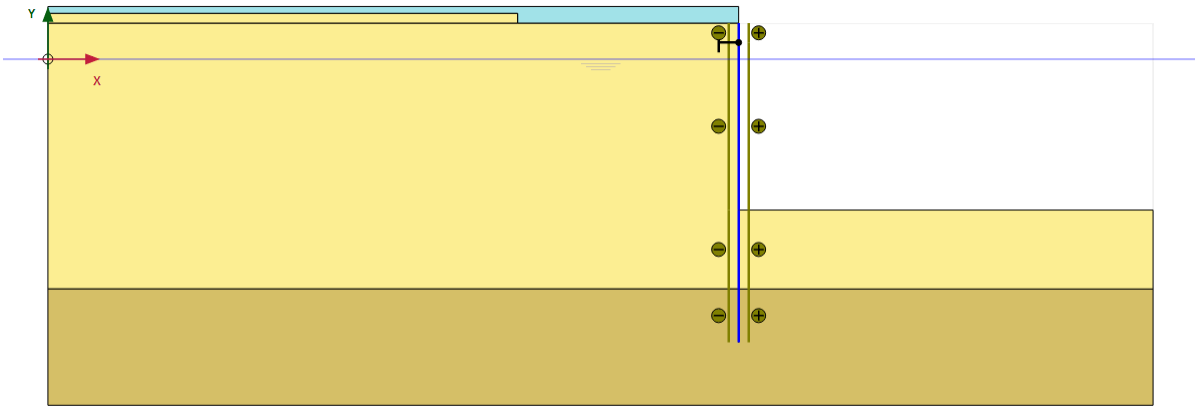

Figure H.1: Basis of the Plaxis 2D Model for Sitio 1

The model frame is from 0 m to +80 m in the x-direction and from +4 m to -25 m in the y-direction. The sheet pile is 23.05 m long and modelled from (50, 2.6) to (50, -19.25). The anchor is located at (50, 1.2). The first soil layer (defined as artificial sand in Chapter 3) is located from +2.6 m to -16.6 m on the y-axis, the second layer (defined as natural sand) from -16.6 m to -25 m. The ground water table (GWT) is located at 0 m on the y axis, same as the sea water level. This is assumed to be the same due to the soil being uniformly graded sand, making it possible for the groundwater level to stay at the same level as the sea water level. On top of the soil layers behind the sheet pile wall, a concrete floor is modelled to reenact the load due to the concrete in real life.

H.2. Nieuw Delft

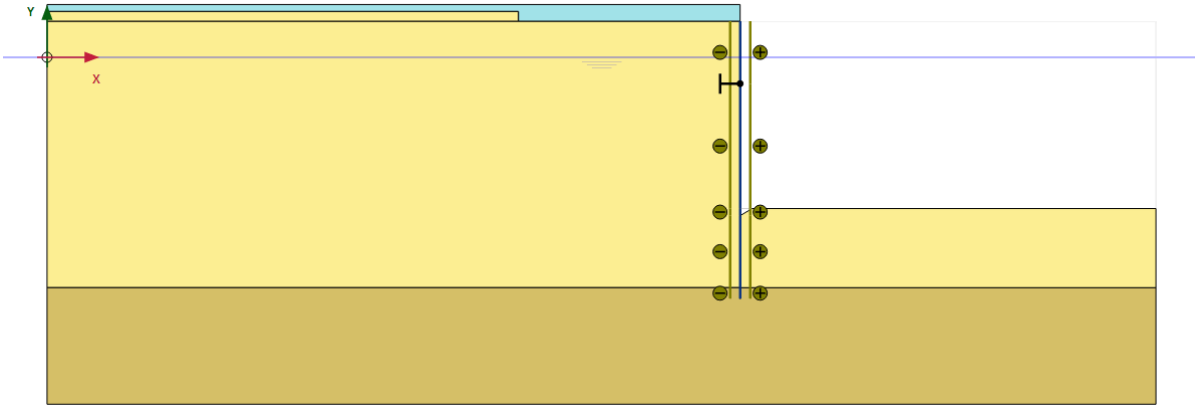

Figure H.2: Basis of the Plaxis 2D Model for NieuwDelft

The model frame is from 0 m to +80 m in the x-direction and from +4 m to -25 m in the y-direction. The sheet pile is 20.00 m long and modelled from (50, 2.6) to (50, -17.4). The anchor is located at (50, -1.9). The first soil layer (artificial sand) is located from +2.6 m to -16.6 m on the y-axis, the second layer (natural sand) from -16.6 m to -25 m. The GWT is located at 0 m on the y-axis, same as the sea water level. This is assumed to be the same due to the soil being uniformly graded sand, making it possible for the groundwater level to stay at the same level as the sea water level. On top of the soil layers behind the sheet pile wall, a concrete floor is modelled to reenact the load due to the concrete in real life.

H.2.1. Concrete founded on piles

Since PLAXIS 2D cannot model a piled foundation effectively, this is left out of the model. To investigate the consequences of this decision on the internal forces of the sheet pile, a piled foundation is simulated in PLAXIS. When the concrete floor is founded on piles, the weight is partly carried by the piles, and partly

directly by the soil. This effect is simulated by reducing the concrete weight in the model by 50% and assessing the effect on the sheet pile wall. The results are given in Table H.1. The effect of the concrete partly carried by the piles on the sheet pile wall is insignificant, as the SF_{SP} only changes by 2.4%.

D_{embed} $[m]$	M_{min} $[kNm/m]$	M_{max} $[kNm/m]$	N $[kN]$	SF_{SP} [-]	$Q_{max.abs}$ $[kN]$	F_{anchor} $[kN]$	u_{max} $[mm]$
-17.4	240	239	176	3.34	160	650	21.6
-17.4	235	228	166	3.43	146	612	20.4

Table H.1: Results of a reduction in concrete weight, simulating the concrete floor being founded on piles and thus not loading the soil directly.

H.2.2. Model load definitions

To assess the sheet pile wall of Sitio 1 and of the new quay design, two loadcases are defined: an operational loadcase and an earthquake loadcase. How these are defined in the model is visualised below.

As mentioned in Section 6.5.5, a scour hole of 0.5 m deep and 0.87 m long is defined in the model. However, the installation of a bottom protection would mean that this scour wont occur. Therefore, the height of the passive soil will be larger than is defined in the model, leading to more stability. Therefore the model will give conservative results.

Operational load definition in the model

The operational load as mentioned in Section 6.3 is modelled in PLAXIS as shown in Figures H.3, H.4, H.5 and H.6.

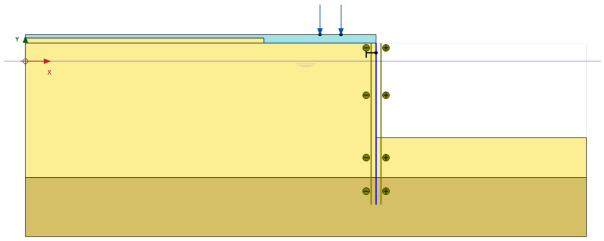

Figure H.3: The operational load case in Plaxis for Sitio 1 with GWT = LAT

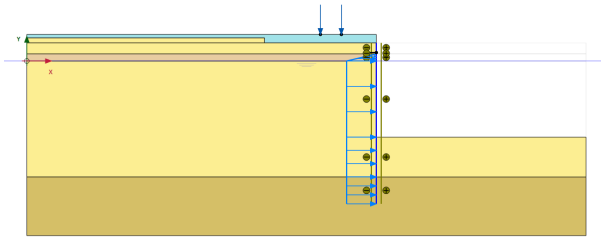

Figure H.4: The operational load case in Plaxis for Sitio 1 with GWT = MSL

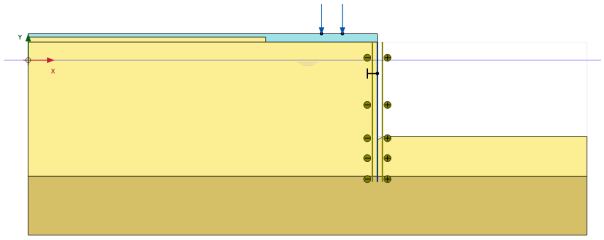

Figure H.5: The operational load case in Plaxis for Nieuw Delft with GWT = LAT

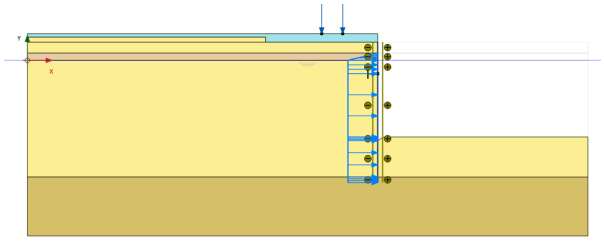

Figure H.6: The operational load case in Plaxis for Nieuw Delft with GWT = MSL

Earthquake load definition in the model

The other load case is the earthquake load case. The way this is modelled in PLAXIS is visualized below, in Figures H.7, H.8, H.9 and H.10. As mentioned in Section 6.3, this depends on the weight of the active soil wedge. However, there are three different soil layers (saturated natural sand at the bottom, saturated artificial sand in the middle and unsaturated artificial sand at the top). Due to this, the weight of the wedge is not completely uniform, as can be seen in the line load in the figures.

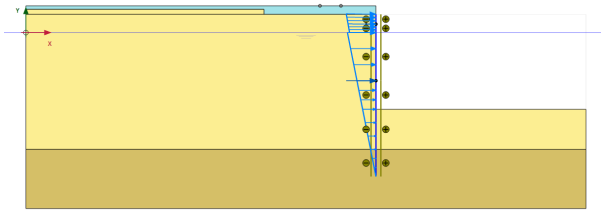

Figure H.7: The earthquake load case in Plaxis for Sitio 1 with GWT = LAT

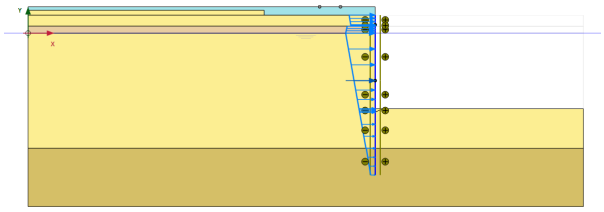

Figure H.8: The earthquake load case in Plaxis for Sitio 1 with GWT = MSL

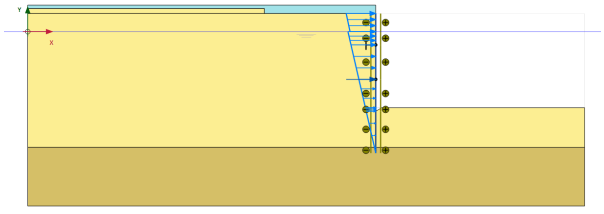

Figure H.9: The earthquake load case in Plaxis for Nieuw Delft with GWT = LAT

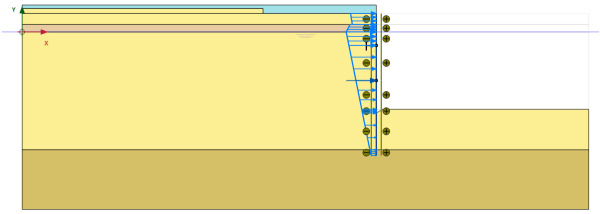

Figure H.10: The earthquake load case in Plaxis for Nieuw Delft with GWT = MSL

The line load is based on the weight of the wedge. This was done in the following way. The wedge is divided in three parts, one per soil layer. The line load for the saturated natural sand part of the wedge (which is triangular) is determined using the following equation.

$$q(y) = C * \gamma_s * tan(\beta) * y \tag{H.1}$$

in which:

- C = seismic coefficient
- γ_s = the unit weight of the soil in kN/m^3
- y = distance from the bottom of the soil layer in upward direction, given in m. The thickness of the soil layer is the maximum value for y.
- β = the angle of the wedge at the toe of the sheet pile (see Section 6.3)

For the other soil layers (for which the wedge part can be split into a rectangular and a triangular part), the line load is determined using the following equation:

$$q(y) = C * \gamma_s * tan(\beta) * y + C * \frac{W_{rectangle}}{H} \tag{H.2}$$

in which $W_{rectangle}$ is the weight of the rectangular part.

For the GWT = LAT scenario, using the soil characteristics given in Section 3.6 and the equations given above, the following line loads are implemented due to the earthquake load case:

- Sitio 1:

Layer	**Line load**
Saturated Natural Sand Layer (thickness = 3.85 m)	$q(y) = 2.68 * y$
Saturated Artificial Sand Layer (thickness = 16.6 m)	$q(y) = 2.65 * y + 10.22$
Unsaturated Artificial Sand Layer (thickness = 2.6 m)	$q(y) = 2.457 * y + 50.25$

- Nieuw Delft:

Layer	**Line load**
Saturated Natural Sand Layer (thickness = 0.8 m)	$q(y) = 2.68 * y$
Saturated Artificial Sand Layer (thickness = 16.6 m)	$q(y) = 2.65 * y + 2.12$
Unsaturated Artificial Sand Layer (thickness = 2.6 m)	$q(y) = 2.457 * y + 42.75$

For the GWT = MSL scenario, using the soil characteristics given in Section 3.6 and the equations given above, the line loads due to earthquake load case are as follows:

- Sitio 1:

Layer	**Line load**
Saturated Natural Sand Layer (Thickness = 3.85 m)	$q(y) = 2.68 * y$
Saturated Artificial Sand Layer (Thickness = 17.64 m)	$q(y) = 2.65 * y + 10.22$
Unsaturated Artificial Sand Layer (Thickness = 2.6 m)	$q(y) = 2.457 * y + 52.79$

- Nieuw Delft:

Layer	Line load
Saturated Natural Sand Layer (Thickness = 0.8 m)	$q(y) = 2.68 * y$
Saturated Artificial Sand Layer (Thickness = 17.64 m)	$q(y) = 2.65 * y + 2.12$
Unsaturated Artificial Sand Layer (Thickness = 2.6 m)	$q(y) = 2.457 * y + 45.3$

Note that for the scenario in which the groundwater level is equal to MSL, the line load used to model the water pressure is added to the line load due to the earthquake load case.
The point load represents the force due to the dynamic water pressure. The size of the force is determined with Equation 6.3, as mentioned in Section 6.3. This gives a force of 175.23 kN. It is situated on a height of 3/5 of the water depth, measured from the water surface.

H.2.3. Dimensioning the anchors and sheet pile

To eventually find the right anchor depth, the model is ran for several depths, to eventually determine the best option. These depths vary around a common anchor depth of $0.25h_{ret}$. Initially, an anchor rod diameter of 80 mm is assumed. This is not the final dimension. Since the length of the anchor should be defined to run the model, and since this length depends on the anchor depth, this length is calculated by hand, according to Equation H.3 and defined in the model for each run, with the embedded depth of the sheet pile wall initially set to 9.55 m, the same as for the Sitio 1 sheet pile wall. This value is only used to define the anchor depth and will change in the final design. As a starting point, the sheet pile particulars are defined as in Table H.2. Based on the results of the model, these particulars might be changed. This analysis is done at two different anchor spacings, being 1.26 m and 2.50 m. By doing so, the possibility of increasing the anchor spacing is assessed. A larger anchor spacing leads to a cost reduction. This analysis is done for the operational load case only. The results of this analysis are given in Table H.4 and H.5.

$$L_{anchor} = H_{SP} * tan(\beta) + \frac{D_{anchor}}{tan(\beta)} + 1.5 \tag{H.3}$$

Parameter	Sitio 1	Initial Nieuw Delft	Unit
Type	YPS B-74	Hat-Type NS-SP-10H	-
A	448	287	cm^2/m
E	200	200	GPa
I	160000	153800	cm^4/m
W	6600	4160	cm^3/m
f_y	173	295	MPa
Mass	148	225	$kg/m/m$
D_{embed}	9.55	9.55	m

Table H.2: Sheet pile characteristics at Sitio 1 [40] and the initially assumed sheet pile for Nieuw Delft to run the model.

Depth $[m]$	$L_{anchor}[m]$
3.5	23
4.5	25
5.5	26

Table H.3: Anchor lengths, calculated by Equation H.3, rounded to the upper integer.

D $[m]$	M_{min} $[kNm/m]$	M_{max} $[kNm/m]$	SF_{SP} [-]	F_{anchor} $[kN]$	SF_{anchor} [-]	u_{top} $[mm]$	u_{max} $[mm]$
3.5	235	258	4.76	358	3.30	4.1	16.5
4.5	209	226	5.43	337	3.51	6.2	13.8
5.5	201	195	6.11	332	3.56	10.0	11.5

Table H.4: Results of anchor depth analysis for $L_{spacing}$ = 1.26 m for the initially assumed sheet pile characteristics under operational conditions.

D [m]	M_{min} [kNm/m]	M_{max} [kNm/m]	SF_{SP} [-]	F_{anchor} [kN]	SF_{anchor} [-]	u_{top} [mm]	u_{max} [mm]
3.5	280	284	4.32	628	1.88	10.0	21.6
4.5	252	242	5.07	611	1.93	14.1	18.8
5.5	227	197	6.23	613	1.93	20.4	20.4

Table H.5: Results of anchor depth analysis for $L_{spacing}$ = 2.50 m for the initially assumed sheet pile characteristics under operational conditions.

By analyzing the results, we find that the safety factor for the sheet pile stress is rather high. To reduce the amount of steel in the design, and thus the cost, another sheet pile is chosen. The sectional modulus W is reduced by approximately 30% to come to the sheet pile given in Table 6.2. Next, the same calculations for different anchor depths are performed with the new sheet pile wall implemented in the PLAXIS model. The results are in Table H.6 and H.7.

D [m]	M_{min} [kNm/m]	M_{max} [kNm/m]	SF_{SP} [-]	F_{anchor} [kN]	SF_{anchor} [-]	u_{top} [mm]	u_{max} [mm]
3.5	223	238	3.68	375	3.15	4.3	18.5
4.5	197	209	4.19	353	3.35	6.7	15.4
5.5	203	184	4.32	346	3.41	10.8	12.8

Table H.6: Results of anchor depth analysis for $L_{spacing}$ = 1.26 m for the improved sheet pile characteristics under operational conditions.

D [m]	M_{min} [kNm/m]	M_{max} [kNm/m]	SF_{SP} [-]	F_{anchor} [kN]	SF_{anchor} [-]	u_{top} [mm]	u_{max} [mm]
3.5	264	263	3.33	665	1.78	10.4	24.1
4.5	237	230	3.81	638	1.85	14.3	20.8
5.5	214	194	4.52	630	1.87	20.9	20.9

Table H.7: Results of anchor depth analysis for $L_{spacing}$ = 2.50 m for the improved sheet pile characteristics under operational conditions.

Looking at the results again, in Table H.7, we can conclude that the material reduction of the sheet pile still gives a sufficiently safe situation, with safety factors around 4.
Although an anchor depth of 5.5 m results in the highest sheet pile safety factor, this option is not chosen as it also results in a relatively big displacement of the sheet pile top. Moreover, such depths for such retaining height are uncommon. Commonly, the anchor depth is around $0.30h_{ret}$. Since the retaining height at Nieuw Delft is 13.5 m this can be seen as another argument not to take 5.5 m depth.
Looking further, we find that the minimum and maximum moment are well distributed when the anchor is at 4.5 m depth. Also the top displacement (<50 mm) and sheet pile safety factor (>1) are acceptable. Moreover, this depth is close to the common value of $0.30h_{ret}$. This depth is therefore chosen for the final design.
By analyzing the results again, it can be concluded that it is safe to use an anchor spacing of 2.5 m. Although the anchor forces increase with the spacing, the safety factor for an anchor depth of 4.5 m is still 1.85, which is well above the desired value of 1.5. Also the maximum displacements of the sheet pile are acceptable at 20.8 mm.

Now a choice has been made on the anchor depth and spacing, and the sheet pile wall has been optimised, the embedded depth of the sheet pile wall can be discussed. In the PLAXIS model, the embedded depth is reduced with a step size of 1 m to find the embedded depth at which failure occurs. A scour depth at the sheet pile bottom of 0.5 meters due to transverse thrusters, as found in Section 6.5.5, is included in the model. the The results of this analysis are given in Table H.8. The embedded depth is the depth op the sheet pile which is fully buried in the soil.

$D_{embed}[m]$	$M_{min}[kNm/m]$	$M_{max}[kNm/m]$	$N_{crit}[kN]$	SF_{SP} [-]	$F_{anchor}[kN]$	$u_{max}[mm]$	SF_{GF} [-]
8.5	244	238	183	3.28	646	21.4	2.25
7.5	243	237	181	3.30	645	21.3	2.25
6.5	240	239	176	3.34	650	21.6	2.36
5.5	214	245	173	3.72	662	22.3	2.68
4.5	198	259	186	3.96	717	24.4	2.20
3.5				Failure			

Table H.8: Altering of the embedded depth in PLAXIS to find the failure point.

Failure of the model means that the soil on the passive side cannot bear the active forces from the other side of the sheet pile. The sheet pile starts rotating around the anchor point. The model gives this kind of failure when the embedded depth is 3.5 m. One step above, at 4.5 m, the anchor force suddenly increases significantly. To be conservative for this kind of failure, the embedded depth is chosen at 6.5 m below LAT. The minimum and maximum moment are well distributed (almost equal) in this situation.
This concludes the dimensioning of the sheet pile wall and its anchors. All determined dimensions are given in Tables 6.1 and 6.2.

H.3. Sheet pile failure check

To check the sheet pile wall stability, the Nieuw Delft sheet pile wall and the Sitio 1 sheet pile wall are modelled for both mentioned load cases, with both groundwater level scenarios. The checks will be based on the stress that will occur in the sheet pile. The checks based on the forces in the anchor are done in Section 6.5.2.
The material properties and orientation of the sheet pile wall determine the maximum stress it can bear. The stresses in the sheet pile walls at Sitio 1 and Nieuw Delft are calculated according to Equation H.4 with their parameters as stated in Tables 6.4 and 6.5. In this equation, N is the axial force, A the area of the section, M is the moment and W the moment capacity of the sheet pile wall. The particulars of the sheet pile wall at Sitio 1 and Nieuw Delft can be found in Table 6.2. It should be noted that the f_y of the sheet pile at Sitio 1 is reduced due to damage of the 2010 earthquake. As the axial forces and moments vary over the height of the sheet pile wall, the most critical point (where N and M lead to the highest stress) should be assessed. Since the moment generally contributes for more than 90% to the stress in the sheet pile, the location at which the highest moment occurs is taken as the critical point (h_{crit}).

$$\sigma(h_{crit}) = \frac{N(h_{crit})}{A} + \frac{M(h_{crit})}{W} \tag{H.4}$$

$$SF_{SP} = \frac{f_y}{\sigma(h_{crit})} \tag{H.5}$$

A scour depth of 0.5 meters in front of the quay (see Section 6.5.5) is included in the model for Nieuw Delft to assess the sheet pile failure. Though, this depth is unlikely to occur and thus implementing this in the model results in conservative results.
Although the foundation piles of the concrete apron floor could not be taken into account in the model, this does not affect the moments in the sheet pile significantly, as found by De Gijt and Broeken.

H.3.1. Sheetpile failure check for Sitio 1

The model for Sitio 1 is ran for both load cases as described above. After running the model, output is given of for the internal forces and the anchor force of the sheet pile. The output for the internal forces is visualised. The internal forces for the load case are shown in Figures H.11 and H.12. Note that the figures don't have the same scale. The internal forces for the earthquake load case are given in H.13 and H.14.

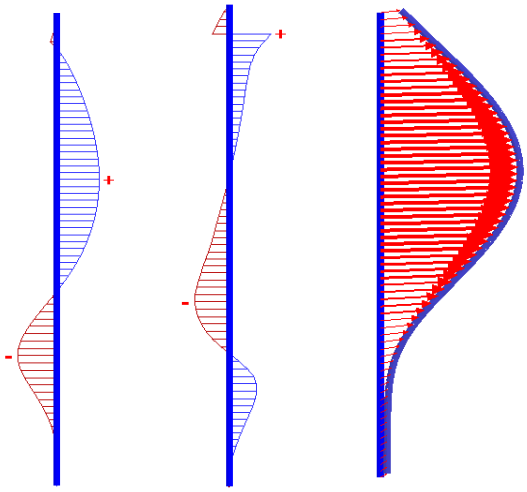

Figure H.11: (a) Bending moment in the sheet pile (b) Shear force in the sheet pile (c) Deformation in the sheet pile, all for Sitio 1 in the operational load case where GWT = LAT

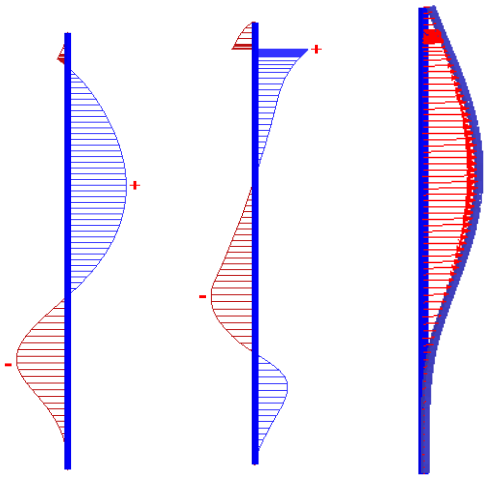

Figure H.12: (a) Bending moment in the sheet pile (b) Shear force in the sheet pile (c) Deformation in the sheet pile, all for Sitio 1 in the operational load case where GWT = MSL

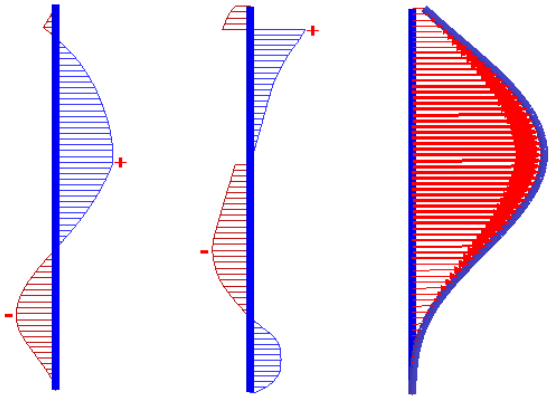

Figure H.13: (a) Bending moment in the sheet pile (b) Shear force in the sheet pile (c) Deformation in the sheet pile, for Sitio 1 in the Earthquake load case, where GWT = LAT

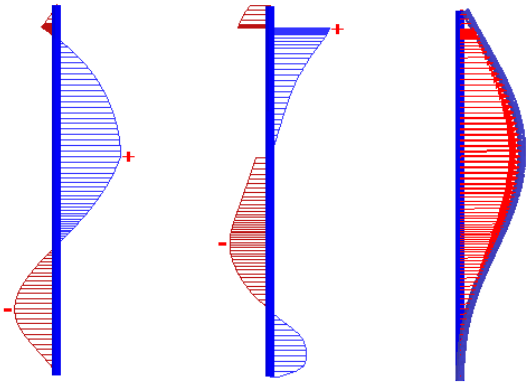

Figure H.14: (a) Bending moment in the sheet pile (b) Shear force in the sheet pile (c) Deformation in the sheet pile, for Sitio 1 in the Earthquake load case, where GWT = MSL

The most important output values for the momentum, forces and deformation of the sheet pile are determined and these are given in Table6.4. The anchor forces for both cases are given in Table 6.6.

H.3.2. Failure check sheet pile Nieuw Delft

For Nieuw Delft the same procedure is followed as for Sitio 1. Both load cases are ran in the model, and the output given for the sheet pile wall was visualised. It should again be noted that the figures are not on the same scale. The internal forces for the operational loadcase are shown in Figures H.15 and H.16. The internal forces for the earthquake loadcase are shown in Figures H.17 and H.18.

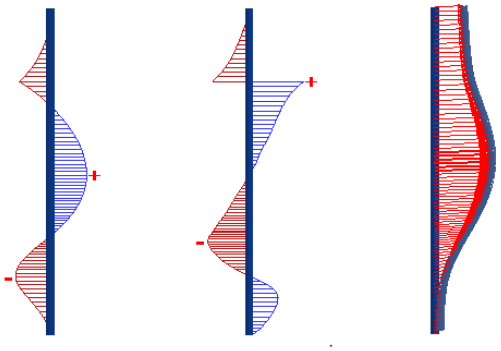

Figure H.15: (a) Bending moment in the sheet pile (b) Shear force in the sheet pile (c) Deformation in the sheet pile, for Nieuw Delft in the operational load case, where GWT = LAT

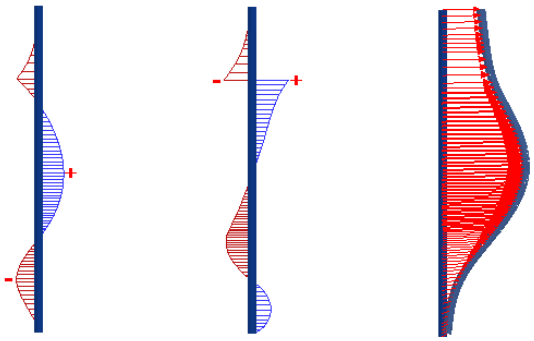

Figure H.16: (a) Bending moment in the sheet pile (b) Shear force in the sheet pile (c) Deformation in the sheet pile, for Nieuw Delft in the operational load case, where GWT = MSL

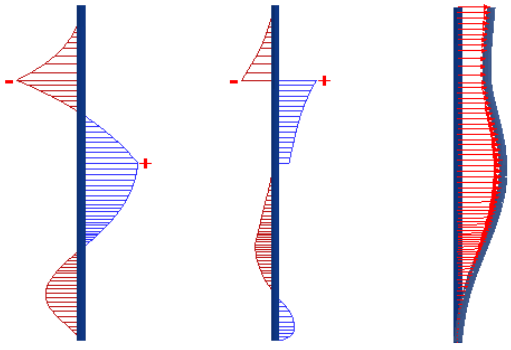

Figure H.17: (a) Bending moment in the sheet pile (b) Shear force in the sheet pile (c) Deformation in the sheet pile, for Nieuw Delft in the Earthquake load case, where GWT = LAT

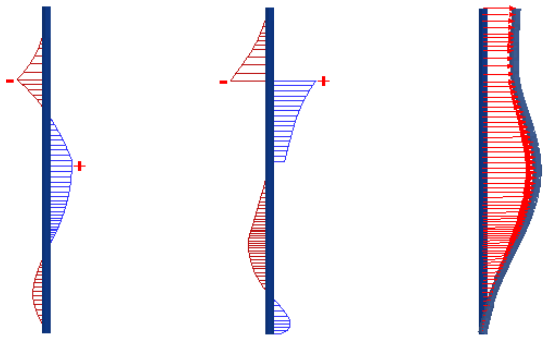

Figure H.18: (a) Bending moment in the sheet pile (b) Shear force in the sheet pile (c) Deformation in the sheet pile, for Nieuw Delft in the Earthquake load case, where GWT = MSL

The most important output values for the sheet pile wall are once again determined and given in Table 6.5. The anchor forces are given in Table 6.6.

Visualisation Quay "Nieuw Delft"

In this Appendix, some visualisations of the quay "Nieuw Delft" are shown.

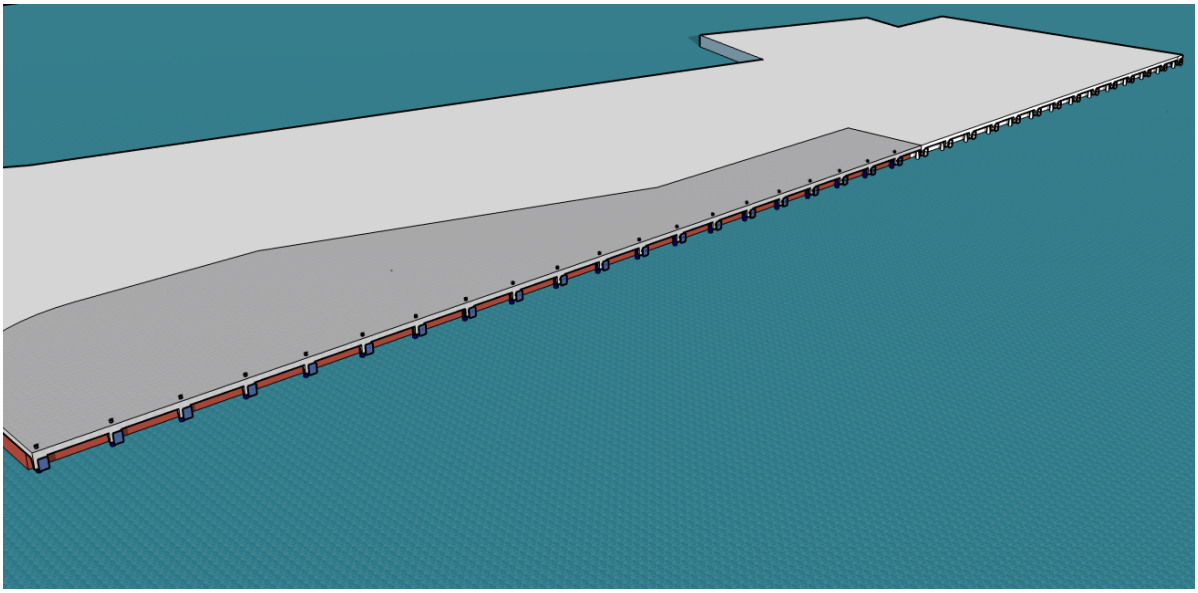

Figure I.1: Nieuw Delft 3D Full View

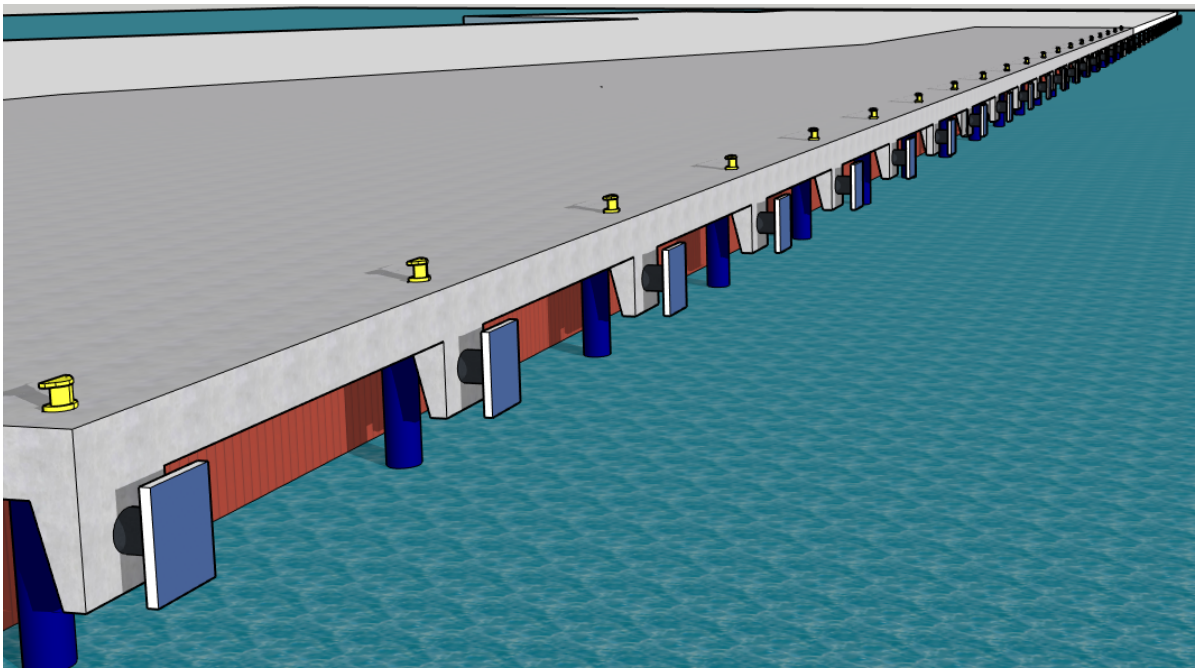

Figure I.2: Nieuw Delft 3D Sideview

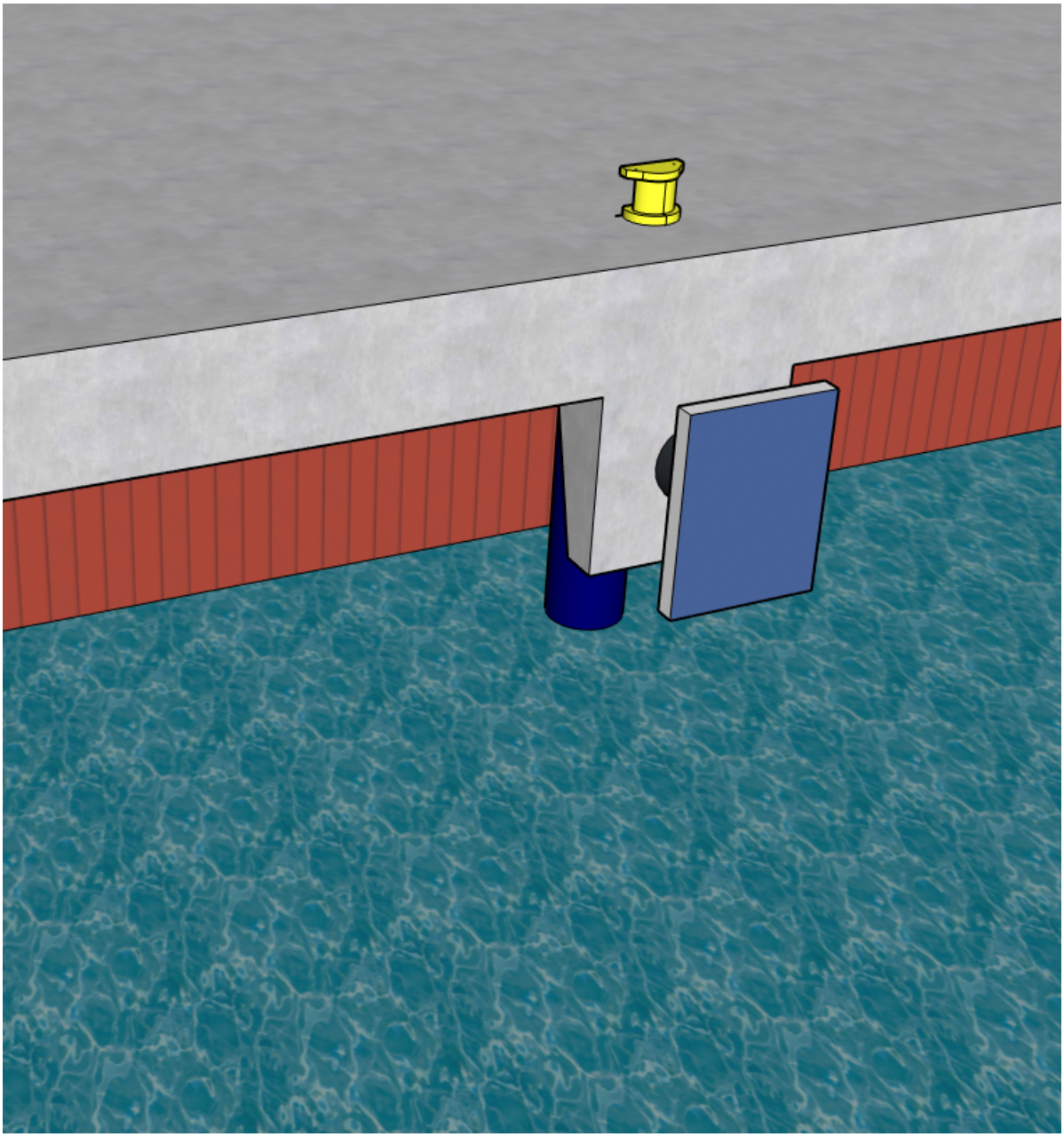

Figure I.3: Nieuw Delft 3D Detail

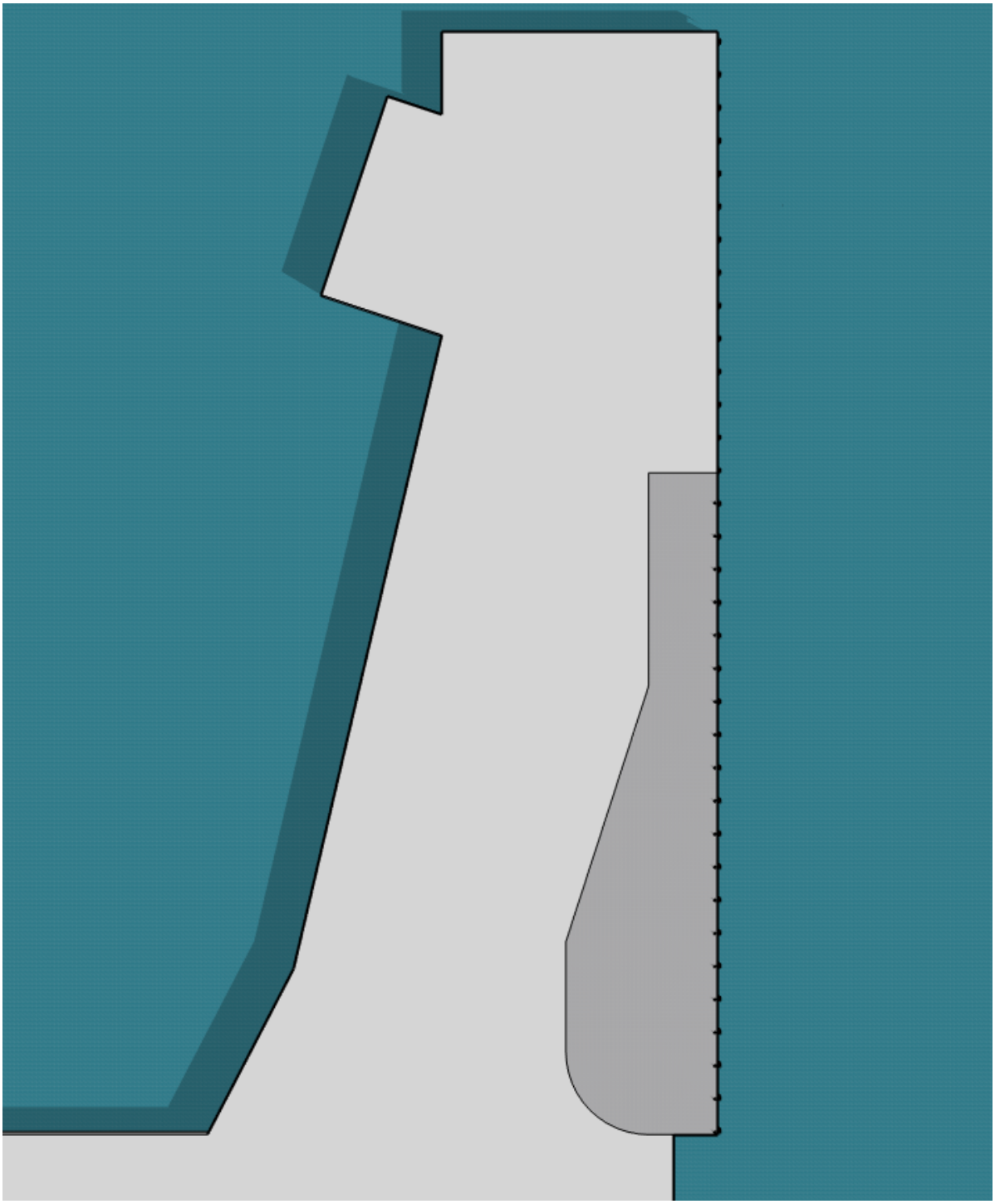

Figure I.4: Nieuw Delft 3D Overview

J

Design Concrete Apron Floor

In this Appendix, the hand calculations for the design of the concrete apron floor are shown. The first two pages consist of the calculation of the maximum moment in the concrete and doing a stress check. The second part consists of the reinforcement calculations in the concrete, which are subdivided into the main reinforcement and the stirrup reinforcement. Due to the limited time, these calculations were done by hand.

Subject: Calculation Mmax & Stress Check Concrete Apron
page: 1/2

1) Model

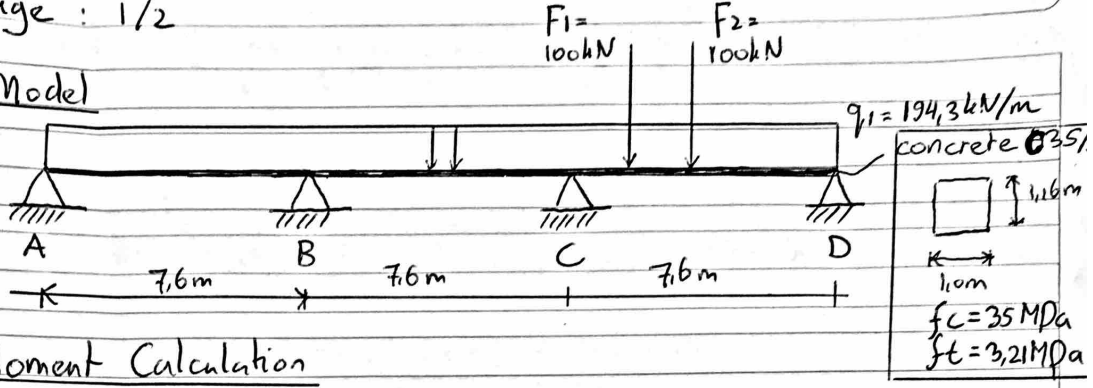

2) Moment Calculation

The maximum moment can be calculated by splitting up the load cases and adding them afterwards.

2.1 Moment due to q-load

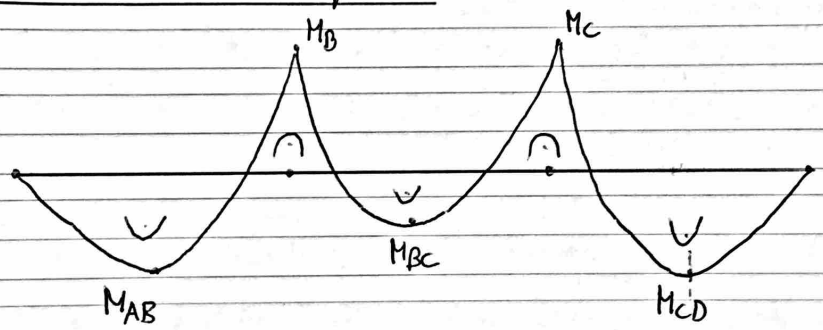

- $M_{AB} = 0{,}08 \cdot q_1 \cdot l^2 = 0{,}08 \cdot 194{,}3 \cdot 7{,}6^2 = 898\,kNm$
- $M_B = M_C = 0{,}1 \cdot q \cdot l^2 = 0{,}1 \cdot 194{,}3 \cdot 7{,}6^2 = 1123\,kNm$
- $M_{BC} = M_B - \frac{1}{8} \cdot q \cdot l^2 = 281\,kNm$
- $M_{CD} = M_{AB} = 899\,kNm$

2.2 Moment due to point loads

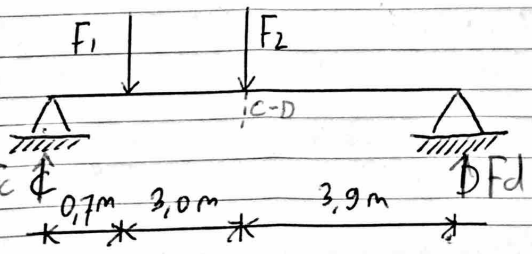

$F_d = \frac{F_1 \cdot 0{,}7 + F_2 \cdot 3{,}7}{7{,}6} = 58kN \quad (\Sigma M = 0)$

$F_c = 200 - 58 = 142kN \quad (\Sigma V = 0)$

$M_{CD_2} = F_d \cdot 3{,}9 = [illegible]\,kNm$

227

Figure J.1: Page 1 calculation maximum moment and stress check concrete apron floor

Subject: Calculation Mmax & Stress Check Concrete Apron
Page: 2/2

2.3 Adding up §2.1 & §2.2

Mmax happens in section C-D.

$M_{max} = M_{CD1} + M_{CD2} = 898 + 227 = 1125$ kNm

3) Stress Check

$$\sigma_{max} = \frac{M_{max}}{W} + \frac{F_N}{A}$$

For simplicity, F_N is assumed to be 0. Only the influence of the moment is considered.

$$\sigma_{max} = \frac{1125 \cdot 10^6}{(\frac{1}{6} \cdot 1{,}0 \cdot 1{,}16^2) / 10^9} = 5{,}0 \text{ N/mm}^2$$

$$U.C = \frac{\sigma_{max}}{f_{compression} \cdot \gamma} = \frac{5{,}0}{35 \cdot 0{,}66} = 0{,}22 \text{ §}$$

Figure J.2: Page 2 calculation maximum moment and stress check concrete apron floor

Subject: Calculation Reinforcement Concrete.

Page: 1/5

1) Analysis

The maximum stress calculated is 5,0 N/mm². The tensile strength of the chosen C35/45 is f_t = 3,21 MPa. This means reinforcement is necessary in order for the concrete to not fail. Since there is a tensile stress in the upper part of the section at supports B and C, reinforcement is needed on both sides of the concrete. (main reinforcement). Afterwards, it is investigated if stirrup reinforcement is needed.

2) Calculating main reinforcement due to Mmax

2.1 Model concrete beam

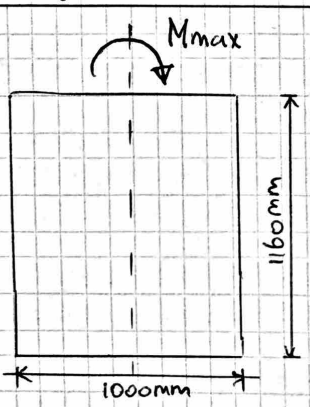

Stresses in the concrete

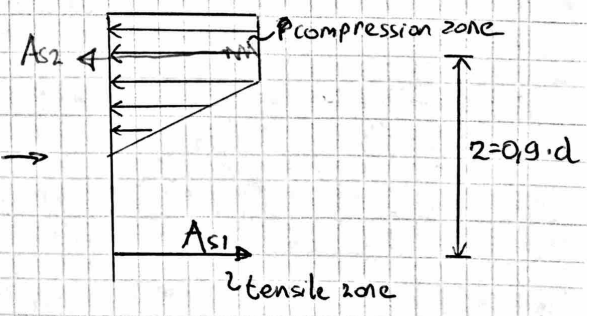

2.2 Main reinforcement

First, we have to calculate d.

$$d = h - c - \varnothing_{stirrup} - \frac{\varnothing_{main}}{2}$$

h = 1160mm, c = 30mm (distance main reinforcement from top), $\varnothing_{stirrup}$ = 12mm (first guess), $\varnothing_{main}$ = 28mm

Figure J.3: Page 1 calculation reinforcement calculation concrete apron floor

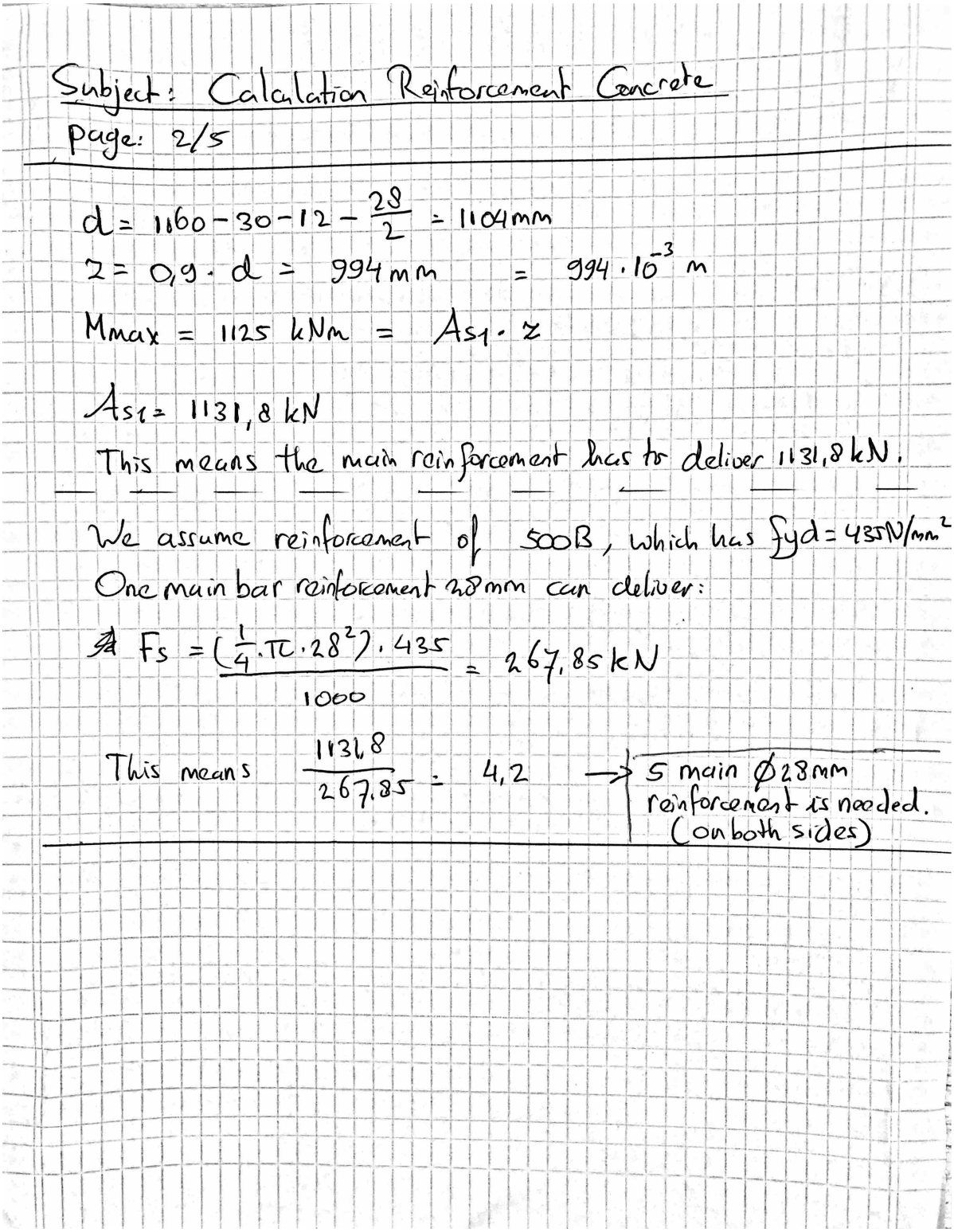

Figure J.4: Page 2 calculation reinforcement calculation concrete apron floor

Subject: Calculation Reinforcement Concrete
Page: 3/5

3) Calculation maximum shear force

3.1 Shear force line

Just like the moment line, the shear force line can be split up in the shear force due to the q-load and the shear force due to the point loads.

3.1.1 Shear force line due to q-load

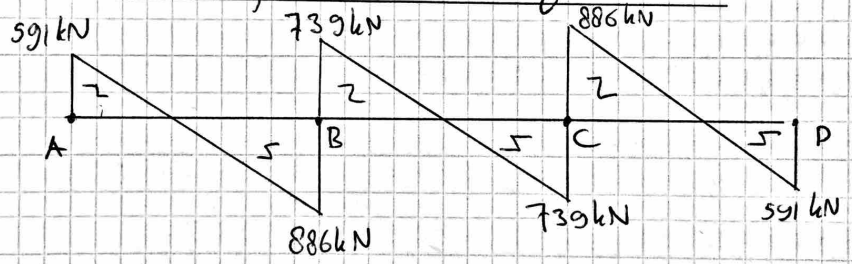

3.1.2 Shear force line due to point loads

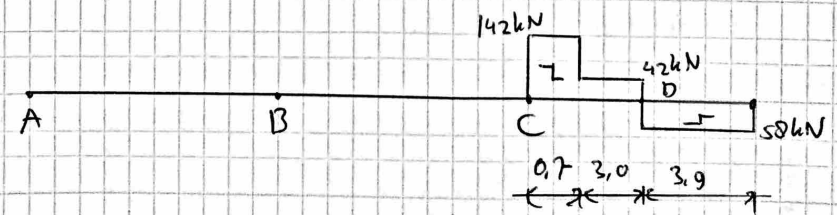

3.1.3 Adding up §3.1.1 & §3.1.2

The maximum shear force happens in section C-D, just on the right side of support C.

$V_{max} = 886 + 142 = \boxed{1028\ kN}$

Figure J.5: Page 3 calculation reinforcement calculation concrete apron floor

Subject: Calculation Reinforcement Concrete
Page: 4/5

4) Designing stirrup reinforcement

In order to know whether stirrup reinforcement is needed, the shear capacity of concrete without stirrup reinforcement needs to be calculated.

4.1 $V_{RD,c}$: shear capacity concrete

$$V_{RD,c} = v_{RD,c} \cdot b \cdot h$$

$$v_{RD,c} = 0{,}12 \cdot k \cdot (100 \cdot \rho_l \cdot f_{ck})^{1/3}$$

$$k = 1 + \sqrt{\frac{200}{1104}} = 1{,}43$$

$$\rho_l = \frac{A_s}{b \cdot d} = \frac{(\frac{1}{4} \cdot \pi \cdot 28^2) \cdot 10}{1000 \cdot 1160} = 0{,}0053$$

$f_{ck} = 35\ N/mm^2$

$$v_{RD,c} = 0{,}12 \cdot 1{,}43 \cdot (100 \cdot 0{,}0053 \cdot 35)^{1/3} = 0{,}45\ N/mm^2$$

$$V_{RD,c} = \frac{0{,}45 \cdot 1000 \cdot 1160}{1000} = 527\ kN$$

$V_{RDC} < V_{max}$ which means stirrup reinforcement is needed

4.2 Calculating stirrup reinforcement

According to the book of Concrete & Steel structures:

$$V_{RDS} = \frac{A_{sw}}{s} \cdot z \cdot \cot\theta \cdot f_{ywd}$$ (shear cap. concrete with stirrup reinforcement).

$z = 994\ mm$

$\theta = 21{,}8°$ (minimum compression angle)

$f_{ywd} = 435\ N/mm^2$

Figure J.6: Page 4 calculation reinforcement calculation concrete apron floor

Subject: Calculation Reinforcement Concrete
page: 5/5

For choosing a diameter of 14mm and a distance between the stirrups of 250mm, the following values are obtained:

$A_{sw} = \left(\frac{1}{4} \cdot \pi \cdot 14^2\right) \cdot 2 = 307,87 \text{ mm}^2$

$s = 250 \text{ mm}$

$V_{RDs} = \frac{307,87}{250} \cdot 994 \cdot \cot(21,8) \cdot 435 = 1331,2 \text{ kN}$

4.3 U.C. Shear force

$$U.C = \frac{V_{max}}{V_{RDs}} = \frac{1028}{1331,2} = 0,77$$

5) Conclusion reinforcement

The following reinforcement is needed in the concrete:

- Main reinforcement
  5 Ø28mm both sides
- Stirrup reinforcement
  Ø14mm , per 250 mm

Figure J.7: Page 5 calculation reinforcement calculation concrete apron floor

K

Scour depth calculations

K.1. Transverse thruster scour

To determine the scour due to the tugboats, the scour depth due to transverse thrusters has to be calculated. The scour due to transverse thrusters at a quay wall can be determined by the following formula's as given in PIANC [54]:

$$\frac{S}{d_{85}} = \begin{cases} C_M * 0.1 * \left(\frac{B}{B_c r}\right)^{13}, & 1.0 < \frac{B}{B_{cr}} < 1.4 \\ C_M * 4.6 * \left(\frac{B}{B_c r}\right)^{2.25}, & \frac{B}{B_{cr}} > 1.4 \end{cases} \tag{K.1}$$

in which:

- C_M = coefficient, for manoeuvring (0.3) and at rest (0.1)
- B = stability coefficient $\left(= \frac{v_{bottom}}{\sqrt{d_{85} * g * \Delta}}\right)$
- B_{cr} = critical stability factor (= 1.2)
- $\Delta = \left(\frac{\rho_s - \rho_w}{\rho_w}\right) = 1.65$

Due to the type of tugboats being unknown, the Azistern 3360 is taken as reference vessel. The vessels stats are given in Table K.1.

Azistern 3360		
Thruster type	Azimuthing	
Draft	5	m
Diameter thruster	2.2	m
Distance thruster to bottom	8.6	m
Distance thruster to wall	4.5	m
Power thruster	1654	kW

Table K.1: Azistern 3360 stats [52]

To calculate the scour, first the velocities of the jet stream have to be calculated. This is done using the following equations for scour at a quay wall due to transverse thrusters, as given in PIANC 180 [54].

$$V_{thruster} = 1.15 \left(\frac{P}{\rho_w D^2}\right)^{0.33} \tag{K.2}$$

This leads to a $V_{thruster}$ of 7.82 m/s. Using this value, the velocity at the bottom can be calculated using the following equation:

$$V_{b,max} = V_{thruster} 1.0 \left(\frac{D_{thruster}}{h_{thruster}}\right) \tag{K.3}$$

A value of 2.0 m/s is found for $V_{b,max}$. The sieve test results E give a D_{85} of 0.00042 m. Using this data, together with the assumption that the tugs are manoeuvring (which gives C_m = 0.3), the scour can be calculated using equation K.1 This leads to a maximum scour of 0.5 m.

K.2. Main propeller scour

The scour due to the main propeller is calculated with the assumption that the seabed does not contain obstacles. The parameters needed for the calculation are given in Table K.2. B is calculated in the same manner as for transverse thruster scour, B_{cr} is again assumed at 1.2. The value for Δ is again 1.65. Some dimensions of the design vessel are unknown, like the propeller type, the propeller diameter (D_p) and the distance from the propeller axis to the seabed (h_p). For this, the assumptions are made based on reference general cargo vessels. D_p is assumed to be 6 m. The distance from the keel to the propeller is assumed at 2 m, making the distance from the keel to the propeller axis 5 m. The under keel clearance in the berthing pocket is 0.9 m. This leads to a value of 5.9 for h_p.

Parameter	**Value**	
Power (P)	7900	kW
D_p	6	m
h_p	5.9	m

Table K.2: Input parameters for main propeller scour calculation

Using the following equations it is possible to calculate the depth of the maximum scour hole [54]. First the initial jet stream velocity is calculated, using Equation K.4

$$V_o = C_3 \left(\frac{f_p P_D}{\rho_w D_p^2} \right)^{0.33} \tag{K.4}$$

The value of C_3 is taken at at 1.48, which is for a manoeuvring vessel, since the jet stream will be produced during a berthing/unberthing manoeuvre. The value for f_p is taken at 5%, since the engine is in slow ahead mode and the conditions are sheltered. The following initial velocity is found to be 3.24 m/s. The velocity at the bed can now be computed using Equation K.5 (assuming the propeller is non-ducted). This is the Dutch method [54], as is also used in the Port of Rotterdam for their maintenance plan.

$$V_{b,max} = 0.216 * V_o * \frac{D_p}{h_p} \tag{K.5}$$

The value found is a stream velocity at the bottom of 0.712 m/s. It is now possible to calculate the maximum depth of the scour hole (S):

$$S = h_p C_{ad} C_{m,r} \left[a_\alpha \frac{B}{B_{crit}} - 1 \right] \tag{K.6}$$

In which C_{ad} = 1 [54], a_α = 0.65 and C_{mr} is taken at 0.44, with the rudder angle being unknown it is taken that it can assume the maximum angle of 40 degrees during the manoeuvring away from the berth. The calculated scour depth is 9.7 m.

L

Reinforced Soil

Several techniques are available for reducing active horizontal soil pressures on the sheet pile wall of the quay. Such reduction allows for the sheet pile wall to be less rigid, saving material and thus money. One of these techniques is reinforcing the soil. Layers of horizontal grids (the dashed lines in Figure L.1) can be placed in the soil, transforming the active horizontal soil pressure into tensile forces in the grids. A soil column reinforced with such grids can be stable on its own. The sheet pile wall will not be in contact with the soil, and only functions to protect the soil from washing away by the water movement, or as protection for vessel impact. Since the active soil pressure is completely eliminated, a significant saving in material and cost can be realised. Applying such grids with the presence of piles in the ground is still feasible.
Reinforced soil performs well under earthquake conditions. As the grids absorb a large part of the pressures in the soil, it limits the risk of liquefaction and reduction of the bearing capacity of the soil. For these reasons, this technique might be interesting to implement in the design of the quay.
A preliminary design calculation has been made by Tensar International BV to assess the feasibility of the technique for the port of Talcahuano under the earthquake load case, for the situation with foundation piles in the ground and GWT = LAT. The results are positive. A column of soil fully stable on its own can be created using the grids, taking away all horizontal soil pressures and allowing for significant material and cost reduction. The design is checked successfully against the following failure mechanisms.
The complete preliminary design proposal for the application of these grids in the soil is provided in the remainder of this appendix.

- Bearing capacity
- Horizontal sliding
- Tilting
- Breaking of the grids
- Sliding over the grids
- Sliding between grid layers

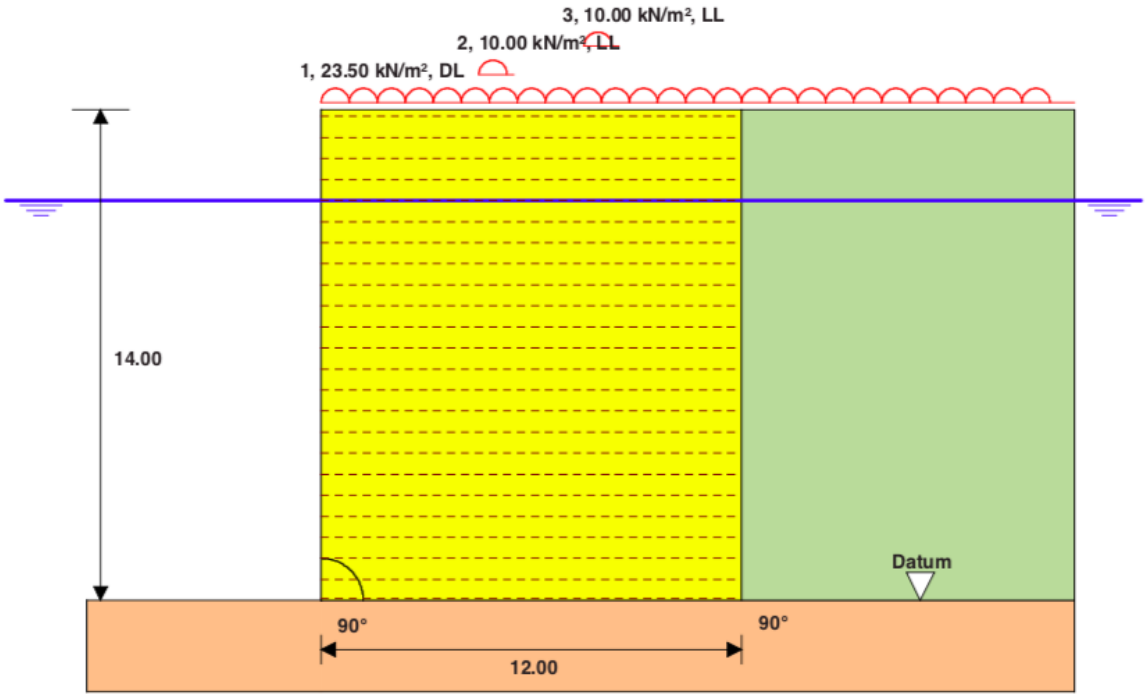

Figure L.1: An impression of reinforced soil in Nieuw Delft, the dashed lines representing the grids [11].

Client:	**Port of Talcahuano**
Project:	**Port of Talcahuano - Thrust releif of sheet pile wall H=14m**

Tensar
Structural Systems

TensarTech Wraparound Facing System

Method of analysis

The calculation method used to create this Tensar software output is the two-part wedge reinforced soil retaining wall designmethod as defined originally in Deutsches Institut für Bautechnik Certificate No Z20.1-102 adapted to take into account facing connectionstrength and serviceability for static loading and seismic loading.

Tensar International BV

Telephone: **+31 73 6241916**
Fax: **+31 73 6240652**
E-mail: **info@tensar.nl**
www.tensar.nl

Helftheuvelweg 11
5222 AV 's-Hertogenbosch
Netherlands

Input data and Section **Project:** **Port of Talcahuano - Thrust releif of sheet pile wall H=14m**

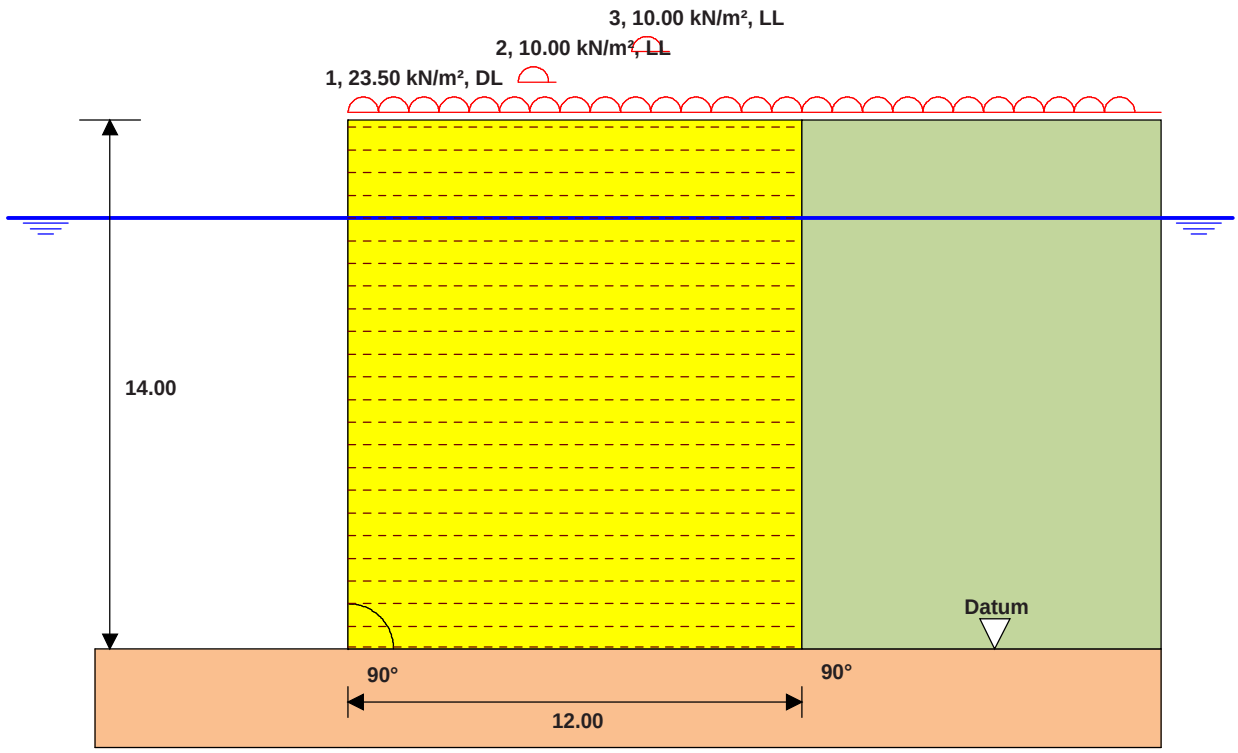

Tensar Structural Systems **TensarTech** **Wraparound Facing System**

Seismic loading case

All dimensions in metres Scale 1:200

Fill/foundation properties
Design soil strength parameters are constant volume values

Soil zone	Drained/ undrained	c' (kN/m²)	ϕ' (°)	γ_{bulk} (kN/m³)
Reinforced fill	Drained	0.0	30.0	20.0
Retained fill	Drained	0.0	30.0	20.0
Foundation soil	Drained	0.0	30.0	20.0

Seismic design data
g = acceleration due to gravity

Input	External mechanisms	Internal mechanisms
A_h = 0.2g	k_h(ext) = 0.1g	k_h(int) = 0.25g
A_v = 0.2g	k_v(ext) = 0.1g	k_v(int) = 0.25g
Vertical accelerations may act either downwards or upwards		

Surcharges
x coordinates are measured from the top of the wall.

No	Load acts from x (m)	To x (m)	Load (kN/m²)	Temporary/Permanent
1	0.00	100.00	24	Permanent
2	4.50	5.50	10	Temporary
3	7.50	8.50	10	Temporary

Water pressure data

Location	Height of water level above datum (m)	r_u
In front of structure	11.40	
Within fill	11.40	NA

Verification of external stability

Mechanism	Result	Max/Min	Critical case	OK?
Eccentricity	e = 0.36 m	2.00 m max	Static check only, Max. OT	OK
Sliding on base	1.579	1.125 min	Seismic	OK
Bearing	1.66	1.5 min	Seismic, A	OK

Verification of internal stability

Mechanism	OK?	Mechanism	OK?
Wedge check	NO	Internal sliding	OK
Post-construction strain (wedges)	< 1.0%		

Reinforcement layout
Starting and finishing levels are related to datum

Tensar Geogrid	No of layers	Starting level (m)	Vertical spacing (m)	Finishing level (m)	Coverage (%)	f_b
RE570	22	1.20	0.60	13.80	80	0.85
RE570	1	0.60	-	0.60	80	0.85
RE570	1	0.00	-	-	100	0.85

Required minimum factors of safety

Check	Static loading	Seismic loading
Eccentricity	Resultant in middle third	NA
Overturning	NA	1.5
Bearing	2.0	1.5
Sliding on base	1.5	1.125
Geogrid rupture	1.75	1.75
Geogrid pullout	2.0	2.0
Connection with facing	1.75	1.75
Internal sliding on geogrid	1.5	1.125

Further information relevent to this Tensar Earth Retention System	Further information, specifications and bill of quantities descriptions for this TensarTechEarth Retaining Structure are given in the following documents which form part of this Design Analysis	System overview Installation guide Case histories
	The current versions of these documents may be found by following the website link to "Tensar Documentation" in the Help menu of the TensarSoil® program	
	For program users who do not have a link to the internet contact your nearest Tensar representative or distributor	Tensar International GmbH +49 (0) 228 / 9 13 92-0 +49 (0) 228 / 9 13 92-11 info@tensar.de Web: www.tensar.co.uk

Detailed calculation results

The following tables provide the detailed results from the design Analysis, including geogrid design data, together with both external and internal analysis results.

External stability - characteristic (unfactored) calculated forces
Note: negative forces are upwards and to the right

Loading direction	Units	Vertical	Horizontal
Characteristic static force components			
Forces in or above reinforced block:			
Soil mass	kN/m	3360.000	0.000
Facing	kN/m	0.000	0.000
Dead loads	kN/m	282.000	0.000
Live loads	kN/m	20.000	0.000
From water pressure on base	kN/m	-1341.598	0.000
From water pressure on face	kN/m	0.000	-637.259
Forces behind reinforced block:			
From soil	kN/m	134.506	369.552
From dead loads	kN/m	33.455	91.917
From live loads	kN/m	0.000	0.000
From water pressure	kN/m	0.000	637.259
Additional characteristic static force components due to seismic loading			
Forces in or above reinforced block:			
Soil mass	kN/m	196.000	196.000
Facing	kN/m	0.000	0.000
Dead loads	kN/m	16.450	16.450
Live loads	kN/m	0.000	0.000
From water pressure on base	kN/m	0.000	0.000
From water pressure on face	kN/m	0.000	0.000
Forces behind reinforced block:			
From soil	kN/m	22.070	60.637
From dead loads	kN/m	5.489	15.082
From live loads	kN/m	0.000	0.000
From water pressure	kN/m	0.000	0.000

Verification of external stability - sliding

Sliding resistance is verified for Load combination B.

Loads given below are design values (factored).

Calculation	Units	Static loading	Seismic loading
Design horizontal driving force	kN/m	461.469	704.830
Sliding coefficient on foundation α_{sf}		0.85	0.85
Design horizontal resisting force	kN/m	1211.344	1112.606
Sliding on base		2.625	1.579
Requirement		> 1.50	> 1.125
OK?		OK	OK

Verification of external stability - bearing resistance check

Calculations carried using Meyerhof load distribution to take into account eccentricity.

Characteristic bearing resistance is calculated using unfactored loads.

Bearing resistance is verified for Load combination A, Load combination A (max overturning) and Load combination B.

Static load case:

Calculation	Units	Load case A	LCA max overturning	Load case B
Total vertical load on base (unfactored)	kN/m	3830	3820	3810
Total horizontal load on base (unfactored)	kN/m	461	461	461
Total moment on base (unfactored)	kNm/m	1350	1370	1360
Factor N_c		30.140	30.140	30.140
Factor N_q		18.401	18.401	18.401
Factor N_b		10.047	10.047	10.047
Factor i_c		0.761	0.760	0.759
Factor i_q		0.774	0.773	0.772
Factor i_y		0.680	0.680	0.679
Effective length L'	m	11.295	11.283	11.286
Characteristic ultimate bearing capacity	kN/m²	899	897	896
Design bearing resistance	kN/m	10151	10121	10117
Design applied load	kN/m	3830	3820	3810
F (bearing resistance)		2.650	2.649	2.655
Requirement		> 2.00	> 2.00	> 2.00
OK?		OK	OK	OK

Seismic load case (vertical acceleration downwards):

Calculation	Units	Load case A	LCA max overturning	Load case B
Total vertical load on base (unfactored)	kN/m	4050	4050	4050
Total horizontal load on base (unfactored)	kN/m	750	750	750
Total moment on base (unfactored)	kNm/m	3964	3964	3964
Factor N_c		30.140	30.140	30.140
Factor N_q		18.401	18.401	18.401
Factor N_b		10.047	10.047	10.047
Factor i_c		0.645	0.645	0.645
Factor i_q		0.664	0.664	0.664
Factor i_y		0.541	0.541	0.541
Effective length L'	m	10.042	10.042	10.042
Characteristic ultimate bearing capacity	kN/m²	668	668	668
Design bearing resistance	kN/m	6711	6711	6711
Design applied load	kN/m	4050	4050	4050
F (bearing resistance)		1.657	1.657	1.657
Requirement		> 1.50	> 1.50	> 1.50
OK?		OK	OK	OK

Seismic load case (vertical acceleration upwards):

Calculation	Units	Load case A	LCA max overturning	Load case B
Total vertical load on base (unfactored)	kN/m	3609	3609	3609
Total horizontal load on base (unfactored)	kN/m	705	705	705
Total moment on base (unfactored)	kNm/m	2624	2624	2624
Factor N_c		30.140	30.140	30.140
Factor N_q		18.401	18.401	18.401
Factor N_b		10.047	10.047	10.047
Factor i_c		0.627	0.627	0.627
Factor i_q		0.648	0.648	0.648
Factor i_y		0.521	0.521	0.521
Effective length L'	m	10.546	10.546	10.546
Characteristic ultimate bearing capacity	kN/m²	675	675	675
Design bearing resistance	kN/m	7113	7113	7113
Design applied load	kN/m	3609	3609	3609
F (bearing resistance)		1.971	1.971	1.971
Requirement		> 1.50	> 1.50	> 1.50
OK?		OK	OK	OK

Verification of external stability - eccentricity

Eccentricity is verified for Load case A, Load case A (max overturning), Load case B , and serviceability.

Static load case:

Calculation	Units	Load case A	LCA max overturning	Load case B
Design vertical load on base	kN/m	3830	3820	3810
Design moment on base about centreline	kNm/m	1350	1370	1360
Eccentricity	m	0.353	0.359	0.357
Maximum permitted	m	2.000	2.000	2.000
OK?		OK	OK	OK

Verification of external stability - overturning

Safety against overturning about the toe is verified for Load case B

Seismic load case (vertical acceleration downwards):

Calculation	Units	Load case B
Total overturning moments about toe	kNm/m	7028
Total restoring moments about toe	kNm/m	24942
F (overturning)		3.549
Requirement		> 1.50
OK?		OK

Verification of external stability - overturning
Safety against overturning about the toe is verified for Load case B
Seismic load case (vertical acceleration upwards):

Calculation	Units	Load case B
Total overturning moments about toe	kNm/m	6652
Total restoring moments about toe	kNm/m	23259
F (overturning)		3.497
Requirement		> 1.50
OK?		OK

Geogrid reinforcement design data
Geogrid design strength is calculated using the strengths and factors given below
Strength values quoted are per metre width of geogrid, and do not take into account percentage coverage

Design temperature (°C)	10	Design life (years)	120	Limit state	ULS

Tensar geogrid	Creep rupture strength (kN/m)	Installation damage factor	Calculated safety factor	Permissible working load at 10°C (kN/m)	Sliding coefficient
	F_B/A_1	A_2	γ	P_{des}	f_{ds}
RE570	61.31	1.0	1.75	35.03	0.85

Geogrid reinforcement design data
Geogrid design strength is calculated using the strengths and factors given below
Strength values quoted are per metre width of geogrid, and do not take into account percentage coverage

Design temperature (°C)	10	Design life (years)	Seismic	Limit state	ULS

Tensar geogrid	Tensile limit (kN/m)	Installation damage factor	Calculated safety factor	Permissible working load at 10°C (kN/m)	Sliding coefficient
		A_2	γ	P_{des}	f_{ds}
RE570	128.97	1.0	1.75	73.7	0.85

Geogrid reinforcement design data
Geogrid design strength is calculated using the strengths and factors given below
Strength values quoted are per metre width of geogrid, and do not take into account percentage coverage

Design temperature (°C)	10	Design life (years)	120	Limit state	SLS

Tensar geogrid	Load tolimit creepstrain (kN/m)	Installation damage factor	Calculated safety factor	Permissible working load at 10°C (kN/m)	Sliding coefficient
	F_B/A_1	A_2	γ	P_{sls}	f_{ds}
RE570	26.61	1.0	1.0	26.61	0.85

Connection strength

T_c for each layer of reinforcement is determined for ULS as follows:

For modular block facings, T_c is determined on the basis of block properties and connection test results as follows:

Modular block parameters			
Block length	L_u	0.000	(m)
Block height	H_u	0.000	(m)
Block width	W_u	0.000	(m)
Weight incl. infill	G_u	0.0	kg
Dist to CoG	D_u	0.000	(m)
Inclination of face	α_u	0.0	o
Max. grid spacing		0.900	(m)

Geogrid parameters				
Type	T_{uu} (kN/m)	A_{cs} (kN/m)	λ_{cs} (o)	T_{cmax} (kN/m)
RE570	100.950	100.950	0.0	100.950

Note that a partial factor of1.75 is applied to the connection strength

Grid coordinates and serviceability results

Levels are measured from the datum and horizontal location is measured from the toe of the wall

Tensar geogrid	Level	Left end	Right end	Length	Coverage	Pullout interaction factor f_b	Post construction strain
	(m)	(m)	(m)	(m)	%		%
RE570	13.80	0.00	12.00	12.00	80	0.85	0.82
RE570	13.20	0.00	12.00	12.00	80	0.85	0.86
RE570	12.60	0.00	12.00	12.00	80	0.85	0.90
RE570	12.00	0.00	12.00	12.00	80	0.85	0.92
RE570	11.40	0.00	12.00	12.00	80	0.85	0.94
RE570	10.80	0.00	12.00	12.00	80	0.85	0.96
RE570	10.20	0.00	12.00	12.00	80	0.85	0.97
RE570	9.60	0.00	12.00	12.00	80	0.85	0.98
RE570	9.00	0.00	12.00	12.00	80	0.85	0.98
RE570	8.40	0.00	12.00	12.00	80	0.85	0.97
RE570	7.80	0.00	12.00	12.00	80	0.85	0.97
RE570	7.20	0.00	12.00	12.00	80	0.85	0.94
RE570	6.60	0.00	12.00	12.00	80	0.85	0.89
RE570	6.00	0.00	12.00	12.00	80	0.85	0.81
RE570	5.40	0.00	12.00	12.00	80	0.85	0.74
RE570	4.80	0.00	12.00	12.00	80	0.85	0.66
RE570	4.20	0.00	12.00	12.00	80	0.85	0.57
RE570	3.60	0.00	12.00	12.00	80	0.85	0.49
RE570	3.00	0.00	12.00	12.00	80	0.85	0.41
RE570	2.40	0.00	12.00	12.00	80	0.85	0.33
RE570	1.80	0.00	12.00	12.00	80	0.85	0.25
RE570	1.20	0.00	12.00	12.00	80	0.85	0.16
RE570	0.60	0.00	12.00	12.00	80	0.85	0.08
RE570	0.00	0.00	12.00	12.00	100	0.85	0.00

Internal stability results

For static conditions:

Level:	Inclined wedges				Sliding between grids		Sliding on grids
	θ c_{rit}	R	Z	R/Z	θ_u	F	F
13.2	59.0	28.0	8.4	3.339	2.862	10.563	36.15
12.6	59.0	56.1	17.5	3.205	2.862	9.103	22.73
12.0	59.0	84.1	29.0	2.902	2.862	8.11	16.985
11.4	59.0	112.1	42.9	2.615	2.862	7.36	13.707
10.8	59.0	140.1	58.6	2.393	2.862	6.662	10.904
10.2	59.0	168.2	75.5	2.228	2.862	6.022	9.141
9.6	59.0	196.2	93.6	2.095	2.862	5.519	7.922
9.0	59.0	224.2	113.0	1.984	2.862	5.111	7.026
8.4	59.0	252.2	133.6	1.888	2.862	4.773	6.335
7.8	59.0	280.3	155.4	1.804	2.862	4.487	5.786
7.2	59.0	308.3	178.4	1.728	2.862	4.24	5.337
6.6	59.0	336.3	202.7	1.659	2.862	4.025	4.962
6.0	59.0	364.3	229.9	1.585	2.862	3.836	4.644
5.4	59.0	392.4	258.6	1.518	2.862	3.667	4.37
4.8	59.0	420.4	288.3	1.458	2.862	3.516	4.131
4.2	59.0	448.4	317.5	1.412	2.862	3.379	3.921
3.6	59.0	476.4	347.8	1.37	2.862	3.255	3.735
3.0	59.0	504.5	379.4	1.33	2.862	3.142	3.568
2.4	59.0	532.5	412.2	1.292	2.862	3.038	3.417
1.8	59.0	560.5	446.2	1.256	2.862	2.942	3.281
1.2	59.0	588.5	482.6	1.22	2.862	2.853	3.157
0.6	59.0	616.6	521.0	1.183	2.862	2.77	3.043
0.0	59.0	644.6	560.7	1.15	2.862	2.693	2.939
Requirement				≥ 1.0		≥ 1.50	≥ 1.50

For dynamic conditions, vertical acceleration acting downwards:

Level:	Inclined wedges				Sliding between grids		Sliding on grids
	θ c_{rit}	R	Z	R/Z	θ_u	F	F
13.2	50.0	59.0	14.9	3.955	2.862	5.002	7.042
12.6	50.0	117.9	31.1	3.797	2.862	4.666	6.269
12.0	50.0	176.9	51.5	3.437	2.862	4.392	5.699
11.4	50.0	235.8	76.1	3.098	2.862	4.159	5.249
10.8	50.0	294.8	104.5	2.82	2.862	3.869	4.596
10.2	50.0	353.7	136.1	2.599	2.862	3.56	4.128
9.6	50.0	412.7	170.8	2.416	2.862	3.316	3.773
9.0	50.0	471.7	208.8	2.259	2.862	3.119	3.493
8.4	50.0	530.6	249.9	2.124	2.862	2.954	3.265
7.8	47.0	589.6	294.4	2.003	2.862	2.813	3.076
7.2	47.0	648.5	342.1	1.896	2.862	2.692	2.915
6.6	47.0	707.5	393.1	1.8	2.862	2.585	2.776
6.0	50.0	766.4	446.1	1.718	2.862	2.49	2.654
5.4	50.0	825.4	501.2	1.647	2.862	2.406	2.547
4.8	53.0	884.3	556.7	1.588	2.862	2.329	2.45
4.2	53.0	943.3	615.2	1.533	2.862	2.259	2.364
3.6	35.0	739.5	499.9	1.479	2.862	2.195	2.286
3.0	35.0	742.6	546.1	1.36	2.862	2.137	2.214
2.4	35.0	745.7	592.6	1.258	2.862	2.082	2.148
1.8	35.0	748.8	637.1	1.175	2.862	2.032	2.088
1.2	35.0	751.8	679.5	1.106	2.862	1.985	2.032
0.6	35.0	754.9	719.8	1.049	2.862	1.941	1.98
0.0	35.0	758.0	758.1	1.0	2.862	1.899	1.931
Requirement				≥ 1.0		≥ 1.125	≥ 1.125

For dynamic conditions, vertical acceleration acting upwards:

Level:	Inclined wedges				Sliding between grids		Sliding on grids
	θ c_{rit}	R	Z	R/Z	θ_u	F	F
13.2	41.0	59.0	11.5	5.138	2.862	4.669	6.38
12.6	41.0	117.9	23.9	4.933	2.862	4.374	5.724
12.0	41.0	176.9	39.6	4.465	2.862	4.131	5.234
11.4	41.0	235.8	58.6	4.025	2.862	3.921	4.842
10.8	38.0	294.8	80.5	3.663	2.862	3.641	4.22
10.2	35.0	350.3	104.5	3.354	2.862	3.334	3.775
9.6	32.0	396.5	130.1	3.046	2.862	3.093	3.438
9.0	35.0	454.4	161.3	2.816	2.862	2.898	3.173
8.4	38.0	512.9	193.7	2.648	2.862	2.735	2.958
7.8	41.0	571.9	226.5	2.525	2.862	2.597	2.779
7.2	38.0	609.6	254.0	2.4	2.862	2.479	2.628
6.6	38.0	653.4	285.2	2.292	2.862	2.375	2.498
6.0	26.0	484.0	227.3	2.129	2.862	2.283	2.385
5.4	26.0	487.7	258.8	1.885	2.862	2.201	2.285
4.8	26.0	491.5	289.4	1.698	2.862	2.128	2.196
4.2	26.0	495.3	317.7	1.559	2.862	2.061	2.116
3.6	26.0	496.8	343.7	1.446	2.862	2.0	2.044
3.0	29.0	564.9	417.3	1.354	2.862	1.944	1.979
2.4	29.0	566.5	445.1	1.273	2.862	1.893	1.919
1.8	29.0	568.0	470.6	1.207	2.862	1.845	1.863
1.2	29.0	569.6	493.9	1.153	2.862	1.801	1.812
0.6	29.0	571.1	514.9	1.109	2.862	1.76	1.765
0.0	29.0	572.7	533.6	1.073	2.862	1.721	1.721
Requirement				≥ 1.0		≥ 1.125	≥ 1.125

Notes:
(1) Elevation measured from base of reinforced soil wall.
(2) For wedge checks, Z is the resultant of all applied forces and R is the resistance provided by the reinforcement.
(3) For sliding on grid, Z is the sum of the activating forces and R is the sum of the resisting forces.
(4) For sliding between grids, forces are calculated for the steepest plane between the grid at the given elevation and the grid immediately above.

Construction Sequence for thrust relief structures using a wraparound face

Introduction

Tensar reinforced soil thrust relief structures may be used where an existing structure has failed or is showing signs of distress. The material behind the face of the existing structure may be excavated and the Tensar structure rebuilt in its place. In many cases the excavated fill material may be re-used. It is normal to leave a void between the face of the new reinforced soil structure and the rear face of the existing wall face. When post constructional strain is complete, this void may be retro filled with an uncompacted rounded stone (pea-gravel) or proprietary compressible filler.

Where applicable, the Contractor shall ensure that the installation fully complies with CDM Regulations 2007 and should refer to the Designer's Risk Assessment and COSHH statements.

Construction Sequence

Wraparound face using external climbing formwork

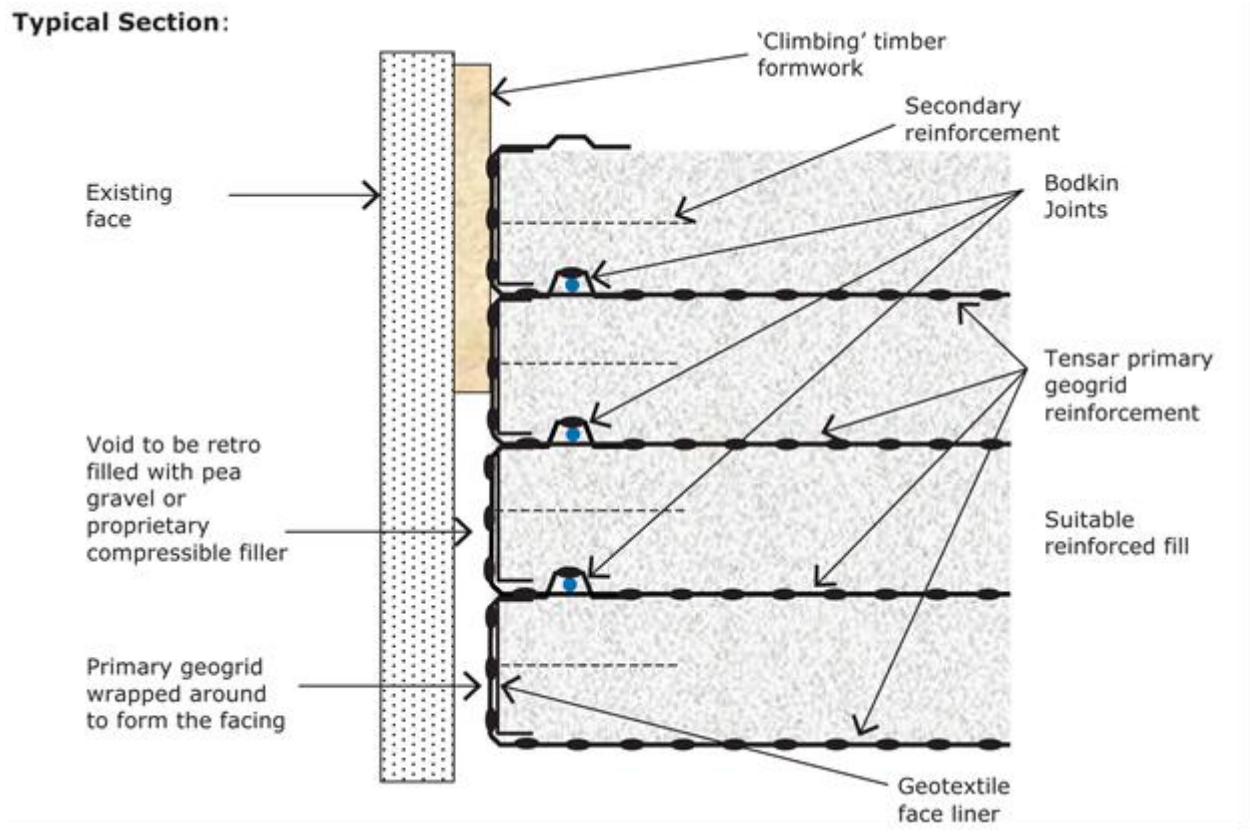

1. Cut and position the base layer of Tensar geogrid and temporarily secure the wraparound geogrid length to the climbing formwork. Adjacent lengths of geogrid are butt jointed at the face.
2. Geogrids should be installed to the levels, lengths and orientations as shown on the drawings.
3. Place and secure a suitable geotextile liner in accordance with the specification to the inside face of the wraparound geogrid length which will prevent loss of fill through the face.

4. Place a quantity of selected structural fill on the base geogrid close to the face. Pull the geogrid taut at the free end and secure with fill or by hammering pegs in front of the geogrid's rearmost transverse bar.
5. Place and compact approved fill in layers to the Contract Specification up to the next layer of primary geogrid reinforcement.
6. Install 1m lengths of secondary geogrid reinforcement to limit the vertical spacing between geogrid layers to 300mm. The front edge of the secondary reinforcement simply abuts the face liner and the geogrid remains horizontal.
7. Fill should be placed by plant such as an excavator bucket or a dozer with an opening bucket which causes the fill to cascade onto the geogrid. A 150mm thick cover of fill must be maintained between the tracks of any plant and the geogrid to avoid damage
8. Compact fill to latest version of Manual of Contract Documents For Highway works (MCHW) volume 1 Specification for Highway Works (MCHW1) Series 600 for Earthworks, Highways Agency document November 2009. Use a vibrating plate compactor or a vibrating roller with a mass per metre width ≤1300kg and a total mass ≤1000kg within 2m of the face.
9. Release the wraparound length of geogrid from the formwork and fold it over the fill.
10. Cut and position the next layer of geogrid. Form a facing joint between this and the lower geogrid length using a suitable Tensar bodkin.

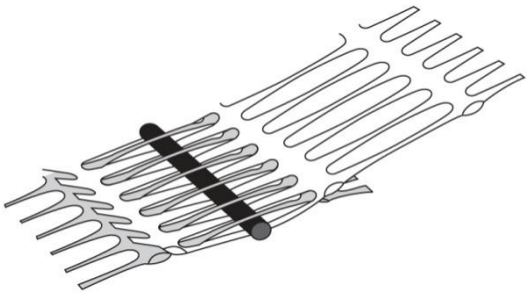

Bodkin connection detail

11. Apply a load to the free end of the upper geogrid, using a tensioning beam [1] inserted through the apertures, until the slack is removed from the bodkin joint and the lower geogrid is pulled taut around the face.
12. Whilst maintaining tension, place a layer of fill on the geogrid which will be sufficient to restrain it when the tension is removed.
13. Release the tension and remove the beam.
14. Secure the wraparound geogrid face to the inside of the formwork, place liner and repeat steps 4 – 13.
15. When necessary the temporary climbing formwork should be lifted to enable the layers of geogrid to be accurately wrapped around and the void formed.
16. The top layer of geogrid should be secured with a longer wraparound length buried beneath the top surface of the fill with the sufficient surcharge to restrain it permanently.
17. When complete and the engineer is happy that any post constructional strain has fully occurred the void between the wraparound face and the rear of the existing face may be filled with a self compacting rounded gravel or a proprietary preformed compressible material.
18. The Contractor must fully assess the safety risk associated with working at height and where appropriate install any necessary temporary edge protection.

Notes

1. Tensar Technical Note – TN Uniaxial Beam.

Tensar International Limited

Tel: +44 (0) 1254 262431
Fax: +44 (0) 1254 266867
E-mail: sales@tensar.co.uk
www.tensar-international.com

UK Head Office
Units 2 - 4 Cunningham Court
Shadsworth Business Park
Blackburn
BB1 2QX
United Kingdom

M

Landfill possibilities dredging

Behind the sheet pile wall of the new quay, landfill is needed to level the area. As the unloaded goods are stacked on the trucks the soil is compressed. The load on this area is very large and therefore the foundation needs to able to resist a large force. Depending on its quality, the dredged material can be used for this landfill. A rough estimation gives a volume of 50,000 m^3 that needs to be filled. The dredged volume more than covers the landfill volume. The most ideal situation for the planning and logistics would be to fill the extension of the quay with the sand dredged in the extended manoeuvring area. By doing so the source and the sink of the material are close together. The landfill can only start when the sheet wall is in place, just as the dredging cannot start before the wetted structure of the new quay is finished.

At this point in time it is unknown whether the soil in the dredging volume has the right characteristics to be used as landfill. Soil samples should be taken and analyzed before the dredging plan is finalized so that it can be said with certainty whether the soil is usable or not. It is recommended for the port to discuss the possibilities for this with the dredging firm beforehand.

When the use of dredged material for landfill is possible, the technical challenge would be to get the material to land in the right place and let the water out. A possible solution to this is feeding the slurry through a pipeline to the landfill area and let gravity push out the water. Another option is to unload the material at a location on the shoreline where the soil can be processed before it is transported by truck to the landfill area. A third option would be to berth the dredging vessel to the new quay and then unload the soil with a digger. All options are to be researched before a decision can be made. It is recommended to consults a dredging firm before this is done.

N

Financial Analysis

For the financial analysis, data from the years 2014,2015,2016,2017 and 2018 have been used to estimate throughput and prices. The data that has been used is listed and can be found in Figure N.1:

- Throughput commmercial berth
- Throughput Fishery
- MEH Commercial berth Sitio 1
- MEH Fishery Sitio 2

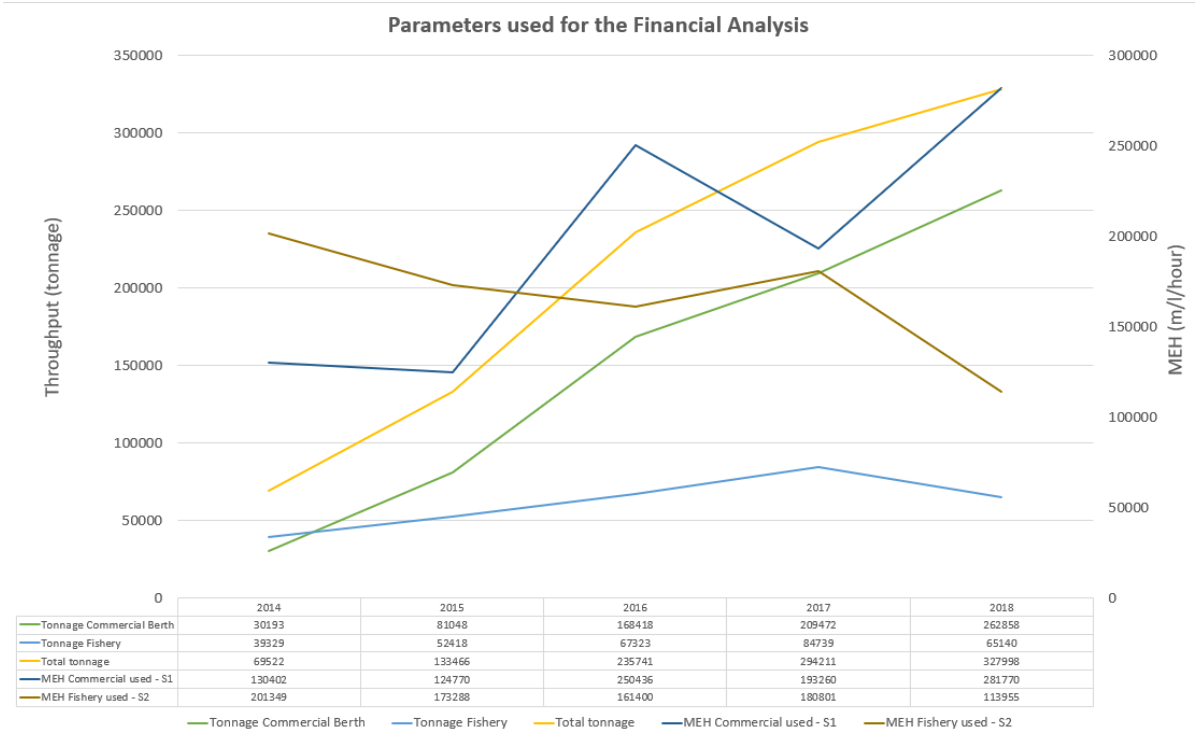

Figure N.1: Financial Analysis Parameters

In Figure N.2, the future cash flow projection for the base case is presented.

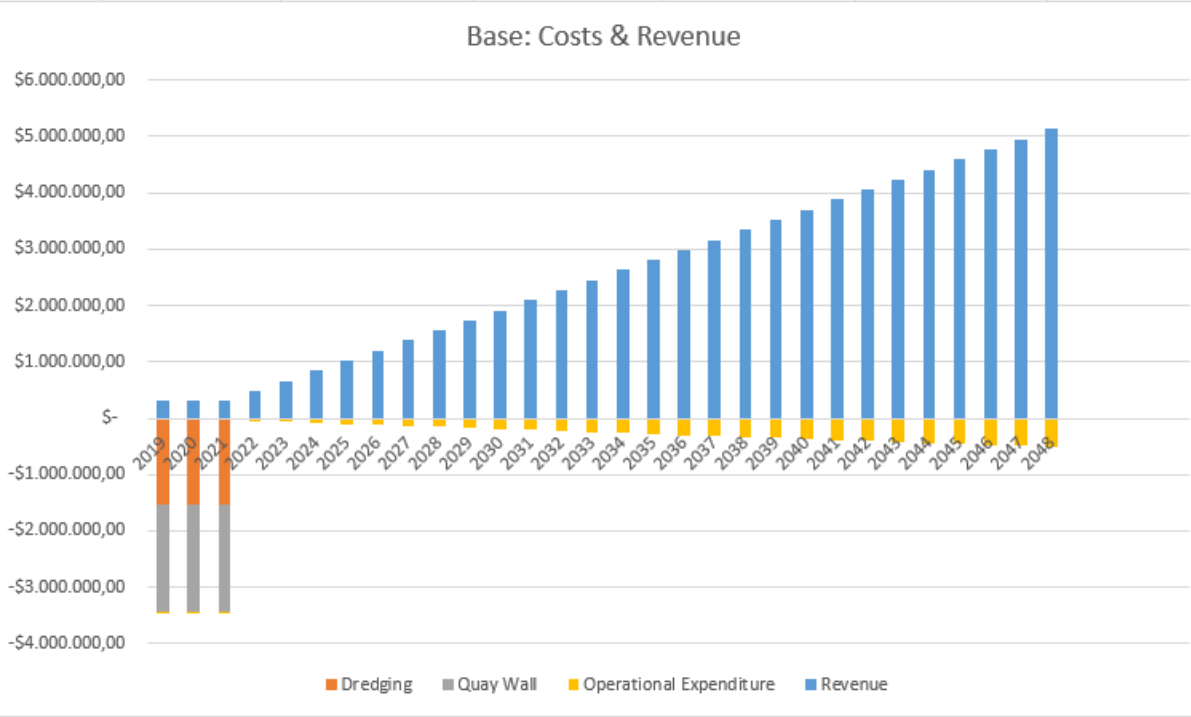

Figure N.2: Cash Flow Projection (not discounted)

In Figure N.3, the estimated throughputs for the low, base and high case are presented.

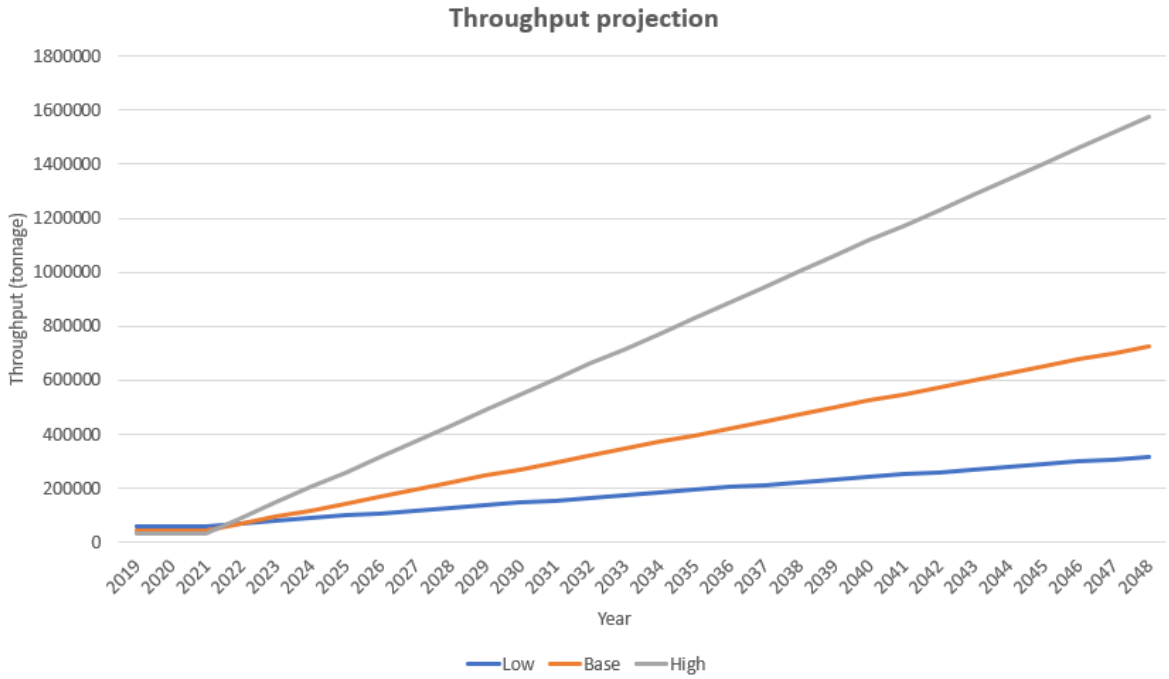

Figure N.3: Throughput projection low, base and high case

0

Dredging Cost Calculation

Rough costprice calculation of TSHD's and CSD's

1 Introduction

The weekly cost of a TSHD is the sum of:

1. DI: Depreciation And Interest
2. Maintenance and Repairs
3. Insurance
4. Crew
5. Fuel and Lubricants
6. Wear and Tear

The actual cost price of a piece of dredging equipment is depending on a large number of parameters. The capital cost form a large part of these costs and it was recognized that a standard method was needed to establish these costs. A method is described in CIRIA 2005. With this method Depreciation and Interest and Maintenance and repairs can be determined.

2 The hopper dredger

2.1 Computation of D+I and M&R

The value of these components can be established in case the following information is known:

W: Lightweight ship [ton]
P_t : Power dredgpumps during suction [kW]
J_t : Power jetpumps during suction
S: Free sailing power

SH: Service hours per week
Discharge method : dumping or pumping/rainbowing

The fist step is the calculation of the Computation of Value:

$$V = 4400W + 894000W^{0.35} - 4766000 + 1400P_t + 580J_t + 670S \quad [€]$$

2.2 Computation of D+I

When the 'value' of the vessel is known the depreciation and interest can be computed. Several methods are used. One of the methods is based on annuity.

The weekly costs for D+I follows in that case from the following equation:

$$DI = A \cdot V$$

$$A = \frac{i}{p^n - 1} \frac{1}{u} \left(p^n - z \right)$$

Where:

i	interest rate	[-]
n	Service life	[yr]
p	1 + i	[-]
u	utilization	[week/year]
z	residual value at rest of service life as a fraction of V	[-]

example:
i=0.07, n =18 years, u = 33 weeks per year and z = 0.1 (10% restvalue):

DI = 0.00292V [€/week]

2.3 Computation of MR

The amount for maintenance and repair is also related to the value V of the vessel. A certain percentage per week is given in the table below:

V [€]	% per week
7,840,000	0.23
9,480,000	0.225
11,300,000	0.219
13,000,000	0.213
14,600,000	0.206
17,800,000	0.185
20,000,000	0.17
24,700,000	0.151
30,100,000	0.133
36,900,000	0.123
42,800,000	0.114
50,500,000	0.107
59,100,000	0.103
66,000,000	0.101
71,900,000	0.1
94,200,000	0.099
104,000,000	0.099
116,000,000	0.098
135,000,000	0.098
156,000,000	0.098

The value per week is divided by a fixed and a variable (as function of the working hours) part. The discharge method has an influence on the M+R costs. Rainbowing and pumping will lead to more M+R because these discharge methods will create a lrager workload for the dredging installation.

Step 1: Compute M1 which is the percentage of the value V from the table above. For values of V in between given values use linear interpolation.

In case the discharge method is rainbowing or pumping ashore increase the value of M1 by 15 %.

M1T=1.15 *M1

Now split this cost in a fixed part of 30 % and variable past of 70 %. The variable part must be adjusted in case the number of service hours is not equal to 84 h per week with the following formula:

M1var=0.7*M1T*((SH – 84)/84+1)

Hence the total MR per week is:

M1tot=0.7*M1T*((SH – 84)/84+1) +0.3 * M1T

Example:

Suppose the value V = 71,900,000 €. The discharge method is rainbowing. Number of service hours per week is 168 Then:

M1T=1.15*0.1*0.01*71,900,000 = 82,685 €./wk.

Variable part of M&R = 0.7*82,685*(168-84)/84+1)=115,759 €./wk
Fixed part of M&R =0.3*82,685=24806 €./wk

Total M&R per week:
M1tot=115,759 €./wk+24806 €./wk=140,565 €./wk

2.4 Insurance

A first guess for the insurance cost per week is 0.03 % of the Value V.

2.5 Crew

The total cost for crew depends on the number of working hours per week, the size of the ship and where the vessel is working, since local regulations might dictate the number and origin of the crew. (for instance in Australia, due to Union regulations only local crew is permitted).

The crew cost is the sum of the expat and local crew.

For the exercise the following table can be used. Here we relate the costs to the length of theship.:

Expat crew:

L [m] from	to	cost [euro /wk]
	< 65	21,000
65	80	24,500
80	90	28,000
90	110	42,000
110	135	52,500
	> 135	64,750

Local crew:
Cost = 100*L-3660 €./wk

L is the length of the ship.

2.6 Fuel and Lubricants

2.6.1 Fuel Costs

The fuel cost per week is equal to the fuel consumption per week [ton/wk] times the unit price for fuel. The fuel unit price is expressed in US $ per ton and can be found on the internet. For the fuel consumption a specific consumption can be used:

For IFO 380 : consumption = 0.19 litre /(hour * kW)
For MDO : consumption = 0.26 litre (hour * kW)

Example :

Propulsion power installed : 25,000 kW
Diesel load during sailing: 95 %.
Fuel : IFO 380:

Fuel consumption : 0.95*25,000*0.19 = 4512 litre/hour.

2.6.2 Lubricants

Take 10 % of the fuel cost as costs for lubricants.

2.7 Wear and Tear

Depending on the abrasiveness of the dredged material extra costs must be taken into account for replacement of worn pipelines, pumps etc. on board. These costs are related to the production of the dredger and are expressed in euro's per m^3 dredged. The amount is related to the grain size of the material and can vary from 0.05 €/m^3 for silt (fine

grained sediment) up to several €/m^3 for very coarse sediments. For this exercise 0.25 €/m^3 can be taken into account.

3 The cutter suction dredge

The method is comparable with the procedure described for the TSHD.
For the value of V two formula's are used. One for a self-propelled and the other for a non propelled CSD.

Self Propelled:

$$V = 3300C + 1000\left(P + J\right) + 6000W + 100000W^{0.35} + 650S$$

Not propelled:

$$V = 3300C + 1000\left(P + J\right) + 6400W + 10000W^{0.35}$$

Where:

C	Cutter power	[kW]
P	Power dredge pumps	[kW]
J	Power jet pumps	[kW]
W	Lightweight	[ton]

3.1 Depreciation and interest

Calculated with the same method as for the hopper

3.2 Maintenance and Repairs

This is a factor times the Value V per week, based on 84 hr/week. For different hours see section 2.3.

3.3 Insurance

See section 2.4

3.4 Crew

The following table can be used . The cost for expat and local crew based on 168 service hrs per week

Large CSD	cutter power > 2500 kW	45,000 €./wk
Medium size CSD	cutterpower between 250 – 2500 kW	36,000 €./wk
Small CSD	cutterpower < 250 kW	23,000 €./wk

3.5 Fuel

The same method is applied as in section 2.6

3.6 Wear and Tear

For wear and tear an amount per m^3 is reserved as was the case for the hopper. Apart from that an extra amount must be taken into account for wear of pick points and adapters used on the cutter head. These costs as well are strongly dependent on the soil conditions encountered.

The order of magnitude for teeth consumption :
Sand : 2000 – 4000 m3 / tooth
Rock: 200 – 300 m3/tooth

Price per tooth: 100 €
Price per adapter 400 €